



Universitat  
Autònoma  
de Barcelona



Doctoral thesis

Removal of water pollutants by adsorption  
on activated carbon prepared from olive-  
waste cakes and by biological treatment  
using ligninolytic fungi

**Rim Baccar Ep Yangui**

Bellaterra, July 2013





Universitat  
Autònoma  
de Barcelona



Doctoral thesis

Removal of some water contaminants by adsorption on activated carbon prepared from olive-waste cakes and biological treatment using fungi

**Rim Baccar Ep Yangui**

Bellaterra, July 2013

**Title:** Removal of some water contaminants by adsorption on activated carbon prepared from olive-waste cakes and biological treatment using fungi

**Realized by:** Rim Bacchar Ep Yangui

**Supervised by:** Montserrat Sarrà Adroguer, Paqui Blázquez Cano and Jalel Bouzid

PhD program in Environmental Science and Technology/Biological Engineering

Department of Chemical engineering/ Laboratory Water Energy and Environment

Engineering School / National School of Engineers of Sfax

Universitat Autònoma de Barcelona/ University of Sfax

*Don't aim for success if you want it,  
first do what you love and believe in,  
and it will come naturally*

David Frost



## **Dedication**

### ***A mes chers parents***

Pour les sacrifices déployés à mon égard, pour leur patience, leur amour et leur confiance en moi. Ils ont tout fait pour mon bonheur et ma réussite. Leurs conseils prodigieux et leur principe dans la vie demeurent toujours présents dans mon esprit. Qu'ils trouvent dans ce travail, le témoignage de ma profonde affection et de mon attachement indéfectible. Que dieu leur réserve bonne santé et longue vie.

### ***A mon cher Ahmed***

Aucun mot ne saurait t'exprimer mon profond attachement et ma reconnaissance pour l'amour, la tendresse et la gentillesse dont tu m'as toujours entouré. Cher mari j'aimerais bien que tu trouves dans ce travail l'expression de mes sentiments de reconnaissance les plus sincères car grâce à ton aide, tes conseils et ton encouragement que ce travail a pu voir le jour. Que Dieu le tout puissant nous accorde un avenir meilleur.

### ***Aux membres des deux familles BACCAR et YANGUI***

Que ce projet soit l'expression de mon affection, ma reconnaissance et mon profond attachement. Que Dieu les protège et leurs offre un meilleur avenir.

### ***A tous mes amis de la Tunisie et d'Espagne***

Pour la tendre affection qu'ils m'ont fait témoigner et pour leur support, je leur souhaite la réussite et le bonheur. Sans citer des noms parce que la liste est longue et pour ne pas oublier personne.





## Acknowledgment

This dissertation would not have been possible without the guidance and the help of several individuals who in one way or another contributed and extended their valuable assistance in the preparation and completion of this study.

First, I would like to sincerely express my great gratitude and special appreciation to my supervisors Prof. Montserrat Sarrà Adroguer and Prof. Paqui Blánquez from Autonomous University of Barcelona and Prof. Jalel Bouzid from University of Sfax for their valuable advice, guidance, wonderful encouragement and patience throughout the research and thesis preparation without forgetting their good human relationships. I am really indebted to them because they challenged me in ways that enhanced my professional growth.

Special thanks to Prof Mongi Feki from University of Sfax, who greatly enriched my knowledge and who help me a lot in the fulfilling of this thesis. From deep inside thank you for your support and help.

I would like to thank all the members of the Department of Chemical Engineering in UAB and especially members of Toxic group for their nice treatment and friendship during my stay, many thanks to all of you with a special thanks to Teresa and Gloria.

I would like also to thank all the personal and colleagues of the laboratory Water Energy and Environment from University of Sfax for their help and collaboration.

It is always impossible to personally thank everyone who has helped successful completion of this study. To those of you without specifically name, my sincere thanks go to all of you, my friends and colleagues in Spain and Tunisia. Really, this is a great opportunity to express my acknowledgement, respect and gratefulness to you for your friendship, encouragement and assistance.

I would like also to thank La Agencia Española de Cooperación Internacional para el Desarrollo (AECID) for the pre-doctoral scholarship.

I specially wish to express my sincere thankfulness to my beloved parents for your tremendous love and many prayers that have been always very valuable and for teaching me how to be a strong person unconsciously by making me gets back up whenever I stumble

I am the most grateful to my husband Ahmed who overflows me with love and inspiration day by day; I share this accomplishment with you. Thank you for your encouragement, for believing in my capabilities, moral supports in all the good and hard times and patience during these years.

Special thanks to families BACCAR and YANGUI members especially my sisters, their husbands, my brother and his wife, all my nephews and my father and mother -in-law for their continuous support and love.

Last but not least, always thank God for giving me so much blessings, without the guidance of ALLAH, this work would not have been done successfully.



## ABSTRACT

Nowadays, increasing public concern and tighter international regulation have challenged the environmental problem associated with wastewater. Indeed, the removal of contaminants from wastewater is still far away from a satisfactory solution. Different processes are used for the treatment of wastewaters. However, these technologies are either frequently ineffective, or they generate secondary products or worse, they are too expensive. In fact, the selection of a particular wastewater treatment technology should not be based uniquely on its efficiency, but should rather integrate environmental and economical aspects. Within this framework, the main objective of this dissertation is the removal of various contaminants in water including metals, dyes and pharmaceuticals products via two environmentally- friendly technologies. The first consists in a physico-chemical treatment- by adsorption on activated carbon prepared from the by-product olive-waste cakes. The second is about a biological treatment using white-rot fungi.

At a first stage, the adsorbent preparation, its characterization and the study of the environmental impact associated with its production are considered. Chemical activation of the feedstock olive-waste cakes, using phosphoric acid as dehydrating agent, is adopted for activated carbon preparation and main process parameters (such as acid concentration, impregnation ratio, temperature of pyrolysis step) are varied to optimize the best conditions. The activated carbon prepared under the optimal conditions is then fully characterized considering its adsorption properties as well as its chemical structure and morphology. The results show that the most efficient adsorbent is that obtained under the following optimal conditions: an acid concentration equal to 60%  $H_3PO_4$ , an impregnation ratio of 1.75, and a pyrolysis temperature of 450 °C. The adsorption characteristics of the adsorbent prepared under such conditions presents good characteristics compared with the previous reports for activated carbon in the literature. To minimize the environmental impact, certain modifications could be incorporated in the process of adsorbent preparation such as recovery of the gas derived from the pyrolysis step, its reuse as an energy source, and the recovery of phosphoric acid after activated carbon washing.

After establishing the optimal conditions, the efficiency of the optimal activated carbon for the removal of inorganic and organic pollutants is then evaluated. For heavy metals, considering the adsorption of  $Cu^{2+}$  ions as a model, column adsorption tests show the

high capacity of the activated carbon to reduce  $\text{KMnO}_4$  into insoluble manganese (IV) oxide ( $\text{MnO}_2$ ) which impregnated the sorbent surface. The results also indicate that the adsorption of  $\text{Cu}^{2+}$  can be significantly improved by the presence of  $\text{MnO}_2$  fixed on activated carbon. Concerning the organic pollutants, the study shows the effectiveness of the activated carbon to remove dyes from individual and real effluents and pharmaceutical products from single and mixture solutions. Many models are used to understand the adsorption behavior and in the most cases Langmuir and pseudo-second order models present the best fit for the isotherm and kinetics, respectively. Temperature is found to affect the adsorption of dyes, however, the pH variation has no influence. The opposite case is found for drugs adsorption.

Regarding the biological process adapted, the potential of three white-rot fungi (WRF) (*Trametes versicolor*, *Ganoderma lucidum* and *Irpex lacteus*) to decolorize the commercial tannery dye – Black Dycem – is investigated in solid and liquid media. The results indicate that *Trametes versicolor* is the best strain both in terms of extent and rapidity of decolorization. The experiment, performed in single and repeated batches in an air-pulsed bioreactor with biomass reuse of the fungus *Trametes versicolor*, shows that the decolorization capability of the fungus does not decrease during the repeated batches and the fungus is able to remove 86–89% of the dye despite the low enzyme activity detected. The results also show that the biodegradation mechanism plays a noticeable role in the decolorization process of the dye by means of laccase activity in addition to the adsorption phenomenon occurring on the fungal surface.

Finally a combination of biological and physico-chemical treatments is adopted to remove the textile dye and the results show that further studies are needed to explore the efficiency of the combined processes.

## RÉSUMÉ

De nos jours, l'augmentation de la conscience du public et les normes de qualité qui sont devenues de plus en plus drastiques, ont posé plus de défis aux problèmes environnementaux associés aux eaux usées. En effet, l'élimination des contaminants dans les eaux usées est encore loin de la satisfaction. Différents procédés sont utilisés pour le traitement des eaux usées. Cependant, ces derniers sont souvent inefficaces, génèrent des produits secondaires, ou ils sont trop chers. A cet égard, l'objectif des travaux réalisés dans le cadre de cette thèse est l'élimination de divers polluants de l'eau, y compris les métaux lourds, les colorants et les produits pharmaceutiques, moyennant deux types de traitements: l'adsorption sur charbon actif préparé à partir d'un sous produit agricole et le traitement biologique par des champignons.

Dans un premier temps, la préparation de l'adsorbant, sa caractérisation et l'étude de l'impact environnemental lié à sa production sont considérées. Le charbon actif est préparé par voie chimique en utilisant l'acide phosphorique comme agent d'activation. Une étude systématique de l'effet de différents paramètres opératoires (concentration de l'acide, taux d'imprégnation et température de la pyrolyse) sur les performances des charbons actifs préparés est conduite pour optimiser les meilleures conditions.

Avant son utilisation, le charbon actif préparé sous les conditions optimales est entièrement caractérisé compte tenu de ses propriétés d'adsorption, sa structure chimique et sa morphologie. L'étude de l'effet des différents paramètres opératoires montre que les conditions optimales permettant la préparation d'un charbon actif performant correspondent à une concentration d'acide égale à 60%  $H_3PO_4$  et une température de pyrolyse de 450 °C. En se référant à plusieurs travaux dont la littérature fait état sur les charbons actifs, il ressort que notre charbon optimal présente des bonnes caractéristiques. Afin de minimiser l'impact environnemental, certaines modifications pourraient être incorporées dans le processus de préparation du charbon actif: comme la récupération du gaz issu de l'étape de pyrolyse et sa réutilisation comme source d'énergie et la récupération de l'acide phosphorique contenue dans les eaux de lavage de l'adsorbent.

Dans un second temps, après l'établissement des conditions optimales, l'efficacité du charbon actif optimal pour l'élimination des polluants organiques et inorganiques est évaluée. En ce qui concerne les métaux lourds, des essais d'adsorption en colonne ont

permis de mettre en évidence la grande capacité du charbon actif, préparé dans les conditions optimales, à réduire et à fixer le manganèse ainsi que la grande aptitude de ce charbon, préalablement garni de  $\text{MnO}_2$ , à fixer les ions  $\text{Cu}^{2+}$ .

S'agissant des polluants organiques, les résultats montrent l'efficacité de l'adsorbent préparé à éliminer les colorants des effluents synthétiques et réels ainsi que les produits pharmaceutiques en solutions individuelles et en mélange. Dans la majorité des cas, les modèles de Langmuir et celui du premier-ordre permettent une bonne description des isothermes expérimentaux et de la cinétique, respectivement. L'étude de l'effet de la température sur l'adsorption des colorants, montre que celle-ci influe sur ce phénomène cependant, la variation du pH n'a aucun effet. Contrairement, pour les produits pharmaceutiques, ces deux facteurs influent de manière inverse.

Concernant le traitement biologique, trois champignons *Trametes versicolor*, *Irpex lacteus* et *Ganoderma lucidum* sont testés dans le processus de décoloration du colorant de tannerie, Noir dycem TTO, dans des milieux solides et liquides. Les résultats indiquent que le champignon *Trametes versicolor* présente le pouvoir de dégradation le plus important en termes de rapidité et d'efficacité. Les résultats d'expériences réalisées en batch et en continu, dans un réacteur à lit fluidisé, montrent que la capacité de décoloration du champignon ne diminue pas au cours des batch répétés et que le champignon est capable d'éliminer 86 à 89% du colorant, malgré la faible activité enzymatique détectée. Des tests in vitro montrent que l'enzyme laccase joue un rôle dans la dégradation de ce colorant en plus de l'adsorption de ce dernier à la surface des champignons.

Finalement, une tentative de combinaison du traitement biologique et physico-chimique est adoptée pour dépolluer le colorant textile et les résultats montrent que d'autres études sont nécessaires pour explorer l'efficacité des procédés combinés.

## RESUMEN

Hoy en día, la creciente preocupación pública y la estricta regulación internacional han desafiado la problemática ambiental asociada a las aguas residuales. De hecho, la eliminación de contaminantes de las aguas residuales está todavía lejos de obtener una solución satisfactoria. Se utilizan diferentes procesos para el tratamiento de las aguas residuales. Sin embargo, estas tecnologías son ineficaces, generan productos secundarios o son demasiado caras. De hecho, la selección de una tecnología determinada de tratamiento de aguas residuales no debe basarse únicamente en su eficiencia sino que debe integrar aspectos medioambientales y económicos. En este contexto, el objetivo principal de esta tesis es la eliminación de diversos contaminantes en el agua, incluyendo metales, tintes y productos farmacéuticos a mediante dos tecnologías respetuosas con el medio ambiente. La primera consiste en un tratamiento físico-químico de adsorción sobre carbón activo preparado a partir de un residuo de la industria agroalimentaria. El segundo se trata de un tratamiento biológico con hongos.

En cuanto a la adsorción sobre carbón activo, en una primera etapa se consideran aspectos tales como la preparación del adsorbente, su caracterización y el estudio del impacto ambiental asociado a su producción. Para la preparación de carbón activo se realiza la activación química a partir de orujo de oliva, utilizando ácido fosfórico como agente deshidratante. Los parámetros principales del proceso (tales como la concentración del ácido, la relación de impregnación, la temperatura de la etapa de pirolisis) son variados para optimizar las condiciones de la activación. El carbón activo preparado en las condiciones óptimas, se caracteriza teniendo en cuenta sus propiedades de adsorción, su estructura química y su morfología. Los resultados muestran que el adsorbente más eficaz es el que se obtiene bajo las siguientes condiciones: una concentración de ácido igual a 60% de  $H_3PO_4$ , una relación de impregnación de 1,75, y una temperatura de pirolisis de 450 °C. El adsorbente preparado en estas condiciones presenta buenas características en comparación con los que se encuentran en la literatura. Para minimizar el impacto ambiental, ciertas modificaciones podrían incorporarse en el proceso de preparación del adsorbente tales como la recuperación del gas derivado de la etapa de pirolisis y su reutilización como fuente de energía, y la recuperación de ácido fosfórico después de lavar el carbón activado.

Después de establecer las condiciones óptimas se evalúa la eficiencia del carbón activo para la eliminación de los contaminantes inorgánicos y orgánicos. Para los metales,

cogiendo  $\text{Cu}^{2+}$  como un modelo, los ensayos de adsorción en columna muestran la alta capacidad del carbón activo para reducir  $\text{KMnO}_4$  en óxido insoluble de manganeso (IV) ( $\text{MnO}_2$ ) que impregna la superficie del adsorbente. Los resultados también muestran que la adsorción de  $\text{Cu}^{2+}$  puede mejorar significativamente por la presencia de  $\text{MnO}_2$  fijado sobre el carbón activo.

En cuanto a los contaminantes orgánicos, el estudio muestra la eficacia del carbón activado para eliminar los colorantes de los efluentes sintéticos y reales y los productos farmacéuticos de soluciones de compuestos puros y formando parte de una mezcla de fármacos. Se han aplicado muchos modelos para entender el comportamiento de la adsorción y en la mayoría de los casos los modelos de Langmuir y pseudo-primero orden presentan el mejor ajuste para la isoterma y la cinética, respectivamente. La temperatura afecta la adsorción de colorantes, sin embargo, la variación de pH no tiene ninguna influencia. Al contrario que en la adsorción de los fármacos.

En cuanto al proceso biológico adaptado, se ha comprobado el potencial de tres hongos ligninolíticos (*Trametes versicolor*, *Ganoderma lucidum* y *Irpex lacteus*) para la decoloración de una mezcla comercial del colorante órgano metálico de la industria de curtidos en medios sólidos y líquidos. Los resultados indican que *Trametes versicolor* es la mejor cepa tanto en términos de extensión como de rapidez en la decoloración. El experimento, realizado en discontinuo y en discontinuos repetidos en un reactor fluidizado por pulsos de aire y con renovación de biomasa del hongo *Trametes versicolor*, muestra que la capacidad de decoloración del hongo no disminuye durante los discontinuos repetidos y que el hongo es capaz de eliminar 86-89% del colorante a pesar de la baja actividad enzimática detectada. Los resultados también muestran que el mecanismo de biodegradación es responsable del proceso de decoloración es la enzima lacasa, además del fenómeno de adsorción que ocurre en la biomasa fúngica.

Finalmente, se realiza la combinación del proceso biológico y físico-químico con la finalidad de tratar un colorante de la industria textil, y se concluye que se necesitan más estudios para explorar la eficacia de los procesos combinados.



## TABLE OF CONTENTS

	<b>ABSTRACT</b>	i
	<b>RÉSUMÉ</b>	iii
	<b>RESUMEN</b>	v
<b>Chapter 1</b>	<b>GENERAL INTRODUCTION, OBJECTIVES AND THESIS OUTLINE</b>	<b>1</b>
<b>1.1</b>	<b>General introduction</b>	<b>2</b>
<b>1.2</b>	<b>Objectives</b>	<b>3</b>
<b>1.3</b>	<b>Thesis outline</b>	<b>4</b>
<b>Chapter 2.</b>	<b>LITTERATURE REVIEW</b>	<b>7</b>
<b>2.1</b>	<b>Water Pollution and water pollutants</b>	<b>8</b>
2.1.1	Heavy metals	11
2.1.2	Textile and tannery dyes	11
2.1.3	Pharmaceutical products	14
<b>2.2.</b>	<b>Wastewater treatment technologies</b>	<b>15</b>
2.2.1	Generalities	15
2.2.2	Techniques for the treatment of the considered pollutants	16
<b>2.3.</b>	<b>Adsorption on activated carbon</b>	<b>17</b>
2.3.1	Generalities	18
2.3.2	Precursors and preparation process of activated carbons	22
2.3.3	Modeling of Adsorption	24
2.3.4	Life Cycle Assessment of the prepared activated carbon	31
<b>2.4.</b>	<b>Biological treatment</b>	<b>32</b>
2.4.1	Aerobic digestion	32
2.4.2	Anaerobic digestion	33
<b>Chapter 3.</b>	<b>GENERAL MATERIALS AND METHODS</b>	<b>51</b>
<b>3.1.</b>	<b>Preparation of activated carbons</b>	<b>52</b>
3.1.1	Raw Material	52
3.1.2	Preparation of activated carbons	53
3.1.3	Characterization of the prepared adsorbents	54
3.1.4	Adsorption on column	56
<b>3.2.</b>	<b>Adsorbates</b>	<b>58</b>
3.2.1.	Metallic species	58
3.2.2.	Dyes	58
3.2.3.	Pharmaceuticals products	59
3.2.4.	Adsorption studies	61

<b>3.3.</b>	<b>Biological treatment</b>	<b>61</b>
3.3.1.	Microorganisms	61
3.3.2.	Culture methods	62
3.3.3.	Media	63
3.3.4.	Reactor	63
<b>3.4.</b>	<b>Analytical methods</b>	<b>65</b>
3.4.1	pH measurements	65
3.4.2	Conductivity	65
3.4.3	Turbidity	65
3.4.4	Metals contents	65
3.4.5	Organic matter	65
3.4.6	Dry cell weight	66
3.4.7	Glucose	67
3.4.8	Laccase activity	67
3.4.9	Toxicity	67
3.4.10	Dye concentrations	67
3.4.11	Statistical analyses	67
<hr/>		
<b>Chapter 4.</b>	<b>RESULTS AND DISCUSSIONS</b>	<b>71</b>
<b>4.1.</b>	<b>Preparation, characterization and environmental impact</b>	<b>73</b>
4.1.1	Preparation of activated carbon from Tunisian olive-waste cakes and its application for adsorption of heavy metal ions	75
4.1.2.	Environmental impact associated with activated carbon preparation from olive-waste cake via life cycle assessment	101
<b>4.2.</b>	<b>Modeling of adsorption</b>	<b>121</b>
4.2.1.	Equilibrium, thermodynamic and kinetic studies on adsorption of commercial dye by activated carbon derived from olive-waste cakes	122
4.2.2.	Modeling of adsorption isotherms and kinetics of a tannery dye onto an activated carbon prepared from an agricultural by-product	149
4.2.3.	Removal of pharmaceutical compounds by activated carbon prepared from agricultural by-product	175
<b>4.3.</b>	<b>Biological treatment</b>	<b>203</b>
4.3.1	Decolorization of a tannery dye: from fungal screening to bioreactor application	205

---

---

<b>Chapter 5.</b>	<b>GENERAL CONCLUSIONS AND SUGGESTIONS FOR FURTHER RESEARCH</b>	<b>223</b>
<b>5.1.</b>	<b>General conclusions</b>	<b>224</b>
<b>5.2.</b>	<b>Suggestions for further research</b>	<b>226</b>
<hr/>		
<b>ANNEXES</b>		<b>229</b>
<b>Annex 1</b>	<b>Metal complex dye degradation by the fungus <i>Trametes versicolor</i> followed by metal adsorption with a low cost activated carbon derived from Tunisian olive-waste cakes</b>	<b>230</b>
<b>Annex 2</b>	<b>Technical specifications of the textile dye Lanaset grey G</b>	<b>241</b>
<b>Annex 3</b>	<b>Technical specifications of the tannery dye Black dycem TTO</b>	<b>247</b>

---







# **Chapter 1:**

## **General introduction, objectives and thesis outline**

---

In this chapter, a brief introduction about the water contaminants and the reasons behind the selection of the two processes adopted in this thesis, the adsorption process on a low-cost activated carbon based precursor and the biological treatment using fungi, are explained. The main objective and the specific ones are listed and finally the thesis outline is presented.

## **1.1. GENERAL INTRODUCTION**

Water is a limited natural resource and fundamental for life and health (UNWWDR, 2002). With the growth of mankind, society, science and technology the world is reaching to new high horizons but the cost which is being paid or will be paid in the near future is surely going to be too high. Among the consequences of this rapid growth, the environmental disorder with a big pollution problem has been translated to a critical aspect (Grover, 2006). Water accumulates different type of compounds during its use becoming wastewater and unsuitable to be reused. Water pollution with toxic compounds is one of major concerns for human health as well as for the environmental quality. Toxic substances can be due to industrial pollution, urban pollution or agricultural pollution through the application of fertilizers and pesticides. Toxic pollution can have an immediate (acute) or a chronic (long-term toxicity) impact on the environment.

The pollutants frequently found are heavy metals (cadmium, chromium, copper, mercury, lead ...), organic substances (solvents, hydrocarbons, dyes...) and / or chemical products (pharmaceutical products, personal care products...)

Discharging different kinds of wastewater and polluted waters such as domestic, industrial and agricultural wastewaters into environment, especially to surface water, produce effluents which are often contaminated with harmful/poisonous substances. There are various methods for the removal of these substances. These broadly fall into three categories: Physical, Chemical and Biological. Any of these treatment processes have their own advantages and disadvantages. The major disadvantage of physico-chemical methods has been largely due to the high cost, low efficiency, limited versatility, interference by other wastewater constituents and the handling of the waste generated. Biological treatment is method in which the removal of organic compounds is brought about by biological activity (Metcalf and Eddy, 1991). However, the main disadvantageous of the biological treatment is the low removal yields.

With regard to increasing effluent discharge standards to the environment, high considerations should be taken when selecting proper treatment processes. Considering economical aspects are important, too. In addition, employing environmentally-friendly methods for treatment is emphasized much more these days. Application of some waste



products that could help in this regard, in addition to reuse of these waste materials, can be an advantage.

## **REFERENCES**

- Grover V.I., 2006. Water global commen and global problems. Science publishers, Enfield, USA.
- Metcalf and Eddy, 1991. Wastewater engineering. Treatment, disposal and reuse. MC.Graw-Hill, Inc 3<sup>nd</sup> ed, New York, USA.
- UNWWDR (United Nations World Water Development Report), 2002. Water for People Water for Life. UNESCO, Paris, France.

## **1.2. OBJECTIVES**

In a view of the above facts, the present work is aimed to the use of two friendly technologies: adsorption process on an activated carbon prepared from an agricultural by-product and biological treatment with white-rot fungi for the removal of some pollutants i.e textile dye, tannery dye, heavy metal and pharmaceutical products. To achieve this general objective, the work comprised in the thesis has been organized according to fit the following specific objectives:

a) Specific objectives regarding the adsorption process using the activated carbon prepared from olive-waste cakes:

- To optimize the preparation method of the activated carbon by analysing the effect of the main process parameters including acid concentration, impregnation ratio, and temperature of pyrolysis step on the performances of the prepared activated carbons.
- To quantify the environmental impacts and critical life stages associated with the AC production process by using LCA methodology.
- To evaluate the adsorption potential of the adsorbent prepared from Tunisian olive-waste cakes for metal complex dyes, particularly Lanaset Grey G
- To study the removal of pharmaceuticals from aqueous media by activated carbons, considering the kinetic and thermodynamic aspects of the retention process and single and mixture drug solutions.

- To investigate the efficiency of the prepared AC towards the Black Dycem TTO tannery dye and a real effluent dye solution from an industrial bath.

b) Specific objectives regarding biological treatment:

- To assess the potential of three common WRF (*Trametes versicolor*, *Ganoderma lucidum* and *Irpex lacteus*) to decolourize a commercial tannery dye, Black Dycem TTO in Petri dishes and liquid media.
- To assess the potential of the best strain to remove the tannery dye in single and repeated batches in an air-pulsed bioreactor and to elucidate the enzymatic system involved in the degradation process

### **1.3. THESIS OUTLINE**

The thesis, presented as a compendium of publications, is divided in the following chapters: General Introduction Objectives and Thesis outline, Literature review, Materials and General Methods, Results and Discussion and finally Conclusions and Annexes.

A brief introduction of the context of the dissertation, the main and specific objectives and the thesis outline are presented in the chapter 1.

The literature review, presented in chapter 2, highlights those aspects which are more significant for the present experimental work understanding. This chapter is devised in two parts: the first part is regarding the activated carbon: definition, precursors and procedures used for the preparation of activated carbon, adsorption process and a brief introduction to the Life Cycle Assessment (LCA) as a tool for quantitative evaluation of environmental impact of the activated carbon preparation. The second part is devoted to the biological treatment, mainly treatment using the white-rot fungus *Trametes versicolor*.

Materials and general methods implemented to carry out this work are the focus of the chapter 3. This chapter is included into the thesis in order to extent and detail the experimental section of publications, thus facilitating repeatability and further research in the application field.

The fourth chapter is devoted to the presentation of experimental results and their discussion; it compromises the following six publications articulated into three topics:

**Topic 1:** Preparation, characterization and environmental impact

Article 1: **Preparation of activated carbon from Tunisian olive-waste cakes and its application for adsorption of heavy metal ions**

*Journal of Hazardous Materials, 162 (2009) 1522–1529*

Article 2: **Environmental impact associated with activated carbon preparation from olive-waste cake via life cycle assessment**

*Submitted to a peer review journal*

**Topic 2:** Modeling of adsorption

Article 3: **Equilibrium, thermodynamic and kinetic studies on adsorption of commercial dye by activated carbon derived from olive-waste cakes**

*Chemical Engineering Journal, 165 (2010) 457–464*

Article 4: **Modeling of adsorption isotherms and kinetics of a tannery dye onto an activated carbon prepared from an agricultural by-product**

*Fuel Processing Technology, 106 (2013) 408–415*

Article 5: **Removal of pharmaceutical compounds by activated carbon prepared from agricultural by-product**

*Chemical Engineering Journal, 211-212 (2012) 310–317*

**Topic 3:** Biological treatment

Article 6: **Decolourization of a tannery dye: from fungal screening to bioreactor application**

*Biochemical Engineering Journal, 56 (2011) 184–189*

The conclusion and future work chapter summarizes the general conclusions drawn from the present work and presents suggestions for future research.

Finally the Annexed information presented some unpublished results and provides some useful supporting information. In the annexed information Annex 1, the results related to a tentative of combination of the two studied processes: the biological treatment and the adsorption on activated carbon to remove a metal complex dye are presented.

Annexes 2 and 3 presented the technical specifications of the dyes Lanaset grey G and Black dycem TTO, respectively.

## **Chapter 2:**

### Literature review

---

This chapter is divided in two parts: the first part is regarding the activated carbon: definition, precursors and procedures used for the preparation of activated carbon, adsorption process and a brief introduction to the Life Cycle Assessment (LCA) as a tool for quantitative evaluation of environmental impact of the adsorbent preparation. The second part makes reference to the biological treatment, mainly treatment using the white-rot fungus *Trametes versicolor*.

Environmental pollution is the unfavorable alteration of our surrounding. It is the introduction of contaminants into the environment that causes harm or discomfort to humans or other living organisms, or that damage environment. The word "pollution" has been taken from the Latin word "pollutionem" meaning to make dirty. Pollution can be in the form of chemical substances or energies, but are considered contaminants when in excess of natural levels. It is mainly linked with human activities, discharge of domestic, industrial and agricultural wastes, application of pesticides by farmers, leaks of radioactive materials, gas emissions into the atmosphere etc (Goel, 2006).

For decades back, water was considered to be pure and unpolluted if it was odorless, colorless and tasteless. But now the whole concept of water pollution has changed. Even if the water is clear, it may be polluted, it may contain dissolved impurities like toxic metals, organic pollutants, radioactive nuclides, emerging contaminants etc (Davis, 2008).

### **2.1. Water Pollution and water pollutants**

Water pollution is any undesirable change in the physical, chemical, or biological characteristics of water that can harmfully affect the health, survival, or activities of human or other living organisms. Two types of water pollutants exist: point source and non-point source (Agrawal, 2009). Point sources of pollution occur when harmful substances are emitted directly into a body of water. They include factories, wastewater treatment facilities, septic systems, and other sources that are clearly discharging pollutants into water sources. A non-point source delivers pollutants indirectly through environmental changes. An example of this type of water pollution is when fertilizer from a field is carried into a stream by rain, in the form of run-off which in turn affects aquatic life. Non point sources are much more difficult to control. Pollution arising from nonpoint sources accounts for a majority of the contaminants in streams and lake (EPA, 2006).

The major sources of water pollution can be classified as municipal, industrial and agricultural. Municipal water pollution consists of wastewater from homes and commercial establishments. The characteristics of industrial wastewaters depend on the type of industry and the manufacturing process in question (Haas and Vamos, 1995). The impact of industrial discharges depends not only on their collective characteristics,

such as biochemical oxygen demand and the amount of suspended solids, but also on their content of specific inorganic compounds.

The most common water pollutants are nutrients, organic matter, heavy metals, microbial contaminants, toxic organic compounds (oil, pesticides, some plastics, and other industrial chemicals), salts, acids, sediments and suspended solids, and high temperature (Revenga and Mock, 2001). Table 2.1 presents the important contaminants in wastewater and their reason of importance. These components are either in solution or as particulate matter and can have (bio-) cumulative, persistent and synergetic characteristics affecting ecosystem health and function, food production, human health and wellbeing (Corcoran et al., 2010).

**Table 2.1.** Important contaminants in wastewater (Source adapted from Metcalf and Eddy, 1991)

Contaminants	Reason for importance
Sediments and suspended solids (SS)	Can interfere with fish spawning because they can cover gravel beds and block light penetration making food harder to find. Can also damage gill structures directly, smothering aquatic insects and fish. Organic sediments can deplete the water of oxygen creating anaerobic conditions and may create unsightly conditions and cause unpleasant odors.
Biodegradable organics	Principally made up of proteins, carbohydrates and fats. They are commonly measured in terms of BOD and COD. If discharged into inland rivers, streams or lakes, their biological stabilization can deplete natural oxygen resources and cause septic conditions that are detrimental to aquatic species.
Pathogens and microbial contaminants	Spreads infectious diseases through contaminated drinking water supplies.
Priority pollutants, including organic and inorganic compounds such as calcium, sodium and sulfate.	May be highly toxic, carcinogenic, or mutagenic.
Refractory organics	That tend to resist conventional waste-water treatment include surfactants, phenols and agricultural pesticides
Heavy metals	Usually derived from industrial activities, can harm aquatic organisms or bioaccumulate in the food chain, even if the metal concentration in water is relatively low.
Dissolved inorganic constituents such as calcium, sodium and sulfate.	They are often initially added to domestic water supplies, and may have to be removed as they present a negative effect when present in excessive amounts.
Nutrients	Over-stimulates growth of algae (eutrophication) which then decomposes, robbing water of oxygen and harming aquatic life. High levels of nitrate in drinking water lead to illness in humans.
High temperature	Changes in oxygen levels and decomposition rate of organic matter in the water column. May shift the species composition of the receiving water body.
Emerging contaminants including pharmaceuticals and personal care products	They are found at trace levels but they present an adverse effect and can affect the health of human and animal species.



Mentioned below are the pollutants that have been considered in this study.

### **2.1.1. Heavy metals**

Heavy metals are considered to be one of the most hazardous water contaminants. They are major pollutants in marine, ground, industrial and even treated wastewaters (Metcalf and Eddy, 1991). Unlike organic pollutants, metals are non-biodegradable and to accumulate in living organisms and many heavy metal ions are known to be toxic or carcinogenic (Drinan, 2001). The presence of heavy metals in drinking water can be hazardous to consumers; these metals can damage nerves, liver and bones and block functional groups of vital enzymes (Ewan and Pamphlet, 1996). Metal ions in water can occur naturally from leaching of ore deposits and from anthropogenic sources, which mainly include industrial effluents and solid waste disposal. Due to rapid development of industrial activities in recent years, the levels of heavy metals in water system have substantially increased over time (Nouri et al., 2006). Certain metals are regulated because they are toxic to operation. Regulated metals include arsenic, barium, cadmium, chromium, copper, lead, mercury, nickel, selenium, silver and zinc (Edwards, 1995).

Copper is a very common metal, which is widely used in electroplate, light industry, mechanical manufacturing industry and architecture. Additionally copper is an indispensable micronutrient to humans and other life form. Conversely, exposure to high levels of copper can cause a toxic leath effect to microorganisms (Trevors and Cotter, 1990).

Faced with more and more stringent regulations, nowadays heavy metals are the environmental priority pollutants and are becoming one of the most serious problems. So these toxic heavy metals should be removed from wastewater to protect the people and the environment (Fu and Wang, 2011).

### **2.1.2. Textile and tannery dyes**

Among industrial wastewater, dye wastewater from textile, tannery and dyestuff industries is one of the most difficult to treat. This is because dyes usually have a synthetic origin and complex aromatic molecular structures which make them stable and more difficult to be biodegraded (Zollinger, 1991). The presence of very low concentrations of dyes in effluent can be highly visible and undesirable on aesthetic grounds. Their presence disturbs aquatic communities present in ecosystem by

obstructing light penetration and oxygen transfer into water bodies. It is reported that there are over 100 000 commercially available dyes with a production over  $7 \times 10^5$  metric tons per year (Christie, 2007). It has been estimated that about 9 % (or 40,000 tons) of the total amount (450, 000 tons) of dyestuffs produced in the world are discharged in textiles wastewaters (O'Neil et al., 1999).

Dye molecules comprise of two key components: the chromophores, responsible for producing the colour, and the auxochromes, which can not only supplement the chromophore but also render the molecule soluble in water and give enhanced affinity towards the fiber type (Christie, 2001). Dyes exhibit considerable structural diversity and are classified in several ways. These can be classified both by their chemical structure and their application over the substrate. Dyes may also be classified on the basis of their solubility: soluble dye which include acid, mordant, metal complex, direct, basic, and reactive dyes; and insoluble dyes including azoic, sulfur, vat and disperse dyes (Christie, 2001). According to Fu and Viraraghavan (2001), dyes are classified as follows anionic dyes which include direct, acid and reactive dyes, cationic dyes which include the basic dyes, and nonionic dyes which include the disperse dyes. Table 2.2 summarized the application classes of dyes and their characteristics (Hunger, 2003). Examples of structure of basic and acid dyes are given in Figure 2.1.

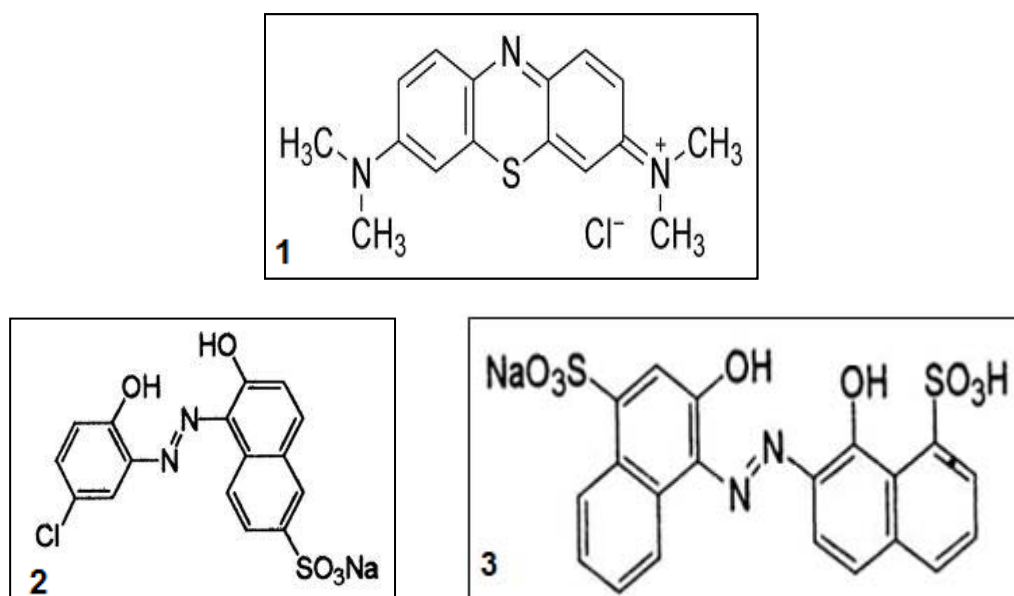


**Figure 2.1.** Example of molecular structure of a basic dye (methylene blue) (1) and acid dyes: acid violet (2) and acid blue (3)

**Table 2.1.** Color index application classes (Hunger, 2003)

<b>Characteristics</b>	
<b>Acid dyes</b>	Highly water-soluble due to the presence of sulphonic acid groups. Form ionic interactions between the protonated functionalities of the fibers ( $-\text{NH}_3^+$ ) and the negative charge of the dyes. Also Van-der-Waals, dipolar and hydrogen bonds are formed. The most common structures are azo, anthraquinone and triarylmethane.
<b>Basic dyes</b>	Basic dyes work very well on acrylics due to the strong ionic interaction between dye functional groups such as $-\text{NR}_3^+$ or $=\text{NR}_2^+$ and the negative charges in the copolymer. The most common structures are azo, diarylmethane, triarylmethane and anthraquinone.
<b>Direct dyes</b>	Their flat shape and length enables them to bind along-side cellulose fibers and maximize the Van-der-Waals, dipole and hydrogen bonds. Only 30% of the 1600 structures are still in production due to their lack of fastness during washing. The most common structures are almost always sulphonated azo dyes.
<b>Disperse dyes</b>	Non-ionic structure, with polar functionality like $-\text{NO}_2$ and $-\text{CN}$ that improve water solubility, Van-der-Waals forces, dipole forces and the color. They are usually used with polyester. The most common structures are azo, nitro, anthraquinones or metal complex azo.
<b>Reactive dyes</b>	Form covalent bonds with $-\text{OH}$ , $-\text{NH}$ or $-\text{SH}$ groups in cotton, wool, silk and nylon. The problem of colored effluents associated to the use of these dyes is due to the hydrolysis of the reactive groups that occurs during the dyeing process. The most common structures are azo, metal complex azo, anthraquinone and phthalocyanine.
<b>Solvent dyes</b>	Non-ionic dyes that are used for dyeing substrates in which they can dissolve as plastics, varnish, ink and waxes. They are not often used for textile processing. The most common structures are diazo compounds that undergo some molecular rearrangement, triarylmethane, anthraquinone and phthalocyanine.
<b>Sulfur dyes</b>	Sulphur dyes are water-insoluble and complex polymeric aromatics, representing about 15% of the global dye production. Dyeing with sulphur dyes (mainly on cellulose fibers) involves reduction and oxidation processes, comparable to vat dyeing.
<b>Vat dyes</b>	Vat dyes are insoluble in water, but may become solubilized by alkali reduction (sodium dithionite in the presence of sodium hydroxide). The produced <i>leuco</i> form is absorbed by the cellulose (Van-der-Waals forces) and can be oxidized back, usually with hydrogen peroxide, to its insoluble form. The most common structures are anthraquinones or indigoids.
<b>Other dye classes</b>	Food dyes are not used as textile dyes. Natural dyes use in textile processing operations is very limited. Fluorescent brighteners mask the yellowish tint of natural fibers by absorbing ultraviolet light and weakly emitting blue light. Not listed in a separate class in the Color Index, many metal complex dyes can be found. These are strong complex of one metal atom (generally chromium, copper, cobalt or nickel) and or two dye molecules. The metal complex dyes are usually azo compounds.

**2.1.3. Pharmaceutical products**

In recent years it has been recognized that among the so-called emerging contaminants, pharmaceuticals and personal care products, present in waters are problematic compounds in regard to their disposal (EPA, 2006). Drugs often have similar physico-chemical behavior as other harmful xenobiotics that are accumulated or induce adverse effects in terrestrial or aquatic organisms (Hernando et al., 2006). The occurrence of several pharmaceutical compounds have been reported in sewage treatment plant effluents as well as in surface waters in Germany (Ternes, 1998; Putschew et al., 2000), the Netherlands (Belfroid et al., 1999), Switzerland (Soulet et al., 2002), Canada (Ternes et al., 1999; Miao et al., 2004), Brazil (Ternes et al., 1999), Italy (Castiglioni et al. 2004), Spain (Brceló and Petrovic, 2008), and the United States (Kolpin et al., 2002). The detected compounds included antibiotics, anticonvulsants, painkillers, cytostatic drugs, hormones, lipid regulators, beta-blockers, antihistamines, and X-ray contrast media. The concentrations of these pharmaceuticals were in the range of ng/L to mg/L in sewage treatment plant effluents and surface water. In addition, a number of polar pharmaceutical compounds and metabolites, such as diclofenac, carbamazepine, sulfamethoxazole, and amidotrizoic acid, have been detected in groundwater samples at concentrations up to 1 mg/L (Sacher et al., 2001; Clara et al., 2004). There are several possible sources and routes for the occurrence of pharmaceutical compounds in the aquatic environment (Figure 2.2). For human pharmaceuticals, non-prescription drugs and some prescription drugs are consumed in households, and other prescription drugs are consumed in healthcare facilities such as hospitals and clinics. These drugs are partially metabolized and excreted in the urine and feces and go into a wastewater collection system (Heberer, 2002; Jones et al., 2005). Some unused, surplus, or expired drugs may be disposed according to special waste management. Wastewater from the hospitals may be treated separately or mixed with municipal wastewater and then treated at sewage treatment plants. Some of the pharmaceuticals and (human) metabolites in wastewater are degraded completely or partially, giving rise to a mixture of parent compounds and a variety of microbial metabolites (Ternes, 1998; Miao et al., 2002; Soulet et al., 2002; Jones et al., 2005). Some pharmaceuticals such as ibuprofen and bezafibrate are relatively biodegradable, while others such as carbamazepine and diazepam are practically non-biodegradable (Gros et al., 2010).

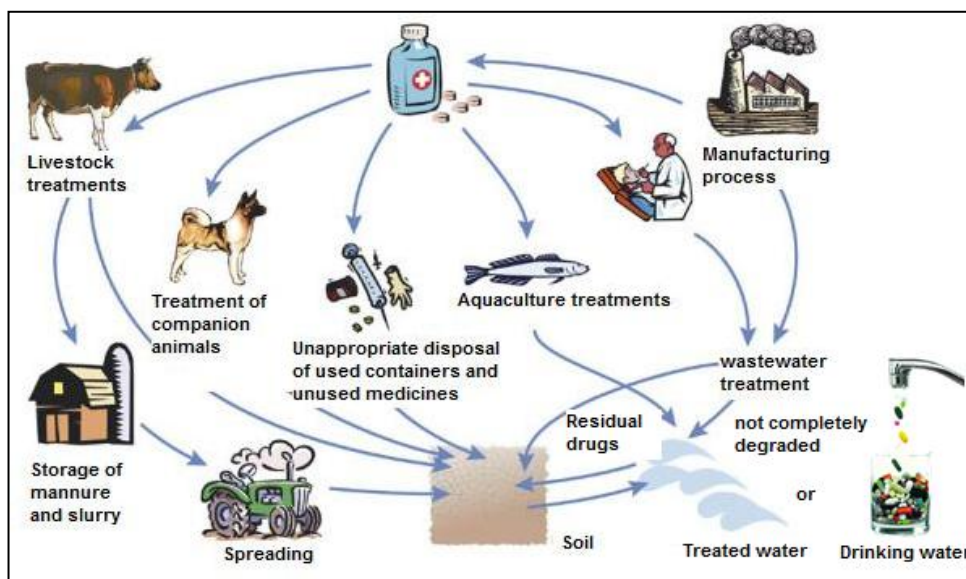


**Figure 2.2.** Sources and fate of pharmaceutical compounds in the environment

## 2.2. Wastewater treatment technologies

### 2.2.1. Generalities

Technologies for treating wastewaters can be divided into three categories: chemical methods, physical methods, and biological methods. Chemical methods rely upon the chemical interactions of the contaminants we wish to remove from water and the application of chemicals that either aid in the separation of contaminants from water or assist in the destruction or neutralization of harmful effects associated with contaminants (Cheremisinoff, 2002). Physical treatment methods include sedimentation, flotation, filtering, stripping, ion exchange, adsorption, and other processes that accomplish removal of dissolved and undissolved substances without necessarily changing their chemical structures. Biological methods are those that involve living organisms using organic, or in some instances, inorganic, substances for food, completely changing their chemical and physical characteristics (Woodard, 2001).

Each technique provides a different and unique approach and perhaps provides certain advantages over others for particle situation. All three of these technology groups can be combined in water treatment, or they may be used in selected combinations depending upon the objectives of water treatment. Among each of the general technology classes, there is a range of both hardware and individual technologies that one may select from. The selection of the optimum combinations depends on factors such as:

1. How depurated the final water effluent from our plant must be;
2. The quantities and nature of the influent water we need to treat;
3. The physical and chemical properties of the pollutants that we need to remove or render neutral in the effluent water;
4. The physical, chemical and thermodynamic properties of the solid wastes generated from treating water; and
5. The cost of treating water, including the cost of treating, processing and disposal of the solid wastes.

### **2.2.2. Techniques for the treatment of the considered pollutants**

#### **2.2.2.1. Methods to remove metals**

Heavy metals are getting importance for their non-degradable nature and often accumulate through tropic level causing a deleterious biological effect (Jain, 1978). Anthropogenic activities like mining, ultimate disposal of treated and untreated waste effluents containing toxic metals as well as metal chelates from different industries, e.g. tannery, steel plants, battery industries, thermal power plants etc. and also the indiscriminate use of heavy metal containing fertilizers and pesticides in agriculture resulted in deterioration of water quality rendering serious environmental problems posing threat on human beings and sustaining aquatic biodiversity (Lantzy and Mackenzie, 1979; Nriagu, 1979; Ross, 1994). The most important and currently used methods for removing heavy metals from effluents are adsorption, ion exchange, membrane techniques, precipitation, electrolytic removal process (Fu and Wang, 2011). And phytoremeddiation (Raskin et al., 1997) Nevertheless, many of these approaches can be marginally cost-effective or difficult to implement in developing countries. Therefore, the need exists for a treatment strategy that is simple, robust, and that addresses local resources and constraints (Mier et al., 2001). In the last few years, adsorption has been shown to be an economically feasible alternative method for removing trace metals from wastewater and water supplies (Allen and Brown, 1995). The adsorption process offers flexibility in design and operation and in many cases will produce high-quality treated effluent. In addition, because adsorption is sometimes reversible, adsorbents can be regenerated by suitable desorption process (Fu and Wang, 2011).

#### **2.2.2.2. Methods to remove organic pollutants**

Wastewater often contains a mixture of organic and inorganic compounds, in addition to solid or soluble material, and because of this diverse feature no universal strategy of remediation is feasible. As to the treatment of effluents polluted with organic compounds, biological oxidation is the cheapest process, but the presence of toxic or biorefractory molecules may hinder this approach (Panizza and Cerisola, 2009). For this reason, a diverse range of physico-chemical methods as filtration, coagulation, adsorption, flocculation, chemical oxidation with use of chlorine, ozone, hydrogen peroxide, and advanced oxidation processes (AOPs) as Fenton's reaction, ozone/UV etc. are currently used to treat industrial effluents, depending on the specific needs. However, these methods are either economically unfavorable or technically complicated, which make them difficult to be used in practice. For example, filtration is not always sufficient to achieve the discharge limits; adsorption using commercial adsorbents is expensive, coagulation and flotation generates large amounts of sludge; chemical oxidation processes requires expansive chemical reacts and need transportation and storage of hazardous chemicals; and advanced oxidation processes usually require high investment costs (Panizza and Cerisola, 2009).

Considering all the mentioned above, adsorption on a low cost activated carbon prepared from an agricultural waste, as a general treatment, and biological process using white rot fungi, as a specific treatment, were considered in this study for the treatment of the mentioned pollutants.

#### **2.3. Adsorption on activated carbon**

Adsorption process has been a prominent method of treating aqueous effluent in industrial processes for a variety of separation and purification purposes. Besides, adsorption on activated carbon is very widely used for achieving high water purification (Dabrowski et al, 2005; Fierro et al., 2008; Pan et al., 2008). Activated carbon adsorption has been cited by the US Environmental Protection Agency as one of the best available control technologies (Derbyshire et al., 2001). However, although activated carbon is a preferred sorbent, its widespread use is restricted due to its cost. Commercially available activated carbons are still expensive due to the use of non-renewable and relatively high-cost starting material such as coal, which is unjustified in

pollution control applications. In order to decrease the cost of treatment and expand its use in wastewater treatment, attempts have been made to find low-cost adsorbents, namely by using waste materials for that purpose (Dias et al., 2007).

### **2.3.1. Generalities**

#### **2.3.1.1. Definition of Activated Carbon**

The most concise definition of an activated carbon, which includes a wide range of amorphous-based materials, is “a material prepared to exhibit a high degree of porosity and an extended inter-particulate surface area” (Bansal et al., 1988).

Activated carbons (AC) are known as very effective adsorbents due to their highly developed porosity, large surface area, variable characteristics of surface chemistry, and high degree of surface (Dias et al., 2007). These unique characteristics make AC very versatile materials, which have been studied not only as adsorbents, but also used as catalysts and catalyst supports (Derbyshire et al., 2001). It can be produced from carbonaceous material in order to provide adsorptive properties.

#### **2.3.1.2. Porous structure and surface area**

An understanding of the molecular and crystalline structure of activated carbon is necessary to discuss the surface chemistry of this material. The basic structural unit of activated carbon is closely approximated by the structure of pure graphite (Figure 2.3). The graphite crystal is composed of layers of fused hexagons held by weak Van der Waals forces. The layers are held by carbon–carbon bonds. Activated carbon is a disorganized form of graphite, due to impurities and the method of preparation (activation process).



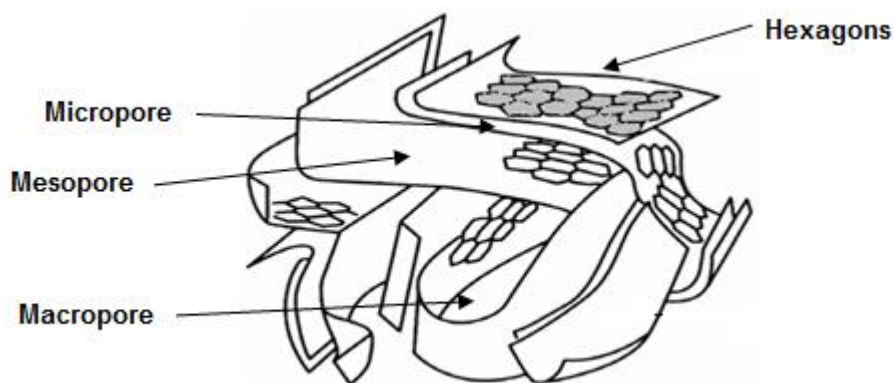


**Figure 2.3.** Schematic structure of an activated carbon

The structure of granular activated carbon is highly heterogeneous and porous. Difference in pore size affects the adsorption capacity for molecules of different shapes and sizes, and thus is one of the criteria by which carbons are selected for a specific application. Porosity is classified by IUPAC into three different groups of pore sizes micro, meso and macropores (Figure 2.4).

Typical ranges are given in Table 2.3 but by special procedures it is possible to prepare activated carbons with even higher porosity, surface area and adsorptive capacity (ASTTE, 2006).

**Table 2.2.** Different types of pores sizes of typical activated carbons (ASTEE, 2006)

	<b>Diameter (nm)</b>	<b>Pore Volume (cm<sup>3</sup>/g)</b>	<b>Surface area (m<sup>2</sup>/g)</b>
<b>Macropores</b>	> 50	0.20- 0.80	0.5-2
<b>Mesopores</b>	2- 50	0.02	20-70
<b>Micropores</b>	< 2	0.10	600-1900

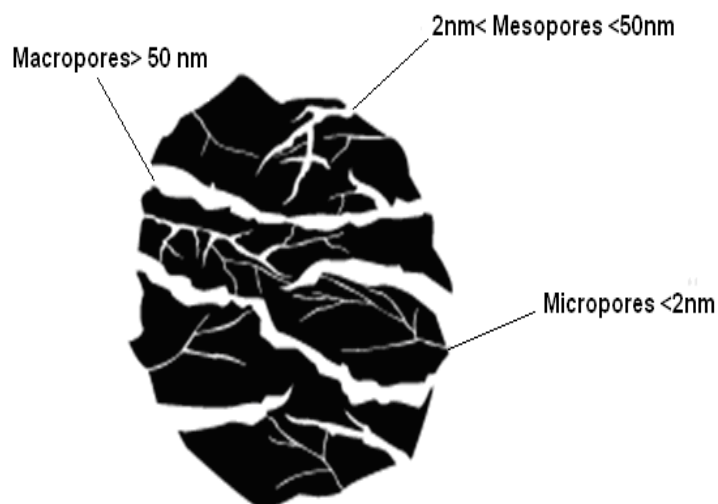


**Figure 2.4.** Schematic activated carbon model

Activated carbons are highly developed internal surface area and porosity, sometimes described as solid sponges. The large surface area results in a high capacity for adsorbing chemicals from gases or liquids. The most widely used commercial active carbons have a specific surface area of the order of  $800\text{-}1500\text{ m}^2\text{ g}^{-1}$ , which is determined typically by nitrogen gas adsorption. Difference in pore size affects the adsorption capacity for molecules of different shapes and sizes, and thus is one of the criteria by which carbons are selected for a specific application.

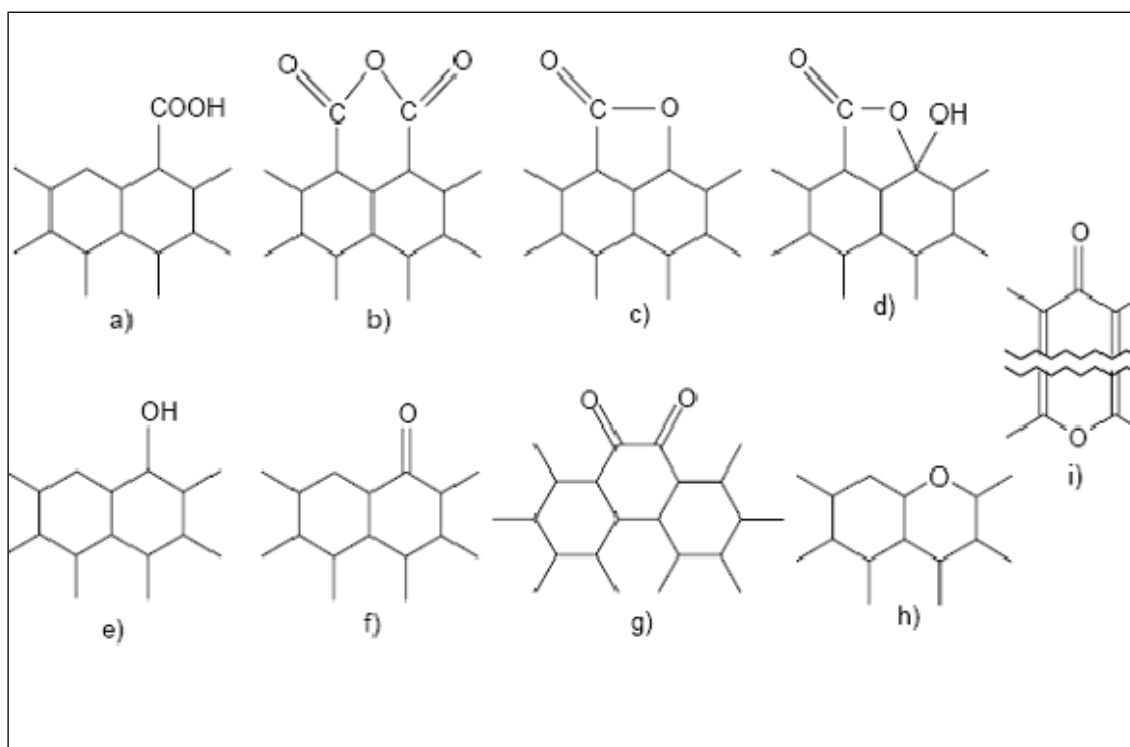
### **Chemical structure**

Although activated carbons are mainly built of graphite layers with a slit-shaped porous structure, the carbonaceous matrix also contains heteroatoms such as oxygen, nitrogen, hydrogen, sulfur or phosphorus. Table 2.4 reports the elemental chemical composition of four activated carbons prepared from different precursors. Those heteroatoms are present in functional groups analogous to well-known groups studied in organic chemistry. They have a key role on the chemical character of carbon surface, acidic or basic, and on its hydrophobicity (Diaz et al., 2005).

**Table 2.3.** Elemental chemical composition of four activated carbons prepared from different precursors

Precursor	C (%)	H (%)	N (%)	S (%)	O (%)	Ash	References
Apricot stones	89.5	2.4	0.90	0.80	6.4	1.96	Gergova et al., 1993
Cherry stones	84.0	2.2	1.0	0.41	12.5	4.19	Gergova et al., 1993
Grapes stones	84.7	1.3	1.60	0.25	12.1	13.12	Gergova et al., 1993
Uruguayan eucalyptus	47.2	6	0.1	-	46.7	0.30	Tancerdi et al., 1996

Previous works were performed by Boehm and Donnet in the 60s for the identification of surface functions. In a more recent reference, Boehm (1994) has identified several groups of acidic character on the surface of activated carbon (Figure 2.5): (a) carboxylic acid, (b) carboxylic anhydride, (c) lactone, (d) lactol, (e) hydroxyl, (f) carbonyl, (g) quinone (h) etheral (xanthene) and (i) pyrone.

**Figure 2.5.** Acid functional groups of the surface of activated carbon

The functional groups of basic character were identified as Chromenes and Pyrones (Julien et al., 1994) (Figure 2.6).

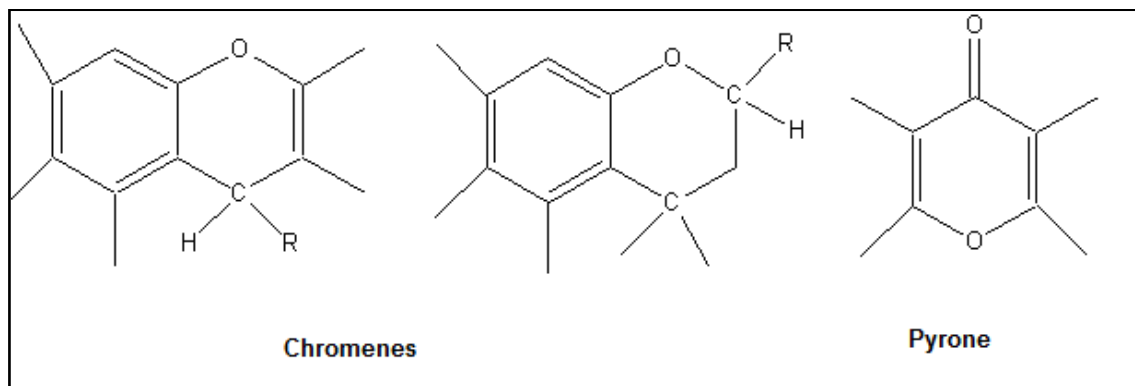


Figure 2.6. Basic functional groups of activated carbon

### 2.3.2. Precursors and preparation process of activated carbons

The characteristics of activated carbon depend on the physical and chemical properties of the precursor as well as on the activation method (Gomez-Serrano et al., 2005).

#### 2.3.2.1. Process of preparation of activated carbon

Activated carbons can be produced by physical or chemical activation (Bansal and Goyal, 2005).

**a) Physical activation process** is usually carried out in two stages. The first stage is the carbonization stage followed by an activation stage (Haimour and Emeish, 2006). The step of carbonization is carried out in an inert atmosphere (pyrolysis) for 5-6 hours at a temperature ranging from 400 to 850 °C and can sometimes reach 1000 °C. The objective of this step is to remove organic compounds (CO, H<sub>2</sub>, CH<sub>4</sub> and other hydrocarbons) to produce a solid residue with high carbon content. Thus, an initial porosity corresponding to a specific surface area of around 5-10 m<sup>2</sup> g<sup>-1</sup> is created. Finally, to further develop the porosity, an activation step at 800-1000 °C is performed in the presence of steam, carbon dioxide, air or their mixtures (Diao et al., 2002, Ioannidou and Zabaniotou, 2007) for 24 to 72 hours. As a consequence of the activation

step, a certain mass of the carbonized material is lost due to the formation of gaseous carbon oxides (Ould-Idriss et al., 2011).

#### **b) Chemical activation process**

This process involve only single step of carbonization process. The activated agent must be used before carbonization takes place. The most activated agents used are zinc chloride, sulphuric acid, potassium hydroxide and phosphoric acid. However, phosphoric acid is preferred because of the problems of corrosion, inefficient chemical recovery, and environmental disadvantages associated with zinc chloride (Gomez Serrano et al., 2005). The chemical activation process is most popular because only required single heating and the temperature used is usually lower than that of physical activation. But the process can generate secondary environmental pollution due to the use of the chemical (Stavropoulos and Zabaniotou, 2005).

In the chemical activation process the two steps are carried out simultaneously, with the precursor being mixed with chemical activating agents, as dehydrating agents and oxidants at very low temperatures. This agent will increase the surface area and reduce the ash content of final carbonized products: the chemical incorporated to the interior of the precursor particle reacts with the products resulting from the thermal decomposition of the precursor, reducing the evolution of volatile matter and inhibiting the shrinking of the particle; in this way, the conversion of the precursor to carbon is high, and once the chemical is eliminated after the heat treatment, a large amount of porosity is formed (Rodriguez-Reinoso and Molina-Sabio, 1992). Chemical activation offers several advantages since it is carried out in a single step, combining carbonization and activation, performed at lower temperatures and therefore resulting in the development of a better porous structure, although the environmental concerns of using chemical agents for activation could be developed.

The yield and the characteristics of the prepared activated carbon depend on the process of preparation used. Thus, applying the two processes on lignocellulosic materials, Rodriguez- Reinoso and Molina-Sabio (1992) showed that the yield of activated carbon is higher in the case of chemical activation with  $Zn Cl_2$  than when using physical activation with  $CO_2$ . Moreover, Laine and Younes (1992) reported that the physical activation with  $CO_2$  leads to an activated carbon with a porous structure which consists mainly of narrow micropores and macropores, while a broad structure with micropores

and a larger high mesoporosity was obtained in the case of chemical activation with phosphoric acid.

### **2.3.2.2. Activated carbons from solid wastes**

Commercially available activated carbons (AC) are usually derived from natural materials such as wood, coconut shell, lignite or coal, but almost any carbonaceous material may be used as precursor for the preparation of carbon adsorbents (Rozada et al., 2003). Because of its availability and cheapness, coal is the most commonly used precursor for AC production (Carrasco-Marin et al., 1996). Coal is a mixture of carbonaceous materials and mineral matter, resulting from the degradation of plants. The sorption properties of each individual coal are determined by the nature of the origin vegetation and the extent of the physical-chemical changes occurring after deposition (Karaca et al., 2004).

Plentiful agricultural and wood by-products may also offer an inexpensive and renewable additional source of AC. These materials have little or no economic value and often present a disposal problem. Therefore, there is a need to valorise these low cost by-products. So, their conversion into AC would add economic value, help reduce the cost of waste disposal and most importantly provide a potentially inexpensive alternative to the existing commercial activated carbons. A wide variety of carbons have been prepared from agricultural and wood wastes, such as rice husk (Guo et al., 2003, Mohamed, 2004), corn cob (Juang et al., 2002) pinewood (Tseng et al., 2003), sawdust (Malik, 2003), coconut tree sawdust (Kadirvelu et al., 2000, 2003), bamboo-based (Hameed et al., 2007a), rattan sawdust (Hameed et al., 2007b), rubber wood sawdust (Prakash Kumar et al., 2005) coconut husk and oil palm fibre (Tan et al., 2007).

### **2.3.3. Modeling of adsorption**

The term adsorption includes the uptake of gaseous or liquid components of mixture from the external and/or internal surface of porous solid. In chemical engineering, adsorption is called the separation process during which specific components of one phase of a liquid or gas are transferred onto the surface of a solid adsorbent (McCabe et al., 1993).

Adsorption is a well known equilibrium separation process and an effective method for water decontamination applications (Dabrowski, 2001). Adsorption has been found to

be superior to other techniques for water re-use in terms of initial cost, flexibility and simplicity of design, ease of operation and insensitivity to toxic pollutants.

### 2.3.3.1. Types of adsorption

The adsorption at surface or interface is largely as a result of binding forces between atoms, molecules and ions of adsorbate and surface (Robert, 1989). According to the nature of forces involved, therefore, adsorption can conveniently be divided into two types:

**a) Physical adsorption** (or physisorption) no exchange of electrons is observed between the adsorbent and the adsorbate. The adsorbate is held to the surface by physical and non-specific forces type Van der Waals and hydrogen binding and multiple layers may be formed with approximately the same heat of adsorption. The heat of adsorption for physisorption is at most a few kcal mol<sup>-1</sup>. Physical adsorption is a non-specific and a reversible process.

**b) Chemical adsorption** (or chemisorption) involves reaction of transfer and sharing of electrons between the adsorb species and the adsorbent. The resulting chemisorption bond is usually stronger than the derived from the physical adsorption (tens of kcal mol<sup>-1</sup>) and is consequently much stronger and more stable at high temperatures than physisorption. Generally only a single molecular layer can be adsorbed.

### 2.3.3.2 Adsorption Isotherm

When the retention of a solute on solid particles is investigated, the remaining solute concentration of the compound C (mol L<sup>-1</sup> or kg L<sup>-1</sup>) can be compared with the concentration of this compound retained on solid particles Q (mol kg<sup>-1</sup> or kg kg<sup>-1</sup>). The relationship  $Q = f(C)$  is named the “sorption isotherm”. The uniqueness of this relation requires several conditions to be met: (i) the various reaction equilibria of retention/release must have been reached, and (ii) all other physico-chemical parameters are constant. The word “isotherm” was specifically chosen because of the influence of the temperature on sorption reactions; temperature must be kept constant (Cornelissen et al., 1997; Werth and Reinhard, 1997).

The adsorption isotherm of dilute solutions are classified into four main classes, according to the nature of the slope of the initial portion of the curve (isotherm) and thereafter into sub-groups, based on the shapes of the upper part of curve: the main

classes are S-curve, L-curve (Langmuir type), H-curve (high affinity) and C-curve (constant partition) (Figure 2.7).

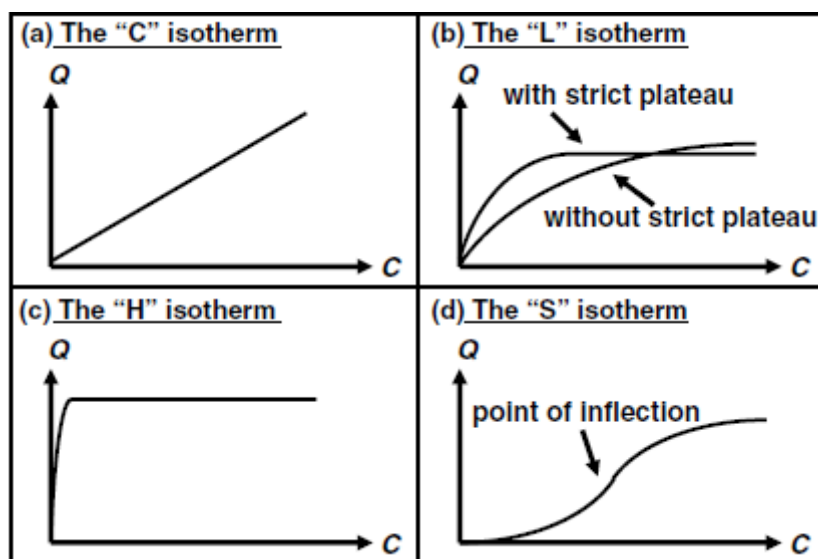


Figure 2.7. The four main types of isotherms

**a) The “C” isotherm**

The curve is a line of zero-origin (Figure 2.7a). It means that the ratio between the concentration of the compound remaining in solution and adsorbed on the solid is the same at any concentration. This ratio is usually named “distribution coefficient” or “partition coefficient”:  $K_d$  or  $K_p$  ( $L\ kg^{-1}$ ). The “C” isotherm is often used as an easy-to-use approximation (for a narrow range of concentration or very low concentrations such as observed for trace pollutants) rather than an accurate description.

But the simplicity of this isotherm must not justify its use without verification; otherwise it could lead to erroneous conclusions. For example, if the solid has a limited quantity of adsorption sites, the isotherm could be nonlinear because of a possible saturation plateau.

**b) The “L” isotherm**

The ratio between the concentration of the compound, remaining in solution and adsorbed on the solid, decreases when the solute concentration increases providing a concave curve (Figure 2.7b). It suggests a progressive saturation of the solid. One usually makes two sub-groups: (i) the curve reaches a strict asymptotic plateau (the solid has a limited sorption capacity), and (ii) the curve does not reach any plateau (the



solid does not show clearly a limited sorption capacity). But it often appears practically difficult to know if an isotherm belongs to the first or to the second sub-group.

**c) The “H” isotherm**

This is only a particular case of the “L” isotherm, where the initial slope is very high (Figure 2.7c). This case was distinguished from the others because the compound exhibits sometimes such a high affinity for the solid that the initial slope cannot be distinguished from infinity, even if it does not make sense from a thermodynamic point of view (Toth, 1995).

**d) The “S” isotherm**

The curve is sigmoidal and thus has got a point of inflection (Figure 2.7d). This type of isotherm is always the result of at least two opposite mechanisms. Non-polar organic compounds are a typical case: they have a low affinity with clays. But as soon as a clay surface is covered by these compounds, other organic molecules are adsorbed more easily (Pignatello, 2000). This phenomenon is called “cooperative adsorption” (Hinz, 2001) and is also observed for surfactants (Smith et al., 1990; Smith and Galan, 1995). The presence of a soluble ligand can also provide a sigmoidal isotherm for metallic species. At low metal concentrations, the adsorption is limited by the presence of the ligand. The ligand must be saturated and then the adsorption occurs normally (Sposito, 1984). The point of inflection illustrates the concentration for which the adsorption overcomes the complexation.

**2.3.3.3 Adsorption mechanism**

To understand the adsorption mechanism many empirical relations have appeared connecting the amount adsorbed with principal variable such as concentration and temperature. Traditional adsorption isotherm models, relating to adsorption equilibrium, such as Freundlich, Langmuir, Temkin and Dubinin-Radushkevich (D-R) isotherm model have been used in the present study. These isotherms are presented by the equations 1, 2, 4 and 5.

### 2.3.3.3.1. The Freundlich model

The model is based on adsorption on the heterogeneous surface and is a widely used isotherm (“L” or “H” isotherms). The first model is empirical (Van Bemmelen, 1888; Freundlich, 1906) and model which is known to be satisfactory for low concentrations is expressed by the equation 1:

$$q_e = K_F C_e^{1/n} \quad (1)$$

where  $q_e$  is the equilibrium sorption concentration of solute per gram of adsorbent ( $\text{mg g}^{-1}$ );  $C_e$  is the equilibrium aqueous concentration of the solute ( $\text{mg L}^{-1}$ );  $K_F$  and  $n$  are Freundlich constants which are related to the adsorption capacity and the intensity of adsorption. A value of  $n$  between 2 and 10 shows good adsorption.

### 2.3.3.3.2. The Langmuir model

The Langmuir adsorption is valid for monolayer adsorption. It is a very common model and is based on reaction hypotheses (Langmuir, 1918). The solid is assumed to have a limited adsorption capacity  $q_{\max}$ . All the adsorption sites (i) are assumed to be identical, (ii) each site retains one molecule of the given compound and (iii) all sites are energetically independent of the adsorbed quantity. The Langmuir isotherms model is described by the equation (2):

$$q_e = \frac{q_{\max} K_L C_e}{1 + K_L C_e} \quad (2)$$

where  $q_{\max}$  and  $K_L$  represented the maximum adsorption capacity and the Langmuir constant, respectively. The essential characteristics of a Langmuir isotherm can be expressed in terms of dimensionless constant separation factor  $R_L$  defined as:

$$R_L = \frac{1}{1 + K_L C_0} \quad (3)$$

where  $C_0$  is the initial concentration.  $R_L$  values less than unity confirm the favorable uptake of the sorbent.

### 2.3.3.3.3. The Temkin model

This isotherm contains a factor that explicitly takes into account of adsorbent-adsorbate interactions. The Temkin isotherm can be expressed by the following equation 4:

$$q_e = \frac{RT}{b} \ln(AC_e) \quad (4)$$

where  $RT/b = B$  ( $\text{J mol}^{-1}$ ), which is the Temkin constant related to heat of sorption whereas  $A$  ( $\text{L g}^{-1}$ ) is the equilibrium binding constant corresponding to the maximum binding energy.  $R$  ( $8.314 \text{ J mol}^{-1} \text{ K}^{-1}$ ) is the universal gas constant and  $T$  (K) is the absolute solution temperature.

#### 2.3.3.3.4. Dubinin-Radushkevich (D-R) isotherm

This model is applied to distinguish between physical and chemical adsorption. The D-R equation is given as follows (5):

$$q_e = q_m \exp(-\beta \varepsilon^2) \quad (5)$$

with

$$\varepsilon = RT \ln\left(1 + \frac{1}{c_e}\right) \quad (6)$$

where  $q_m$  is the maximum amount adsorbed and can be called the adsorption capacity,  $\beta$  is a constant related to the adsorption energy ( $\text{mol}^2 \text{ kJ}^{-2}$ ),  $\varepsilon$  is the potential energy of the surface,  $R$  is the gas constant ( $\text{kJ mol}^{-1} \text{ K}^{-1}$ ) and  $T$  is the absolute temperature. The constant  $B$  gives the free energy  $E$  ( $\text{kJ mol}^{-1}$ ) of the transfer of 1 mol of solute from infinity to the surface of an adsorbent, and can be computed using the following relationship (Onyango et al., 2004):

$$E = \frac{1}{\sqrt{2B}} \quad (7)$$

#### 2.3.3.4. Adsorption kinetics

The study of sorption from a kinetic perspective can lead to a better understanding of the mechanism of the process. The kinetic studies describe the rate of adsorption and this rate controls the equilibrium time. These kinetic models are useful for the design and optimization of effluent treatment models. Pseudo first order, pseudo second order, Elovich and Intra-particle diffusion kinetic models were adopted in this work.

##### 2.3.3.4.1. Pseudo-First and pseudo-second order Kinetic Models

The modeling of kinetics of adsorption was investigated by two common models, namely, the Lagergren's pseudo-first order model and pseudo-second order model. The

Lagergen's first order and second order models, in the linear form, are expressed by equations 8 and 9, respectively:

$$\log(q_e - q_t) = \log q_e - K_1 t \quad (8)$$

$$\frac{t}{q_t} = \frac{1}{k_2 q_e} + \frac{1}{q_e} t \quad (9)$$

Where  $q_e$  and  $q_t$  are the amounts of the adsorbent adsorbed at equilibrium and at time  $t$ , respectively, and are expressed in  $\text{mg g}^{-1}$ ,  $K_1$  and  $K_2$  are the pseudo first-order and the second order model rate constant expressed in  $\text{Lmin}^{-1}$  and  $\text{g mg}^{-1} \text{min}^{-1}$  respectively.

#### 2.3.3.4.2. Elovich equation

The Elovich equation is another rate equation in which the absorbing surface is heterogeneous (Chien and Clayton, 1980). It is generally expressed as given as follows:

$$q_t = \frac{1}{b} \ln(ab) + \frac{1}{b} \ln t \quad (10)$$

where  $a$  ( $\text{mg g}^{-1} \text{h}^{-1}$ ) is the initial sorption rate and  $b$  ( $\text{mg g}^{-1}$ ) is related to the extent of surface coverage and activation energy for chemisorption. The parameters  $(1/b)$  and  $(1/b) \ln(ab)$  can be obtained from the slope and intercept of the linear plot of  $q_t$  versus  $\ln t$ . The value of  $1/b$  is indicative of the number of sites available for adsorption, while the  $(1/b) \ln(ab)$  value is the adsorption quantity when  $\ln t$  is equal to zero (Tan et al., 2009).

#### 2.3.3.4.3. Intra-particle Diffusion Model

Intra-particle diffusion model based on the theory proposed by Weber and Morris was tested to identify the diffusion mechanism (Shaarani et al., 2010). According to this theory:

$$q_t = K_{id} t^{1/2} + C \quad (11)$$

where  $C$  is the intercept and  $k_{id}$  ( $\text{mg g}^{-1} \text{h}^{-1/2}$ ) is the intra-particle diffusion rate constant, which can be evaluated from the slope of the linear plot of  $q_t$  versus  $t^{1/2}$ . If intra-particle diffusion is a rate controlling step, then the plots should be linear and pass through the origin. In most cases these plots give general features of three stages; initial curved portion, followed by an intermediate linear portion and a plateau. The initial portion due to external mass transfer, the intermediate linear part is due to intra-particle diffusion

and the plateau to the equilibrium stage where intra-particle diffusion starts to slow down due to extremely low solute concentrations in the solution (Daifullah et al., 2007).

### 2.3.3.5. Adsorption thermodynamic

The temperature has great effect on the adsorption. The equilibrium constant  $K_D$  of the adsorption process, expressed in  $L\ g^{-1}$ , can be used to estimate the thermodynamic parameters due to its dependence on temperature. The changes in standard free energy ( $\Delta G^\circ$ ), enthalpy ( $\Delta H^\circ$ ) and entropy ( $\Delta S^\circ$ ) of adsorption process were determined using the following equations 12, 13 and 14:

$$K_D = \frac{q_e}{c_e} \quad (12)$$

$$\Delta G^\circ = -RT \ln K_D \quad (13)$$

$$\ln K_D = \frac{\Delta S^\circ}{R} - \frac{\Delta H^\circ}{RT} \quad (14)$$

A Van't Hoff plot of  $\ln K_D$  as a function of  $1/T$  yields to a straight line. The  $\Delta H^\circ$  and  $\Delta S^\circ$  parameters were calculated from the slope and intercept of the plot, respectively.

### 2.3.4. Life Cycle Assessment of the prepared activated carbon

Life cycle assessment is a technique used for analyzing the environmental aspects and potential impacts of products and services (ISO, 1997). The analysis is done by bringing together an inventory of relevant inputs and outputs of a system, evaluating the potential impacts associated with those inputs and outputs and relating the results of the inventory analysis and impact assessment phases to the objectives of the study. By comparing the alternatives and studying the technical systems, function of the products or services as well as the impacts on the natural environment is assessed. The comparison may provide improvements in existing products or services and may help in the design of new products or services. Life cycle assessment provides us to describe the natural resource use and pollutant emissions in quantitative terms (Finnveden et al., 2009). The ISO 14040 standard determines four basic stages for LCA studies, schematically represented in figure 2.8.

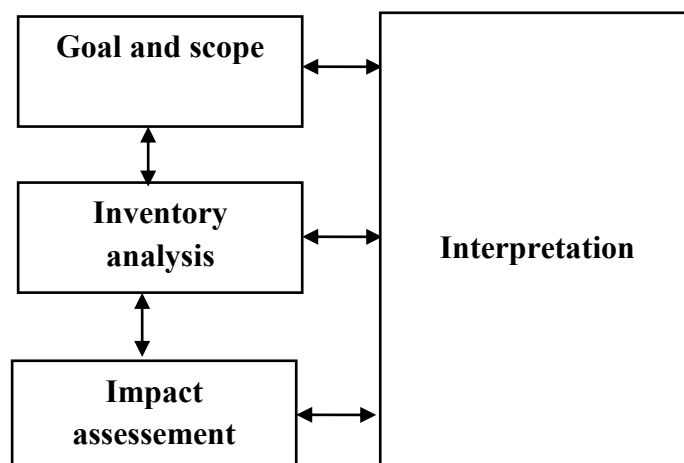


**Figure 2.8.** Stages in a Life Cycle Analysis (Source: ISO 1997)

Within this study, the LCA methodology was used to evaluate the preparation of the activated carbon from the agriculture by-product olive waste cakes.

## **2.4. Biological treatment**

Biological treatment is one of the most economical methods compared to other physical and chemical processes. It has the advantages of lower treatment costs with no secondary pollution (Chan et al., 2009). It includes biosorption and biodegradation in either aerobic or anaerobic treatment process with microorganisms: bacteria, fungi, yeasts and algae or enzymes.

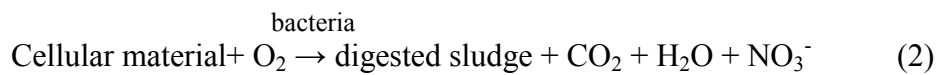
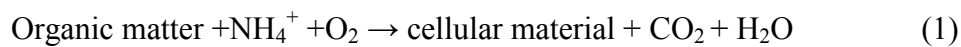
### **2.4.1. Aerobic treatment**

Aerobic biological process involves the use of free or dissolved oxygen by microorganisms (aerobes) in the conversion of organic wastes to biomass and CO<sub>2</sub> (Chan et al., 2009).

When a culture of aerobic heterotrophic microorganisms is placed in an environment containing a source of organic material, the microorganisms will degrade and remove this material. A fraction of the organic material removed is utilized for the synthesis of new microorganisms, resulting in a biomass increase. The remaining material is oxidized to carbon dioxide, water and soluble inert material, providing energy for

synthesis, metabolism and maintenance of the microorganisms' vital functions. Once the external source of organic material is exhausted, the microorganisms will begin endogenous respiration where cellular material is oxidized to satisfy the energy requirements for life support. If such conditions are maintained over an extended period of time, the total quantity of biomass will be reduced considerably and the remaining material will exist at a low energy state and can be considered biologically stable and suitable for disposal to the environment.

The aerobic digestion process, as mentioned above, consists of two steps; direct oxidation of biodegradable matter, and endogenous respiration in which cellular material is oxidized. These processes can be illustrated by the following reactions:



Reaction (1) describes the oxidation of organic matter to cellular material which is the predominant reaction in aerobic digestion systems.

The process described in Reaction (2) is typical endogenous respiration process where cellular material is subsequently oxidized, producing digested sludge.

The main disadvantageous of the aerobic treatment is the production of sludge. It supposes a high contribution to environmental contamination and it is an important point to be solved in aerobic treatment processes (Robinson et al., 1983).

#### 2.4.2. Anaerobic digestion

Anaerobic digestion is a biological process by which the organic matter is degraded in the absence of oxygen and the presence of anaerobic microorganisms. Biogas which mainly composed of methane (CH<sub>4</sub>) and carbon dioxide (CO<sub>2</sub>) is produced as a result of the organic matter digestion, and this produced biogas can be used for electricity generation.

Anaerobic digestion is the consequence of a series of metabolic interactions among various groups of microorganisms. It occurs in four main stages (Figure 2.9): hydrolysis, acidogenesis, acetogenesis and methanogenesis (Metcalf and Eddy, 1991).

**a. Hydrolysis:** in the first stage of hydrolysis, the fermentative bacteria via its extracellular enzymes convert the undissolved complex organic matter like cellulose into simpler soluble compounds such as sugars, amino acids, fatty acids, alcohol and CO<sub>2</sub>. This stage is important especially for complex organic wastes and could represent a limiting factor for the digestion process.

**b. Acidogenesis:** in this stage, the first stage hydrolyzed compounds are converted to simple organic acid (fatty acids mainly composed of acetate, propionate and butyrate), hydrogen and carbon dioxide.

**c. Acetogenesis:** This involves the breakdown of fatty acids and other compounds to form acetic acid, carbon dioxide and hydrogen which will be used by methanogenic bacteria in the last stage.

**d. Methanogenesis:** all the simple compounds obtained in the previous stage (acetate, hydrogen, carbon dioxide) are converted to methane by the methanogenic microorganisms.

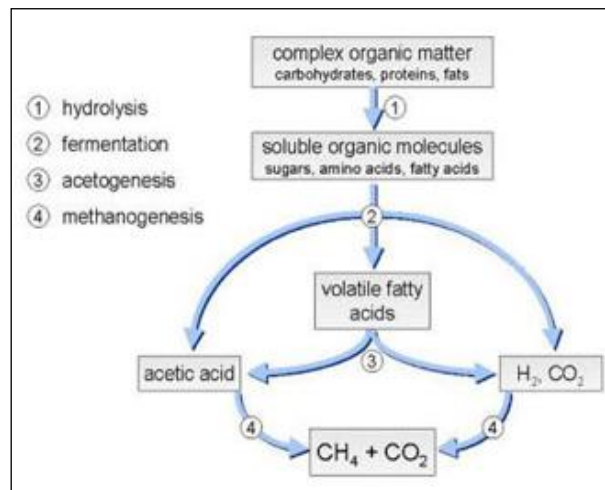


**Figure 2.9.** The different consecutive stages of anaerobic digestion process

Anaerobic treatment has the advantage of a lower energy demand (expansive aeration omitted) and a lower sludge production compared with aerobic treatment (O'Neill et al., 2000). The resulting sludge is also quite well stabilized and usually suitable to be directly deposited at landfill or applied to agricultural fields. Moreover, the resulting methane is combustible and can be later exploited by conversion into thermal or mechanical energy (Metcalf and Eddy, 1991).



### 2.4.3. Treatment with lignolytic fungi

The most widely researched fungi to degrade contaminants are the lignolytic fungi. White rot fungi (WRF) is a physiological group of fungi that can degrade lignin (and lignin-like substances). The role of fungi in the treatment of wastewater has been extensively researched (Coulibaly et al., 2003; Brar et al., 2006). Fungus has proved to be a suitable organism for the removal of pollutants.

To understand the ability to degrade contaminants it is important to analyze the ecological niches of white rot fungi. These fungi are a physiological rather than taxonomic grouping, comprising those fungi that are capable of extensively degrading lignin (a heterogeneous polyphenolic polymer) within lignocellulosic substrates (Pointing, 2001). The name white rot derives from the appearance of wood attacked by these fungi, in which lignin removal results in a bleached appearance of the substrate (Pointing, 2001). Most known white rot fungi are basidiomycetes, although a few ascomycete genera within the *Xylariaceae* are also capable of white rot decay (Eaton and Hale, 1993).

In nature, white rot fungi live on woody tissues that are composed mainly of three biopolymers: cellulose, hemicellulose and lignin. Lignin, which provides strength and structure to the plant, is extremely recalcitrant. It is synthesized in plants by random peroxidase-catalysed polymerization of substituted *p*-hydroxy-cinnamyl alcohols (Field et al., 1993). This polymer is three dimensional, and its monomers are linked by various carbon-carbon and ether bonds and the stereo irregularity of lignin makes it resistant to attack by enzymes.

The white rot fungi have developed very non-specific mechanisms to degrade lignin (Barr and Aust, 1994) extracellularly. The major families of lignin modifying enzymes believed to be involved in lignin degradation are laccases, lignin peroxidases, manganese peroxidases (Reddy and Mathew, 2001) and a recently described family the versatile peroxidase (Martinez et al., 2002). The key step in lignin degradation by laccase or the ligninolytic peroxidases (LiP and MnP) involves the formation of free radical intermediates, which are formed when one electron is removed or added to the ground state of a chemical (Reddy and Mathew, 2001). Different white rot fungi appear to be able to achieve the same effect with different combinations of enzymes (Harvey and Thurston, 2001) with respect to wood degradation. The common features are the random nature of the structure of lignin, which requires its degradation to function in a

non-specific manner. Consequently, other compounds that have an aromatic structure, such as many xenobiotic compounds, are also highly susceptible to degradation by ligninolytic enzymes (Field et al., 1993; Barr and Aust, 1994). This characteristic is the greatest advantage of the use of white-rot fungi in bioremediation, since a mixture of different pollutants are usually found in most contaminated sites (Mester and Tien, 2000).

Aside from the lack of specificity, the ligninolytic system of white rot fungi offers further advantages. It is not induced by either lignin or other related compounds (Cancel et al., 1993). Thus, it is possible to degrade pollutants at relatively low concentrations that may be lower than that required to induce the synthesis of biodegrading enzymes in other microorganisms (Mester and Tien, 2000).

Furthermore, repression of enzyme synthesis does not occur when the concentration of a chemical is reduced to a level that is ineffective for enzyme induction. This is because the induction of the degradative enzymes is not dependent on the presence of the chemical. The fungus can effectively degrade very low concentrations of a pollutant to non-detectable or nearly non-detectable levels (Bumpus and Aust, 1986).

Most lignolytic fungi incorporate also an intracellular degradative system involving cytochrome P450 monooxygenase-epoxide hydrolase. This pathway is present in eukaryotic organisms. It regulates normally the conversion of hormones. In WRF it has been revealed that it can cooperate with lignolytic system in the degradation of PAHs (Bezalel et al., 1996), TCE/PCE (Marco-Urrea et al., 2008) and other xenobiotics.

#### **2.4.4. The white rot fungus *Trametes versicolor***

*Trametes versicolor* formerly known as *Coriolus versicolor* and *Polyporus versicolor* is an extremely common polypore mushroom which can be found throughout the world. *Versicolor* means 'of several colours' (Photo 2.1). *T. versicolor* is commonly called Turkey Tail because of its resemblance to the tail of the wild turkey. *T. versicolor* is recognized as a medicinal mushroom in Chinese medicine. During submerged growth, the filamentous fungus may grow either as free mycelia or as pellets (Photo 2.2), and the growth form is determined by a number of factors such as growth medium, size of inoculum and physical environment. The morphology of filamentous micro-organisms in submerged culture has been shown to play a critical role in many industrial

fermentation and in commercial production of some metabolites (Smith and Lilly, 1990).



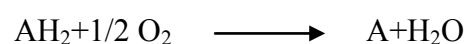
**Photo 2.1.** The fungus *Trametes versicolor* in the wild form



**Photo 2.2.** Growth of the fungus *Trametes versicolor* in the pellets form

The lignonilytic system of the fungus is stimulated by nitrogen limitation. It is capable to produce lignin peroxidase (LiP), manganese peroxidase (MnP) and laccase (lac) (Wesenberg et al., 2003). Laccase is the most characteristic enzyme and can be produced either constitutive or induced, maintaining a similar catalytic activity (Bourbonnais et al., 1995). Laccase is of particular interest, because to difference of peroxidases, it does not use hydrogen peroxide, by such reason displays a greater stability, which allows to use it more efficiently of immobilized way, in addition laccase can oxidize a great variety of substrates, and by means of the use of mediators can expand the reactivity of laccase towards others substrates (Octavio et al., 2006).

Laccase (benzenediol:oxygen oxidoreductases; EC 1.10.3.2) is a multicopper enzyme belonging to the group of blue oxidases, which catalyse reduction of molecular oxygen to water, bypassing hydrogen peroxidase formation (Lee et al., 2002) according the equation:



Laccase catalyzes the oxidation of a variety of phenolic compounds, as well as diamines and aromatic amines, with concomitant reduction of molecular oxygen to water (Thurston, 1994). The laccase molecule, as an active holoenzyme form, is a dimeric or tetradimeric glycoprotein, usually containing four copper atoms per monomer, bound to three redox sites (T1, T2 and T3 Cu pair) (Figure 2.10). T1 oxidizes the substrate and transfers electrons to the T2 and T3 sites, which form a trinuclear copper cluster center.

In this center, O<sub>2</sub> is reduced producing water (Wesenberg et al., 2003). Free radicals resulting from aromatic amines following one-electron abstraction by laccases can either polymerize or be degraded (Thurston, 1994).

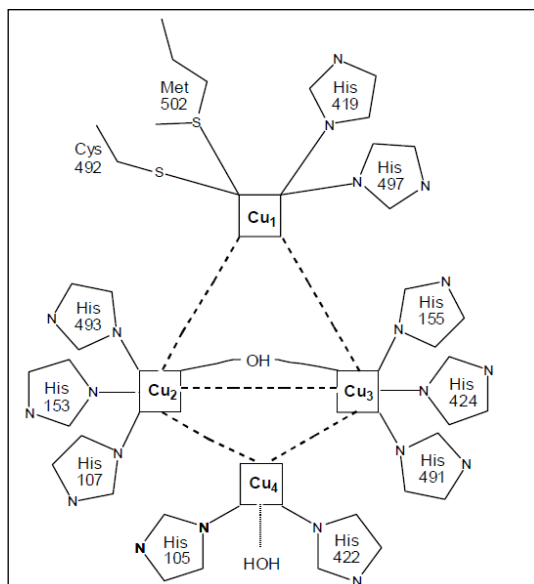


**Figure 2.10.** Copper centers of the laccase (adapted from Claus, 2004)

Mediators are low molecular weight compounds that aid in lignin degradation assisting the lignin degrading enzymes in increasing the effective redox potential. The laccase mediator system involves use of these mediators which are oxidized by laccase to stable radicals which in turn oxidize other compounds which could not have been acted upon by laccase directly (Figure 2.11). The most commonly used mediators are 2,2'-azinobis (3-ethylbenzthiazoline-6-sulfonate) (ABTS) and 1-hydroxybenzotriazole (HOBT) (Bourbonnais et al., 1997). Their structures are shown in Figure 2.12.

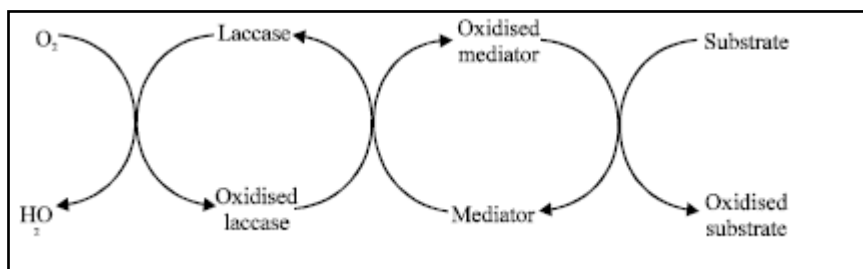


**Figure 2.11.** Mediator-mediated oxidation of substrate by laccase

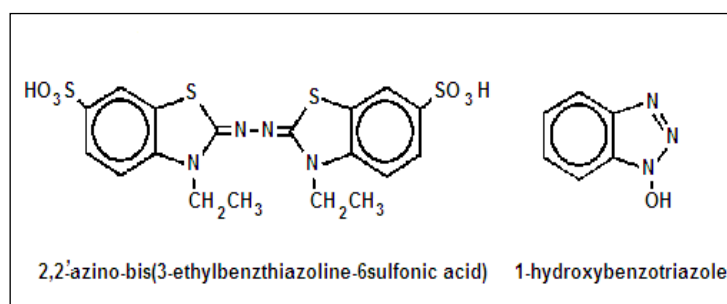


**Figure 2.13.** Structures of the mediators of laccase: ABTS and HOBT (Bourbonnais et al., 1997)

## REFERENCES

- Agrawal S.K., 2009. Water pollution. APH publishing corporation, New delhi.
- Allen S. J., Brown P. A., 1995. Isotherm analyses for single component and multicomponent metal sorption onto lignite. *J. Chem. Technol. Biotechnol.* 62, 7-24.
- ASTEE (Association Scientifique et Technique pour l'Eau et l'Environnement), 2006 Reglementation et traitement des eaux destinés à la consommation humaine, 1<sup>st</sup> Edition, Paris.
- Bansal, R.C., Jean-Baptiste D., Fritz S., 1988. Active carbon Marcel Dekker Inc. New York
- Bansal R.C., Goyal, M., 2005. Activated Carbon Adsorption. Taylor and Francis, New York.
- Barceló D., Petrovic M., 2008. Emerging contaminants from industrial and municipal waste. Removal technologies. *The Handbook of Environmental Chemistry*, vol 5, S 2. Springer-Verlag Berlin Heidelberg.
- Barr D., Aust S., 1994. Mechanisms white rot fungi use to degrade pollutants. *Environ. Sci. Technol.* 28 (2), 78–87.
- Belfroid A.C., Van der Horst A., Vethaak A.D., Schafer A.J., Rijs G.B.J., Wegener J., Cofino W.P., 1999. Analysis and occurrence of estrogenic hormones and their glucuronides in surface water and waste water in the Netherlands. *Sci. Total Environ.* 225 (1–2), 101–108.
- Bezalel L., Hadar Y., Cerniglia C., 1996. Mineralization of polycyclic aromatic hydrocarbons by the white rot fungus *Pleurotus ostreatus*. *Appl. Environ. Microbiol.* 62, 292-295.
- Boehm H. P., 1994. Some aspects of the surface chemistry of carbon blacks and other carbons. *Carbon* 32, 759–769.
- Bourbonnais R., Paice M., Reid, I. D., Lanthier P., Yaguchi M., 1995. Lignin Oxidation by Laccase isozymes from *Trametes versicolor* and role of the mediator 2,2'-Azinobis (3-Ethylbenzthiazoline-6-Sulfonate) in Kraft Lignin Depolymerization. *Appl. Environ. Microbiol.* 61, 1876–1880.
- Bourbonnais R., Paice M. G., Reid I. D., Freiermuth B., 1997. Reactivities of various mediators and laccases with kraft pulp and lignin model compounds. *Appl. Environ. Microbiol.* 63, 4627–4632.

- Brar S.K., Verma M., Surampalli R.Y., Misra K., Tyagi R.D., Meunier N., Blais J.F., 2006. Bioremediation of hazardous wastes-a review. Practice periodical of hazardous, toxic and radioactive. Waste Manage. 10, 59–72.
- Bumpus J., Aust S., 1986. Biodegradation of environmental pollutants by the white rot fungus *Phanerochaete chrysosporium*: involvement of the lignin degrading system. Bioessays 6, 166–170.
- Cancel A., Orth A., Tien M., 1993. Lignin and veratryl alcohol are not inducers of the ligninolytic system of *Phanerochaete chrysosporium*. Appl. Environ. Microbiol. 59, 2909–2913.
- Carrasco-Marin M., Alvarez-Merino A., Moreno-Castilla C., 1996. Microporous activated carbons from a bituminous coal. Fuel 75, 966–970.
- Castiglioni S., Fanelli R., Calamari D., Bagnati R., Zuccato E., 2004. Methodological approaches for studying pharmaceuticals in the environment by comparing predicted and measured concentrations in River Po, Italy. Regul. Toxicol. Pharmacol. 39, 25–32.
- Chan Y. J., Chong M. F., Law C. L., Hassell. D.G., 2009. A review on anaerobic–aerobic treatment of industrial and municipal wastewater. Chem. Eng. J. 155, 1–18.
- Cheremisinoff N. P., 2002. Handbook of water and wastewater treatment. Butterworth-Heinemann. Boston, USA.
- Chien S.H., Clayton W.R., 1980. Application of Elovich equation to the kinetics of phosphate release and sorption on soils. Soil Sci. Soc. Am. J. 44, 265–268.
- Christie R.M., 2001. Colour Chemistry. Royal Society of Chemistry, Cambridge.
- Christie R.M., 2007. Environmental aspects of textile dyeing. Woodhead, Boca Raton, Cambridge.
- Claus H., 2004. Laccases: structure, reactions, distribution: Micron. 35, 93-96.
- Clara M., B. Strenn, Kreuzinger N., 2004. Carbamazepine as a possible anthropogenic marker in the aquatic environment: Investigations on the behaviour of carbamazepine in wastewater treatment and during groundwater infiltration. Water Res. 38, 947–954.
- Corcoran E., Nellesmann C., Baker E., Bos R., Osborn D., Savelli H., (eds). 2010. Sick Water? The central role of wastewater management in sustainable development. A

- rapid response assessment. United Nations Environment Programme, UN-HABITAT, GRID-Arendal.
- Cornelissen G., Van Noort P.C.M., Parsons J.R., Govers H.A.J., 1997. The temperature dependence of slow adsorption and desorption kinetics of organic compounds in sediments. *Environ. Sci. Technol.* 31, 454–460.
- Coulibaly L., Gourene G., Agathos N.S., 2003. Utilization of fungi for biotreatment of raw wastewaters. *Afr. J. Biotechnol.*, 2: 620–30.
- Dabrowski A., 2001. Adsorption: from theory to practice. *Adv. Colloid Int. Sci.* 93:135–224.
- Dabrowski A., Podkoscielny P., Hubicki Z, Barczak M., 2005. Adsorption of phenolic compounds by activated carbon-a critical review. *Chemosphere* 58, 1049–1070.
- Daifullah A.A.M., Yakout S.M., Elreefy S.A., 2007. Adsorption of fluoride in aqueous solutions using KMnO<sub>4</sub>-modified activated carbon derived from steam pyrolysis of rice straw. *J. Hazard. Mater.* 147, 633–643.
- Davis M.L., Cornwell D.A., 2008. *Introduction to Environmental Engineering*. 4 th edition. McGraw-Hill, NY.
- Derbyshire F., Jagtoyen M., Andrews R., Rao A., Martin-Gullon I., Grulke E., 2001. *Carbon Materials in Environmental Applications*. Marcel Decker, New York.
- Dias J. M., Alvim-Ferraz M.C.M., Almeida M. F., Riverra-Urtella J., Sánchez-Polo M., 2007. Waste materials for activated carbon preparation and its use in aqueous-phase treatment: A review. *J. Environ. Manage.* 85, 833–846.
- Diaz E., Ordonez S., Vega A., Coca J., 2005. Comparison of adsorption properties of a chemically activated and a steam-activated carbon, using inverse gas chromatography. *Microporous Mesoporous Mater.* 82, 173–181.
- Diao Y., Walawender, W.P., Fan L.T., 2002. Activated carbon prepared from phosphoric acid activation of grain sorghum. *Bioresour. Technol.* 81, 45–52.
- Drinan J.E., 2001. *Water and wastewater treatment*. CRC press, Florida.
- Eaton R., Hale M., 1993. *Wood, decay, pests and prevention*. Chapman and Hall, London.
- Edwards J.D., 1995. *Industrial wastewater treatment: a guide book*. CRC Press, Florida, USA.



- EPA, 2001. United States Environmental Protection Agency. Origin and fate of Pharmaceuticals and personal care products (PPCPs) in the environment. Online in the internet from <http://www.epa.gov/ppcp/basic2.html>
- EPA, 2006. United States Environmental Protection Agency. Technical Fact sheet on Nitrate/Nitrite. Online on the internet from <http://www.epa.gov/ogwdw/dwh/t-ioc/nitrates.html>.
- Ewan K. B., Pamphlet R., 1996. Increased inorganic mercury in spinal motor neurous following chelating agents. *Neur. Tox.* 17(2):343-9.
- Field J., Jong E., Feijo-Costa G. and Bont J., 1993. Screening for ligninolytic fungi applicable to the biodegradation of xenobiotics. *Trends in Biotechnology*; 11: 44-49.
- Fierro V., Torne Fernandez V., Montane D., Celzard A. 2008. Micropor. Mesopor. Mater. 111, 276–284.
- Finnveden G., Hauschild M. Z., Ekvall T., Guinée J., Heijungs R., Hellweg S., Koehler A., Pennington D., Suh S., 2009. Recent developments in life cycle assessment. *Journal of Environmental Management* 91, 1-21.
- Freundlich H.M.F., 1906. Over the adsorption in solution. *J. Phys. Chem.* 57, 385–471.
- Fu Y., Viraraghavan T., 2001. Fungal decolourization of dye wastewaters: a review. *Bioresour Technol.* 79, 251–62.
- Fu F., Wang Q., 2011. Removal of heavy metal ions from wastewaters: A review. *J. Environ Manage.* 92, 407–418.
- Gergova K., Petrov N., Minkova V.A., 1993. Comparaison of adsorption characteristics of various activated carbons. *Chem.Technol. Biotechnol.* 56, 77–82.
- Goel P.K., 2006. *Water pollution:causes effect and control.* New Age International, New Delhi.
- Gomez-Serrano V., Cuerda-Correa M.C., Fernandez-Gonzaleza E.M., Alexandre-Francoa M.F., Macias-Garcia A., 2005. Preparation of activated carbons from chestnut wood by phosphoric acid-chemical activation. Study of microporosity and fractal dimension. *Mater. Lett.* 59, 846–853.
- Gros M., Petrovic M., Barceló D., 2010. Removal of pharmaceuticals during wastewater treatment and environmental risk assessment using hazard indexes. *Environ. Inter.* 36, 15–26.

- Guo Y., Yang S., Fu W., Qi J., Li R., Wang Z., and Xu H., 2003. Adsorption of malachite green on micro- and mesoporous rice husk-based active carbon. *Dyes Pigm.* 56, 219–229.
- Haas C. N., Vamos R. J., 1995. Hazardous and industrial waste treatment. Prentice Hall. Englewood Cliffs.
- Haimour N.M., Emeish S., 2006. Utilization of date stones for production of activated carbon using phosphoric acid. *Waste Manage.* 26, 651–660.
- Hameed B. H., Din A.T.M., Ahmad A.L., 2007 a. Adsorption of methylene blue onto bamboo-based activated carbon: Kinetics and equilibrium studies. *J. Hazard. Mater.* 141 (3), 819–825.
- Hameed B. H., Ahmad A. L., Latiff K. N. A., 2007 b. Adsorption of basic dye (methylene blue) onto activated carbon prepared from rattan sawdust. *Dyes Pigm.* 75, 143-149.
- Harvey P., Thurston C., 2001. The biochemistry of ligninolytic fungi. In: Gadd G. (Ed.) *Fungi in bioremediation*. Cambridge University Press. Cambridge, U.K.
- Heberer T., 2002. Occurrence, fate, and removal of pharmaceutical residues in the aquatic environment: a review of recent research data. *Toxicol. Lett.* 131, 5–17.
- Hernando M.D., Mezcuca M., Fernandez-Alba A.R., Barceló D., 2006. Environmental risk assessment of pharmaceuticals residues in wastewater effluents, surface waters and sediments. *Talanta* 69, 334-342.
- Hinz C., 2001. Description of sorption data with isotherm equations. *Geoderma* 99, 225–243.
- Hunger K., 2003. *Industrial dyes: Chemistry, properties, applications*. Germany: Wiley-VCH.
- Ioannidou O., Zabaniotou A., 2007. Agricultural residues as precursors for activated carbon production—a review. *Renew. Sustain. Energy Rev.* 11, 1966–2005.
- ISO, 1997. ISO 14040: Environmental management-Life cycle assessment- Principales and Framework. Geneva, Switzerland.
- Jain V. K., 1978. Studies on effect of cadmium on the growth pattern of phaseolus aurius varieties. *Absi. I. Bot. Conf. WHO. World Health Organization technical report JIBS*, 57-84.
- Jones O.A., Lester J.N., Voulvoulis N., 2005. Pharmaceuticals: A Threat to Drinking Water? *Trends Biotechnol.* 23(4), 163–167.

- Juang R. S., Wu F. C., Tseng R. L., 2002. Characterization and use of activated carbons prepared from bagasses for liquid-phase adsorption. *Colloid Surf. A: Physicochem. Eng. Aspect* 201, 191–199.
- Julien F., Baudu M., Mazet M., 1994. Effects of the modification of the activated carbon physico-chemical characteristics onto the organic compounds adsorption. *Aqua London* 43 (6), 278-286.
- Kadirvelu K., Palanivel M., Kalpana R., Rajeswari S., 2000. Activated carbon prepared from an agricultural by-product for the treatment of dyeing industry wastewater. *Bioresour. Technol.* 74, 263–265.
- Kadirvelu K., Kavipriya M., Karthika C., Radhika M., Vennilamani N., Pattabhi, S., 2003. Utilization of various agricultural wastes for activated carbon preparation and application for the removal of dyes and metal ions from aqueous solutions. *Bioresour. Technol.* 87, 129–132.
- Karaca S., Gürses, A. and Bayrak, R., 2004. Effect of some pre-treatments on the adsorption of methylene blue by *Balkaya lignite*. *Energy Convers. Manage.* 45, 1693–1704.
- Kolpin D.W., Furlong E.T., Meyer M.T., Thurman E.M., Zaugg S.D., Barber L.B., Buxton H.T., 2002. Pharmaceuticals, Hormones, and Other Organic Wastewater Contaminants in U.S. Streams, 1999–2000: A National Reconnaissance”. *Environ. Sci. Technol.* 36 (6), 1202–1211.
- Laine J. Yunes S., 1992. Effect of the preparation method on the pore size distribution of activated carbon from cocount shell. *Carbon* 30, 601–604.
- Langmuir I., 1918. The adsorption of gases on plane surfaces of glass, mica, and platinum. *J. Am. Chem. Soc.* 40, 1361–1403.
- Lantzy R. J., Mackenzie F. T., 1979. Atmospheric trace metals: global cycles and assessment of man’s impact. *Geochim. Cosmochim. Acta.* 43, 511–525.
- Lee S.K., George S.D., Antholine W.E., Hedman B., Hodgson K.O., Solomon E.I., 2002. Nature of the intermediate formed in the reduction of O<sub>2</sub> to H<sub>2</sub>O at the trinuclear copper cluster active site in native laccase. *J. Am. Chem. Soc.* 124 (7), 6180–6193.
- Malik P.K, 2003. Use of activated carbons prepared from sawdust and rice-husk for adsorption of acid dyes: a case study of Acid Yellow 36. *Dyes Pigm.* 56, 239–249.

- Marco-Urrea E., Teodor Parella, Gabarrell, X., Caminal, G., Vicent, T., Reddy, C. A., 2008. Mechanistics of trichloroethylene mineralization by the white-rot fungus *Trametes versicolor*. *Chemosphere* 70 (3), 404–410.
- Martinez, A. T. (2002). Molecular biology and structure–function of lignin-degrading heme peroxidases. *Enzyme Microb. Technol.* 30, 425–444
- McCabe W.L., Smith J.C., Harriott P., 1993. *Unit Operations of Chemical Engineering*, 5th ed. New York: McGraw-Hill.
- Mester T., Tien M. 2000. Oxidation mechanism of ligninolytic enzymes involved in the degradation of environmental pollutants. *Int. Biodeteor. Biodegrad.* 46, 51-59.
- Metcalf and Eddy, 1991. *Wastewater engineering. Treatment, disposal and reuse*. MC.Graw-Hill, Inc 3<sup>rd</sup> ed, New York, USA
- Miao X.S., Bishay F., Chen M., Metcalfe C.D., 2004. Occurrence of antimicrobials in the final effluents of wastewater treatment plants in Canada. *Environ. Sci. Technol.* 38 (13), 3533–3541.
- Mier M. V., Callejas R. L., Gehr R., Jimenez-Cisneros B. E., Álvarez J. P.J. 2001. Heavy metal removal with mexican clinoptilolite: multi-component ionic exchange. *Water Res.* 35 (2), 373-378.
- Mohamed M. M., 2004. Acid dye removal: comparison of surfactant-modified mesoporous FSM-16 with activated carbon derived from rice husk. *J. Colloid Int. Sci.* 272, 28–34.
- Nouri J., Mahvi A.H., Babaei A. A., Jahed G. R., Ahmadpour E., 2006. Investigation of heavy metals in groundwater Pakistan. *J. Biol. Sci.* 9 (3), 377-384.
- Nriagu J. O., 1979. Global inventory of natural and anthropogenic emissions of trace metals to the atmosphere. *Nature* 279, 409–411.
- Octavio L.C., Pérez P. Cristina Ma., Barbosa I. J. R. Rodríguez, Villaseñor, Francisco O., 2006. Laccases. *Adv. Agr. Food Biotechnol.* 37/661 (2), 323-340.
- O’Neil C, Hawkes FR, Hawkes DL, Lourenc, ND, Pinheiro HM, Delee W., 1999. Colour in textile effluents-sources, measurement, discharge consents and simulation: a review. *J. Chem. Technol. Biotechnol.* 74, 1009–18.
- O’Neill C., Hawkes F.R., Hawkes D.L., Esteves S., Wilcox S.J., 2000. Anaerobic-aerobic biotreatment of simulated textile effluent containing varied ratios of starch and azo dye. *Water Res.* 34, 2355–61.

- Onyango M.S., Kojima YAoyi O., 2004. Adsorption equilibrium modeling and solution chemistry dependence of fluoride removal from water by trivalent-cation exchanged zeolite F-9. *J. Colloid. Interface Sci.* 279, 341–350.
- Ould-Idriss A., M. Stitou, E.M. Cuerda-Correa, C. Fernández-González, A. Macías-García, M.F. Alexandre-Franco, Gómez-Serrano V., 2011. Preparation of activated carbons from olive-tree wood revisited. II. Physical activation with air. *Fuel Process. Technol.* 92, 266–270.
- Pan B., Pan Bi., Zhang W., Zhang Q., Zhang Q., Zheng S., 2008. Adsorptive removal of phenol from aqueous phase by using a porous acrylic ester polymer. *J. Hazard. Mater.* 157 (2-3), 293–299.
- Panizza, M Cerisola G., 2009. Direct and mediated anodic oxidation of organic pollutants. *Chem. Rev.* 109, 6541-6569.
- Prakash Kumar B.G., Miranda L.R., Velan M., 2005. Adsorption of Bismark Brown dye on activated carbons prepared from rubber wood sawdust (*Hevea brasiliensis*) using different activated methods. *J. Hazard. Mater. B* 126, 65–70.
- Pignatello J.J., 2000. The measurement and interpretation of sorption and desorption rates for organic compounds in soil media. *Adv. Agron.* 69: 1–73.
- Pointing S., 2001. Feasibility of bioremediation by white-rot fungi. *Appl. Microbiol. Biotechnol.* 57, 20-33.
- Putschew A., Wischnack S., Jekel, M. 2000. Occurrence of Triiodinated X-ray contrast agents in the aquatic environment'. *Sci. Total Environ.* 255 (1–3), 129–134.
- Raskin I., Smith R.D., Salt E:D., 1997. Phytoremediation of metals: using plants to remove pollutants from the environment. *Curr. Opin. Biotechnol.* 8, 221–226
- Reddy C., Mathew Z., 2001. Bioremediation potential of white rot fungi. In. Gadd G. (Eds.) *Fungi in bioremediation*. Cambridge University Press. Cambridge, U.K.
- Revenga C., Mock, G., 2001. Dirty water: pollution problems persist, *Earth Trends: Featured Topic*, 1-6.
- Robert L., 1989. Opérations unitaires Adsorption. *Techniques d'ingénieurs J 2730: 1-22*. Editions Technique de l'Ingenieur, Paris, France.
- Robinson H. D., Maris P.J., 1983. Aerobic biological treatment of a medium-strength leachate. *Water Res.* 17, 153- 154.

- Rodriguez-Reinso, Molina-Sabio M., 1992. Activated carbons from lignocellulosic materials by chemical and / or physical activation: an overview. *Carbon* 30, 1111-1118.
- Ross S. M., 1994. Toxic metals in soil-plant systems. Wiley, Chichester, U. K.
- Rozada F., Calvo L.F., Garcia A.I., Martin Villacorta J., Otero M., 2003. Dye Adsorption by Sewage Sludge-Based Activated Carbons in Batch and Fixed Bed Systems. *Bioresour. Technol.* 87, 221–230.
- Sacher F., Lange F.T., Brauch H.J., Blankenhorn I., 2001. Pharmaceuticals in Groundwaters- Analytical Methods and Results of a Monitoring Program in Baden-Wurttemberg, Germany. *J. Chromatogr. A* 938 (1–2), 199–210.
- Sariaslani F.S. 1989. Microbial enzymes for oxidation of organic molecules. *Critical Review in Microbial.* 9, 171–257.
- Shaarani F.W., Hameed B.H., 2010. Batch adsorption of 2,4-dichlorophenol onto activated carbon derived from agricultural waste. *Desalination* 255, 159–164.
- Siddique M., Farooq R., Shaheen A., 2011. Removal of reactive blue 19 from wastewaters by physicochemical and biological processes-a Review. *Pakistan J. Chem. Society* 33 (2), 284.
- Smith J.A., Galan A., 1995. Sorption of non-ionic organic contaminants to single and dual organic cation bentonite from water. *Environ. Sci. Technol.* 29, 685–692.
- Smith J.A., Jaffe P.R., Chiou C.T., 1990. Effect of ten quaternary ammonium cations on tetrachloromethane sorption to clay from water. *Environ. Sci. Technol.* 24, 1167–1172.
- Smith J.J., Lilly M.D., 1990. The effect of agitation on the morphology and penicillium production of *Penicillium chrysogenum*. *Biotechnol. Bioeng.* 35, 1011–1023.
- Soulet B., Tauxe A., Tarradellas J., 2002. Analysis of acidic drugs in Swiss wastewaters. *Int. J. Environ. Anal. Chem.* 82 (10), 659–667.
- Sposito G., 1984. *The Surface Chemistry of Soils*. Oxford University Press, New York, USA.
- Stavropoulos G.G, Zabaniotou A., 2005. Production and characterisation of activated carbon from olive seed waste residue. *Microporous Mesoporous Mater.* 82, 79–85.
- Tan I.A.W., Hameed B.H., Ahmad A.L., 2007. Equilibrium and kinetic studies on basic dye adsorption by oil palm fiber activated carbon. *Chem. Eng. J.* 127, 111–119.

- Tan I.A.W., Ahmad A.L., Hameed B.H., 2009. Adsorption isotherms, kinetics, thermodynamics and desorption studied of 2,4,6-trichlorophenol on oil palm empty fruit bunch- based activated carbon, *J. Hazard. Mater.* 164, 473–482.
- Ternes T.A., 1998. Occurrence of drugs in German sewage treatment plants and rivers. *Water Res.* 32, 3245–3260.
- Ternes T.A., Stumpf M., Mueller J., Haberer K., Wilken R.D., Servos M., 1999. Behavior and occurrence of estrogens in municipal sewage treatment plants I. Investigations in Germany, Canada and Brazil. *Sci. Total Environ.* 225 (1/2), 81–90.
- Thurston C.F., 1994. The structure and function of fungal laccases. *Microbiol.* 140: 19–26.
- Toth J., 1995. Thermodynamical correctness of gas/solid adsorption isotherm equations. *J. Colloid Interf. Sci.* 163, 299–302.
- Trevors J.T., Cotter C.M., 1990. Copper toxicity and uptake in microorganisms: a review. *J. Indus. Micob.* 6, 77– 84.
- Tseng R. L., Wu, F. C., Juang R. S., 2003. Liquid-phase adsorption of dyes and phenols using pinewood-based activated carbons. *Carbon* 41,487–495.
- Werth C.J., Reinhard M., 1997. Effects of temperature on trichloroethylene desorption on silica gel and natural sediments. 2. Kinetics. *Environ. Sci. Technol.* 31, 697–703.
- Wesenberg D, Kyriakides I, Agathos S.N., 2003. White-rot fungi and their enzymes for the treatment of industrial dye effluents. *Biotechnol. Adv.* 22, 161–187.
- Woodard F., 2001. *Industrial Waste Treatment Handbook*, by Butterworth–Heinemann Page 335 Chapter 8 Methods for Treating Wastewaters from Industry.
- Yhdego M., 1995. Environmental pollution management for Tanzania: towards pollution prevention. *J. Clean. Prod.* 3, 143–155.
- Zollinger H., 1991. *Color chemistry. Synthesis, properties and application of organic dyes and pigments.* VCH 2<sup>ed</sup>, New York, US





## **Chapter 3:**

### **Materials and general methods**

---

This chapter includes the materials and general methods implemented to carry out this work and which are not completely described through the research articles content. It is devised into four parts, the first one concerned the preparation of activated carbon and its characterization, the second part described the different adsorbates, the third part is devoted to biological treatment and the fourth part listed the analytic methods used in the both processes.

### 3.1. Preparation of activated carbons

#### 3.1.1. Raw Material

Exhausted Olive-waste cakes, obtained from an oil factory “Agrozitex” located in Sfax, Tunisia, was used as raw material for the production of activated carbons. The olive-waste cake presents the solid by-product generated from the traditional press extraction method as well as the continuous three phase system used for extraction of olive oil. The solid waste olive-waste cakes (OWC) or “orujo” is a combination of olive pulp and stones (Fernández-Bolaños et al., 2006). Exhausted olive-waste cake was obtained after extraction of the oil remaining in the olive-waste cakes as indicated in Figure 3.1.

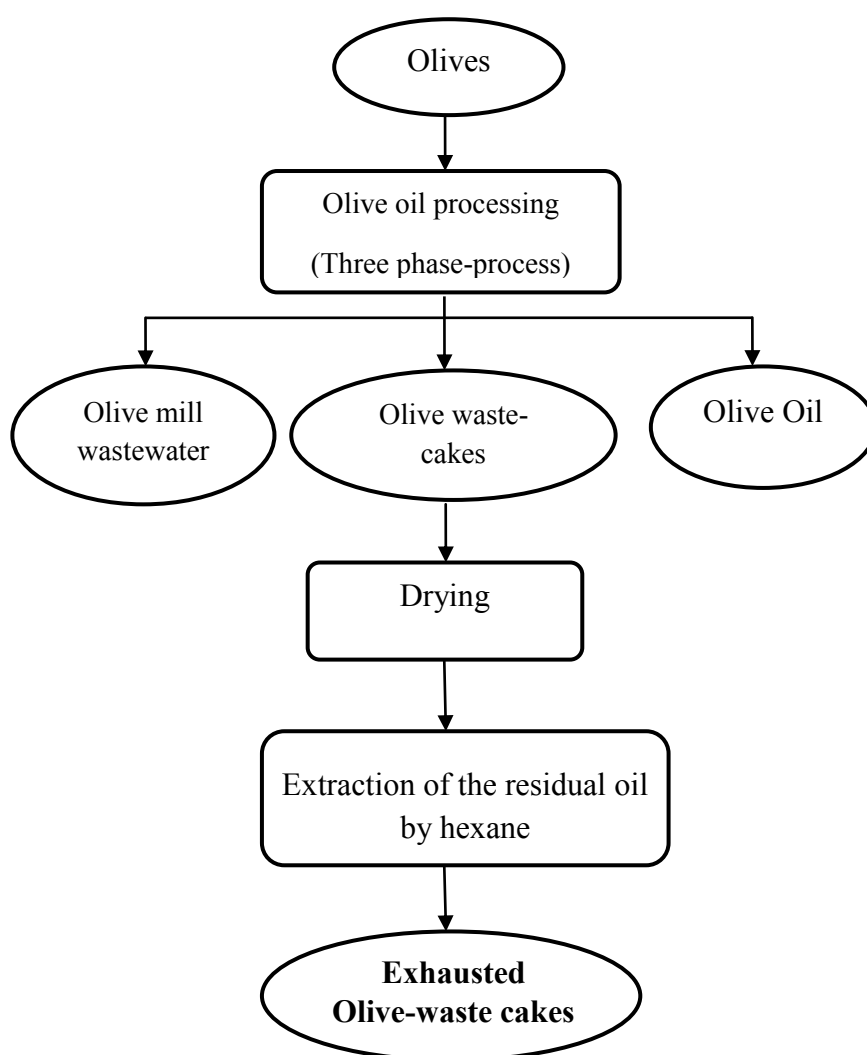


**Figure 3.1.** Three phase of olive oil processing

Exhausted Olive-waste cake was then dried at 105 °C for 24 hours and finally ground using an electric grinder equipped with a sieve of 1.5 mm diameter.

### 3.1.2. Preparation of activated carbons

Chemical activation method was adapted for the production of activated carbons. For this purpose, phosphoric acid (analytical grade) was retained as a dehydrating agent. Each preparation test was conducted as follows: 40 g of the crushed ( $\text{Ø} < 1.5$  mm) and dried precursor was mixed with  $\text{H}_3\text{PO}_4$  solutions having different concentrations: 30, 45, 60 and 85%  $\text{H}_3\text{PO}_4$  in weight. The impregnation ratio, defined by the weight ratio of impregnant ( $\text{H}_3\text{PO}_4$ ) to precursor, was 1; 1.25; 1.5; 1.75; 1.85 and 2. The impregnation was carried out in a stirred pyrex reactor equipped with a reflux condenser (Figure 3.2). Stirring was used to ensure the access of the acid to the interior of the olive-waste cake particles. The temperature and the duration of the reaction were 104 °C and 2 hours, respectively. Agitation and heating were ensured by a heating magnetic stirrer with connected temperature regulator probe made of Teflon. The pyrolysis of the impregnated material was conducted in a cylindrical stainless steel reactor, inserted into a tubular regulated furnace under continuous nitrogen flow ( $0.5 \text{ Lmin}^{-1}$ ) (Figure 3.3). Pyrolysis temperature ranged from 350 to 650 °C, while pyrolysis time was maintained at 2 hours. After cooling down to room temperature, under the same flow of nitrogen, the obtained activated carbon was thoroughly washed with hot distilled water until neutral pH. The sample was then dried at 105 °C overnight, ground (until a granulometry ranging between 100 and 160  $\mu\text{m}$ ) and finally kept in hermetic bottle for subsequent uses.

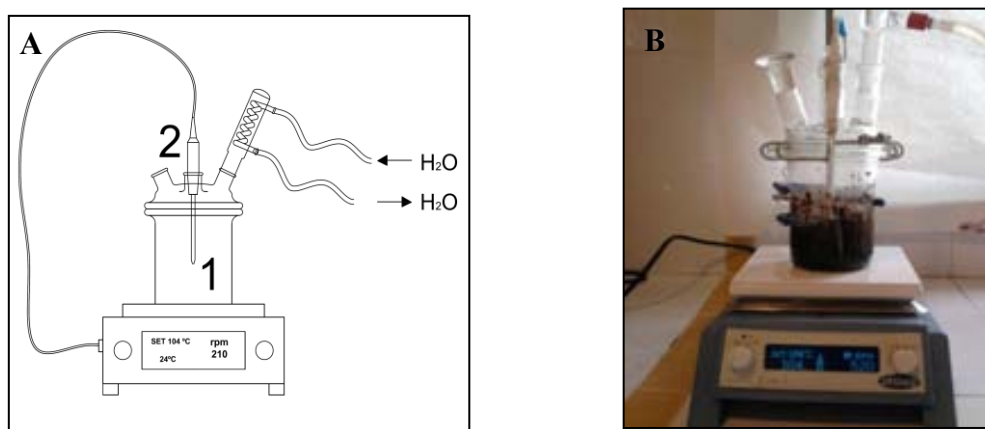


**Figure 3.2.** Schematic representation (A) and photography (B) of the reactor used for impregnation step

1: Pyrex reactor

2: Probe

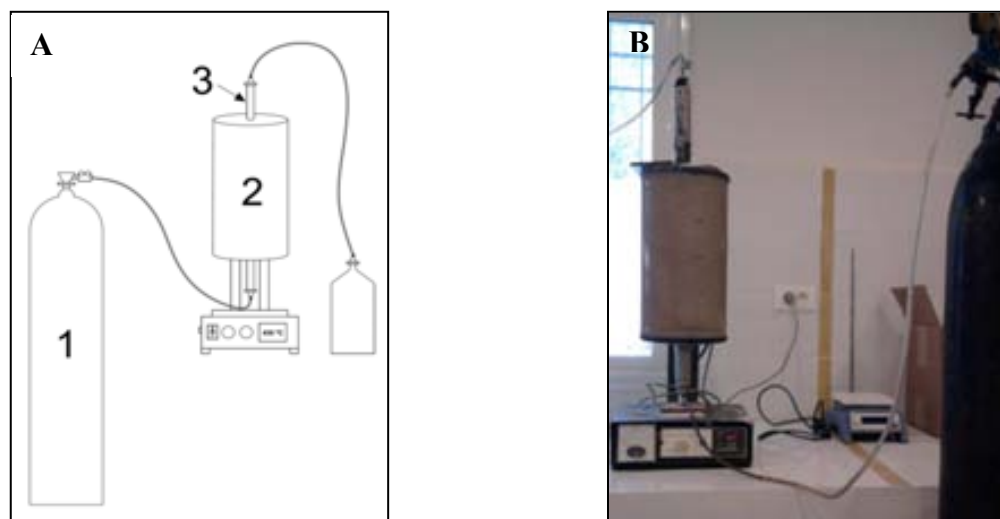


**Figure 3.3.** Schematic representation (A) and photography (B) of the reactor used for pyrolysis step

1: Nitrogen bottle      2: Tubular furnace      3: Reactor

### 3.1.3. Characterization of the prepared adsorbents

#### 3.1.3.1. Iodine number

The iodine number is defined in term of the milligrams of iodine ( $I_2$ ) adsorbed by 1 g of activated carbon when the iodine equilibrium concentration is 0.01M (ECCMF, 1986). In this work, the three- point method was adopted. The latter avoid the use of the correction factor usually employed in the less accurate single point-method (ASTM, 1999). The procedure of the iodine number determination is as follows: three dry samples of activated carbon were weighed out into three 250-ml conical flasks (sample weight ranged between 300 and 600 mg). Ten millilitres of 5% (in weight) hydrochloric acid solution were added to each flask and then mixed until the carbon became wet. The mixtures were then boiled for 30 seconds and finally cooled. One hundred millilitres of 0.05M standard iodine solution were added to each flask. The contents were vigorously shaken for 30 seconds and then immediately filtered. A 50 ml aliquot of each filtrate was titrated by a standardized 0.1M sodium thiosulfate solution. For each sample, the obtained iodine residual concentration should be included into 0.004 and 0.02 M. The plot of the amount of iodine fixed per gram of sorbent versus residual iodine concentration gives a straight line which allows determining graphically the iodine number (ordinate corresponding to a residual concentration of 0.01M).

### **3.1.3.2. Methylene blue (MB) adsorption**

Methylene blue adsorption tests were conducted by mixing 0.300 g of the prepared activated carbon with 100 ml of 1000 mg L<sup>-1</sup> methylene blue solution (Yang, and Chong Lua, 2006). After agitation during 24 hours, the suspension was filtered and the MB residual concentration was measured at 660 nm, using an UV/Visible spectrophotometer (OPTIMA, SP-3000 plus). A linear Beer–Lambert relationship was established and used for the concentration determination.

### **3.1.3.3. Chemical surface properties**

#### ***a) Cation-exchange capacity***

In studies on activated carbons, Bohem's titration was widely used to determine the cation-exchange capacity (CEC) of sorbents (El sheikh et al., 2004). A weighted amount of adsorbent (0.100 g) was placed into an Erlenmeyer flask. A volume of 20 ml of 0.1 M NaOH solution was added. To attain equilibrium, the suspension was shaken for 24 hours. After filtration, the residual NaOH concentration was determined by titration with 0.1M hydrochloric acid solution, using phenolphthalein as indicator. The quantity of NaOH consumed was converted to CEC and expressed in meq g<sup>-1</sup> (Puziy et al., 2002).

#### ***b) pH at the point of zero charge***

The Point of Zero Charge, pH<sub>PZC</sub> is defined as the pH of the aqueous solution in which the solid presents a neutral electric potential: pH at which the initial value is the same as the final value. It allows quantifying the acidic or basic character of the carbon. Depending on the precursor origin and the preparation mode (chemical or physical), activated carbons can have an acidic, basic or neutral nature depending on the pH<sub>pzc</sub>: the carbon surface is positively charged at pH < pH<sub>PZC</sub> and negatively charged at pH > pH<sub>PZC</sub>. pH<sub>pzc</sub> has been determined according to the method described by Furlan et al. (2010). It is noted that pH<sub>pzc</sub> is considered as the pH at which the electric charge density of a given surface equals zero. This parameter was obtained through mixtures of 0.1 g of activated carbon with 50 mL of 0.01 M NaCl standard solution in nine Erlenmeyer flasks to which appropriate quantities of HCl or NaOH were added to obtain the following pH values: 2.5; 4.0; 5.0; 6.0; 7.0; 8.0; 9.0; 10.0 and 11.0. The mixtures were shaken for 48 h at room temperature. Then, the final pH of each mixture

was measured. The  $\text{pH}_{\text{PZC}}$  is the point where the curve  $\text{pH}_{\text{final}}$  versus  $\text{pH}_{\text{initial}}$  intersects the line  $\text{pH}_{\text{initial}} = \text{pH}_{\text{final}}$ .

A high precision pH meter (Metrohm, model 632) equipped with a combined glass electrode (Metrohm) was used.

#### **3.1.3.4. Bulk density**

Activated carbon sample was placed in a graduated cylinder, tapped several times until constant volume and then weighted. The bulk density was calculated as the ratio of the weight sample to its volume and expressed in  $\text{g cm}^{-3}$  (ECCMF, 1986).

#### **3.1.3.5. Textural characteristics**

Specific surface area of the prepared activated carbons, total pore volume ( $V_{\text{tot}}$ ) and pore size distribution were determined through  $\text{N}_2$  adsorption at 77K, using an Autosorb1-Quantachrome instrument. The BET (Brunauer-Emmet and Teller) model was applied to fit nitrogen adsorption isotherm and evaluate the surface area ( $S_{\text{BET}}$ ) of the sorbent (BET, 1938).

#### **3.1.3.6. Morphology analysis**

In order to know the structure sight of activated carbon, scanning electron microscopy (SEM) was generally employed to visualise sample morphology. Pore structure and structural changes happening after chemical activation could be also observed. In the present work, the raw material (olive-waste cakes) and the activated carbon prepared in the optimal conditions were analyzed by this technique using a Philips XL30 microscope.

#### **3.1.3.7. Infrared spectroscopy analysis**

The surface functional groups and structure were studied by Fourier transform infrared (FTIR) spectroscopy. The FTIR spectra of the raw material and the resulting activated carbon were recorded between 400 and 4000  $\text{cm}^{-1}$  in a NICOET spectrometer.

#### **3.1.4. Adsorption on column**

The adsorptive properties of activated carbon without and after impregnation with  $\text{KMnO}_4$  towards the heavy metal copper were studied in a column. The experimental

device (Figure 3.4) includes a Pyrex chromatographic column and a peristaltic pump type (Gilson).

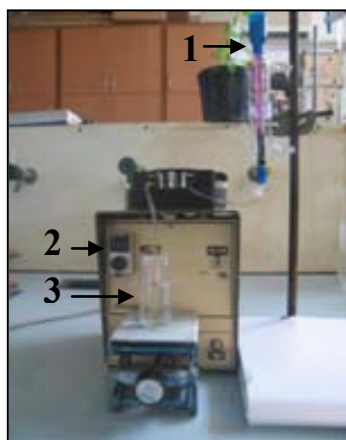


**Figure 3.4.** Experimental device for activated carbon impregnation

1: Column                      2: Peristaltic pump      3: Collected effluent

#### 3.1.4.1. Preparation of $\text{KMnO}_4$ -modified activated carbon

The modified activated carbon was prepared as follows: the adsorbent was transferred into a laboratory column (SIGMA chemical Company) packed at the bottom with glass wool and previously filled with distilled water. The column was performed in a Pyrex glass tube of 0.7 cm internal diameter and 14 cm in effective height. It is equipped with fixed polypropylene end caps, polyethylene bed support and Luer-Look inlet and outlet fittings (Figure 3.4). After settlement, by gravity, of the activated carbon particles, the adsorbent bed was covered with a thin layer of glass wool in order to avoid disturbance during the inlet of the influent. The level of water or solution present at the top of the bed was always fixed at the same level as that of the glass wool. A peristaltic pump (Gilson-Minipuls 2) - connected to the bottom of the column by a silicon tube of low internal diameter ( $\text{Ø} = 1.2 \text{ mm}$ ) and very limited length (to minimize dead volume)-ensured a flow-rate of  $0.5 \text{ mL min}^{-1}$ . The total dead volume fraction of the column ((bed void volume + connection tubing volume)/ fixed bed volume) was 53.3 %.

To modify the activated carbon surface, a  $10^{-3} \text{ M KMnO}_4$  solution was pumped down through the column. The effluent, collected at the bottom of the column with an automatic fraction collector (Gilson), was sampled in 30 mL-tubes, and stored for Mn analysis and pH measurement. Thereafter, the modified activated carbon column was washed with doubly distilled water.

## **3.2. Adsorbates**

### **3.2.1. Metallic species**

Effluent samples, collected from column tests, were analysed for metal species (Mn and Cu).

Samples collected from the textile effluent Lanaset grey G, treated biologically, were analysed for metallic species (Cr and Co).

### **3.2.2. Dyes**

#### **3.2.2.1. Textile dye**

Lanaset Grey G, a dark blue powder composed of a mixture of metal complex dyes, was purchased from Ciba (Specialty Chemicals, Barcelona ref. 080173.5). The chemical formula of this water-soluble dye is unavailable. However, this material is known to contain cobalt II (0.79 wt %) and chromium III (2.5 wt %) as organo-metal complexes.

The additives used industrially with the dye Lanaset Grey G (Esterol 126, Citric acid, Amplex DG and Antifoam) were supplied by the industry “Artextil S.A” located in Sabadell-Barcelona. The component Esterol 126 is an equalizer, the acid citric is used for the adjustment of pH, the Amplex DG is an additive used for avoiding the reduction and the antifoam is used for avoiding the formation of the foam.

#### **3.2.2.2. Tannery dye**

Black Dycem TTO is a commercial patented dye, extensively used in a tannery industry located in Sfax, Tunisia. It was supplied to this factory by “Colorantes Industriales, S.A” (Barcelona, Spain). According to its technical specifications, this dye, with a black color, is water soluble, it is not rapidly biodegraded and the effluent containing this dye must be recycled. It is classified as an acid dye.

The tannery effluent was collected from a tannery industry located in Sfax, Tunisia. Many techniques were used for the characterization of the effluent such as pH, conductivity, turbidity, metals contents and organic matter. More details of the analytic methods used were described and given before in the section analytic methods.

More details concerning the two dyes are provided in the technical reports presented in Annexes 2 and 3.



### 3.2.3. Pharmaceuticals products

The pharmaceuticals products studied in this work were ibuprofen, ketoprofen, diclofenac and naproxen.

#### 3.2.3.1. Ibuprofen

Ibuprofen is one of the most consumed medicines all over the world. For instance, in the United Kingdom it is one of the top five most consumed drugs, having an estimated annual production of several kilotons (Sebastine and Wakeman, 2003). It is a nonsteroidal anti-inflammatory (NSAID), analgesic and antipyretic drug widely used in the treatment of rheumatic disorders, pain and fever. Being slightly soluble in water is readily soluble in organic solvents, and so it has high mobility in the aquatic environment (Mestre et al., 2007). Ibuprofen was synthesized by Shasun Chemicals and Drugs Ltd. (lot IBU0307598). It has a molecular weight of  $206.28 \text{ g mol}^{-1}$  and its molecular structure is depicted in Figure 3.5.

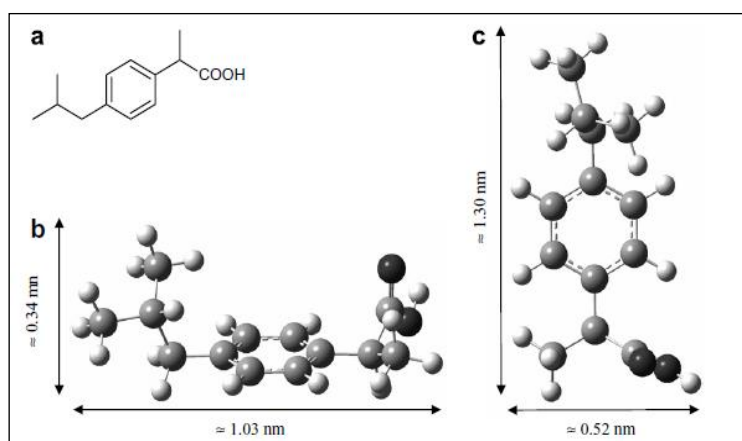


**Figure 3.5.** Molecular structure of ibuprofen (a) General structure (b) and (c) arrangement of its atoms in space (Mestre et al., 2007)

#### 3.2.3.2. Ketoprofen

Ketoprofen, (RS) 2-(3-benzoylphenyl)-propionic acid (chemical formula  $\text{C}_{16}\text{H}_{14}\text{O}_3$ ), is a type of nonsteroidal anti-inflammatory drug (NSAID) that is used for general pain relief and to treat symptoms of arthritis (Kantor, 1986). The medication is effective in reducing pain, inflammation, and joint swelling associated with different forms of arthritis and painful conditions. It has a molecular weight of  $254.28 \text{ g mol}^{-1}$  and its molecular structure is depicted in Figure 3.6.

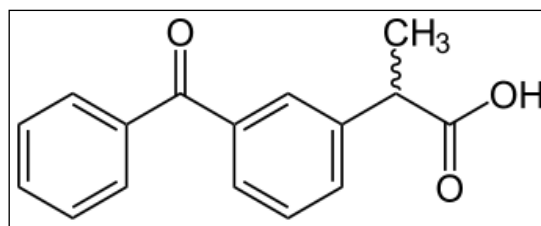


**Figure 3.6.** Molecular structure of Ketoprofen

### 3.2.3.3. Diclofenac

Diclofenac, 2-(2,6-dichloranilino) phenylacetic acid (chemical formula  $C_{14}H_{11}Cl_2NO_2$ ) is a non-steroidal anti-inflammatory drug (NSAID) taken to reduce inflammation and as an analgesic reducing pain in certain conditions. Diclofenac is often used to treat chronic pain associated with cancer, in particular if inflammation is also present (Step I of the World Health Organization (WHO) scheme for treatment of chronic pain). It has a molecular weight of  $296.25 \text{ g mol}^{-1}$  and its molecular structure is depicted in Figure 3.7.

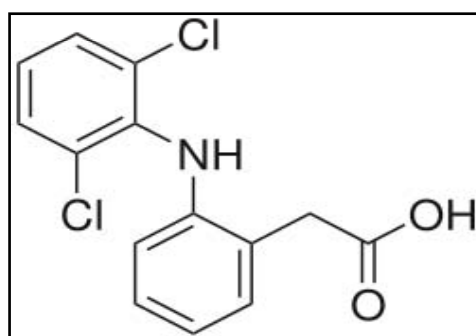


**Figure 3.7.** Molecular structure of Diclofenac

### 3.2.3.4. Naproxen

Naproxen, (*S*)-6-methoxy-methyl-2-naphthalene acetic acid (chemical formula  $C_{14}H_{14}O_3$ ), is a widely used non-steroidal anti-inflammatory drug in the treatment of rheumatoid arthritis, spondylitis, and osteoarthritis. This drug is recognized to be highly effective and clinically safe (Yokoyama et al., 2006). It has a molecular weight of  $230.25 \text{ g mol}^{-1}$  and its molecular structure is depicted in Figure 3.8.

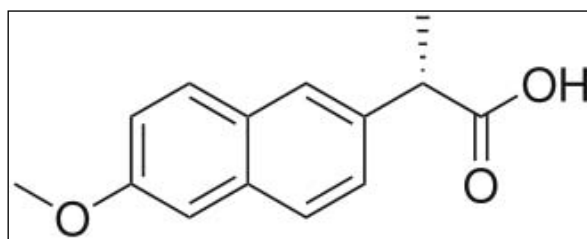


**Figure 3.8.** Molecular structure of Naproxen

### 3.2.4. Adsorption studies

Equilibrium and kinetics of adsorbates were studied essentially at 25 °C. In general, adsorption tests were carried out in batch system by adding various amounts of adsorbent to a series of 500 mL Erlenmeyer flasks filled with a 300 mL solution of one of the adsorbate either: textile dye, tannery dye or one of the selected drugs. The flasks were shaken at 200 rpm with a magnetic stirrer until the concentration of the adsorbate become constant (equilibrium). Then each solution was separated from the sorbent by centrifugation at 13000 rpm for 5 min.

For a given pH, the amount of adsorbate fixed at equilibrium  $q_e$  ( $\text{mg g}^{-1}$ ) was calculated from the following equation:

$$q_e = \frac{(C_0 - C_e)V}{m_{AC}} \quad (1)$$

where  $C_0$  and  $C_e$  ( $\text{mg L}^{-1}$ ) are the liquid phase concentrations of the adsorbate at initial and equilibrium, respectively,  $V$  the volume of the solution (L) and  $m_{AC}$  is the mass of activated carbon used in the experiment (g).

The effect of pH and temperature on the adsorption of the different adsorbates, were also investigated. More details are given in chapter 3 in the experimental part of the articles relatives to each adsorbate.

## 3.3. Biological treatment

### 3.3.1. Microorganisms

The potential of three strains of white-rot fungi was investigated for biological treatment of a tannery dye, Black Dycem TTO: *Trametes versicolor*, *Ganoderma lucidum* and *Irpex lacteus* (Figure 3.9). The strain *T. versicolor* 42530 was acquired

from the American type Culture Collection (ATCC). *G. lucidum* (Leysser) Karsten FP-58537-Sp was provided by the US Department of Agriculture Forest Products Laboratory, Madison, Wis. *I. lacteus* (AX1) was isolated from agricultural soils at the Long Term Ecological Research site at Michigan State University. *G. lucidum* and *I. lacteus* were a gift from Dr. C. A. Reddy (Michigan State University). All fungi were maintained on 2% malt extract agar slants at 25 °C until use. Subcultures were routinely made.



*Trametes vesicolor*

*Ganoderma lucidum*

*Irpex lacteus*

**Figure 3.9.** White-rot fungi tested for the degradation of the tannery dye Black dycem TTO

### 3.3.2. Culture methods

Mycelial suspension of each fungus was obtained by inoculation of four 1 cm diameter plugs from the fungus growing zone on 2% malt agar, in a 500 mL Erlenmeyer flask containing 150 mL of 2% (w/v) malt extract medium. This was incubated at 25 °C under orbital agitation (135 rpm, r = 25 mm). After 4-5 days, a dense mycelial mass was formed. It was separated from the culture medium, resuspended in an equal volume of a sterile saline solution (0.85% (w/v) NaCl) and then disrupted with an X10/20 homogenizer (Ystral GmbH). The resulting mycelial suspension was stored at 4 °C until use. The suspension was used to obtain fungal pellets by inoculating 1 mL of the suspension in 250 mL malt extract medium (2%) (adjusted to pH 4.5) in 1 L Erlenmeyer flask. The flask was incubated in an orbital shaker (135 rpm, r = 25 mm) at 25 °C for 5–6 days. The pellets thus obtained can be stored in sterilized saline solution (0.85% NaCl) at 4 °C where they will remain active for up to 2 months without losing their morphology (Blánquez et al., 2004). A diagram of the process, for the obtaining of

mycelial suspension and pellets of the fungus *Trametes versicolor* can be observed in Figure 3.10.

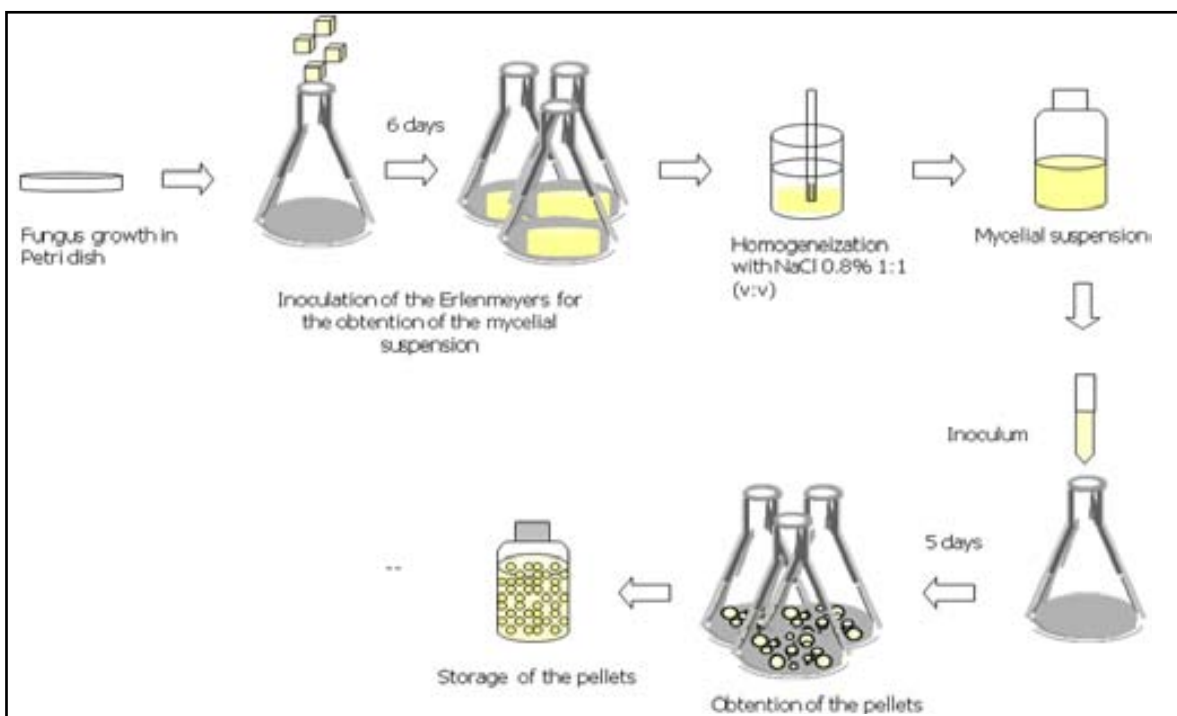


**Figure 3.10.** Scheme of the methodology to obtain pellets of *Trametes versicolor* (Blánquez, 2005)

### 3.3.3. Media

Two different liquid media were employed:

Malt extract medium (ME): The ME contained  $20 \text{ g L}^{-1}$  malt extract (Sharlau, Barcelona, Spain).

Defined medium (DM): The DM contained per liter: 8 g glucose, 1.9g  $\text{NH}_4\text{Cl}$ , 1.168 g 2,2-dimethylsuccinate (DMS) buffer, 10 mL macronutrients solution (per liter:  $\text{KH}_2\text{PO}_4$  20g,  $\text{MgSO}_4 \cdot 7\text{H}_2\text{O}$  5 g,  $\text{CaCl}_2$  1g) and 1 mL micronutrients solution (per liter: nitrilo tri-acetic acid 1.5g,  $\text{MgSO}_4 \cdot 7\text{H}_2\text{O}$  3.0g,  $\text{MnSO}_4 \cdot \text{H}_2\text{O}$  0.5g,  $\text{NaCl}$  1.0g,  $\text{FeSO}_4 \cdot 7\text{H}_2\text{O}$  0.1g,  $\text{CoSO}_4$  0.1g,  $\text{ZnSO}_4 \cdot 7\text{H}_2\text{O}$  0.1g,  $\text{CaCl}_2 \cdot 2\text{H}_2\text{O}$  0.1g,  $\text{CuSO}_4 \cdot 5\text{H}_2\text{O}$  0.01g,  $\text{AlK}(\text{SO}_4)_2 \cdot 12\text{H}_2\text{O}$  0.01g,  $\text{H}_3\text{BO}_3$  0.01g,  $\text{NaMoO}_4$  0.01g) and 10 mg thiamine.

### 3.3.4. Reactor

A glass air-pulsed bioreactor, with a working volume of 1500 mL, was used for the decolorization process. The air pulse frequency was  $0.16 \text{ s}^{-1}$ , allowing fluidization and

liquid phase homogenization of the biomass. The bioreactor was equipped with a pH controller in order to maintain pH at 4.5 by adding HCl 1M or NaOH 1M when it was required and the temperature was maintained at 25 °C (Figure 3.11) (Blázquez, 2005).

Table 2.1 shows the main dimensions of the reactor. Its heads feature several ports that are used for the pH probe, air exit system, foam collection system, acid and basic entry and sampling (Figure 3.12). The homogenization in the reactor is achieving by entering air in pulses. The pulsating flow is generated by a pneumatic transmission disturbance in the air pulse form to the culture broth contained in the bioreactor.

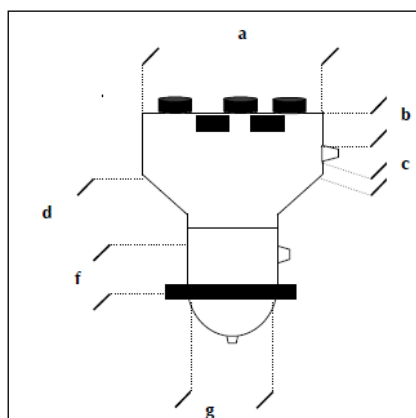


**Table 3.1:** Geometric characteristics of the 1.5 L air fluidized bioreactor

Piece	Dimensions (cm)
a	14
b	2
c	5.5
d	2
f	11.5
g	7.5

**Figure 3.11.** Scheme of the the 1.5 L air fluidized bioreactor



**Figure 3.12:** Experimental device of the tannery dye decolorization in the reactor

### **3.4. Analytical methods**

#### **3.4.1. pH measurements**

The pH of the samples was measured using a Basic 20 pH meter (Crison, Barcelona, Spain). Preliminary standardization was systematically carried out using suitable buffer solutions.

#### **3.4.2. Conductivity**

The electrical conductivity was determined using an electronic conductivity TACUSSEL (CD6NG type), equipped with an immersion probe. The determination of the cell constant was first performed through a standard solution of KCl 0.1 M.

#### **3.4.3. Turbidity**

Turbidity is the reduction of transparency of a liquid due to the presence of undissolved matter (suspended particulate matter). The apparatus used (WTW Turb 550 IR) is equipped with an infrared lamp for making measurements at wavelengths above 800nm, which avoids interference from the colored substances.

The turbidimeter was previously calibrated using commercial standards: 0.02, 10 and 1000 NTU (Nephelometric Turbidity Unit).

#### **3.4.4. Metals contents**

The metal species were analyzed using acetylene-air flame/atomic absorption spectrophotometer (HITACHI Model Z-6100).

#### **3.4.5. Organic matter**

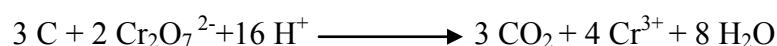
A number of different tests were used to determine the organic contents of the effluent: (1) biological oxygen demand BOD<sub>5</sub> (2) chemical oxygen demand COD and (3) total organic compound TOC.

##### **a) Biological Oxygen Demand (BOD)**

The most widely used parameters of organic pollution applied to both wastewater and surface water is the 5-day BOD (BOD<sub>5</sub>). It corresponds to the measurement of the dissolved oxygen used by microorganisms in the biochemical oxidation of organic matter at 20 °C in dark. BOD<sub>5</sub> is measured by the manometric method, using a digital respirometer WTW (BSB-Controller Model 620 Controller Model T).

**b) Chemical Oxygen Demand (COD)**

The COD test is used to measure the content of organic and inorganic matter of both wastewater and natural waters. The COD is determined according to a standard method (AFNOR, 1997). The oxygen equivalent of the organic matter that can be oxidized is measured by using a strong chemical oxidizing agent in an acidic medium. Potassium dichromate has been found to be excellent for these purposes. The test must be performed at an elevated temperature. The oxidation was performed by potassium dichromate, that was found to be excellent for these purposes, and acts as a strong oxidizing agent and oxidizes the organic and inorganic matter in the waste water. The reaction can be expressed as:



The  $\text{Cr}^{3+}$  obtained by the oxidation reaction was measured by spectrophotometer at 620 nm.

**c) Total Organic Carbon TOC:**

Another means for measuring the organic matters present in the water is the TOC test, which is especially applicable to small concentrations of organic matter. This test is performed by injecting a known quantity of sample into a high-temperature furnace or chemically-oxidizing environment. The organic carbon is oxidized to carbon dioxide in the presence of a catalyst.

The carbon dioxide that was produced was quantitatively measured by means of an infrared analyzer. Acidification and aeration of the sample prior to analysis eliminate errors due to the presence of inorganic carbon. The test can be performed rapidly and is becoming more popular. The TOC value was given directly by the instrument TOC 500.

**3.4.6. Dry cell weight**

Pellets dry weight was determined after vacuum filtration through reweighed glass microfiber filters (Whatman GF/A, 47 mm diameter) and drying at 105 °C to a constant weight.



#### **3.4.7. Glucose**

Glucose concentrations were measured with an YSI 2700 enzymatic analyzer (Yellow Springs Instruments and Co). The available range of this glucose concentration analyzer is 0 to 20 g L<sup>-1</sup> with an accuracy of ± 2% or 0.04 g L<sup>-1</sup>. The analysis is based on the glucose enzymatic oxidation to peroxide using glucose oxidase immobilized on the membrane and the subsequent reduction of peroxidase in a platinum anode.

#### **3.4.8. Laccase activity**

Laccase activity was measured using a modified version (Kaal et al., 1993) based on the first step of the method used for the determination of manganese peroxidase (MnP) (Wariishi et al., 1992), where 2,6-dimethoxyphenol (DMP) is oxidized by laccase, even in the absence of a cofactor. One activity unit (AU) was defined as the number of micromoles of DMP oxidized per minute. The DMP extinction coefficient was 24800 M<sup>-1</sup> cm<sup>-1</sup>.

#### **3.4.9. Toxicity**

A Microtox system from Microbics Corporation was used. This method is based on the percentage of decrease in the amount of light emitted by the bioluminescent marine bacterium *Vibrio fischeri* upon contact with the sample. Toxicity is, then, inversely proportional to the intensity of light emitted after the contact with the toxic substances. The effective concentration, EC<sub>50</sub>, is defined as the concentration that produces a 50% light reduction. EC<sub>50</sub> was measured after 5 and 15 min contact time. A color correction was done according to the Microtox instructions. To obtain 50% inhibition the fractions were diluted wherever necessary with purified water containing 2% NaCl. This diluent is also used as non-toxic control. Effluent toxicity was expressed in units of EC<sub>50</sub>.

#### **3.4.10. Dye concentrations**

Absorbances of samples were measured with a Varian UV/vis Cary spectrophotometer. Standardization curve was plotted by measuring the absorbances of different dye solutions at maximum absorption wavelength.

#### **3.4.11. Statistical analyses**

Analysis of variance (ANOVA) of the data was performed using SPSS (17) for Windows.

## REFERENCES

- AFNOR, 1997. Recueil des normes AFNOR: Qualité de l'eau, Méthodes d'analyse, AFNOR, La Plaine Saint-Denis, (In French).
- ASTM, 1999. Standard Test Method for Determination of Iodine Number of Activated Carbon. ASTM Committee on Standards, ASTM D 4607-94, ASTM, Philadelphia, PA.
- Brunauer S., Emmett P. H., Teller E., 1938. J. Am. Chem. Soc. 60, 309
- Blánquez P., Casas N., Font X., Gabarrell X., Sarrà M., Caminal G., Vicent T., 2004. Mechanism of textile metal dye biotransformation by *Trametes versicolor*. Water Res. 38, 2166-2172.
- Blánquez P., 2005. Desenvolupment d'un process a escala pilot per el tractament del colorant textil Gris Lanaset G amb *Trametes versicolor*. PhD thesis. Universitat Autònoma de Barcelona.
- ECCMF (European Council of Chemical Manufacturers' Federations), 1986. Test Methods for activated carbon: [http://www.cefic.org/Documents/Other/Test-method-for-Activated Carbon 86.pdf](http://www.cefic.org/Documents/Other/Test-method-for-Activated-Carbon-86.pdf).
- El-Sheikh A.H., Newman A.P., Al Daffae H.K., Phull S., Creswell N., 2004. Characterisation of activated carbon prepared from a single cultivar of Jordanian olive stones by chemical and physicochemical techniques. J. Anal. Appl. Pyrolysis 71, 151–164.
- Fernández-Bolaños J., Rodríguez G., Rodríguez R., Guillén R., Jiménez A., 2006. Potential use of olive by-products. Extraction of interesting organic compounds from olive oil waste. Grasas y Aceites 57 (1), 95–106.
- Furlan F.R., Da Silva L.G.M., Morgado A.F., De Souza A.A.U., De Souza S.M.A.G.U., 2010. Removal of reactive dyes from aqueous solutions using combined coagulation/ flocculation and adsorption on activated carbon. Res. Conserv. Recycling 54, 283–290.
- Haimour N.M., Emeish S., 2006. Utilization of date stones for production of activated carbon using phosphoric acid. Waste Manage. 26, 51–60.
- Kaal E.E.J., De Jong E., Field J.A., 1993. Stimulation of ligninolytic peroxidase activity by nitrogen nutrients in the white rot fungus *Bjerkandera sp.* Strain BOS55. Appl. Environ. Microb. 59, 4031–4036.
- Kantor T. G., 1986. "Ketoprofen: a review of its pharmacologic and clinical properties". Pharmacotherapy 6 (3), 93–103.

- Mestre A.S., Pires, J.M.F. Nogueira, Carvalho A.P., 2007. Activated carbons for the adsorption of ibuprofen. *Carbon* 45, 1979–1988.
- Puziy A.M., Poddubnaya O.I., Martinez-Alonso A., Suarez-Garcia F., Tascon J.M.D., 2002. Synthetic carbons activated with phosphoric acid. I. Surface chemistry and ion binding properties. *Carbon* 40, 1493–1505.
- Sebastine I.M., Wakeman R.J., 2003. Consumption and environmental hazards of pharmaceutical substances in the UK. *Process Saf. Environ. Protect.* 81 (B4), 229–35.
- Vernersson T., Bonelli P.R., Cerrela E.G. Cukierman A.L., 2002. Arundo donax cane as a precursor for activated carbons preparation by phosphoric acid activation. *Bioresour. Technol.* 83, 95–104.
- Wariishi H., Valli K., Gold M.H., 1992. Manganese (II) oxidation by manganese peroxidase from the basidiomycete *Phanerochaete chrysosporium*. *J. Biol. Chem.* 267, 23688-23695.
- Yang T., Chong Lua A., 2006. Textural and chemical proprieties of zinc chloride activated carbons prepared from pistachio-nut shells. *Mater. Chem. Phys.* 100, 438–444.
- Yokoyama H., Horie T., Awazu S., 2006. Naproxen-induced oxidative stress in the isolated perfused rat liver. *Chem. Biol. Interact.* 160, 150–158.



## Chapter 4:

### Results and discussions

---

In the present thesis, two environmentally friendly processes are employed for the removal of some water contaminants i.e, metallic species, textile and tannery dyes, and pharmaceuticals products. The first process is one of adsorption on activated carbon prepared from a by-product and the second consists in biological treatment using white-rot fungi. The results obtained within this framework, presented in chapter 4, are significant and are the subject of six articles. These articles are incorporated into three topics:

**Topic 1:** is related to the preparation, characterization and environmental impact of the prepared activated carbons

**Topic 2:** Modeling of adsorption

**Topic 3:** Biological treatment



## **Topic 1: Preparation, characterization and environmental impact**

---

The methodology conducted for the preparation of the activated carbon from the feedstock olive-waste cakes, its characterization and the environmental impact associated with its preparation are presented in this topic. The below two articles, corresponding to sections 4.1.1 and 4.1.2, encompass the above-mentioned aspects. The first one is already published while the second is under revision.

### **4.1.1: Preparation of activated carbon from Tunisian olive-waste cakes and its application for adsorption of heavy metal ions.**

*Journal of Hazardous Materials, 162 (2009) 1522–1529*

### **4.1.2: Environmental impact associated with activated carbon preparation from olive-waste cake via life cycle assessment**

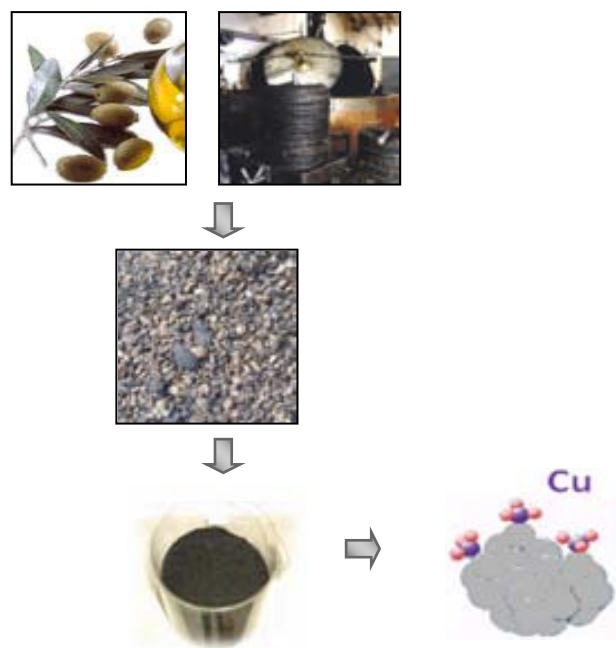
*Journal of Environmental Management, under revision.*





#### 4.1.1: Preparation of activated carbon from Tunisian olive-waste cakes and its application for adsorption of heavy metal ions.

---



**Abstract**

The present work explored the use of Tunisian olive-waste cakes, a by-product of the manufacture process of olive oil in mills, as a potential feedstock for the preparation of activated carbon. Chemical activation of this precursor, using phosphoric acid as dehydrating agent, was adopted. To optimize the preparation method, the effect of the main process parameters (such as acid concentration, impregnation ratio, temperature of pyrolysis step) on the performances of the obtained activated carbons (expressed in terms of iodine and methylene blue numbers and specific surface area) was studied. The optimal activated carbon was fully characterized considering its adsorption properties as well as its chemical structure and morphology. To enhance the adsorption capacity of this carbon for heavy metals, a modification of the chemical characteristics of the sorbent surface was performed, using  $\text{KMnO}_4$  as oxidant. The efficiency of this treatment was evaluated considering the adsorption of  $\text{Cu}^{2+}$  ions as a model for metallic species. Column adsorption tests showed the high capacity of the activated carbon to reduce  $\text{KMnO}_4$  into insoluble manganese (IV) oxide ( $\text{MnO}_2$ ) which impregnated the sorbent surface. The results indicated also that copper uptake capacity was enhanced by a factor of up to 3 for the permanganate-treated activated carbon.

**Keywords:** Activated carbon, Olive-waste cakes, chemical activation, modification, metal adsorption.

## **1. Introduction**

Various technologies such as precipitation, ion exchange, membrane filtration and reverse osmosis have been applied for the removal of pollutants from wastewaters (Chen and Wang, 2000; Vinod and Imran, 2000). However, these methods have somehow proven disadvantageous in as much as they require expensive equipments and/or continuous need of chemicals (Malkoc et al., 2006). Moreover, sometimes the above-mentioned methods fail to meet the Environmental Protection Agency requirements (Borba et al., 2007). Considering limitations of conventional methods for metal removal, the most promising alternative appears to be the adsorption process. This method is a cost-effective and user friendly technique for the removal of metallic micropollutants from water. Additionally, adsorption has been found to be superior to other techniques for water re-use in terms of the initial cost, simplicity of design, ease of operation and insensibility to toxic substances (Jusoha et al., 2007).

Activated carbon (AC) is the most commonly used and most effective adsorbent (Vinod and Imran, 2000, Chen et al., 2003, Daifullah et al., 2007). Nevertheless, its application fields are restricted due to its high cost. The use of low-cost wastes and agriculture by-products to produce activated carbon has been shown to provide economical solution to this problem (Cimino et al., 2005, Ioannidou, and Zabaniotou, 2007). The adsorption of organic micropollutants by activated carbon is being widely used in water and wastewater treatments and the advantages of this adsorbent have been well documented (Strelko and Malik, 2010). In other respect, there is evidence in the literature that activated carbon can remove metal ions, especially  $\text{Cu}^{2+}$ , from aqueous solutions (Chen et al., 2003, Strelko and Malik, 2010). However, sorptive capacity of untreated activated carbons towards heavy metals is rather low (Strelko and Malik, 2010). To enhance sorption capacity for cationic and oxyanionic metal species, modifications of activated carbon using oxidant agents have been reported, among which we can state  $\text{HNO}_3$ ,  $\text{H}_2\text{O}_2$  and  $\text{O}_3$  (El-Hendawy, 2003, Cimino et al., 2005, Daifullah et al., 2007, Quintanilla et al., 2007, Takaoka et al., 2007, Strelko and Malik, 2010). These reagents introduce weakly acidic oxygen groups through surface oxidation of the sorbent. The most widely used carbonaceous materials for the industrial production of activated carbons are coal, wood and coconut shell (Vernersson et al., 2002, Yang and Chong Lua, 2006). These types of precursors are expensive and are often imported, making it necessary for

developing countries to find a cheap and available feedstock for the preparation of activated carbon for use in industry, drinking water purification and wastewater treatment. Several suitable agricultural by-products (lignocellulosics) including peach stones (Molina-Sabio et al., 1995), date stones (Girgis and El-Hendawy, 2002, Haimour and Emeish, 2006) waste apple pulp in cider production (Suarez-Garcia et al., 2002), rice husks (Chuah et al., 2005), pistachio-nut shells (Yang and Chong Lua, 2006) and grain sorghum (Diao et al., 2002) have been investigated in the last years as activated carbon precursors and are still receiving renewed attention. In comparison, olive-waste cakes received much less consideration as lignocellulosic material for activated carbon production (Baçaoui et al., 2001, Cimino et al., 2005).

Tunisia is the fourth largest olive oil producer in the world. During the manufacture process of the olive oil in mills, about 20% of oil, 30% of waste solids and 50% of wastewater are obtained (Moreno-Castilla et al., 2001). Olive-waste cakes (olive pomace), corresponding to the remaining residue of oil extraction process, represent a yearly average of  $2 \times 10^5$  tons depending on the crop (Sellami et al., 2008). The use of this material as precursor for the preparation of activated carbon produces not only a useful adsorbent for the purification of contaminated environments, but also contributes to minimizing the solid wastes.

From another angle, Tunisian fertilizer industry is a great world producer of wet-process phosphoric acid which can be used as activating agent in chemical activation method of any carbonaceous precursor. It is noteworthy that phosphoric acid is widely used in the chemical processing of activated carbon (Molina-Sabio et al., 2003) since it offers some advantages such as its non-polluting character (compared to  $Zn Cl_2$ ) and its ease of elimination by water extraction after carbonization (Suarez-Garcia et al., 2002, Gomez-Serrano et al., 2005).

The adsorptive properties of activated carbon depend on the nature of the precursor, the type of activation (chemical or physical) as well as on the processing conditions (Rivera-Utrilla et al., 1991, ASTM, 1999, Yun et al., 2001, Girgis and El-Hendawy, 2002, Puziy et al., 2002, El-Sheikh et al., 2004, Stavropoulos and Zabaniotou, 2005, Mudoga et al., 2007). It has been shown that in case of chemical activation, concentration of the dehydrating agent, impregnation ratio and pyrolysis temperature globally govern the properties of the resulting activated carbon (Diao et al., 2002, Girgis

and El-Hendawy, 2002, Haimour and Emeish, 2006). Performances of the obtained carbons are generally expressed in terms of some properties, among which: surface area, cation-exchange capacity (CEC), bulk density and adsorption efficiency towards iodine, phenol and methylene blue are frequently considered (Vernersson et al., 2002, Haimour and Emeish, 2006, Yang and Chong Lua, 2006).

The present work explored the use of Tunisian olive-waste cakes as a potential feedstock for AC preparation. For this purpose, chemical activation, using phosphoric acid as dehydrating agent, was adopted. To optimize the preparation method, the effect of the main process parameters (acid concentration, impregnation ratio, temperature of pyrolysis step) on the performances of the prepared activated carbons (expressed in terms of iodine and methylene blue numbers and specific surface area) was studied. Characterization of the activated carbon obtained in the optimal conditions was conducted, using the following techniques: infrared spectroscopy for chemical structure and scanning electron microscopy for morphology. Adsorption characteristics of this sorbent were also determined. To enhance the adsorption capacity of this carbon for heavy metals, a modification of the chemical characteristics of the sorbent surface was performed, using  $\text{KMnO}_4$  as oxidant. The efficiency of this treatment was evaluated considering the adsorption of  $\text{Cu}^{2+}$  ions as a model for metallic species.  $\text{KMnO}_4^-$  treatment and  $\text{Cu}^{2+}$  adsorption tests were carried out in a small-scale column.

## **2. Materials and methods**

### **2.1. Preparation of activated carbons**

Exhausted Olive-waste cakes, obtained from an oil factory “Agrozitex” located in Sfax, Tunisia, was used as raw material for the production of activated carbons via chemical activation. For this purpose, phosphoric acid was retained as a dehydrating agent. Each preparation test was conducted as follows: 40 g of the crushed (diameter < 1.5 mm) and dried precursor were mixed with  $\text{H}_3\text{PO}_4$  solution having different concentrations (30 to 85 %  $\text{H}_3\text{PO}_4$  in weight). The impregnation ratio, defined by the weight ratio of impregnant ( $\text{H}_3\text{PO}_4$ ) to precursor, was 1; 1.25; 1.5; 1.75; 1.85 and 2. The impregnation was carried out in a stirred Pyrex reactor equipped with a reflux condenser. Stirring was used to ensure the access of the acid to the interior of the olive-waste cake particles. The temperature and the duration of the reaction were 104 °C and 2 hours, respectively. Agitation and heating were ensured by a heating magnetic stirrer with connected

temperature regulator probe made of teflon. The pyrolysis of the impregnated material was conducted in a cylindrical stainless steel reactor, inserted into a tubular regulated furnace under continuous nitrogen flow ( $0.5 \text{ L min}^{-1}$ ). Pyrolysis temperature ranged from 350 to 650 °C, while activation time was maintained at 2 hours.

After cooling down to room temperature, under the same flow of nitrogen, the obtained activated carbon was thoroughly washed with hot distilled water until neutral pH. The sample was then dried at 105 °C overnight, ground (until a particle size ranging between 100 and 160  $\mu\text{m}$ ) and finally kept in hermetic bottle for subsequent uses.

## **2.2. Characterization of the prepared adsorbents**

### **2.2.1. Iodine number**

The iodine number is defined in terms of the milligrams of iodine ( $\text{I}_2$ ) adsorbed by 1 g of activated carbon when the iodine equilibrium concentration is 0.01M (Haimour and Emeish, 2006). In this work, the three-point method was adopted. The latter avoid the use of the correction factor usually employed in the less accurate single point-method (ASTM, 1999). The procedure of the iodine number determination is as follows: three dry samples of activated carbon were weighed out into three 250-ml conical flasks (sample weight ranged between 300 and 600 mg). Ten milliliters of 5% (in weight) hydrochloric acid solution were added to each flask and then mixed until the carbon became wet. The mixtures were then boiled for 30 s and finally cooled. One hundred milliliters of 0.05M standard iodine solution were added to each flask. The contents were vigorously shaken for 30 s and then immediately filtered. A 50-ml aliquot of each filtrate was titrated by a standardized 0.1M sodium thiosulfate solution. For each sample, the obtained iodine residual concentration should be included into 0.004 and 0.02 M. The plot of the amount of iodine fixed per gram of sorbent versus residual iodine concentration gives a straight line which allows determining graphically the iodine number (ordinate corresponding to a residual concentration of 0.01M).

### **2.2.2. Methylene blue (MB) adsorption**

Methylene blue adsorption tests were conducted by mixing 0.300 g of the prepared activated carbon with 100 mL of  $1000 \text{ mg L}^{-1}$  methylene blue solution (Yang and Chong Lua, 2006). After agitation during 24 h, the suspension was filtered and the MB

residual concentration was measured at 660 nm, using an UV/vis spectrophotometer (OPTIMA, SP-3000 plus). A previously established linear Beer–Lambert relationship was used for the concentration determination.

### **2.2.3. Cation-exchange capacity**

In studies on activated carbons, Bohem's titration was widely used to determine the CEC of sorbents (El-Sheikh et al., 2004). A weighted amount of adsorbent (0.100 g) was placed into an Erlenmeyer flask. A volume of 20 ml of 0.1M NaOH solution was added. To attain equilibrium, the suspension was shaken for 24 h. After filtration, the residual NaOH concentration was determined by titration with 0.1M hydrochloric acid solution, using phenolphthalein as indicator. The quantity of consumed NaOH was converted to CEC and expressed in mequiv. g<sup>-1</sup> (Puziy et al., 2002).

### **2.2.4. Specific surface area**

Specific surface area of the prepared activated carbons was evaluated through N<sub>2</sub> adsorption at 77 K, using an Autosorb1- Quantachrome instrument. The BET (Brunauer–Emmet and Teller) model was applied to fit nitrogen adsorption isotherm and evaluate the surface area ( $S_{\text{BET}}$ ) of the sorbent (Vernersson et al., 2002).

### **2.2.5. Bulk density**

Activated carbon sample was placed in a graduated cylinder, tapped several times until constant volume and then weighted. The bulk density was calculated as the ratio of the weight sample to its volume and expressed in gcm<sup>-3</sup> (Mudoga et al., 2007).

### **2.2.6. Morphology analysis**

In order to know the structure sight of activated carbon, scanning electron microscopy (SEM) was generally employed to visualize sample morphology. Pore structure and structural changes happening after chemical activation could be also observed. In the present work, the raw material (olive-waste cakes) and the activated carbon prepared in the optimal conditions were analyzed by this technique using a Philips XL30 microscope.

### 2.2.7. IR spectroscopy analysis

The surface functional groups and structure were studied by FTIR spectroscopy. The FTIR spectra of the raw material and the resulting activated carbon were recorded between 400 and 4000  $\text{cm}^{-1}$  in a NICOET spectrometer.

## 2.3. Column studies

### 2.3.1. Preparation of $\text{KMnO}_4$ -modified activated carbon

The modified activated carbon was prepared as follows: the adsorbent was transferred into a laboratory column (SIGMA chemical Company) packed at the bottom with glass wool and previously filled with distilled water. The column was performed in a Pyrex glass tube of 0.7 cm internal diameter and 14 cm in effective height. It is equipped with fixed polypropylene end caps, polyethylene bed support and Luer-Look inlet and outlet fittings. After settlement, by gravity, of the activated carbon particles, the adsorbent bed was covered with a thin layer of glass wool in order to avoid disturbance during the inlet of the influent. The level of water or solution present at the top of the bed was always fixed at the same level as that of the glass wool. A peristaltic pump (Gilson-Mnipuls 2) - connected to the bottom of the column by a silicon tube of low internal diameter (diameter = 1.2 mm) and very limited length (to minimize dead volume) - ensured a flow-rate of 0.5  $\text{mL min}^{-1}$ . The total dead volume fraction of the column ((bed void volume + connection tubing volume)/carbon bed volume) was 53.3%.

To modify the activated carbon surface, a  $10^{-3}\text{M}$   $\text{KMnO}_4$  solution (pH equal to 6.06) was pumped down through the column. The effluent, collected at the bottom of the column with an automatic fraction collector (Gilson), was sampled in 30-ml tubes, and stored for Mn analysis and pH measurement. Thereafter, the modified activated carbon column was washed with doubly distilled water.

### 2.3.2. Copper adsorption

A copper solution, with a concentration of 470  $\text{mg Cu}^{2+} \text{L}^{-1}$ , was fed through the column containing unmodified or modified activated carbon. The same peristaltic pump was used to ensure an influent flow-rate of 0.5  $\text{mL min}^{-1}$ . The influent pH was 4.79. Column effluent was collected in 30-ml tubes for subsequent copper analysis.



For column studies, the breakthrough curve relative to each considered metallic specie (Mn and Cu) was plotted. This curve translates the metal concentration evolution in the collected effluent versus the effluent cumulative volume, which is expressed in term of number of bed volumes (BVs). This number is defined as follows (Chen and Wang, 2000, Chen et al., 2003):

$$\text{Number of bed volumes} = \frac{\text{Volume of collected effluent}}{\text{volume of carbon bed}} \quad (1)$$

For all solute/sorbent combinations, the breakthrough curves are approximately S-shaped (or are approaching an S-shape). The breakthrough point is defined as the phenomenon when the solute begins to appear in the effluent, while exhaustion point occurs when the outflow concentration reaches the inflow concentration (Chen and Wang, 2000, Chen et al., 2003). The  $\text{KMnO}_4^-$  modification of the activated carbon bed and the copper retention studies were carried out at room temperature (23–25 °C).

#### **2.4. Metallic species analysis and pH measurement**

Effluent samples, collected from column tests, were analysed for metal species (Mn and Cu) using Acetylene-Air Flame/ Atomic Absorption spectrophotometer (HITACHI Model Z-6100). The pH of solutions were measured by a high precision pH-meter (Metrohm, model 632), equipped with a combined glass electrode (Metrohm). Preliminary standardisation was systematically carried out using suitable buffer solutions.

#### **2.5. Chemicals**

All chemicals used ( $\text{H}_3\text{PO}_4$ ,  $\text{I}_2$ , methylene blue,  $\text{Na}_2\text{S}_2\text{O}_3 \cdot 2\text{H}_2\text{O}$ , NaOH, HCl,  $\text{KMnO}_4$  and  $\text{CuSO}_4 \cdot 5\text{H}_2\text{O}$ ) were of analytical grade. Solutions were prepared by dissolving the corresponding reagent in doubly distilled water.

### **3. Results and discussion**

#### **3.1. Preparation of activated carbons: effect of processing parameters**

Within the scope of our researches, an attempt has been made to optimize the process parameters which lead to an activated carbon with good characteristics. As illustrations Figures. 1–3 show the effect of phosphoric acid concentration, pyrolysis temperature

and impregnation ratio on some properties of the prepared activated carbons. As it can be discerned from Figure 1, the surface area of the sorbent increases first rapidly (from 716 to 1020  $\text{m}^2 \text{g}^{-1}$ ) with an increase of acid concentration from 35 to 60%  $\text{H}_3\text{PO}_4$ , and then slightly beyond 60%  $\text{H}_3\text{PO}_4$  (1062  $\text{m}^2 \text{g}^{-1}$  for 85%  $\text{H}_3\text{PO}_4$ ). Taking into account the slight increase of the specific area occurring in the acid concentration range 60–85%  $\text{H}_3\text{PO}_4$ , and the handling difficulties of the most concentrated commercial phosphoric acid (85%  $\text{H}_3\text{PO}_4$  in weight) owing especially to its high viscosity, a concentration of 60%  $\text{H}_3\text{PO}_4$  seems to be the most suitable for the development of a high specific surface area of the adsorbent material.

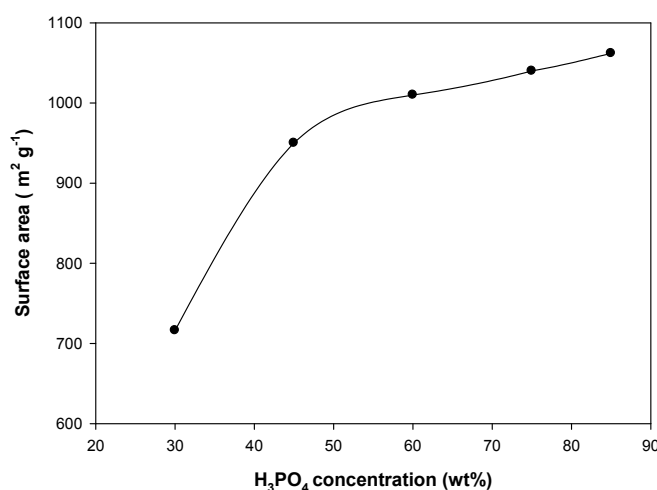


**Figure 1:** Effect of  $\text{H}_3\text{PO}_4$  concentration on the surface area of the activated carbon  
(Impregnation ratio: 1.75; Pyrolysis temperature: 450 °C;  
Pyrolysis duration: 2H)

The effect of pyrolysis temperature on the methylene blue number of the adsorbent (Figure 2) shows that the quantity of methylene blue adsorbed begins to increase with an increase of the temperature from 350 to 450 °C, and then decreases when the temperature exceeds 450 °C. Thus, keeping the pyrolysis temperature at around 450 °C leads to a better development of the sorbent porosity.

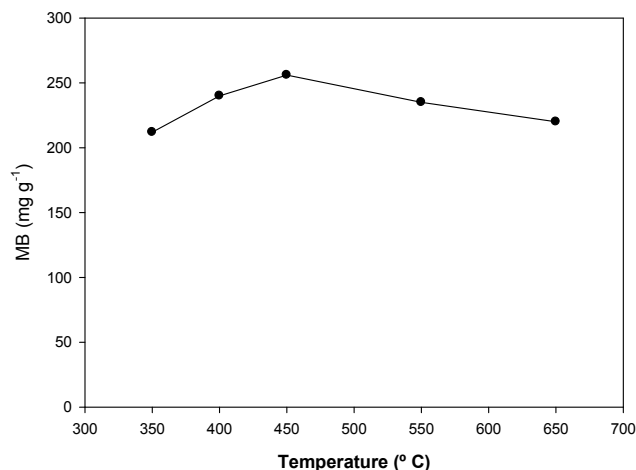


**Figure 2:** Effect of pyrolysis temperature on MB adsorption (H<sub>3</sub>PO<sub>4</sub> concentration: 60%; Impregnation ratio: 1.75; Pyrolysis duration: 2H)

Several investigators have established that in the case of H<sub>3</sub>PO<sub>4</sub> activation of other agricultural materials (woods, coconut shell, date pits, grain sorghum), temperatures neighbouring 450 °C were also suitable to obtain optimal properties of the activated carbons (Jagtoyen and Derbyshire, 1993, Molina-Sabio et al., 1995, Diao et al., 2002, Girgis and El-Hendawy, 2002).

Contrary to methylene blue, which is the most recognized probe molecule for assessing the ability of the sorbent to remove large molecules via its macroporosity (pore diameter greater than 1.5 nm), iodine number gives an indication on microporosity (pores less than 1 nm in diameter). The effect of the impregnation ratio on the iodine number is illustrated in Figure 3. The highest iodine number was obtained at an impregnation ratio of 1.75. At a value more or less than 1.75, the iodine number decreased. Therefore, 1.75 is the suitable impregnation ratio value leading to the best iodine number and, consequently, to the best development of microporous structure.

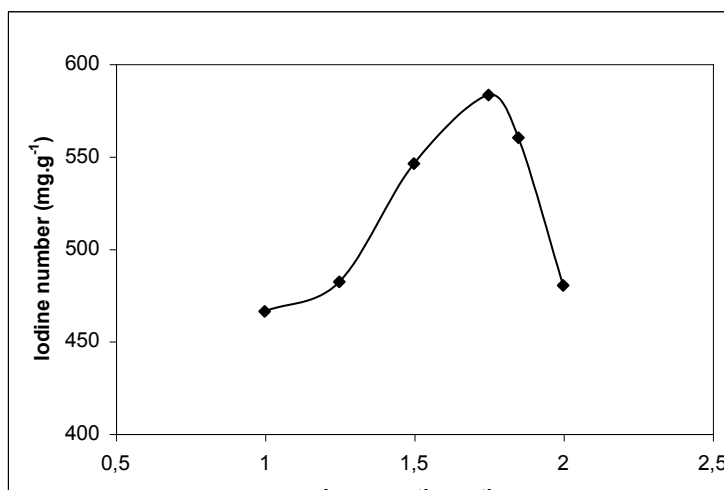


**Figure 3:** Effect of impregnation ratio on the Iodine number  
( $\text{H}_3\text{PO}_4$  concentration: 60%; Pyrolysis temperature: 450 °C;  
Pyrolysis duration: 2H)

The above results show that the most efficient activated carbon is that obtained under the following optimal conditions: an acid concentration equal to 60% in weight, an impregnation ratio of 1.75 and a pyrolysis temperature of 450 °C. It is to note that results obtained when studying the effect of each parameter (acid concentration, impregnation ratio and pyrolysis temperature) on the whole considered properties, namely iodine and methylene blue numbers and specific area (results not shown), lead to the same optimal conditions.

### 3.2. Characterization of the optimal activated carbon

#### 3.2.1. Adsorption characteristics

Characteristics of the activated carbon prepared under the optimal conditions mentioned above, are given in Table 1. For the sake of comparison, we have shown in the same table the values of some activated carbon characteristics available in literature. As it can be seen, the characteristics of the carbon obtained in this work compare well and sometimes more favourable than the other sorbents. The yield of the activated carbon – which is defined as the weight ratio, on a dry basis, of the resulting activated carbon to that of the original olive-waste cakes (Diao et al., 2002) – is in our case 42.9%. This value is significantly higher than those observed for other lignocellulosic materials such as holm-oak sawdust (25.5%), rockrose (20.0%) and olive-wood sawdust (22.9%) (Gomez-Serrano et al., 2005)

**Table 1** : Compared characteristics of the optimal activated carbon

	Activation process (activation agent)	Adsorbent characteristics					Reference
		I <sub>2</sub> (mg g <sup>-1</sup> )	BM (mg g <sup>-1</sup> )	CEC (meq g <sup>-1</sup> )	S <sub>BET</sub> (m <sup>2</sup> g <sup>-1</sup> )	Bulk density (g cm <sup>-3</sup> )	
Olive-waste cakes	Chemical (H <sub>3</sub> PO <sub>4</sub> )	583	312.5	2.42	1020	0.551	This work
Coconut shell	Chemical (H <sub>3</sub> PO <sub>4</sub> )	*-	-	2.33	-	-	ASTEE, 2006
Grain sorghum	Chemical (H <sub>3</sub> PO <sub>4</sub> )	-	-	-	182-508	-	Diao et al., 2001
Peach stones	Chemical (H <sub>3</sub> PO <sub>4</sub> )	-	-	-	632	0.56	Molina-Sabio et al., 1995
Olive-seed waste	Chemical (KOH)	-	190-262	-	367-506	-	Stavropoulos and Zabaniotou, 2005
Olive-waste cakes	Physical (steam)	-	-	-	514-1271	-	Baçauoui et al., 2001
Olive stones	Physical (steam and N <sub>2</sub> gas mixture)	574	-	-	-	-	Galiatsatou et al., 2002

\*- : not available

### 3.2.2. IR spectra and SEM micrographs

Pore structure of the AC is very important in determining adsorption properties of the sorbent. However, the importance of the surface chemistry of AC should not be ignored. In this work, infrared spectroscopy was used to obtain informations about the chemical structure and functional groups of the raw material and the prepared activated carbon (Zawadzki, 1989, Jagtoyen et al., 1992, Pastor-Villegas et al., 1993, Vinke et al., 1994, Solum et al., 1995, Gomez-Serrano et al., 1996). The FTIR spectrum of the olive-waste cakes is shown in Figure 4. This spectrum is quite similar to that of other lignocellulosic materials such as pistachio-nut shell and rockrose (Pastor-Villegas et al., 1993, Gomez-Serrano et al., 1996). The band located at  $2929\text{ cm}^{-1}$  corresponds to the C–H vibrations in methyl and methylene groups. The band at  $1738\text{ cm}^{-1}$  is ascribed to carbonyl C=O groups. The olefinic (C=C) vibrations cause the emergence of the band at about  $1651\text{ cm}^{-1}$ , while the skeletal C=C vibrations in aromatic rings cause another two bands at  $1510$  and  $1425\text{ cm}^{-1}$ . The vibrations at  $1462$  and  $1377\text{ cm}^{-1}$  are assigned to the bands –CH<sub>3</sub> and –CH<sub>2</sub>– (Jagtoyen et al., 1992, Gomez-Serrano et al., 1996). The band at  $1323\text{ cm}^{-1}$  can be attributed to (C–O) vibrations in carboxylate groups. The band at  $1246\text{ cm}^{-1}$  may be attributed to esters (e.g. R–CO–O–R'), ethers (e.g. R–O–R') or phenol groups. The relatively intense band at  $1048\text{ cm}^{-1}$  can be assigned to alcohol groups (R–OH). The C–H out-of-plane bending in benzene derivative vibrations causes the band at  $895\text{ cm}^{-1}$ .

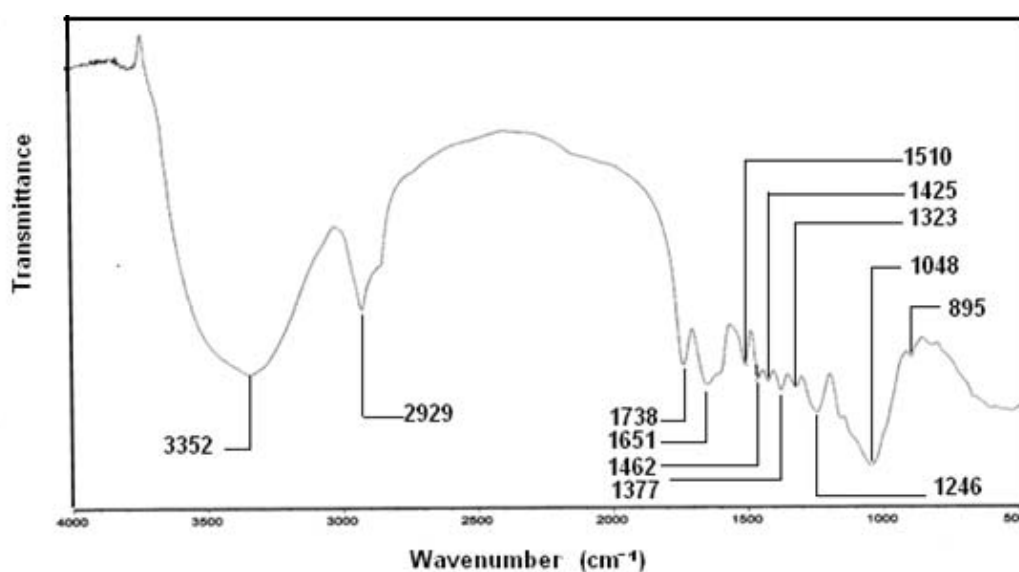


**Figure 4:** FTIR spectrum of the olive-waste cakes

The above-IR analysis shows the absence of nitrogen and sulphur groups in the olive-waste cakes structure, whereas we note the presence of different oxygen groups, mainly: carbonyl, alcohol and phenol groups, ethers and esters. The spectrum of the optimal adsorbent prepared in this work is given in Figure 5. We essentially mentioned that the absorption in the region 1300–1000  $\text{cm}^{-1}$  is generally ascribed to phosphorous and phosphocarbonaceous compounds (Jagtøyen et al., 1992, Solum et al., 1995). Due to the overlap of absorption bands from many oxygen and phosphorous compounds in this region, an unambiguous assignment is difficult. However, based on our analysis data, activated carbon obtained in this work contains about 1.5 wt% phosphorous (dry basis), which suggests the incorporation of this element in the activated carbon structure.

When comparing the two spectra, we can show that deep modifications take place in the wave number range 1700–1000  $\text{cm}^{-1}$ . These modifications make the spectrum of the activated carbon less complicated than that of the precursor. Considering the spectrum of the carbon, we can essentially notice:

- a dramatic decrease in intensity of the band corresponding to C=O groups ( $\sim 1700 \text{ cm}^{-1}$ ). This suggests that phosphoric acid activated carbon contains less C=O groups than the raw material.

The decrease of the amount of carbonyl groups may be due to hydrolysis effect of  $\text{H}_3\text{PO}_4$ , resulting in the decomposition of these groups and subsequent release of their by-products as volatile matter;

- a disappearance of the weak band set located between 1500 and 1200  $\text{cm}^{-1}$ , and a shift of the C–O band from 1048 to 1169  $\text{cm}^{-1}$ ;
- a disappearance of the olefinic C=C band (1651  $\text{cm}^{-1}$ ) and the appearance of a strong absorption band (1555  $\text{cm}^{-1}$ ) corresponding to aromatic C=C groups. This translates the fact that the activated carbon structure is richer in aromatics.

Taking into account the whole observations and comments given above, we can conclude that the acid impregnation of the raw material followed by the pyrolysis step lead to a more carbonaceous and aromatic structure due to the dehydration effect of  $\text{H}_3\text{PO}_4$  and evolution of volatiles during pyrolysis. In another respect, IR and chemical analysis suggest that phosphoric acid chemical activation leads to the incorporation of phosphorous element in the structure of the obtained carbon.

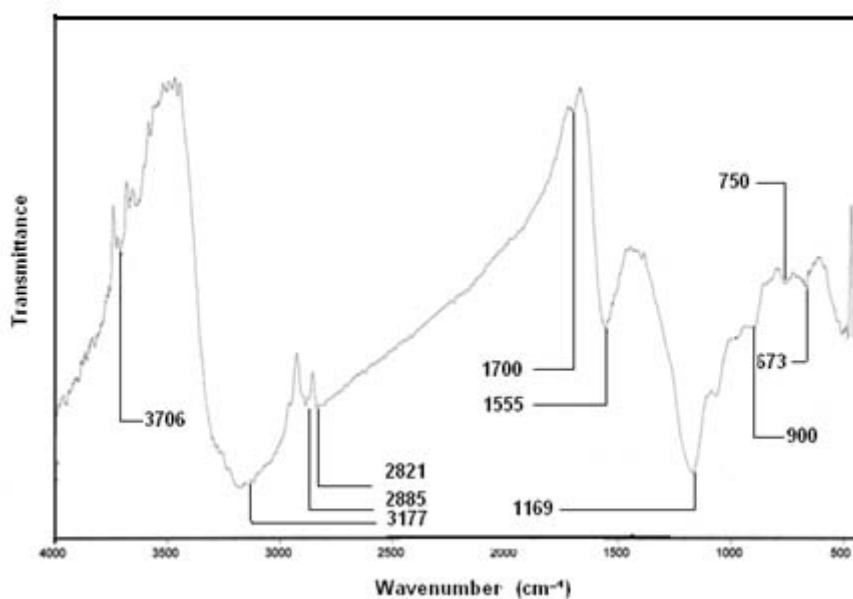


**Figure 5: FTIR spectrum of the optimal activated carbon**

The microstructure of the raw olive-waste cakes and the resulting activated carbon prepared in the optimal conditions are shown in Figure 6. For the olive-waste cakes (Figure 6a), the surface was quite smooth without any porous structure except for some occasional cracks or curves. Comparison of the precursor morphology with that of the derived carbon (Figure 6b) attests substantial changes occasioned by phosphoric acid activation. The sorbent surface exhibits a clear porous structure and a predominately microporous character which is responsible of the high developed surface area of this material and of its high iodine number.

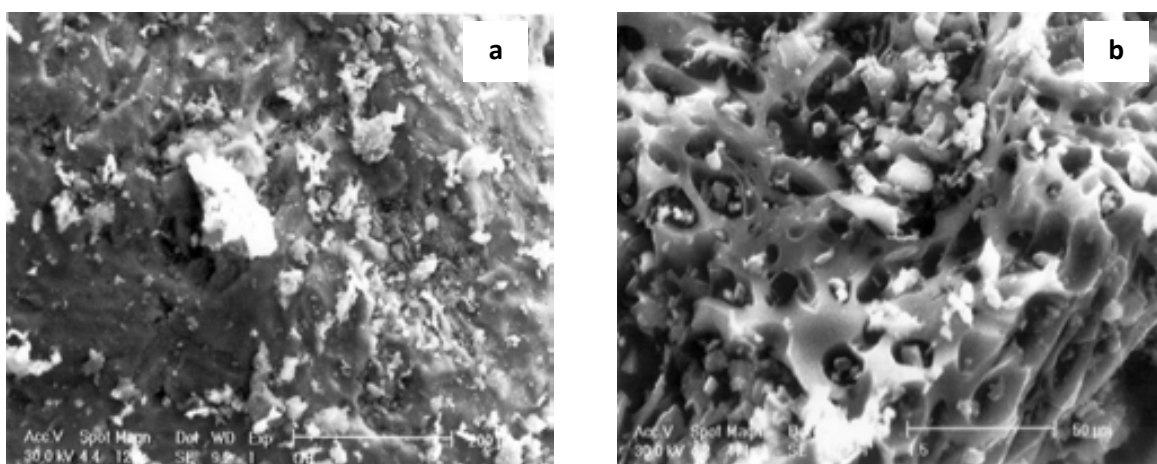


**Figure 6: SEM micrographs of olive-waste cakes (a) and optimal activated carbon (b)**



### **3.3. Column studies: $\text{KMnO}_4$ -modification of the optimal activated carbon and copper adsorption**

Modification of the surface chemistry of carbons is recognized as an attractive route towards the novel application of these materials as polyfunctional adsorbents as well as catalyst supports (El-Hendawy, 2003, Vladimir and Danish, 2002).

Metal uptake by activated carbon is assumed to be function of the amount of polar or acidic groups present on the sorbent surface (Toles et al., 1999).

Sorptive capacity of conventional carbons towards heavy metals is rather low. However, metal sorption can be considerably enhanced by the introduction of weakly acidic functional groups through surface oxidation using different agents such as nitric acid, hydrogen peroxide, potassium permanganate and ammonium persulfate (El-Hendawy, 2003). Boehm titrations show that surface oxidation of activated carbons greatly increases the concentration of oxygen-containing surface acidic groups (essentially carboxylic and phenolic surface groups) which improve cation-exchange and complexation properties of these sorbents (El-Hendawy, 2003, Vladimir and Danish, 2002).

As surface modifier agent,  $\text{KMnO}_4$  behave differently in accordance with the treatment way. When  $\text{KMnO}_4$  is used in mixture with a concentrated strong acid, like  $\text{HNO}_3$ , the result of this treatment is a considerable increase of the amount of oxygen-containing functional groups on the sorbent surface (Chen et al., 2007). The reduction products of  $\text{KMnO}_4$  and  $\text{HNO}_3$  are in this case water-soluble species which are eliminated during the subsequent washing step of the treated carbon. In return, in alkaline, neutral and slightly acidic media,  $\text{KMnO}_4$  is reduced by activated carbon to insoluble  $\text{MnO}_2$  which impregnates the sorbent surface (Okoniewska et al., 2008). In this connection, recent studies have shown that some filtration materials with a little or no sorptive properties, such as sand and crushed brick, act as good sorbents for cationic and anionic species when coated with oxides (oxyhydroxides) of iron (III) and essentially manganese (IV) (Benjamin et al., 1996, Boujelben et al., 2008). For these engineered coated sorbents, solutes adsorb at the iron or manganese oxyhydroxide surface by forming complexes with the surface sites (Chen et al., 2007, Benjamin et al., 1996). Since the combination of activated carbon and insoluble  $\text{MnO}_2$  (composite media) would take advantage of the strength of these two materials, the second treatment strategy was adopted in this work.

### 3.3.1. $\text{KMnO}_4$ -modification of the optimal activated carbon

To impregnate the activated carbon with manganese (IV) oxide, a  $10^{-3}\text{M}$   $\text{KMnO}_4$  solution (natural pH 6.06) was used. Figure 7 shows the evolution during the permanganate treatment of the outflow Mn concentration and pH as a function of the collected effluent (expressed in BV). In the course of this chemical treatment, we did not detect any trace of  $\text{MnO}_4^-$  in the collected fractions, in spite of the percolation of 300 BV of effluent. The quantity of reduced Mn (VII), corresponding to 300 BV, is amounting to  $37.9 \text{ mg Mn g}^{-1}$  of sorbent. Since the activated carbon was not yet saturated for 300 BV, it might be deduced that the capacity of the carbon column to reduce  $\text{MnO}_4^-$  is higher than  $37.9 \text{ mg Mn g}^{-1}$ . However, when the effluent volume reached approximately 150, a very clear yellow-chestnut colour, which could be assigned to  $\text{MnO}_2$ , was visually detected in the collected fractions. To make certainty that manganese (IV) oxide is effectively at the origin of this colour, chemical tests were applied to the collected effluent (Charlot, 1983). The following chemical tests, which were positive, consisted in:

- oxidation of  $\text{MnO}_2$  with persulphate, under heating and in the presence of  $\text{Ag}^+$  ion as catalyst, which leads to the formation of  $\text{MnO}_4^-$  having the characteristic purple colour;
- reduction of  $\text{MnO}_2$  with oxalic acid, which leads to the formation of  $\text{Mn}^{2+}$  ions characterized by their pink colour.

In addition, when some drops of  $10^{-3}\text{M}$   $\text{KMnO}_4$  solution were added to a diluted solution of  $\text{Mn}^{2+}$  ions, the same colour in the collected fractions was obtained. In this connection, it is well known that  $\text{MnO}_4^-$  reacts with  $\text{Mn}^{2+}$  ions yielding to  $\text{MnO}_2$ . Thus, this additional test confirms once again that  $\text{MnO}_2$  was at the origin of the observed colour.

To quantify the amounts of  $\text{MnO}_2$  present in the different effluent fractions, analysis of Mn element was carried out. Simultaneously, the pH of each fraction was measured (Figure 7). It should be noted that for manganese analysis,  $\text{MnO}_2$  present in the collected Samples was first reduced to  $\text{Mn}^{2+}$  ions with crystallized oxalic acid in the presence of one drop of concentrated  $\text{H}_2\text{SO}_4$ .

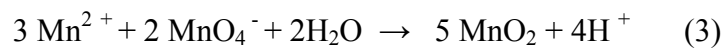
According to Figure 7, the curve representing the evolution of Mn concentration have firstly a shape similar to that of a breakthrough curve (effluent volume  $<150$  BV). From this plot, it appears that  $\text{MnO}_2$  begins to leak out the column at an effluent volume equal

to 16.6 BV, and not at 150 BV as visually detected. The increase of the outflow  $\text{MnO}_2$  concentration until 150 BV is accompanied by a simultaneous increase of the effluent pH. This pH evolution may be assigned to the reduction of  $\text{MnO}_4^-$  to  $\text{MnO}_2$  with activated carbon, which is an alkalizing reaction:



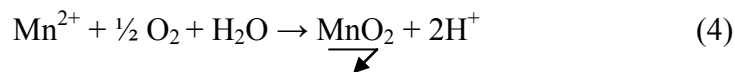
When the effluent volume is nearly 150 BV, the concentration of Mn (in fact  $\text{MnO}_2$ ) increased significantly while effluent pH slightly decreased. Therefore, it might be suggested that there is possibly a secondary reaction producing  $\text{MnO}_2$  and increasing in the same time the effluent acidity. According to the literature (Charlot, 1974, Charlot, 1983), it appears that the only acidifying reactions leading to  $\text{MnO}_2$  formation are:

- the reduction of  $\text{MnO}_4^-$  with  $\text{Mn}^{2+}$  ions according to:

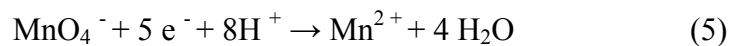


This reaction is known to be slow at ambient temperature. However, it can be catalyzed by activated carbon, following the example of the well known reduction reaction of chlorine with water (Lyonnaise des eaux, 1983);

- the oxidation of  $\text{Mn}^{2+}$  ions with dissolved oxygen in water:



which is well known to be catalyzed by  $\text{MnO}_2$  settled on the surface of activated carbon (Okoniewska et al., 2008). Reactions (3) and (4) suppose that the reduction of  $\text{MnO}_4^-$  by activated carbon (Reaction (2)) produces  $\text{Mn}^{2+}$  in addition to  $\text{MnO}_2$  as principal product. This  $\text{Mn}^{2+}$  production might result even directly according to Charlot (1983):



or via  $\text{Mn}_2\text{O}_3$  formation (Charlot, 1983):



which then spontaneously disproportionates to give  $\text{MnO}_2$  and  $\text{Mn}^{2+}$  according to Charlot (1983):

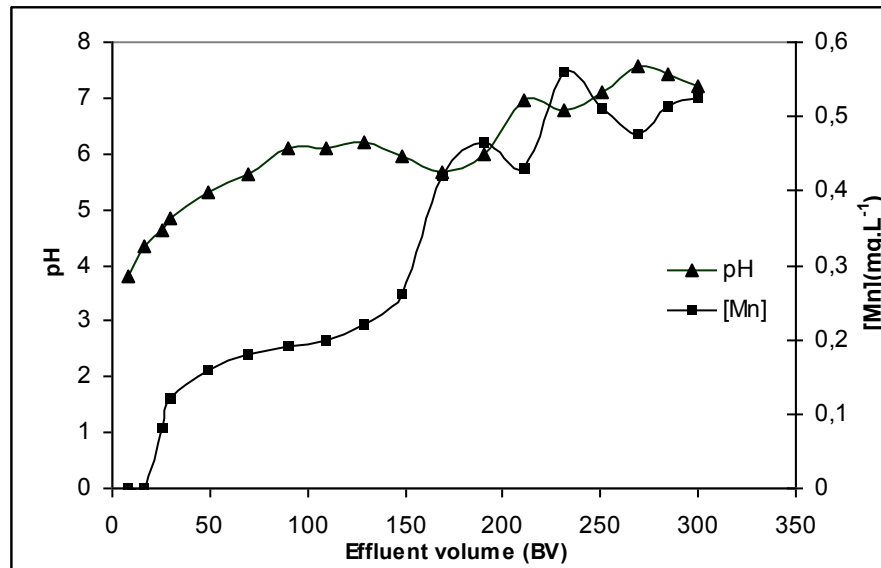
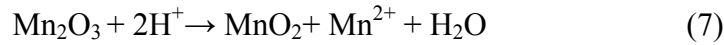


**Figure 7:**  $\text{KMnO}_4$ -modification of activated carbon: evolution of Mn concentration and pH of the collected fractions of effluent

Coming back to Figure 7, we show that – at an effluent volume greater than 150 BV – the concentration of manganese in the effluent increases while the pH decreases and vice versa. This suggests that Reactions (2) and (3) or (4) are periodically alternated in the carbon column.

### 3.3.2. $\text{Cu}^{2+}$ adsorption

Adsorption experiments of copper were conducted through the both treated and untreated activated carbon bed with  $\text{KMnO}_4$ . The obtained breakthrough curves are shown in Figure 8. As it can be seen, the breakthrough occurs at 2.7 and 25.6 BV for unmodified and  $\text{KMnO}_4$ -modified adsorbent, respectively. From these plots, the adsorption capacity ( $q_{\max}$ ) of the carbons for  $\text{Cu}^{2+}$  ions was determined using the following relation (Tremillion, 1965):

$$(V_{\text{PI}} - V_{\text{D}}) [\text{Cu}^{2+}]_0 = m \cdot q_{\max}$$

where  $V_{\text{PI}}$  is the effluent volume corresponding to the point of inflexion of each breakthrough curve,  $V_{\text{D}}$  is the total dead volume of the column,  $[\text{Cu}^{2+}]_0$  is the influent concentration and  $m$  is the amount of activated carbon present in the column.

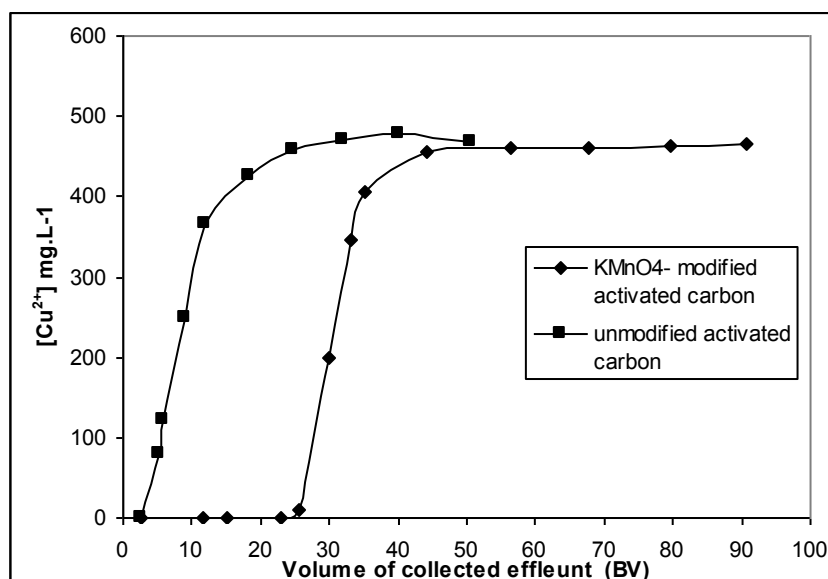


**Figure 8:** Breakthrough curves for copper adsorption relating to  $\text{KMnO}_4$ -modified and unmodified activated carbon

The obtained values were:

$$q_{\max} = 12.0 \text{ mg Cu}^{2+} \text{ g}^{-1} \text{ for unmodified carbon}$$

$$q_{\max} = 35.3 \text{ mg Cu}^{2+} \text{ g}^{-1} \text{ for modified carbon}$$

Thus, a marked increase in the copper uptake capacity of the modified activated carbon is observed. Indeed, this capacity is enhanced by a factor of up to 3 for the  $\text{MnO}_2$ -impregnated carbon. In these conditions, we can conclude that  $\text{KMnO}_4$  treatment of conventional activated carbon considerably improves the adsorption capacity of this sorbent towards copper as a typical transition metal. Copper uptake capacities ( $q_{\max}$ ) depend on the nature of the starting materials, the activation process and the modification method used for the preparation of the sorbent. Copper (II) uptake capacities ( $q_{\max}$ ) equal to 5.08 and 18.22  $\text{mg g}^{-1}$  were for example obtained by Vladimir and Danish (2002) when using unoxidized and  $\text{HNO}_3$ -oxidized commercial activated carbon, respectively. On the other hand, when considering rice husk modified by tartaric acid under particular conditions,  $\text{Cu}^{2+}$  uptake capacity of 29  $\text{mg g}^{-1}$  was observed (Wong et al., 2003, Chuah et al., 2005).

#### 4. Conclusion

Based on the results obtained within the framework of this study, it appears that olive-waste cakes may constitute a suitable precursor for the manufacture of a powerful

activated carbon through chemical activation with phosphoric acid. The most efficient activated carbon is that obtained under the following optimal conditions: an acid concentration equal to 60% H<sub>3</sub>PO<sub>4</sub>, an impregnation ratio of 1.75, and a pyrolysis temperature of 450 °C. The adsorption characteristics of the activated carbon prepared under these conditions compare well, and sometimes more favorably than the previously reports for activated carbon in literature.

The main conclusions that can be drawn from the current investigation are given below:

- the capacity of the optimal activated carbon to reduce MnO<sub>4</sub><sup>-</sup> exceeds 37.9 mg Mn g<sup>-1</sup> of adsorbent;
- a marked increase in the copper uptake capacity of the modified activated carbon is observed. Thus, the capacity for copper sorption was enhanced by a factor of up to 3 after modification of the produced activated carbon by permanganate treatment under specified conditions.

## **REFERENCES**

- ASTEE, 2006. Association Scientifique et Technique pour l'Eau et l'Environnement. Réglementation et traitement des eaux destinés à la consommation humaine, 1ère edition, Paris.
- ASTM, 1999. Standard Test Method for Determination of Iodine Number of Activated Carbon. ASTM Committee on Standards, ASTM D 4607-94, ASTM, Philadelphia, PA.
- Baçaooui A., Yaacoubi A., Dahbi A., Bennouna C., Phan Tan Luu R., Maldonado-Hodar F.J., Rivera-Utrilla J., Moreno-Castilla C., 2001. Optimization of conditions for the preparation of activated carbons from olive-waste cakes. *Carbon* 39, 425–432.
- Benjamin M.M., Slatten R.S., Bailey R.P., Bennett T., 1996. Sorption and filtration of metals using iron oxide coated sand. *Water Res.* 30, 2609–2620.
- Borba E.A., Da Silva, Fagundes-Klen M.R., Kroumov A.D., Guirardello R., 2008. Prediction C.E. of the copper (II) ions dynamic removal from a medium by using mathematical models with analytical solution. *J. Hazard. Mater.* 152, 366–372.

- Boujelben N., Bouzid J., Elouar Z., Feki M., Jamoussi F., Montiel A., 2008. Phosphorous removal from aqueous solution using iron coated natural and engineered sorbents, *J. Hazard. Mater.* 151, 103–110.
- Charlot G., 1974. *Chimie analytique quantitative, Tome 2. Méthodes Sélectionnées d'Analyse Chimique Des Eléments*, 6ème edition, Masson, Paris.
- Charlot G., 1983. *Les réactions chimiques en solution aqueuse et caractérisation des ions*, Masson, Paris.
- Chen J.P., Wang X., 2000. Removing copper, zinc and lead ion by granular activated carbon pretreated fixed-bed columns. *Sep. Purif. Technol.* 19, 157–167.
- Chen J. P., Yoon J.T., Yiacoumi S., 2003. Effects of chemical and physical properties of influent on copper sorption onto activated carbon fixed-bed columns. *Carbon* 41, 1635–1644.
- Chen W., Parette R., Zou J., Cannon F.S., Dempsey B.A., 2007. Arsenic removal by iron modified activated carbon. *Water Res.* 41, 1851–1858.
- Chuah T.G., Jumariah A., Azni I., Katayon S., Thomas Choong S.Y., 2005. Rice husk as a potentially low-cost biosorbent for heavy metal and dye removal: an overview. *Desalination* 175, 305–316.
- Cimino G., Cappello R.M., Caristi C., Toscazo G., 2005. Characterisation of carbons from olive cake by sorption of wastewater pollutants. *Chemosphere* 61, 947–955.
- Daifullah A.A.M., Yakout S.M., Elreefy S.A., 2007. Adsorption of fluoride in aqueous solutions using  $\text{KMnO}_4$ -modified activated carbon derived from steam pyrolysis of rice straw. *J. Hazard. Mater.* 147, 633–643.
- Diao Y., Walawender W.P., Fan L.T., 2002. Activated carbon prepared from phosphoric acid activation of grain sorghum. *Bioresour. Technol.* 8, 45–52.
- El-Hendawy A.N.A., 2003. Influence of  $\text{HNO}_3$  oxidation on the structure and adsorptive properties of corncob-based activated carbon. *Carbon* 41, 713–722.
- El-Sheikh A.H., Newman A.P., Al Daffae H.K., Phull S., Creswell N., 2004. Characterization of activated carbon prepared from a single cultivar of Jordanian olive stones by chemical and physicochemical techniques. *J. Anal. Appl. Pyrolysis* 71, 151–164.

- Galiatsatou P., Metaxas M., Arapoglou D., Kasselouri-Rigopoulou V., 2002. Treatment of olive mill wastewater with activated carbons from agricultural by-products. *Waste Manage.* 22, 803–812.
- Girgis B.S., El-Hendawy A.N.A., 2002. Porosity development in activated carbons obtained from date pits under chemical activation with phosphoric acid. *Microporous Mesoporous Mater.* 52, 105–117.
- Gomez-Serrano V., Cuerda-Correa E.M., Fernandez-Gonzalez M.C., Alexandre-Franco M.F., Macias-Garcia A., 2005. Preparation of activated carbons from chestnut wood by phosphoric acid-chemical activation. Study of microporosity and fractal dimension. *Materials Lett.* 59, 846–853.
- Gomez-Serrano V., Pastor-Villegas J., Duran-Valle C.J., Valenzuela-Calahorra C., 1996. Heat treatment of rockrose char in air. Effect on surface chemistry and porous texture. *Carbon* 34, 533–538.
- Haimour N.M., Emeish S., 2006. Utilization of date stones for production of activated carbon using phosphoric acid. *Waste Manage.* 26, 51–60.
- Ioannidou O., Zabaniotou A., 2007. Agricultural residues as precursors for activated carbon production –a review. *Renew. Sust. Energ. Rev.* 11, 1966–2005.
- Jagtoyen M., Derbyshire F., 1993. Some considerations of the origins of porosity in carbons from chemically activated wood. *Carbon* 31, 1185–1192.
- Jagtoyen M., Thwaites M., Stencil J., McEnaney B., Derbyshire F., 1992. Adsorbent carbon synthesis from coals by phosphoric acid activation. *Carbon* 30, 1089–1096.
- Jusoha A., Lam S.S., Noraaini A., Noor M.J.M.M., 2007. A simulation study of the removal efficiency of granular activated carbon on cadmium and lead. *Desalination* 206, 9–16.
- Lyonnaise des eaux, 1989. *Memento Technique de l'eau*, 9<sup>ème</sup> edition Paris.
- Malkoc E., Nuhoglu Y., Dundar M., 2006. Adsorption of chromium (VI) on pomace-An olive oil industry waste: batch and column studies. *J. Hazard. Mater.* 138, 142–151.
- Molina-Sabio M., Almansa C., Rodriguez-Reinoso F., 2003. Phosphoric acid activated carbon discs for methane adsorption. *Carbon* 41, 2113–2119.



- Molina-Sabio M., Rodríguez-Reinoso F., Catarla F., Sellés M.J., 1995. Porosity in granular carbons activated with phosphoric acid. *Carbon* 33, 1105–1113.
- Moreno-Castilla C., Carrasco-Marin F., Lopez-Ramon M., Alvarez-Merino A., 2001. Chemical physical activation of olive-mill waste water to produce activated carbons. *Carbon* 39, 1415–1420.
- Mudoga H.L., Yucel H., Kincal N.S., 2007. Decolorization of sugar syrups using commercial and sugar beet pulp based activated carbons. *Bioresour. Technol.* 99 (9), 3528-3533.
- Okoniewska E., Lach J., Kacprzak M., Neczaj E., 2008. The trial of regeneration of used impregnated activated. Carbons after manganese sorption. *Desalination* 223: 256–263.
- Pastor-Villegas J., Valenzuela-Calahorro C., Bernalte-Garcia A., Gomez-serrano V., 1993. Characterization study of char and activated carbon prepared from raw and extracted rockrose. *Carbon* 31, 1061–1069.
- Puziy A.M., Poddubnaya O.I., Martínez-Alonso A., Suárez-García F., Tascón J.M.D., 2002. Synthetic carbons activated with phosphoric acid. I. Surface chemistry and ion binding properties. *Carbon* 40, 1493–1505.
- Quintanilla A., Casas J.A., Rodríguez J.J., 2007. Catalytic wet air oxidation of phenol with modified activated carbons and Fe/activated carbon catalysts. *Appl. Catal. B: Environ.* 76, 135–145.
- Rivera-Utrilla J., Hidalgo E.U., Garcia M.A., 1991. Comparison of activated carbons from agricultural raw materials and Spanish lignites, when removing chlorophenols from aqueous solutions. *Carbon* 28, 613–619.
- Sellami F., Jarboui R., Achica S., Medhioub K., Ammar E., 2008. Co-composting of oil exhausted olive-cake, poultry manure and industrial residues of agro-food activity for soil amendment. *Bioresour. Technol.* 99, 1177–1188.
- Solum M.S., Pugmire R.J., Jagtoyen M., Derbyshire F., 1995. Evolution of carbon structure in chemically activated wood. *Carbon* 33, 1247–1254.
- Stavropoulos G.G., Zabaniotou A., 2005. Production and characterisation of activated carbon from olive seed waste residue, *Microporous Mesoporous Mater.* 82, 79–85.
- Strelko V., Malik D., 2002. Characterization and metal sorptive properties of oxidized active carbon. *J. Colloid Interface Sci* 250, 213–220.

- Suarez-Garcia F., Martinier-Alonso A., Tascon J.M.D., 2002. Pyrolysis of apple pulp: chemical activation with phosphoric acid. *Anal. Appl. Pyrolysis* 63: 283–301.
- Takaoka M., Yokokawa H., Takeda N., 2007. The effect of treatment of activated carbon by H<sub>2</sub>O<sub>2</sub> or HNO<sub>3</sub> on the decomposition of pentachlorobenzene. *Appl. Catalysis B: Environ.* 74, 179–186.
- Toles C.A., Marshall W.E., Johns M.M., 1999. Surface functional groups on acid activated nutshell carbons. *Carbon* 37, 1207–1214.
- Tremillion B., 1965. *Les séparations par les résines échangeuses d'ions*. Gautier Villars. Paris.
- Vernersson T., Bonelli P.R., Cerrela E.G., Cukierman A.L, 2002. Arundo donax cane as a precursor for activated carbons preparation by phosphoric acid activation. *Bioresour. Technol.* 83, 95–104.
- Vinke P., Van Der E.M., Verbree M., Voskamp A.F., Van Bekkum H., 1994. Modification of the surfaces of a gas-activated carbon and a chemically activated carbon with nitric acid, hypochlorite and ammonia. *Carbon* 32, 675–686.
- Vinod K.G., Imran A., 2000. Utilisation of bagasse fly ash (a sugar industry waste) for the removal of copper and zinc from wastewater. *Sep. Purif. Technol.* 18, 131–140.
- Vladimir S. Jr., Danish J.M., 2002. Characterization and metal sorptive properties of oxidized active carbon. *J. Colloid Interface Sci* 250, 213–220.
- Wong K.K., Lee C.K., Low K.S., Haron M.J., 2003. Removal of Cu and Pb by tartaric acid modified rice husk from aqueous solutions. *Chemosphere* 50: 23–28.
- Yang T., Chong Lua A., 2006. Textural and chemical proprieties of zinc chloride activated carbons prepared from pistachio-nut shells. *Mater. Chem. Phys.* 100, 438–444.
- Yun C.H., Park Y.H., Chong R.P., 2001. Effects of pre-carbonization on porosity development of activated carbons from rice straw. *Carbon* 39: 559–567.
- Zawadzki J., 1989. Infrared spectroscopy in surface chemistry of carbons, in: P.A. Thrower (Ed.). *Chemistry and Physics of Carbon*, vol 21. Marcel Dekker, New York, 147–386.

#### 4.1.2. Environmental impact associated with activated carbon preparation from olive-waste cake via life cycle assessment

---



**Abstract**

The life cycle assessment (LCA) environmental tool was implemented to quantify the potential environmental impacts associated with the activated carbon (AC) production process from olive-waste cakes in Tunisia. On the basis of laboratory investigations for AC preparation, a flowchart was developed and the environmental impacts were determined. The LCA functional unit chosen was the production of 1 kg of AC from by-product olive-waste cakes. The results showed that impregnation using  $H_3PO_4$  presented the highest environmental impacts for the majority of the indicators tested: acidification potential (62%), eutrophication (96%), ozone depletion potential (44%), human toxicity (64%), fresh water aquatic ecotoxicity (90%) and terrestrial ecotoxicity (92%). One of the highest impacts was found to be the global warming potential (GWP) (11.096 kg  $CO_2$  eq/kg AC), which was equally weighted between the steps involving impregnation, pyrolysis, and drying the washed AC. The cumulative energy demand (CED) of the AC production process from the by-product olive-waste cakes was 167.63 MJ. The steps involving impregnation, pyrolysis, and drying the washed AC steps contributed to this total. The use of phosphoric acid and electricity consumption were the main factors responsible for the majority of the impacts. If certain modifications are incorporated into the AC production, such as implementing synthesis gas recovery and reusing it as an energy source and recovery of phosphoric acid after AC washing, additional savings could be realized, and environmental impacts could be minimized.

**Keywords:** Olive-waste cakes, activated carbon, life cycle assessment, environmental impacts.

## **1. Introduction**

Food industries produce large volume of solid and liquid residues, which represent a disposal and potential environmental pollution problem (Fernández-Bolaños et al., 2006). Likewise, olive-oil production, one of the foremost agro-food industries in Mediterranean countries, generates different quantities and types of by-products depending on the production system adopted. Indeed, in most olive growing countries, even in the most advanced ones, especially in the South and East Mediterranean countries where vast planting and processing modernization schemes are underway to expand and upgrade the quality of olive oil produced, no definitive answer has been found for the disposal and treatment of olive mill wastes (liquid or solid). The olive oil manufacturing process has undergone evolutionary changes. The traditional discontinuous pressing process was initially replaced by continuous centrifugation using a three-phase system and, later on, a two-phase system. Depending on the olive oil production method used in each country, there are different types of wastes, most of which involve one type of residue or another (Fernández-Bolaños et al., 2006). The two-phase process generates only one by-product, which has moisture content in the range of 55-70%. The traditional press extraction method and the continuous three-phase system, which is the most widely used system for the production of olive oil, generate three products olive oil (20%) and two streams of waste: a wet solid waste (30%) called olive-waste cakes (orujo) and aqueous waste called olive mill wastewater or “alpechin” (50%) (Tsagaraki et al., 2007). The extraction process of the remaining oil from olive-waste cakes with the solvent hexane produces a solid residue called exhausted olive waste-cakes (orujillo). Exhausted olive-waste cake is a dry material (8%–10% moisture) composed of ground olive stones and pulp. It has a high lignin, cellulose, and hemicellulose content (Niaounakis and Halvadakis, 2006).

For the solid waste, different strategies have been proposed for the efficient elimination or transformation of this waste. For many years, the solid waste was partly used as an inefficient, polluting heating fuel (Jurado et al., 2003, El-Hamouz et al., 2007). It has also been used for feeding animals (Nefzaoui et al., 1999), in agricultural applications as an amendment for composting (Sellami et al., 2008) and in the production of activated carbon (AC) (Baccar et al., 2009). All the cited alternatives seem to be good solutions to valorize the by-product olive-waste cakes. However, environmental issues must be

considered when selecting the appropriate method to avoid creating a worse impact on the environment instead of resolving a problem. Therefore, a complete environmental assessment of any of these solutions must be carried out before considering it. Life cycle assessment (LCA) can be used for such evaluations. LCA is an environmental tool that aims to assess the environmental aspects of a process and potential environmental impacts during the entire process (from cradle to grave): from raw material extraction and acquisition, through energy and material production and manufacturing, to use, end-of-life treatment, recycling and final disposal (ISO14040, 2006). For each operation within a stage, the inputs (raw materials, resources and energy) and outputs (emission to air, water and solid waste) are calculated and then aggregated over the life cycle by means of material and energy balances, which are drawn over the system boundary (Arena et al., 2003). Since the selection of the most environmentally friendly of the cited alternatives for the valorization of olive-waste cakes is beyond the scope of this paper, we focus on the environmental impacts associated with the AC production process from this solid by-product.

The environmental impact associated with a specific AC varies because AC can be produced from various carbonaceous materials by physical or chemical activation or by a combination of the two processes. In this context, Srinivasakannan and Abu Baker (2004) reported that chemical activation using phosphoric acid is widely preferred over zinc chloride because  $ZnCl_2$  has a negative environmental impact and the activated carbon produced when using it cannot be used in the food and pharmaceutical industries. Up to now, to the best of our knowledge, few studies have been conducted to show the corresponding environmental impacts through an LCA of the AC production process. Bayer et al. (2005) studied an LCA of a granular AC produced from hard coal. In work reported by Muñoz et al. (2007), a comparison between granular AC adsorption and a coupled oxidation-biological process for wastewater treatment was conducted to identify the better process from an environmental point of view. In another study, LCA methodology was used to compare the environmental impact of dye treatment using a white rot-fungus with a standard treatment employing granular AC (Gabarrell et al., 2012).

Previous studies demonstrated that olive-waste activated carbon, prepared by chemical activation using phosphoric acid as a dehydrating agent, has the potential to remove metals (Baccar et al., 2009) and various organic pollutants such as dyes (Baccar et al.,

2010) and drugs (Baccar et al., 2012). Therefore, consideration should be given to determining the environmental impact of this AC.

The main objective of this investigation was to quantify the environmental impacts and critical life stages associated with the AC production process from Tunisian olive-waste cakes by using LCA methodology.

## **2. Materials and methods**

### **2.1. Data origin**

The data used were based on a laboratory-scale experiment performed at the National Engineering School of Sfax-Tunisia by the authors (Baccar et al., 2009). The raw material was kindly provided by an oil factory, “Agrozitex”, located 15 km from the laboratory. Although the assessment is based on the experimental data obtained at the laboratory scale, the study can give us an idea where the impacts are concentrated. Indeed, in recent studies, the LCAs were based on data obtained in laboratory experiments (Muñoz et al., 2006; Seigné Itoiz et al., 2012).

### **2.2. Preparation of activated carbon**

The activated carbon was prepared via chemical activation using phosphoric acid (analytical grade) as a dehydrating agent. The preparation of the activated carbon was conducted as follows: the crushed ( $\text{Ø} < 1.5 \text{ mm}$ ) and dried precursor, exhausted olive-waste cakes, was mixed with a  $\text{H}_3\text{PO}_4$  solution with a concentration of 60%  $\text{H}_3\text{PO}_4$  by weight. The impregnation ratio, defined by the weight ratio of impregnant ( $\text{H}_3\text{PO}_4$ ) to precursor, was 1.75. The impregnation was conducted in a stirred Pyrex reactor equipped with a reflux condenser. Stirring was used to ensure the acid had access to the interior of the olive-waste cake particles. The temperature and the duration of the reaction were 104 °C and 2 h, respectively. Agitation and heating were ensured using a heating magnetic stirrer with a connected temperature regulator probe made of Teflon. The pyrolysis of the impregnated material was conducted in a cylindrical stainless steel reactor inserted into a tubular regulated furnace under continuous nitrogen flow ( $0.5 \text{ L min}^{-1}$ ). The pyrolysis temperature and pyrolysis time were maintained at 450 °C and 2 h, respectively. After cooling down to room temperature under the same flow of nitrogen, the obtained activated carbon was thoroughly washed with hot distilled water

until it reached a neutral pH. The sample was then dried at 105 °C overnight, ground (to a granulometry ranging between 100 and 160  $\mu\text{m}$ ), and finally stored in a hermetic bottle for subsequent use.

### **2.3. Application of LCA methodology**

The experimental data obtained in the above-described experiment were used for applying the LCA methodology proposed by ISO 14040 (2006). The structure of an LCA consists of four distinct phases, which contributes to an integrated approach: (1) Goal and scope definition, which serves to define the purpose for carrying out the study, indicate the intended application of results, and identify the intended audience. In the scope definition, the LCA boundary and the functional unit are defined; (2) Inventory analysis (LCI), which consists of collection, quantification, and adaption according to the functional unit, of all the material and energy input and output flows within the LCA boundary; (3) Impact assessment (LCIA), which aims at understanding and evaluating the magnitude and significance of the potential environmental impact of a system. It serves to classify and characterize the main impact categories into environmental impact indicators; and (4) Interpretation, which evaluates the study to derive recommendations and conclusions.

In this study, the environmental impacts associated with each step were evaluated using the software Simapro 7.3 based on the ecoinvent database v2.2 (Swiss Centre for Life Cycle Inventories, SCLCI 2010) to obtain the background data. The impact assessment method used was CML 2 Baseline 2000. Only the obligatory phases defined by ISO 14040 regulations for the impact assessment, namely, classification and characterization were performed because they are more objective (European Commission, 2010, Martínez-Blanco et al., 2010). The impact categories considered in this study were: the (1) abiotic depletion potential (ADP) (kg Sb eq.), (2) acidification potential (AP) (kg SO<sub>2</sub> eq.), (3) eutrophication potential (EP) (kg PO<sub>4</sub><sup>3-</sup>eq.), (4) global warming potential (GWP) (kg CO<sub>2</sub> eq.), ozone layer depletion potential (ODP) (kg CFC<sup>-11</sup> eq.), and photochemical oxidation potential (PO) (kg C<sub>2</sub>H<sub>4</sub> eq.). In addition, toxicological impact categories (human toxicity (HT), fresh water aquatic ecotoxicity (FWE) (kg 1,4-DB eq.), and terrestrial ecotoxicity (TE) (kg 1,4-DB eq.)) and a flow indicator, the



cumulative energy demand (CED) (MJ), were also analyzed. The CED represents the entire energy demand, valued as primary energy, which arises in connection with the production, use and disposal of an economic good (González-García et al., 2012).

### **2.3.1. Goal and Scope Definition**

The main goal of this study is to quantify the environmental impacts of the AC production process from the by-product of olive oil processing. Such environmental information will be relevant to identifying the “environmental weaknesses” through the production process steps. This helps researchers modify and optimize the process and furthermore helps decision makers, scientists, authorities, and AC industries choose between different process/material alternatives.

#### **2.3.1.1 Functional Unit**

The functional unit is the unit of the product or service whose environmental impacts will be assessed or compared (ISO14040, 2006). In this study, the functional unit was defined as the production of 1 kg AC from Tunisian exhausted olive-waste cakes.

#### **2.3.1.2 System Boundary and Flowchart**

The system boundary is a set of criteria specifying which unit processes are part of the product system (ISO 14040, 2006). Figure 1 shows the AC production system, which includes nine steps: 1- transporting the exhausted olive-waste cakes to the laboratory; 2- drying the raw material; 3- crushing the dried raw material; 4- impregnating using  $H_3PO_4$ ; 5- pyrolysis; 6- cooling; 7- washing with water and filtering; 8- drying the washed AC; and 9- crushing the final AC. For each step, the input/output flows were identified.

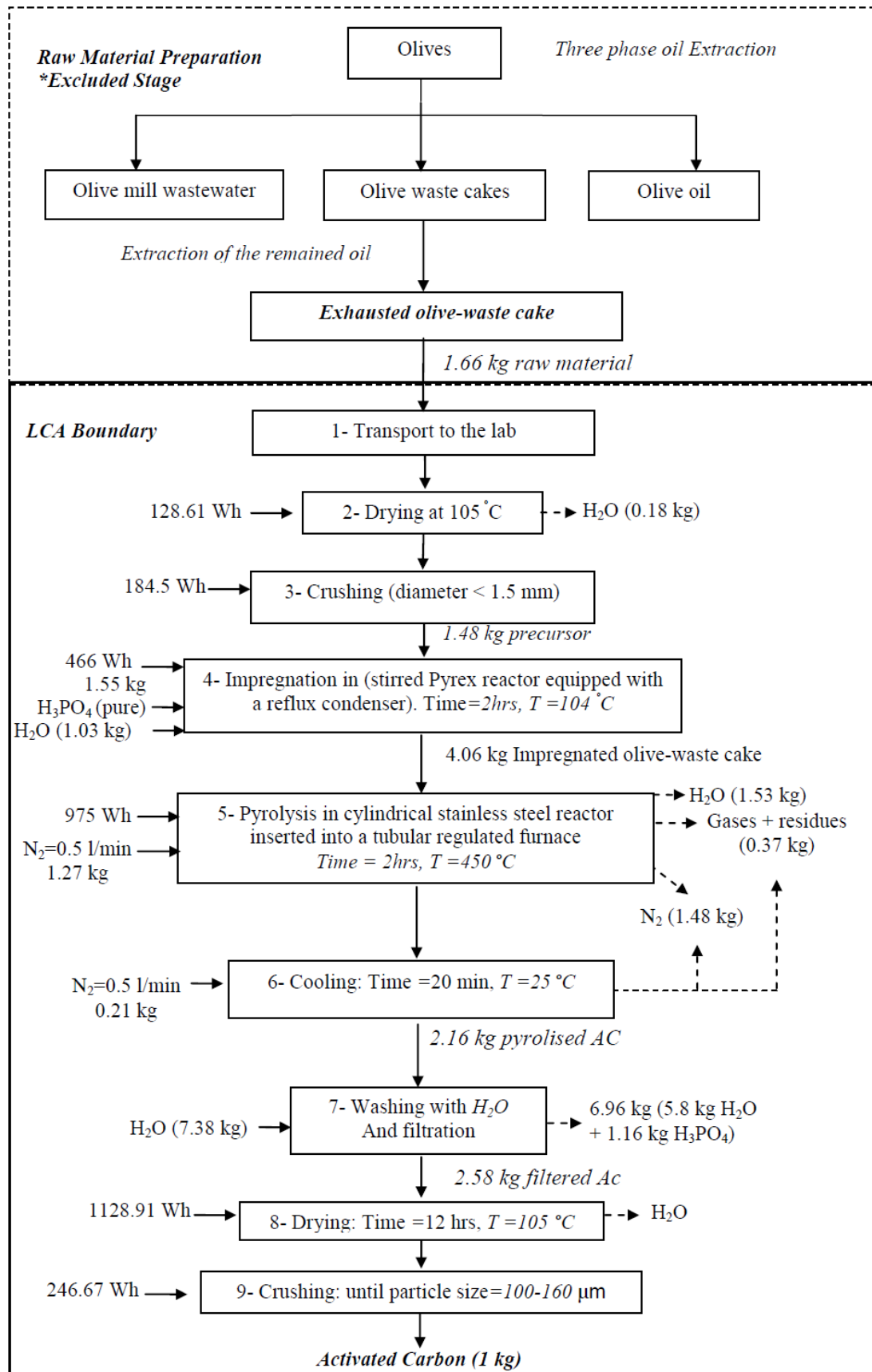


Figure 1: “To produce 1 kg AC production process flowchart from olive-waste cakes”

### **2.3.2. Life Cycle Inventory (LCI)**

Based on a laboratory-scale experimental process, the required inventory primary data were collected, calculated, and analyzed. Input/output data were collected and quantified for each production step. Some data were calculated based on the experimental production process (to produce 54.2 g AC) and then adapted according to the functional unit: 1 kg AC production process. Linear adaptation has been assumed. The amount of H<sub>3</sub>PO<sub>4</sub> (60% concentration) was converted to the corresponding amount of 85% concentration that corresponds to the commercial form.

To complete the life cycle inventories, missing secondary data were obtained from the literature and the ecoinvent database. The energy consumed as a form of electricity was supplied from the Tunisian grid. Tunisian electricity does not exist in the ecoinvent 2.2 database; therefore, it was created as an energy dataset source based on data collected from the Tunisian company of electricity and gas STEG (2007). The drying energies required for steps 2 and 8 were calculated using thermodynamics equations.

Due to the lack of some output analysis and the unavailability of many waste scenarios in the ecoinvent database, different waste scenarios were identified for the output flows based on many assumptions. Thermodynamic equations were used to calculate the drying energies. The ideal gas law was used as the basis to calculate the nitrogen gas flux weight. The Granular Activated Carbon (GAC) inventory and impact results were based on a previous study described by Gabarrell et al. (2012).

All water output flows were assumed to be discharged through one output pipe to a wastewater treatment plant (WWTP). This step up was used due to the large amount of water output from the system.

The water mixed with diluted H<sub>3</sub>PO<sub>4</sub> derived from the washing step was assumed in SimaPro to be “wastewater, untreated, slightly organic and inorganic contaminated” to be discharged to the WWTP; this was done because this waste stream does not exist in the ecoinvent database. Adding to that, this stream is small compared with the total wastewater output, so precise information is less critical in this case

Two types of residues were derived from the pyrolysis step: volatile gases that come from the top of the reactor and a solid residue in the form of viscous oil. The latter was assumed to be disposed to landfills as hard coal ash residues from stove. Concerning the gases, their composition was determined based on the literature (Encinar et al., 2008).

### **3. Results and discussion**

#### **3.1. Inventory analysis results**

Table 1 and Figure 1 summarize the inventory results corresponding to the experimental data and the adapted data for the input and output materials and emissions.

During the production process of AC, 1.66 kg of exhausted olive-waste cake is needed to prepare 1 kg AC with an average percentage yield of 60%. This AC presented a relatively high yield compared with ACs prepared with physical activation, which means it can be produced cheaper compared with other sorbents. In chemical activation, costs are generally lower compared with physical one, primarily because of the increased product yield (Stavropoulos and Zabaniotou, 2009).

To produce 1 kg of AC from olive-waste cakes, 1.55 kg of pure  $H_3PO_4$  is required in the activation process, and 75% of this amount is lost with the output washing water. Such a loss of an expensive and nonrenewable resource is critical, especially for large-scale processes.

After the pyrolysis step, to remove any residual phosphoric acid, the cooled carbon was washed by using 7.38 l of water per 1 kg of AC. Ng et al. (2003) used a higher quantity of water, 40 l per kg carbon, to remove phosphoric acid from AC prepared from pecan shells. Considering all steps of AC production, to produce 1 kg of AC from olive-waste cakes, 8.41 kg of water was used and 10.25 kg of wastewater was generated. Compared with Gabarrell et al. (2012), the quantity of water used in this study is less than that reported by these authors, who cited that 12.0 kg of water was necessary to produce 1 kg of granular AC (GAC).

**Table 1:** LCI Inventory Input- Output materials and emissions

<b>Material Input</b>	<b>Experimental lab. Amount (g)</b>	<b>Adapted amount (kg)</b>
Olive-waste cakes	90	1.66
H <sub>3</sub> PO <sub>4</sub> (pure)	84	1.55
Nitrogen gas N <sub>2</sub>	80.2	1.48
Dematerialized H <sub>2</sub> O for H <sub>3</sub> PO <sub>4</sub> dilution	56	1.03
Dematerialized H <sub>2</sub> O for washing	400	7.38
<b>Material Output</b>	<b>Experimental lab. Amount (g)</b>	<b>Adapted amount (kg)</b>
Wastewater derived from drying the raw material	10	0.18
Wastewater derived from pyrolysis step	83.16	1.53
Wastewater contaminated with H <sub>3</sub> PO <sub>4</sub> derived from washing and filtration	377.22	6.96
Wastewater derived from drying the filtered activated acarbon	85.50	1.58
Gases and residues derived from pyrolysis and cooling steps	19.92	0.37
Nitrogen gas N <sub>2</sub> derived from pyrolysis and cooling steps	80.20	1.48
Activated carbon (AC)	54.20	1.00

Table 2 described the energy amounts required to produce 1 Kg AC. Concerning the power consumption, approximately 3.13 kWh/kg AC is presumed as a form of electricity supplied from the Tunisian Grid, where 36% of this amount is consumed to dry the washed AC. Compared with Bayer et al. (2005), to produce 1 kg of GAC from hard coal, energy power of 1.6 kWh was required. This difference may be due to the distinct preparation methodologies and operation conditions used. Indeed, the AC in this study was prepared on the laboratory scale and the other sorbent was prepared on a larger scale (different equipments were used, and consequently, different amounts of electricity were required). According to Gabarrell et al. (2012), the energy consumption of large-scale processes is usually lower than the consumption of laboratory–or pilot–scale processes due to the increase in the efficiency of industrial systems.

**Table 2:** Energy necessary to produce 1 kg AC from exhausted olive-waste cakes

Energy Process	Equipment Type	Temperature (°C)	Time (h)	Power (W)	Energy (Wh)
Electricity used for drying the raw material	Drying oven	105	-	-	128.61
Electricity used for crushing the dried raw material	Laboratory crusher		0.62	300	184.5
Electricity used for impregnation step	Stirred Pyrex reactor equipped with a reflux condenser	104	2	233	466
Electricity used for pyrolysis step	cylindrical stainless steel reactor inserted into a tubular regulated furnace	450	2	487.5	975
Electricity used for drying the washed AC	Drying oven	105	-	-	1128.91
Electricity used for crushing the final produced AC	Laboratory crusher	-	0.62	400	246.67

### 3.2. Environmental assessment results

By analyzing the AC production, only the steps of impregnation, pyrolysis and cooling and drying the final AC product are considered. The steps involving transport, raw material drying, crushing, and washing the final AC presented reduced environmental impacts (0%–6.4%) and therefore were excluded from the impact assessment. From Table 3, it can be seen that the results show that the majority of the impact was due to the impregnation of the raw material by phosphoric acid, followed by the pyrolysis step, and finally by drying the washed AC. Figure 2 shows the relative impact contributions of the three relevant steps of AC production selected in the categories analyzed. The impregnation step presented the highest environmental impact regarding the majority of impact considered in this study, particularly for EU (96.31%), TE (92.47%), FEW (90.02%), HT (63.99%), AP (62.31%) and ODP (44.31%). The main contribution was due to the use of phosphoric acid especially for AP and HT impacts; the  $H_3PO_4$  contributed 90% and 91%, respectively. The abiotic depletion (AP) category involved three steps impregnation, pyrolysis and cooling, and drying with percentages of 29.13, 26.35 and 29.44%, respectively. The pyrolysis and cooling step presented the highest relative PO impact (45.3% out of 0.007 kg  $C_2H_4$  eq/kg AC), and this is due to the  $C_2H_4$  (eq.) emissions contained in the gases released from the pyrolysis of the precursor olive-waste cakes.

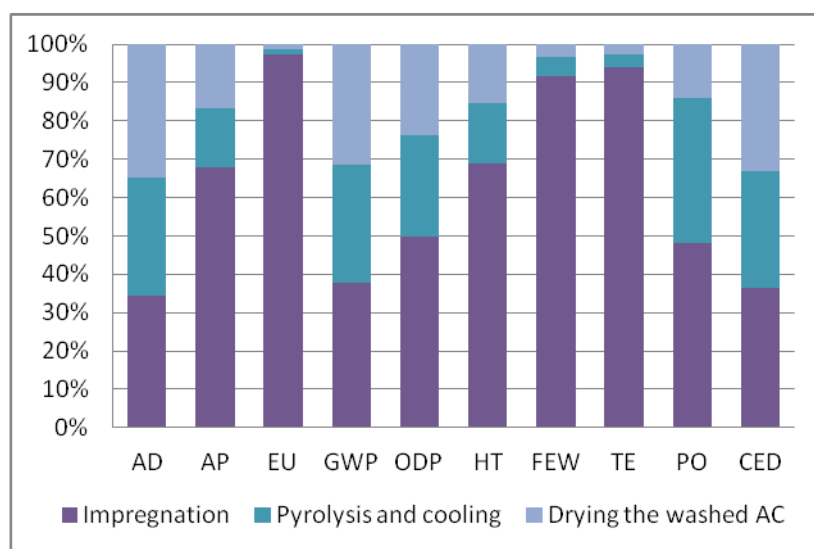


**Figure 2:** Environmental impacts of AC production process from olive-waste cakes

**Table 3:** Environmental impacts of AC production process from olive-waste cakes in Tunisia

Impact category	Unit	Impregnation	Pyrolysis and cooling	Drying the washed AC	Total
Abiotic depletion (AD)	kg Sb eq.	29.13%	26.35%	29.44%	0.079
Acidification potential (AP)	kg SO <sub>2</sub> eq.	62.32%	14.20%	15.37%	0.108
Eutrophication (EU)	kg PO <sub>4</sub> <sup>3-</sup> eq.	96.31%	1.26%	1.28%	0.033
Global warming (GWP)	kg CO <sub>2</sub> eq.	29.89%	30.53%	25.03%	11.096
Ozone layer depletion (ODP)	kg CFC <sup>-11</sup> eq.	44.31%	23.74%	21.12%	5.4584E-07
Human toxicity (HT)	kg 1,4-DB eq.	63.99%	14.41%	14.30%	5.260
Fresh water aquatic ecotox.(FEW)	kg 1,4-DB eq.	90.02%	4.95%	3.34%	4.899
Terrestrial ecotoxicity (TE)	kg 1,4-DB eq.	92.47%	3.25%	2.64%	0.016
Photochemical oxidation potential (PO)	kg C <sub>2</sub> H <sub>4</sub>	37.98%	45.30%	11.04%	0.007
Cumulative energy demand (CED)	MJ	31.11%	26.05%	28.32%	167.630



GWP estimates the relative contribution of each pollutant, compared with carbon dioxide, to heating up the atmosphere (greenhouse effect) (Lashof and Ahuja, 1999). Regarding this impact, the results showed that producing 1 kg AC from olive-waste cakes in Tunisia emits 11.096 kg of CO<sub>2</sub> per kg of AC into the atmosphere. This result is almost as that reported by Bayer et al. (2005), who found that 11 kg of CO<sub>2</sub> was emitted per kg GAC prepared from hard coal. For the pyrolysis and drying steps, the electricity was the main factor responsible for this impact (69.3%). This may be due to the fuel cycle emissions generated from producing electricity from natural gas. Methane has a global warming potential, and it is released in high amounts when natural gas is used to generate electricity (Meier, 2002). Indeed, 98% of Tunisian electricity is based on natural gas systems (STEG, 2007).

The cumulative energy demand (CED) of a product represents the direct and indirect energy used in units of MJ throughout the life cycle, including the energy consumed during the extraction, manufacturing and disposal of the raw and auxiliary materials. In this study, the CED was found to be 167.63 MJ per kg of AC. The contribution to this impact was nearly equal between the impregnation, drying the washed AC and pyrolysis steps with 31.11, 28.32 and 26.05%, respectively. Electrical energy is needed to operate all the equipment used in the three steps.

The results found in this work were compared with those reported by Gabarrell et al. (2012) concerning the GAC production process using hard coal (Table 4). The environmental impacts of the functional unit GAC production process are less than the impacts of the olive-waste cakes AC in the majority of the impact categories. This can be attributed to two factors: the larger amount of energy used as electricity supplied from the Tunisian grid and the use of H<sub>3</sub>PO<sub>4</sub> as an activating agent when producing AC from olive-waste cakes. Moreover, each production process has different inputs, assumptions, production scales, and energy sources. The GAC LCA was analyzed based on industrial-scale data, while the olive waste AC was based on lab-scale data. The GAC production process was based on natural gas and coal as energy inputs, whereas the olive waste AC is based on large amounts of “natural gas-based” electricity. Meanwhile, the GAC production process was based on physical activation, whereas the olive waste AC production process was based on physical and chemical activation (using H<sub>3</sub>PO<sub>4</sub>).

**Table 4:** Total environmental impacts of the AC production from olive-waste cakes and the GAC

Impact category	Unit	Olive-waste cakes AC (this study)	GAC (Gabarrell et al., 2012)
Abiotic depletion (AD)	kg Sb eq.	0.079	0.0757
Acidification potential (AP)	kg SO <sub>2</sub> eq.	0.108	0.0533
Eutrophication (EU)	kg PO <sub>4</sub> <sup>---</sup> eq.	0.033	0.0025
Global warming (GWP)	kg CO <sub>2</sub> eq.	11.096	8.40
Ozone depletion potential (ODP)	kg CFC-11 eq.	5.4584E-07	1.900E-07
Human toxicity (HT)	kg 1,4-DB eq.	5.260	2.08
Fresh water aquatic ecotox.(FEW)	kg 1,4-DB eq.	4.899	0.343
Terrestrial ecotoxicity (TE)	kg 1,4-DB eq.	0.016	0.0169
Photochemical oxidation (PE)	kg C <sub>2</sub> H <sub>4</sub>	0.007	0.0024

### 3.3. Sensitivity Analyses

The LCIA results of the AC production process from Tunisian olive-waste cakes showed that the concentrated H<sub>3</sub>PO<sub>4</sub>, an impregnating agent, and the energy inputs, a form of electricity supplied from the Tunisian grid, are the critical points causing higher environmental impacts in certain categories. Accordingly, reducing those inputs leads to reduced environmental impacts and resource use.

Energy recovery from the gases was not included in this study. The reuse of the gases produced during the pyrolysis step for use as an energy source could be beneficial. Analyzing the hot gases released from the pyrolysis step based on other similar works in the literature (Encinar et al., 2008), it was found that the gases were mostly hydrogen (0.002 kg H<sub>2</sub>), carbon monoxide (2.24 kg CO), methane (0.021 kg CH<sub>4</sub>), and carbon dioxide (3.413 kg CO<sub>2</sub>). The energy that can be recovered from those gases was calculated based on thermodynamic equations to be 624 Wh. This amount of energy, when recovered, could be sufficient for drying the raw material and performing the crushing step.

Another practice to save resources and reduce energy consumption is the recovery of diluted  $H_3PO_4$  generated with the contaminated water from the AC washing step.  $H_3PO_4$  recovery means avoiding the excess energy consumption and emissions resulting from phosphate raw material extraction and thus reducing the environmental impact of the  $H_3PO_4$ . Furthermore, because the  $H_3PO_4$  sources are limited and have a high price, recovery contributes to relative phosphoric acid savings. The corresponding environmental impact reductions are highly dependent on the recovery techniques. Accordingly, further investigations are needed regarding this point.

The residues from the pyrolysis step have been assumed to be disposed of in sanitary landfills; this assumption increases the HT and FEW impacts. To reduce those impacts, further analysis is needed to study the recycling possibilities.

As suggested by Gabarrell et al. (2012), working on an industrial scale rather than on the laboratory scale would lower the energy consumption due to the increase in the efficiency of industrial systems. Moreover, for large-scale systems, the first step of drying could be avoided and the exhausted olive-waste cakes could be crushed directly. Accordingly, energy consumption would be slightly reduced.

Finally, if these suggestions were put into operation, savings in environmental emissions could be realized and could significantly improve the profitability balance of the whole operation.

#### **4. Conclusions**

Based on laboratory-scale data, the AC production process from olive-waste cakes was analyzed to quantify the corresponding environmental impacts. One benefit of the life cycle assessment is the generation of a strategy for improving the activated carbon production process and decreasing the environmental impacts associated with the production.

The results showed that the environmental impacts are dominated by impregnation, followed by pyrolysis of the impregnated precursor, and finally by drying the washed AC. The GWP impact was found to be 11.10 kg CO<sub>2</sub> eq/kg AC, which is comparable to a GAC prepared from hard coal reported in literature. The impregnation step presented the highest environmental impact considered in this study, particularly for EU (96.31%), TE (92.47%), FEW (90.02%), HT (63.99%), AP (62.31%) and ODP

(44.31%). The main contribution was due to the use of phosphoric acid especially for the AP and HT impacts; the  $H_3PO_4$  contributed 90% and 91%, respectively. The total CED (167.63 MJ) is shared equally between the steps involving impregnation, drying the washed AC and pyrolysis.

Finally, if certain modifications are incorporated into the system, such as synthesis gas recovery for reuse as an energy source and recovery of phosphoric acid after AC washing, additional savings could be realized. Accordingly, to minimize the environmental impact, further studies are needed to accomplish the following tasks: first, recover the  $H_3PO_4$  generated with the contaminated water; second, recover the energy from the pyrolysis hot gases; and third, study the regeneration of the used olive waste AC after treatment for further LCA studies.

### **Acknowledgments**

The authors would like to thank the Spanish Ministry of Foreign Affairs and Cooperation, AECID, for the predoctoral scholarship of R. Baccar.

### **REFERENCES**

- Arena U., Mastellone M.L., Perugini F., 2003. The environmental performance of alternative solid waste management options: a life cycle assessment study. *Chem. Eng. J.* 96, 207-222.
- Baccar R., Blázquez P., Bouzid J., Feki M., Sarrà M., 2012. Removal of pharmaceutical compounds by activated carbon prepared from agricultural by-product. *Chem. Eng. J.* 211-212, 310–317.
- Baccar R., Blázquez P., Bouzid J., Feki M., Sarrà M., 2010. Equilibrium, thermodynamic and kinetic studies on adsorption of commercial dye by activated carbon derived from olive-waste cakes. *Chem. Eng. J.* 165, 457–464.
- Baccar R., Bouzid J., Feki M., Montiel A., 2009. Preparation of activated carbon from Tunisian olive waste cakes and its application for adsorption of heavy metal ions. *J. Hazard. Mater.* 162, 1522–1529.
- Bayer P., Heuer E., Karl U., Finkel M., (2005). Economical and ecological comparison of granular activated carbon (GAC) adsorber refill strategies. *Water Res.* 39 (9), 1719–1728.

- El-Hamouz A., Hilal H. S., Nassar N., Mardawi Z., 2007. Solid olive waste in environmental cleanup: Oil recovery and carbon production for water purification J. Environ. Manage. 84, 83–92.
- European Commission, 2010. Joint Research Centre - Institute for Environment and Sustainability: International Reference Life Cycle Data System (ILCD) Handbook General guide for Life Cycle Assessment - Detailed guidance. First edition. Luxembourg. Publications Office of the European Union.
- Encinar J.M., González J.F., Martínez G., González J.M., 2008. Two stages catalytic pyrolysis of olive oil waste. Fuel Process. Technol. 89, 1448 – 1455.
- Fernández-Bolaños J., Rodríguez G., Rodríguez R., Guillén R., Jiménez A., 2006. Potential use of olive by-products. Extraction of interesting organic compounds from olive oil waste. Grasas y Aceites 57 (1), 95–106.
- Gabarrell X., Font M., Vicent T., Caminal G., Sarrà M., Blánquez P., 2012. A comparative life cycle assessment of two treatment technologies for the Grey Lanaset G textile dye: biodegradation by *Trametes versicolor* and granular activated carbon adsorption. Int. J. Life Cycle Ass. 17, 613–624.
- González-García S., Bacenetti J., Murphy R. J., Fiala M., 2012. Present and future environmental impact of poplar cultivation in the Po Valley (Italy) under different crop management systems. J. Cleaner Prod. 26, 56–66.
- ISO, 14040. Environmental Management– Life Cycle Assessment– Principles and Framework. International for Standardisation (ISO). Switzerland 2006.
- Jurado F., Cano A., Carpio J., 2003. Modeling of combined cycle power plants using biomass. Renew. Energ. 28, 743–753.
- Lashof D. A., Ahuja D. R., 1990. Relative contributions of greenhouse gas emissions to global warming. Nature 344, 529–553.
- Martínez-Blanco J., Colón J., Gabarrell X., Font X., Sánchez A., Artola A., Rieradevall J. 2010. The use of life cycle assessment for the comparison of biowaste composting at home and full scale. Waste management 30, 983–994.
- Meier P.J., 2002. Life Cycle Assessment of Electricity Generation Systems and Applications for Climate Change Policy Analysis. PhD research. Fusion technology institute, University of Wisconsin, Madison.

- Muñoz I., Rieradevall J., Torrades F., Peral J., Domenech X., 2006. Environmental assessment of different advanced Oxidation processes applied to a bleaching kraft mill effluent. *Chemosphere* 62 (1), 9-16.
- Muñoz I., Peral J., Ayllón J. A., Malato S., Martin M. J., Perrot J.Y., Vincent M., Domènech X., 2007. Life-Cycle Assessment of a Coupled Advanced Oxidation Biological Process for Wastewater Treatment: Comparison with Granular Activated Carbon Adsorption. *Environ. Eng. Sci.* 24 (5),638–651.
- Nefzaoui A., 1999. Olive tree by-products. In: International Center for Agricultural Research in the Dry Areas (Rabat).
- Ng C., Marshall W. E, Rao R. M., Bansode R. R., Losso J. N., 2003. Activated carbon from pecan shell: process description and economic analysis. *Ind. Crop. Prod.* 17, 209–217.
- Niaounakis N., Halvadakis C.P., 2006. Olive processing waste management: literature review and patent survey. Second Edition by Elsevier Ltd, Italy.
- Sevigné Itoiz E., Fuentes-Grünwald C., Gasol C.M., Garcés E., Alacid E., Rossi S., Rieradevall J., 2012. Energy balance and environmental impact analysis of marine microalgal biomass production for biodiesel generation in a photobioreactor pilot plant. *Biomass Bioenergy* 39, 324-335.
- Stavropoulos G.G., Zabaniotou A.A., 2009. Minimizing activated carbons production cost. *Fuel Process. Technol.* 90, 952–957.
- Sellami F., Jarboui R., Hachicha S., Medhioub K., Ammar E., 2008. Co-composting of oil exhausted olive-cake, poultry manure and industrial residues of agro-food activity for soil amendment. *Bioresour. Technol.* 99, 1177–1188.
- Srinivasakannan C., Abu Bakar M.Z., 2004. Production of activated carbon from rubber wood sawdust. *Biomass Energy* 27, 89-96.
- STEG “La Société Tunisienne de l'Electricité et du Gaz”, 2007. Effort National de Maitrise De L'énergie: Contribution De La STEG. Home page : ([http://www.steg.com.tn/journee\\_sidi\\_salem/maitrise\\_energie.pdf](http://www.steg.com.tn/journee_sidi_salem/maitrise_energie.pdf)).
- Tsagaraki E., Lazardies H.N., Ptrolos K.B., 2007. Utilization of by-products and treatment of waste in the food industry. Vasso Oreopoulou and Winfried Russ Editors pp.1- 316.

## Topic 2: Modeling of adsorption

---

The second topic of the thesis concerns the evaluation of the potential of the activated carbon prepared under optimal conditions to remove a textile and tannery dyes from individual and real effluents and pharmaceuticals products from single and mixture solutions. The effect of time, pH and temperature on the adsorption process of the target contaminants is evaluated. Finally various models are applied to fit the equilibrium and kinetics data. The following publications 4.2.1, 4.2.2 and 4.2.3 enclose this topic:

**4.2.1: Equilibrium, thermodynamic and kinetic studies on adsorption of commercial dye by activated carbon derived from olive-waste cakes**

*Chemical Engineering Journal*, 165 (2010) 457–464

**4.2.2: Modeling of adsorption isotherms and kinetics of a tannery dye onto an activated carbon prepared from an agricultural by-product**

*Fuel Processing Technology*, 106 (2013) 408–415

**4.2.3: Removal of pharmaceutical compounds by activated carbon prepared from agricultural by-product**

*Chemical Engineering Journal*, 211-212 (2012) 310–317

#### 4.2.1: Equilibrium, thermodynamic and kinetic studies on a dsorption of commercial dye by activated carbon derived from olive-waste cakes

---





**Abstract**

Adsorption of Lanaset Grey G, an industrial metal complex dye, on activated carbon derived from Tunisian olive-waste cakes was explored. The equilibrium adsorption data, obtained at 25 °C, were analyzed by Langmuir Freundlich and Temkin models. The results indicate that the Langmuir, model provides the best correlation of the experimental data. The adsorption capacity of the sorbent for Lanaset Grey G was found to be 108.7 mg g<sup>-1</sup> which is better than the capacity of a commercial activated carbon. The kinetic studies, conducted at three temperatures (10, 25 and 37 °C) indicated that the adsorption process followed the pseudo-first-order kinetic model and increase of temperature enhanced both rate and efficiency of the dye uptake. The application of the intra-particle diffusion model revealed that the adsorption mechanism of this dye is rather a complex process and the intra-particle diffusion is involved in the overall rate of the adsorption process but it is not the only rate-controlling step. The calculated thermodynamics parameters showed the spontaneous and the endothermic nature of the adsorption process. The activation energy found to be 32.1 kJ mol<sup>-1</sup>, could indicate a physical adsorption process. The presence of others components, commonly used in the textile industrial bath, did not affect the uptake extent of the target dye by the activated carbon. Olive-waste cakes activated carbon was shown to be a promising adsorbent for the efficient removal of metal complex dyes.

**Keywords:** Low cost adsorbent, metal complex dye, textile wastewater.

## **1. Introduction**

Wastewater generated by textile industries is rated as the most polluting among all industrial sectors considering both volumes discharged and effluent composition. These effluents can damage the environment, if they are discharged directly into the surface waters or into wastewater treatment plant, as they contain dyes with complex and variable chemical structures. The metal complex dye group is one of the most important and widely used dye groups in the textile industry due to their excellent light fastness on substrates (Ozacar and Sengil, 2005). In commercial terms, the more important metal complex dyes are chromium, cobalt and copper complexes with azo ligands. Without adequate treatment, textile dyes can remain in the environment for an extended period of time (Li and Guthrie, 2010). Therefore, their removal from waste effluents becomes environmentally important. Many treatment processes have been applied for the removal of dyes from wastewater such as coagulation, flocculation, ozonation, membrane filtration, Fentons reagent, ion exchange and biological treatment (Robinson et al., 2001, Blázquez et al., 2008, Crini, 2006). These methods, however, display one or more limitations, such as low efficiency, high cost, generation of secondary pollution and narrow appliance range. Overcoming these limitations, chemists have been devoted to search for effective, economic and easily methods (Runping et al., 2009). Adsorption process has gained favour recently as it is one of the most effective methods. Besides, adsorption onto activated carbonic (AC) is proven to be very effective in treating textile effluents (Binupriya et al., 2008, Namasivayam and Kavitha, 2002). However, its widespread use is restricted due to the high cost of conventional and commercial carbons. Therefore, in recent years, many researchers have tried to produce activated carbons using renewable and cheaper precursors which were mainly industrial and agricultural by-products (lignocellulosics) including peach stones (Molina-Sabio et al., 1995), date stones (Girgis et al., 2002, Haimour and Emeish, 2006), waste apple pulp in cider production (Suarez-Garcia et al., 2002), rice husks (Guo et al., 2005), pistachio-nut shells (Yang and Chong, 2006) and coir pitch (Namasivayam and Kavitha, 2002). The use of these materials as precursors for the preparation of activated carbon produces not only a useful and a low cost adsorbent for the purification of contaminated environments, but also contributes to minimizing the solid wastes. Olive-waste cakes are an agro-food waste predominantly produced in the Mediterranean countries and

especially in Tunisia as it is the fourth largest olive oil producer in the world (Sellami et al., 2008).

The main objective of this study is to evaluate the adsorption potential of an activated carbon prepared from Tunisian olive-waste cakes for metal complex dyes, particularly Lanaset Grey G. It is to be noted that only a limited number of studies dealing with the removal of metal complex dyes have been found in the literature (Ozacar and Sengil, 2005, Gupta et al., 1990, Stolz, 2001, Vijaykumar et al., 2006).

The adsorbent used in this work was prepared in the laboratory scale, from olive-waste cakes, via chemical activation using phosphoric acid as a dehydrating agent. Optimization of some process parameters and characterization of the optimal activated carbon were first investigated. Thereafter, the adsorption of the Lanaset Grey G was undertaken. The adsorption isotherms, kinetic and thermodynamic aspects of the retention process were explored. Finally, the effect of the additives, commonly used by the industry to dye the textile, on the uptake of the Lanaset Grey G by the adsorbent, was studied.

Concerning the target dye, Lanaset Grey G, it is a commercial mixture of several metal complex dyes used in the textile industry “Artextil S.A” located in Sabadell, Barcelona. The chemical formula of this water-soluble dye is unavailable. However, this material is known to contain cobalt II (0.79 wt %) and chromium III (2.5 wt %) as organo-metal complexes.

## **2. Materials and methods**

### **2.1. Preparation of activated carbon**

Exhausted olive-waste cakes, obtained from an oil factory “Agrozitex” located in Sfax, Tunisia, was used as raw material for the production of activated carbons via chemical activation. For this purpose, phosphoric acid (analytical grade) was retained as a dehydrating agent. Each preparation test was conducted as follows: 40 g of the crushed ( $\text{Ø} < 1.5 \text{ mm}$ ) and dried precursor was mixed with  $\text{H}_3\text{PO}_4$  solutions having different concentrations (30 to 85 %  $\text{H}_3\text{PO}_4$  in weight). The impregnation ratio, defined by the weight ratio of impregnant ( $\text{H}_3\text{PO}_4$ ) to precursor, was 1, 1.25, 1.5, 1.75, 1.85 and 2. The impregnation was carried out in a stirred pyrex reactor equipped with a reflux condenser. Stirring was used to ensure the access of the acid to the interior of the olive-waste cake particles. The temperature and the duration of the reaction were 104 °C and

2 hours, respectively. Agitation and heating were ensured by a heating magnetic stirrer with connected temperature regulator probe made of Teflon. The pyrolysis of the impregnated material was conducted in a cylindrical stainless steel reactor, inserted into a tubular regulated furnace under continuous nitrogen flow ( $0.5 \text{ Lmin}^{-1}$ ). Pyrolysis temperature ranged from 350 to 650 °C, while pyrolysis time was maintained at 2 hours. After cooling down to room temperature, under the same flow of nitrogen, the obtained activated carbon was thoroughly washed with hot distilled water until neutral pH. The sample was then dried at 105 °C overnight, ground (until a granulometry ranging between 100 and 160  $\mu\text{m}$ ) and finally kept in hermetic bottle for subsequent uses.

## **2.2. Characterization**

### **2.2.1. Characterization of the prepared adsorbents**

To optimize the preparation method, the effect of the main process parameters (acid concentration, impregnation ratio, temperature of pyrolysis step) on the performances of the prepared activated carbons was studied. These performances were expressed in terms of iodine and methylene blue numbers. The choice of these molecules is justified by their properties. Thus, the methylene blue is the most recognized probe molecule for assessing the ability of the sorbent to remove large molecules via its macroporosity (pore diameter greater than 1.5 nm) and this also serves as model compound for adsorption of organic contaminants from aqueous solutions (Baçaoui et al., 2001). On the contrary, the iodine number gives an indication on microporosity (pores less than 1 nm in diameter) and consequently on the specific surface area of the sorbent material.

### **2.2.2. Characterization of the adsorbent prepared under optimal conditions**

Specific surface area of the activated carbon prepared under optimal conditions, which will be used later for the adsorption of the metal complex dye, was evaluated through  $\text{N}_2$  adsorption at 77K, using an Autosorb1-Quantachrome instrument. The BET (Brunauer-Emmet and Teller) model was applied to fit nitrogen adsorption isotherm and evaluate the surface area ( $S_{\text{BET}}$ ) of the sorbent (Vernersson et al., 2002). Crystalline phases eventually present in the adsorbent material were analyzed by powder X-ray diffraction (XRD analyzer Philips X Pert).

## 2.3. Adsorption studies

### 2.3.1. Chemicals

Lanaset Grey G, a dark blue powder composed of a mixture of metal complex dyes, was purchased from Ciba (Specialty Chemicals, Barcelona Ref. 080173.5). The additives used industrially with the dye Lanaset Grey G (Esterol 126, citric acid, Amplex DG and Antifoam) were supplied by the industry “Artextil S.A” located in Sabadell, Barcelona. All other chemicals used were of analytical grade. Solutions were prepared by dissolving the corresponding reagents in bidistilled water.

The activated carbon, prepared under the optimal conditions, was retained for all the following adsorption experiments.

### 2.3.2. Effect of pH on adsorption of Lanaset Grey G

The effect of pH on the dye uptake by the adsorbent was investigated at 25 °C using synthetic solutions containing 150 mg L<sup>-1</sup> Lanaset Grey G. Adsorption tests were carried out by adding 0.50 g of activated carbon to a series of 500 mL Erlenmeyer flasks filled with 300 mL of the above solution at different pH values. The initial pH of the solutions was adjusted between 2 and 11 by adding either HCl (1M) or NaOH (1M). Solution pH's were measured by a high precision pH-meter (Metrohm, model 632), equipped with a combined glass electrode (Metrohm). Preliminary calibration was systematically carried out using suitable buffer solutions. To make sure that the equilibrium was reached, each suspension was magnetically stirred for 3 days at 250 rpm. Then, each dye solution was separated from the sorbent by centrifugation at 13000 rpm for 5 min. The residual concentration of the Lanaset grey G (C<sub>e</sub>) was measured at 590 nm using an UV/Visible spectrophotometer (UNICAM 8625).

For a given pH, the amount of dye adsorbed at equilibrium q<sub>e</sub> (mg g<sup>-1</sup>) was calculated from Eq. (1):

$$q_e = \frac{(C_0 - C_e)V}{m_{AC}} \quad (1)$$

where C<sub>0</sub> and C<sub>e</sub> (mg L<sup>-1</sup>) are the liquid phase concentrations of dye at initial and equilibrium, respectively, V the volume of the solution (L) and m<sub>AC</sub> is the mass of activated carbon used in the experiment (g).

### **2.3.3. Sorption isotherm and kinetic studies**

Equilibrium and kinetics of the dye adsorption were studied here at 25 °C.

For the determination of equilibrium isotherm, adsorption tests were carried out by adding various amounts of adsorbent (0.10, 0.175, 0.30, 0.50 and 0.60 g) to a series of 500 mL Erlenmeyer flasks filled with 300 mL solution containing 150 mg L<sup>-1</sup> of Lanaset Grey G. The solution was maintained at its natural pH (pH= 4.5). The flasks were shaken at 250 rpm with a magnetic stirrer and kept for 3 days to reach adsorption equilibrium. At the end of each experiment, the separation of the dye solution from the sorbent and the measure of the residual concentration ( $C_e$ ) of the Lanaset Grey G were conducted by the same method mentioned above.

The amount of dye adsorbed at equilibrium  $q_e$  (mg g<sup>-1</sup>) was calculated by Eq. (1).

The procedure of Kinetic tests was basically identical to those of equilibrium. Nevertheless, for each suspension, the liquid samples taken for dye analysis were realized at preset time intervals. The amount of dye adsorbed at time  $t$ ,  $q_t$  (mg g<sup>-1</sup>), was calculated by Eq. (1) by substituting  $C_e$  by  $C_t$ . The latter represents the liquid phase concentration of dye at any time  $t$ .

### **2.3.4. Effect of temperature**

The effect of the temperature on the dye sorption process was investigated by time-based analyses, when the adsorption systems were analyzed until residual dye concentration in the solution became constant (equilibrium state). The kinetic adsorption runs were performed at three different temperatures, i.e. 15, 25 and 37 °C, by using the same stock solution containing 150 mg L<sup>-1</sup> Lanaset Grey G at its natural pH (pH= 4.5). The agitation of the mixture was realized by a magnetic stirrer at 250 rpm. For each temperature, the quantities:  $C_t$ ,  $q_t$ ,  $C_e$  and  $q_e$  were determined as described above.

The rate and equilibrium, data obtained at the three temperatures considered were used to evaluate the activation energy ( $E_a$ ) and the thermodynamic parameters ( $\Delta G^\circ$ ,  $\Delta H^\circ$  and  $\Delta S^\circ$ ) of the dye adsorption process.

### **2.3.5. Effect of the additives used in the textile bath on the adsorption**

In textile industry, the bath used to dye textiles contained apart from the dye Lanaset Grey G ( $150 \text{ mg L}^{-1}$ ), other components (additives), i.e. Esterol 126 ( $0.5 \text{ g L}^{-1}$ ); citric acid ( $1.5 \text{ g L}^{-1}$ ); Amplex DG ( $1 \text{ g L}^{-1}$ ) and Antifoam. The additive Esterol 126 is an equalizer, the citric acid is used to adjust the pH and the Amplex DG.

In order to investigate the effect of these additives on the uptake of the Lanaset Grey G by the adsorbent, a solution having the same composition of the industrial bath described above was prepared. The equilibrium isotherm, relating to the adsorption of Lanaset Grey G from this mixture, was established at  $25 \text{ }^{\circ}\text{C}$  following the same procedure used for the individual dye (only Lanaset Grey G). Thus, adsorption tests were carried out by adding various amounts of adsorbent (0.10, 0.20, 0.30, 0.45, 0.60 and 1.00 g) to a series of 500 mL Erlenmeyer flasks filled with 300 mL of the prepared mixture. The separation of the solution from the sorbent and the measure of the residual concentration of Lanaset Grey G were conducted by the same methods described above for the individual dye.

## **3. Results and discussion**

### **3.1. Preparation of activated carbons: effect of processing parameters**

Within the scope of our researches, an attempt has been made to optimize the process parameters which lead to an activated carbon with good characteristics. 3 D response surfaces were plotted to represent our results. This representation showed the relative effects of any two variables when the remaining variables were kept constant.

As illustration, Figure 1 shows the effect of the main process parameters (phosphoric acid concentration, impregnation ratio and temperature of pyrolysis step) and their mutual interactions on the performances of the prepared sorbents expressed in terms of iodine and methylene blue numbers.

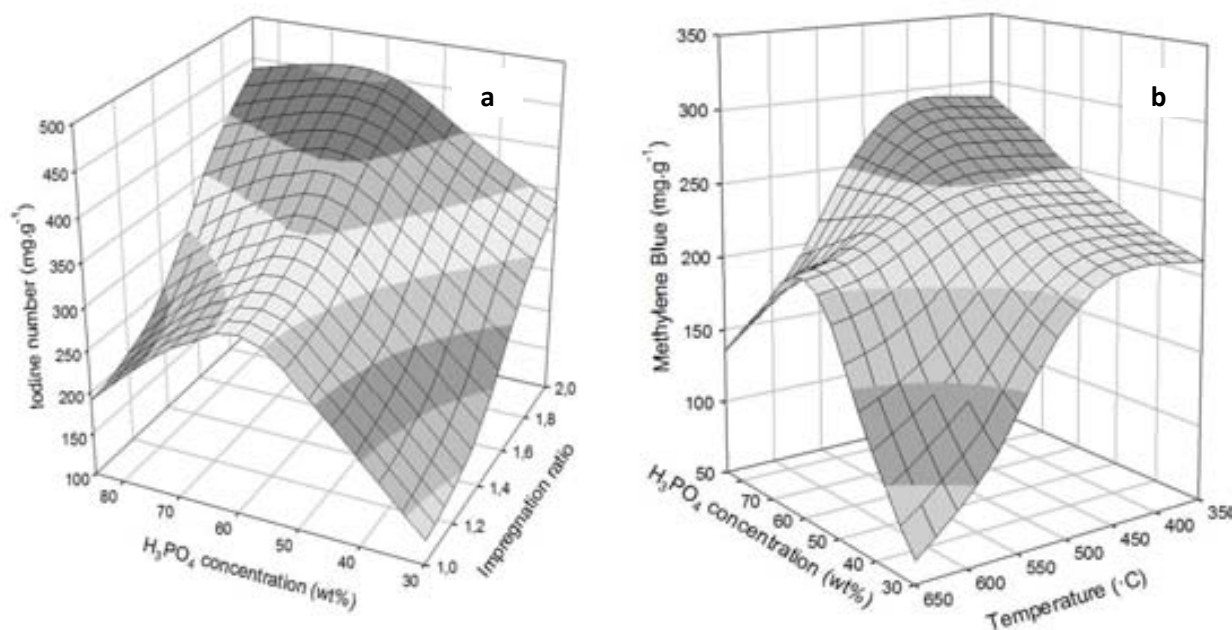


**Figure 1:** (a) Effect of acid concentration and impregnation ratio on iodine number. (b) Effect of acid concentration and temperature on methylene blue number.

Acid concentration and impregnation ratio are important factors that govern the development of porosity of the prepared carbon (Molina-Sabio et al., 1995). The effect of these two parameters on the iodine number of the adsorbent is shown in Figure 1a. As it can be discerned, the iodine number increases rapidly with an increase of acid concentration from 35% to 60%  $\text{H}_3\text{PO}_4$  and until an impregnation ratio of 1.75. Beyond this impregnation ratio, the iodine number decreases while it increases slightly with acid concentration higher than 60%  $\text{H}_3\text{PO}_4$ . Taking into account this slight increase of the iodine number occurring in the acid concentration range 60–85%  $\text{H}_3\text{PO}_4$  and the handling difficulties of the most concentrated commercial phosphoric acid (85%  $\text{H}_3\text{PO}_4$  in weight) owing especially to its high viscosity, a concentration of 60%  $\text{H}_3\text{PO}_4$  and an impregnation ratio of 1.75 seems to be the most suitable values for the development of the best iodine number and, consequently, to the best development of microporous structure.

The effect of temperature and acid concentration on methylene blue number is illustrated in Figure 1b. As it can be seen, the quantity of methylene blue adsorbed increases with an increase of the temperature from 350 to 450 °C and an acid concentration from 30% to 85%  $\text{H}_3\text{PO}_4$ . Thus, keeping the pyrolysis temperature around



its optimal value (i.e. 450 °C), leads to a better development of the sorbent macroporosity. Several investigators have established that in the case of H<sub>3</sub>PO<sub>4</sub> activation of other agricultural materials (woods, coconut shell, date pits, grain sorghum), temperatures neighbouring 450 °C were also suitable to obtain optimal properties of the activated carbons (Jagtoyen and Derbyshire, 1993, Molina-Sabio et al., 1995, Diao et al., 2002, Girgis et al., 2002).

The above results show that the most efficient activated carbon is that obtained under the followings optimal conditions: an acid concentration equal to 60% in weight, an impregnation ratio of 1.75 and a pyrolysis temperature of 450 °C. It is to note that results obtained when studying individually the effect of each parameter (acid concentration, impregnation ratio and pyrolysis temperature) on the whole considered properties, namely iodine and methylene blue numbers (results not shown), lead to the same optimal conditions (Baccar et al., 2009).

### **3.2. Characteristics of the activated carbon prepared under the optimal conditions**

It was found that the BET surface area, total pore volume and average pore diameter of the activated carbon were 793 m<sup>2</sup> g<sup>-1</sup>, 0.49 cm<sup>3</sup> g<sup>-1</sup> and 4.2 nm, respectively. The XRD pattern of the sorbent did not show any peak. This indicates the amorphous nature of the carbon prepared from olive-waste cakes.

### **3.3. Effect of pH on dye adsorption**

In this part, the pH of the dye solution was varied in the range 2-11.

Before presenting the pH dependence of the dye uptake by the sorbent, an important fact deserves to be pointed out. When adjusting at alkaline values the pH of the metal complex dye solutions used in this part, no precipitation of metal hydroxides (Co (OH)<sub>2</sub> and Cr (OH)<sub>3</sub>) was observed. This means that the metallic species (Co<sup>2+</sup> and Cr<sup>3+</sup>), taking part of the chemical composition of the industrial dye, are strongly bounded to the organic groups (ligands) of the dye molecules. In other words, the organo-metal complex dye molecules do not dissociate since the addition of OH<sup>-</sup> ions does not yield a precipitate of metal hydroxide. In fact, the more stable the complex, the smaller is the tendency of the complex to dissociate into its constituents. Thus, the free metal ion concentration is very small, so small in fact that the solubility product of metal hydroxide is not reached.

Concerning the effect of pH on the extent of dye adsorption, our experimental results (Figure 2) showed no significant variation of the amount of solute adsorbed in the pH range explored. According to the findings of several investigations dealing with adsorption of dyes of different chemical structures, the effect of pH on the solute uptake by activated carbons can be high, moderate or slightly significant (Namasivayam and Kavitha, 2002, Guo et al., 2005, Iqbal and Ashiq, 2007, Gupta and Suhas, 2009). Adsorption is affected by the pH change of the solution since this parameter affects the degree of ionization of the dye and the surface properties of the sorbents. As a general rule, low pH values result in lowering the number of negatively charged sites of the activated carbon, increasing the number of positively charged sites thus enhancing the adsorption of anionic dyes. With the increase in pH values, the hydroxyl ion concentration increases and on the surface of the carbon the number of negatively charged sites increases so that the extent of adsorption of cationic dyes is increased (Iqbal and Ashiq, 2007, Gupta and Suhas, 2009). For the dye used in this work, the results related to the pH effect are apparently surprising. However, a plausible explanation of this behavior may be the presence of both negatively and positively charged functional groups in the dye molecules. Independently of the origin of this insignificant effect of the pH, we estimate that this finding is quite meaningful in adsorption process application since it makes not indispensable any pH adjustment of the effluent before treatment.

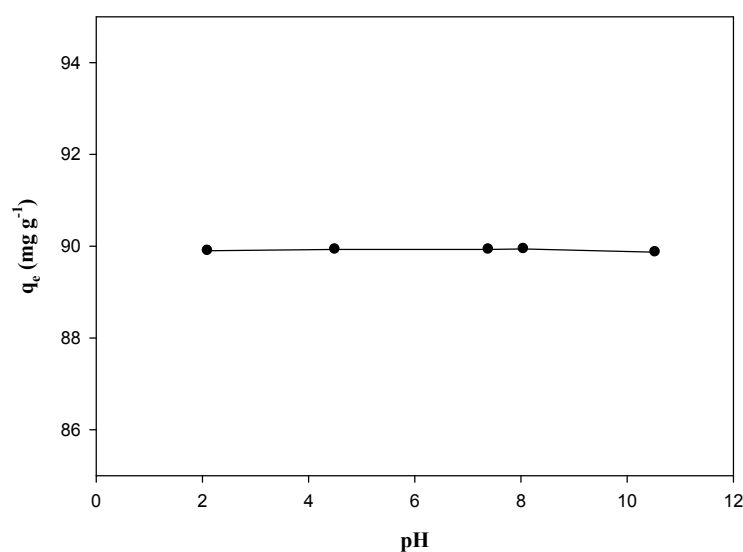


**Figure 2:** Effect of pH on adsorption of Lanaset Grey G ( $C_0=150 \text{ mg L}^{-1}$ ;  $T=25 \text{ }^\circ\text{C}$ ).

### 3.4. Effect of contact time on dye adsorption

Figure 3 shows the residual dye concentration versus contact time. As illustration we presented only the curves relative to 0.10, 0.30 and 0.60 g of adsorbent. The results indicate that the contact time needed to reach adsorption equilibrium of Lanaset Grey G on activated carbon is about 50 hours for all the sorbent loadings considered. Thus, the chosen contact time of 3 days, used in our experiments, is enough sufficient to reach equilibrium state.

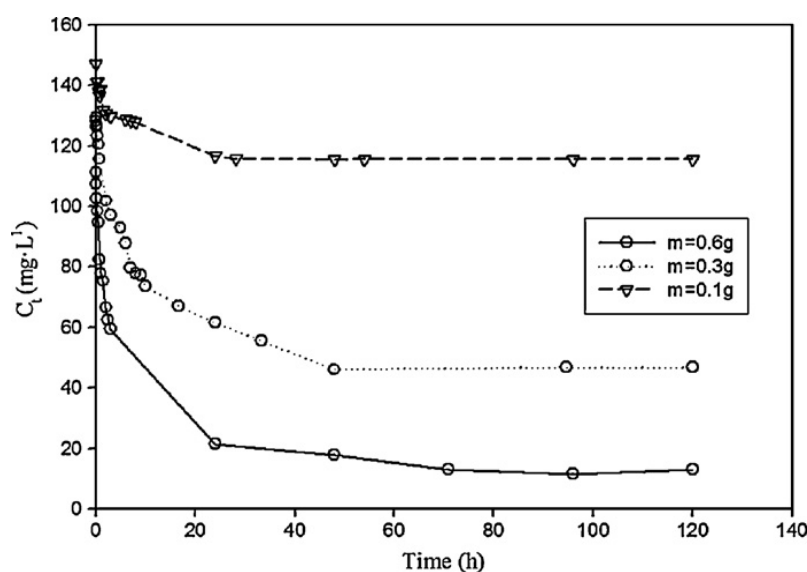


**Figure 3:** Effect of contact time on Lanaset Grey G adsorption for different amounts of adsorbent ( $C_0=150 \text{ mg L}^{-1}$ ;  $T=25 \text{ }^\circ\text{C}$ ).

At the beginning, the dye is adsorbed by the exterior surface of the activated carbon, the adsorption rate is fast (Figure 3). When the exterior adsorption surface reaches saturation, the dye enters into the pores of the adsorbent and is adsorbed by the interior surface of the particles. This phenomenon takes relatively long contact time. Chen et al. (2001), for example, used 5 days as contact time for the adsorption isotherm of dyestuffs on pitch. To make sure that full equilibrium was attained, Hameed et al. (2007) used as a contact time of 48 hours for the adsorption of acid green 25 dye.

It is to be noted that the time-based results described above agree with the general theory of dye adsorption process: initially the dye molecules have to first encounter the boundary layer effect and then diffuse from the boundary layer film onto adsorbent surface and then finally they have to diffuse into the porous structure of the adsorbent

(Tan et al., 2008). Accordingly, the residual concentration of Lanaset Grey G decreases with time and, at some point in time, it reaches a constant value beyond which no more dye is further removed from the solution. At this point, the amount of the dye desorbing from the activated carbon is in a state of dynamic equilibrium with the amount of the dye being adsorbed on the carbon.

### **3.5. Adsorption isotherm**

The adsorption isotherm indicates how the adsorption molecules distribute between the liquid phase and the solid phase when the adsorption process reaches an equilibrium state.

Three isotherm models, relating to adsorption equilibrium, have been tested in the present research, namely Langmuir, Freundlich and Temkin isotherm models.

Langmuir model assumes monolayer adsorption onto a surface containing a finite number of adsorption sites of uniform energies of adsorption with no transmigration of adsorbate in the plane of surface. The Langmuir isotherm is described by Eq. (2):

$$q_e = \frac{q_{\max} K_L C_e}{1 + K_L C_e} \quad (2)$$

where  $q_{\max}$  and  $K_L$  are Langmuir constants related to adsorption capacity (maximum amount adsorbed per gram of adsorbent ( $\text{mg g}^{-1}$ )) and energy of sorption ( $\text{L mg}^{-1}$ ), respectively. Values of  $q_{\max}$  and  $K_L$  can be calculated from the slope and intercept of the linear plot of  $C_e/q_e$  against  $C_e$ .

The essential characteristics of the Langmuir isotherm can be expressed in terms of dimensionless constant separation factor  $R_L$ , defined as:

$$R_L = \frac{1}{1 + K_L C_0} \quad (3)$$

where  $C_0$  is the initial dye concentration. The value of  $R_L$  indicates the type of isotherm to be either unfavorable ( $R_L > 1$ ), linear ( $R_L = 1$ ), favorable ( $0 < R_L < 1$ ) or irreversible ( $R_L = 1$ ).

The empirical Freundlich model, which is known to be satisfactory for low concentrations and based on sorption on a heterogeneous surface, is expressed by Eq. (4):

$$q_e = K_F C_e^{1/n} \quad (4)$$

where  $K_F$  and  $n$  are Freundlich constants related to the adsorption capacity and adsorption intensity, respectively. These parameters can be calculated from the intercept and the slope of the linear plot  $\log q_e$  versus  $\log C_e$ .

Temkin model considers the effects of indirect adsorbate-adsorbate interactions on adsorption isotherm. It assumes that the heat of adsorption of all the molecules in the layer decreases linearly with coverage due to adsorbate-adsorbate interactions.

The Temkin isotherm can be expressed by Eq. (5):

$$q_e = \frac{RT}{b} \ln(AC_e) \quad (5)$$

where constant  $B = RT/b = (RT/\Delta E)q_{max}$ ,  $T$  the temperature (K),  $R$  the universal gas constant ( $8.314 \text{ J mol}^{-1}\text{K}^{-1}$ ),  $\Delta E = (-\Delta H)$  the variation of adsorption energy ( $\text{J mol}^{-1}$ ),  $A$  the Temkin equilibrium constant ( $\text{L mg}^{-1}$ ) corresponding to the maximum binding energy and  $q_{max}$  is the adsorption (maximum) capacity (Kundu and Gupta, 2006, Hamdaoui and Naffrechoux, 2007). If the adsorption obeys Temkin equation,  $A$  and  $B$  can be obtained from the slope and intercept of the plot  $q_e$  against  $\ln C_e$ .

Table 1 presents the parameters corresponding to the Langmuir, Freundlich and Temkin isotherms established at  $25^\circ\text{C}$ . A comparison of  $R^2$  values for the three models indicates that the Langmuir equation provides the best correlation of the experimental data. The fact that the Langmuir isotherm fits the experimental data very well may be due to the homogenous distribution of active sites on the activated carbon surface. Similar observations were reported for the adsorption of metal complex dyes on pine sawdust (Ozacar and Sengil, 2005). The adsorption capacity ( $q_{max}$ ) determined from Langmuir model was  $108.7 \text{ mg g}^{-1}$ . The value of  $R_L$  in the present investigation was found to be 0.031, confirming the favorable adsorption of the Lanaset Grey G.

**Table 1:** Langmuir, Freundlich and Temkin isotherm model parameters and correlation coefficients for adsorption of Lanaset Grey G at 25 °C.

<b>Isotherms</b>	<b>Parameters</b>
Langmuir	$q_{\max} = 108.7 \text{ mg g}^{-1}$ $R_L = 0.031$ $R^2 = 0.998$
Freundlich	$K_F = 48.6 \text{ mg g}^{-1} (\text{L mg}^{-1})^{1/n}$ $n = 5.847$ $R^2 = 0.859$
Temkin	$A = 15.8 \text{ L mg}^{-1}$ $B = 14.4 \text{ J mol}^{-1}$ $R^2 = 0.854$

For the sake of comparison, values of some adsorbent capacities – towards Lanaset Grey G and other dyes – available in the literature are shown in Table 2. As it can be seen, the capacity of the carbon used in this work ( $108.7 \text{ mg g}^{-1}$ ) compare well and sometimes more favorable than those of other sorbents prepared from agricultural wastes or of the commercial activated carbon CAL.

**Table 2:** Comparison of the adsorption capacity of the (AC) prepared from olive-waste cakes and other adsorbents for different dyes

Adsorbent	Adsorbate	Adsorbent capacity $q_{\max}(\text{mg g}^{-1})$	References
AC from olive-waste cakes	Lanaset Grey G	108.7	This work
AC from rice husk	Acid blue	50.0	Mohamed, 2004
AC from orange peel	Direct blue-86	37.3	El Nemr et al., 2009
Pine sawdust	Metal complex blue	82.0	Ozacar and Sengýl, 2004
Pine sawdust	Metal complex yellow	105.0	Ozacar and Sengýl, 2004
Wood	Acid blue 25	17.5	Chen et al., 2001
Hazelnut shell	Acid blue 25	60.2	Ferrero, 2007
Commercial AC F400 (Chemviron)	Lanaset Grey G	454.5	Blánquez and Sarrà, 2010
Commercial AC CAL (Chemviron)	Lanaset Grey G	56.8	Blánquez and Sarrà, 2010

### 3.5. Adsorption kinetics

#### 3.5.1. Pseudo-first and pseudo-second order equations

The modeling of kinetics of adsorption was investigated by two common models, namely, the Lagergren pseudo-first order and pseudo-second order models. The linear forms of these two models are expressed by Eqs. (6) and (7), respectively:

$$\log(q_e - q_t) = \log q_e - K_1 t \quad (6)$$

$$\frac{t}{q_t} = \frac{1}{K_2 q_e^2} + \frac{1}{q_e} t \quad (7)$$

where the terms  $q_e$  and  $q_t$  have the same meaning previously mentioned and are expressed in  $\text{mg g}^{-1}$ ,  $K_1$  and  $K_2$  are the pseudo-first order and the pseudo-second order model rate constants, expressed in  $\text{min}^{-1}$  and  $\text{g mg}^{-1} \text{min}^{-1}$ , respectively.

The calculated  $q_e$ ,  $K_1$ ,  $K_2$  and the corresponding linear regression coefficient  $R^2$  values are presented in Table 3. The applicability of the kinetic model is compared by judging the correlation coefficients  $R^2$  and the agreement between the calculated and the experimental  $q_e$  values. In a view of these both considerations, we may conclude that the pseudo first-order mechanism is predominant. Note that this result is an agreement with those reported in several papers dealing with adsorption of organic solutes on activated carbons (Gupta and Suhas, 2009; Rajeev et al., 2010; Galiatsatou et al., 2002, Belmouden et al., 2001).

**Table 3:** Parameters of the first and second order kinetic models

Adsorbent amounts (g)	First order Kinetic model				Second order Kinetic model		
	$q_{e,\text{exp}}$ ( $\text{mg g}^{-1}$ )	$K_1$ ( $\text{min}^{-1}$ )	$q_{e,\text{cal}}$ ( $\text{mg g}^{-1}$ )	$R^2$	$K_2 \times 10^5$ ( $\text{g mg}^{-1} \text{min}^{-1}$ )	$q_{e,\text{cal}}$ ( $\text{mg g}^{-1}$ )	$R^2$
m=0.10	113.6	0.0019	106.4	0.997	8	71.2	0.961
m=0.30	103.2	0.0009	105.2	0.995	6	60.8	0.869
m=0.50	80.2	0.0019	80.0	0.998	2	41.5	0.968
m=0.60	68.5	0.0014	68.9	0.991	25.5	39.6	0.942



### 3.5.2. Intra-particle diffusion

Intra-particle diffusion model based on the theory proposed by Weber and Morris (1963) was tested to identify the diffusion mechanism. According to this theory, adsorbate uptake  $q_t$  varies almost proportionally with the square root of the contact time,  $t^{1/2}$  rather than  $t$ :

$$q_t = K_{id} t^{1/2} + C \quad (8)$$

where  $C$  is the intercept and  $k_{id}$  ( $\text{mg} \cdot \text{g}^{-1} \text{h}^{-1/2}$ ) is the intra-particle diffusion rate constant. If intra particle diffusion occurs, then  $q_t$  versus  $t^{1/2}$  will be linear and if the plot passes through the origin, then the rate limiting step is only due to the intra particle diffusion. Otherwise, some other mechanisms along with intra-particle diffusion are involved. In most cases, this plot gives general features of three stages: initial curved portion, followed by an intermediate linear portion and a plateau. The initial sharper, is due to the instantaneous adsorption or external surface adsorption (external mass transfer). The intermediate linear part is due to intra-particle diffusion and the plateau to the equilibrium stage where intra particle diffusion starts to slow down due to extremely low solute concentrations in the solution (Daifullah et al., 2007).

Plot of the quantity of Lanaset Grey G adsorbed against square root of time is shown in Figure 4.

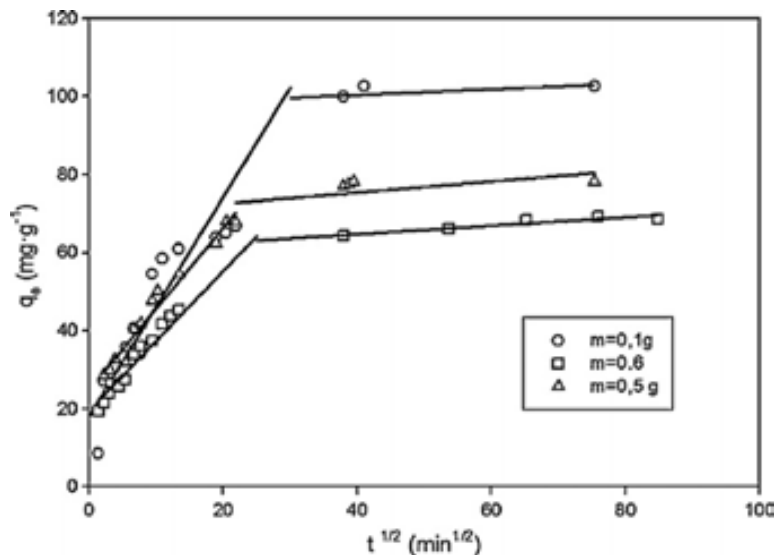


**Figure 4:** Plots of Lanaset grey G uptake against square root of contact time.

It can be observed that the plots are not linear over the whole time range and the graphs of this figure reflect a dual nature, with initial linear portion followed by a plateau. The fact that the first curved portion of the plots seems to be absent implies that the external surface adsorption (stage 1) is relatively very fast and the stage of intra-particle diffusion (stage 2) is rapidly attained and continued to 50 hours. Finally, equilibrium adsorption (stage 3) starts after 50 hours. The dye molecules are slowly transported via intra-particle diffusion into the particles and are finally retained in the pores. The linear portion of the curve does not pass the origin and the latter stage of Lanaset Grey adsorption does not follow Weber-Morris equation. It may be concluded that the adsorption mechanism of this dye is rather a complex process and the intra-particle diffusion was not the only rate-controlling step. The results obtained agreed with those found by Monser and Adhoum (Monser and Adhoum, 2009) for the adsorption of tartrazine onto activated carbon.

### **3.6. Effect of temperature**

Adsorption experiments were carried out for different contact times at three different temperatures 15, 25 and 37 °C. For each temperature considered, the values of  $C_e$  and  $q_e$  corresponding to the equilibrium state were also determined. The results related to the time dependence of  $q_t$  are shown in Figure 5. It was found that the uptake of the dye by the sorbent adsorption capacity increases with the increasing temperature from 15 to 37 °C, indicating that the adsorption is an endothermic process (Hameed et al., 2007; Al-Degs et al., 2008).

The equilibrium constant  $K_D$  of the adsorption process, expressed in  $L g^{-1}$ , can be used to estimate the thermodynamic parameters due to its dependence on temperature. The changes in standard free energy ( $\Delta G^\circ$ ), enthalpy ( $\Delta H^\circ$ ) and entropy ( $\Delta S^\circ$ ) of adsorption process were determined by using Eqs. (9) - (11):

$$k_D = \frac{q_e}{C_e} \quad (9)$$

$$\Delta G^\circ = -RT \ln K_D \quad (10)$$

$$\ln K_D = \frac{\Delta S^\circ}{R} - \frac{\Delta H^\circ}{RT} \quad (11)$$

A Van't Hoff plot of  $\ln K_D$  as a function of  $1/T$  (figure not shown) yields to a straight line. The  $\Delta H^\circ$  and  $\Delta S^\circ$  parameters were calculated from the slope and intercept of the plot, respectively. The values of the thermodynamic parameters are listed in Table 4.

**Table 4:** Thermodynamic parameters for the adsorption of Lanaset Grey G onto activated carbon prepared from Tunisian olive-waste cakes at different temperatures

$\Delta S^\circ$ (J mol <sup>-1</sup> K <sup>-1</sup> )	$\Delta H^\circ$ (kJ mol <sup>-1</sup> )	$\Delta G^\circ$ (KJ mol <sup>-1</sup> )		
		288 K	298K	310 K
169.7	49.0	-0.14	-1.56	-3.60

The positive value of  $\Delta S^\circ$  means an increase in the randomness at the solid/solution interface during the adsorption of the dye on the activated carbon (Aziz et al., 2009). Such positive value may be explained as follows: in the adsorption of the dye, the adsorbate species displace adsorbed solvent molecules to gain more translational entropy than was lost by the adsorbate, thus allowing randomness in the system. The  $\Delta H^\circ$  parameter was found to be 49.02 kJ mol<sup>-1</sup>. The positive value of  $\Delta H^\circ$  further confirms the endothermic nature of the adsorption process (Ruhan et al., 2009). The decrease in  $\Delta G^\circ$  values shows the feasibility of adsorption as the temperature increased. Similar results were reported by Li et al. (2009) for the adsorption of 2-nitroaniline onto activated carbon prepared from cotton stalk fiber.

On considering the time-profiles of dye uptake presented in Figure 5, the effect of temperature on the kinetics of the adsorption was also investigated by the Lagergren pseudo-first order and pseudo-second order models. The parameters related to each model were presented in Table 5.

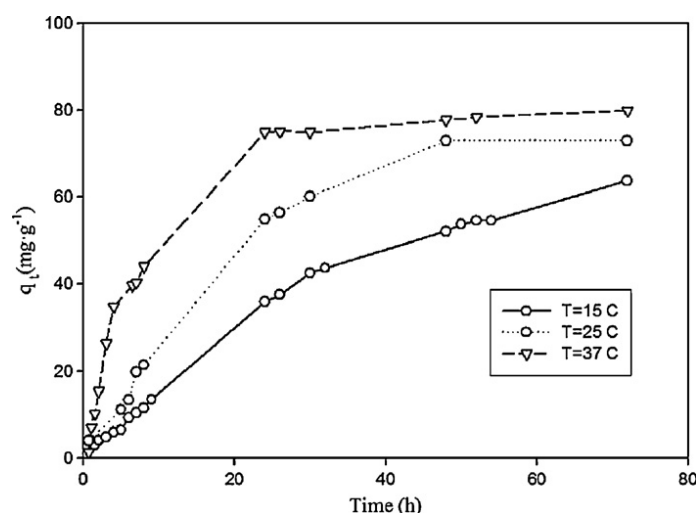


**Figure 5:** Variation of dye uptake with contact time at different temperatures (15, 25 and 37 °C).

**Table 5:** Parameters of the first and second order kinetic models at various temperatures

	First order Kinetic model				Second order Kinetic model		
	$q_{e,exp}$ ( $\text{mg g}^{-1}$ )	$K_1$ ( $1 \text{ min}^{-1}$ )	$q_{e,cal}$ ( $\text{mg g}^{-1}$ )	$R^2$	$K_2 \times 10^6$ ( $\text{g mg}^{-1} \text{ min}^{-1}$ )	$q_{e,cal}$ ( $\text{mg g}^{-1}$ )	$R^2$
<b>T=15 °C</b>	63.7	0.0006	67.5	0.998	1.2	151.5	0.771
<b>T=25 °C</b>	72.9	0.0010	80.6	0.994	4.5	113.6	0.861
<b>T=37 °C</b>	79.9	0.0013	66.4	0.956	12.0	101.0	0.852

As previously observed, the results fitted the first order model for the three temperatures considered. The correlation coefficients of the first order model for 15 °C and 25 °C were higher than 0.99 except for 37 °C which is equal to 0.954. The data given in table 5 also shows that the pseudo-first order rate constant  $K_1$  increases with temperature indicating enhancement of the adsorption kinetics as the temperature increases. This enhancement reflects again the endothermic character of the adsorption process. The activation energy  $E_a$  for Lanaset Grey G adsorption was determined from the slope of the Arrhenius plot of  $\ln K_1$  versus temperature ( $1/T$ ) (figure. not shown) and was found to be  $32.1 \text{ kJ mol}^{-1}$ . The magnitude of activation energy gives an idea about the type of adsorption which is mainly physical or chemical. The physisorption processes usually have energies in the range of  $5\text{-}40 \text{ kJ mol}^{-1}$ , while higher activation energies ( $40\text{-}800 \text{ kJ mol}^{-1}$ ) suggest chemisorptions (Hameed et al., 2007). Consequently, the relatively low

activation energy ( $32.1 \text{ kJ mol}^{-1}$ ) obtained for the adsorption of Lanaset Grey G on the activated carbon may involve a physical sorption.

### 3.7. Adsorption of dye from industrial solution

The adsorption isotherms of the dye present in industrial solution and of the individual Lanaset Grey G are presented in Figure 6. The results relating to the industrial solution were fitted to Langmuir and Freundlich isotherm models. A comparison of  $R^2$  values for the two models indicates that the Langmuir equation ( $R^2= 0.997$ ) fits better the experimental data than the Freundlich equation ( $R^2= 0.897$ ). The same results were found previously for the individual dye (only Grey Lanaset G). When comparing the maximum adsorption capacity ( $q_{\max}$ ) of the activated carbon towards the dye in the industrial solution ( $133.9 \text{ mg g}^{-1}$ ) with that for the individual Lanaset Grey G ( $108.7 \text{ mg g}^{-1}$ ), we can conclude that the added components did not affect the uptake extent of the target solute by the activated carbon. This means that the dye competes well with the additives for the adsorption sites of the sorbent. The value of  $R_L$  was found to be  $0 < 0.072 < 1$  indicating the favorable uptake of the dye from the industrial solution.

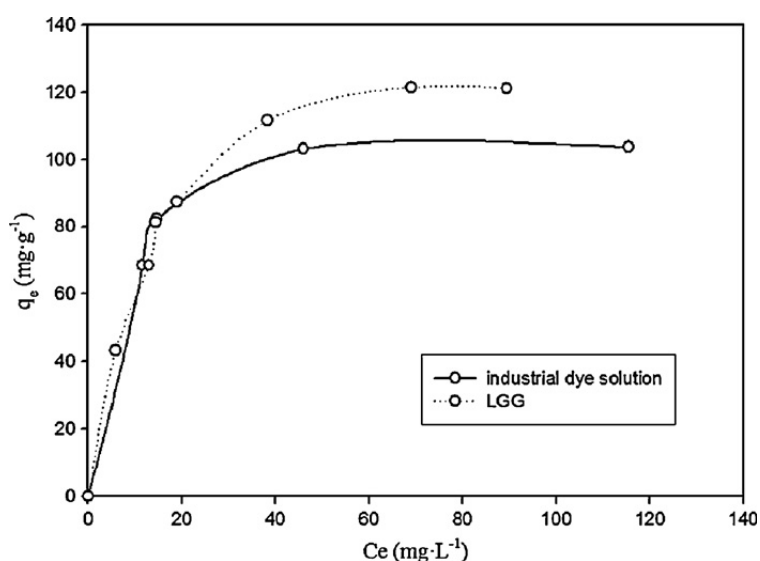


**Figure 6:** Equilibrium adsorption isotherms of individual Lanaset Grey G and industrial dye solution onto activated carbon at 25 °C.

## 4. Conclusions

Based on the results obtained within the framework of this study, it appears that the activated carbon prepared from Tunisian olive-waste cakes constitutes a good adsorbent

for removing a metal complex dye: Lanaset Grey G. The main conclusions that can be drawn from the current investigation are given below:

The Langmuir model provides the best correlation of the experimental equilibrium data. The adsorption capacity of the activated carbon was determined as  $108.7 \text{ mg g}^{-1}$  which compares well those of other sorbents prepared from agricultural wastes and is more favorable than that of the commercial granular activated carbon “CAL” from Chemviron Carbon: CAL ( $56.8 \text{ mg g}^{-1}$ ),

The adsorption system obeys the pseudo first-order kinetic model represented by the Lagergren equation. Moreover, the increase of the temperature enhances the kinetics of dye uptake.

The adsorption mechanism of this dye is rather a complex process and the intra-particle diffusion was not the only rate-controlling step.

The calculated thermodynamic parameters show the spontaneous and endothermic natures of the adsorption process.

The low value of the activation energy shows that dye adsorption process by the activated carbon may involve a physical sorption.

When comparing the adsorption capacity of the activated carbon towards the dye in the industrial solution ( $133.9 \text{ mg g}^{-1}$ ) with that of individual dye ( $108.7 \text{ mg g}^{-1}$ ), we can conclude that the added components do not affect the maximum uptake of the target solute by the sorbent.

### **Acknowledgements**

This work was been supported by the Spanish Ministry of Foreign Affairs and Cooperation, AECID program (project A/016195/08). The Department of Chemical Engineering of the Universitat Autònoma de Barcelona is the Unit of Biochemical Engineering of the Centre de Referència en Biotecnologia de la Generalitat de Catalunya. P. Blánquez and M. Sarrà are members of a Consolidated Research Group of Catalonia (2009SGR656). The authors are grateful to MATGAS (organization of Materials and Gases) for their technical assistance.

## REFERENCES

- Al-Degs Y.S., El-Barghouthi M.I., El-Sheikh A.H., Walker G.M., 2008. Effect of solution pH, ionic strength, and temperature on adsorption behavior of reactive dyes on activated carbon. *Dyes Pigments* 77, 16-23.
- Aziz A., Ouali M.S., El Hadj E., De Menorval L.CH., Lindheimer M., 2009. Chemically modified olive stone: A low-cost sorbent for heavy metals and basic dyes removal from aqueous solutions. *J. Hazard. Mater.* 163, 441-447.
- Bacaoui A., Yaacoubi A., Dahbi A., Bennouna C., Phan Tan Luu, R., Maldonado-Hodar F.J., Rivera-Utrilla J., Moreno-Castilla C., 2001. Optimization of conditions for the preparation of activated carbons from olive-waste cakes. *Carbon* 39, 425-432.
- Baccar R., Bouzid J., Feki M., Montiel A., 2009. Preparation of activated carbon from Tunisian olive-waste cakes and its application for adsorption of heavy metal ions. *J. Hazard. Mater.* 162, 1522-1529.
- Belmouden M., Assabane A., Ait Ichou Y., 2001. Removal of 2,4-dichloro phenoxyacetic acid from aqueous solution by adsorption on activated carbon. A kinetic study. *Ann. Chim. Sci. Mater.* 26 (2), 79-85.
- Binupriya A.R., Sathishkumar M., Swaminathan K., Ku C.S., Yun S.E., 2008. Comparative studies on removal of Congo red by native and modified mycelial pellets of *Trametes versicolor* in various reactor modes. *Bioresour. Technol.* 99, 1080-1088.
- Blázquez P., Sarrà M., 2010. Continuous adsorption process of GLG textile dye onto GAC: a balanced solution between the use of GAC and the treatment capacity" submitted article.
- Blázquez P., Sarrà M., Vicent T., 2008. Development of a continuous process to adapt the textile wastewater treatment by fungi to industrial conditions. *Process Biochem.* 43, 1-7.
- Chen B.N., Hui C.W., McKay G., 2001. Film-pore diffusion modeling and contact time optimization for the adsorption of dyestuffs on pitch. *Chem. Eng. J.* 84 77-94.
- Crini G., 2006. Non-conventional low-cost adsorbents for dye removal: a review. *Bioresour. Technol.* 97, 1061-1085.

- Daifullah A.A.M., Yakout S.M., Elreefy S.A., 2007. Adsorption of fluoride in aqueous solutions using KMnO<sub>4</sub>-modified activated carbon derived from steam pyrolysis of rice straw. *J. Hazard. Mater.* 147, 633-643.
- Diao Y., Walawender W.P., Fan, L.T. 2002. Activated carbon prepared from phosphoric acid activation of grain sorghum. *Bioresource Technol.* 8145-8152.
- El Nemr A., Abdelwahab O., El-Sikaily A., Khaled A., 2009. Removal of direct blue-86 from aqueous solution by new activated carbon developed from orange peel. *J. Hazard. Mater.* 161, 102-110.
- Ferrero F., 2007. Dye removal by low cost adsorbents: hazelnut shells in comparison with wood sawdust. *J. Hazard. Mater.* 142 144-152.
- Galiatsatou P., Metaxas M., Arapoglou D., Kasselouri-Rigopoulou V., 2002. Treatment of olive millwastewater with activated carbons from agricultural by-products. *Waste Manage.* 22, 803–812.
- Girgis B., Abdel- Nasser S., El- Hendawy A., 2002. Porosity development in activated carbons obtained from date pits under chemical activation with phosphoric acid. *Microporous Mesoporous Mater.* 52, 105-117.
- Guo Y., Zhao J., Zhang H., Yang S., Qi J., Wang Z., Xu H., 2005. Use of rice husk-based porous carbon for adsorption of Rhodamine B from aqueous solutions. *Dyes Pigments* 66, 123-128.
- Gupta G.S., Prasad G., Singh V.N., 1990. Removal of chrome dye from aqueous solutions by mixed adsorbents: fly ash and coal. *Water Res.* 24, 45-50.
- Gupta V.K., Suhas, 2009. Application of low-cost adsorbents for dye removal – a review. *J. Environ. Manage.* 90, 2313-2342.
- Haimour N.M., Emeish S., 2006. Utilization of date stones for production of activated carbon using phosphoric acid. *Waste Manage.* 26, 51-60.
- Hamdaoui O., Naffrechoux E., 2007. Modeling of adsorption isotherms of phenol and chlorophenols onto granular activated carbon, Part II. Two-parameter models and equations allowing determination of thermodynamic parameters. *J. Hazard. Mater.* 147, 381-394.
- Hameed B.H., Ahmad A.A., Aziz N., 2007. Isotherms, kinetics and thermodynamics of acid dye adsorption on activated palm ash. *Chem. Eng. J.* 133 195-203.
- Iqbal M. J., Ashiq M. N., 2007. Adsorption of dyes from aqueous solutions on activated charcoal. *J. Hazard. Mater.* B139, 57-66.



- Jagtoyen M., Derbyshire F., 1993. Some considerations of the origins of porosity in carbons from chemically activated wood. *Carbon* 31, 1185-1192.
- Kundu S., Gupta A.K., 2006. Arsenic adsorption onto iron oxide-coated cement (IOCC): regression analysis of equilibrium data with several isotherm models and their optimization. *Chem. Eng. J.* 122, 93-106.
- Li K., Zheng Z., Xingfa H., Guohua Z., Jingwei F., Jibiao Z., 2009. Equilibrium, kinetic and thermodynamic studies on the adsorption of 2-nitroaniline onto activated carbon prepared from cotton stalk fiber. *J. Hazard. Mater.* 166, 213-220.
- Li T., Guthrie J.T., 2010. Colour removal from aqueous solutions of metal-complex azo dyes using bacterial cells of *Shewanella* strain J18 143. *Bioresource Technol.* 101, 4291-4295.
- Mohamed M.M., 2004. Acid dye removal: comparison of surfactant-modified mesoporous FSM-16 with activated carbon derived rice husk. *J. Colloid Interface Sci.* 272, 28-34.
- Molina-Sabio M., Rodríguez-Reinoso F., Caturla F., Sellés M.J., 1995. Porosity in granular carbons activated with phosphoric acid. *Carbon* 33, 1105-1113.
- Monser L., Adhoum N., 2009. Tartrazine modified activated carbon for the removal of Pb(II), Cd(II) and Cr(III). *J. Hazard. Mater.* 16, 263-269.
- Namasivayam C., Kavitha D., 2002. Removal of Congo Red from water by adsorption onto activated carbon prepared from coir pith, an agricultural solid waste. *Dyes Pigments* 54, 47-58.
- Ozacar M., Sengil A.I., 2005. Adsorption of metal complex dyes from aqueous solution by pine sawdust. *Bioresource Technol.* 96, 791-795.
- Ozacar M., Sengyl I.A., 2004. Two-stage batch sorber design using second-order kinetic model for the sorption of metal complex dyes onto pine sawdust. *Biochem. Eng. J.* 39-45.
- Rajeev J., Gupta V.K., Sikarwar S., 2010. Adsorption and desorption studies on hazardous dye Naphthol Yellow. *J. Hazard. Mater.* 182,749-756.
- Robinson T., McMullan G., Marchant R., Nigam P., 2001. Remediation of dyes in textile effluent: a critical review on current treatment technologies with a proposed alternative. *Bioresource Technol.* 77, 247-255.

- Ruhan A.A., Sari A., Tuzen M., 2009. Equilibrium, Thermodynamic and kinetic studies on biosorption of Pb(II) and Cd(II) from aqueous solution by macrofungus (*Lactarius scrobiculatus*) biomass. *Chem. Eng. J.* 15, 255-261.
- Runping H., Zoua L., Zhaoc X., Xua Y., Xua F., Li Y., Wanga Y., 2009. Characterization and properties of iron oxide-coated zeolite as adsorbent for removal of copper (II) from solution in fixed bed column. *Chem. Eng. J.* 149, 123-131.
- Sellami F., Jarboui R., Achica S., Medhioub K., Ammar E., 2008. Co-composting of oil exhausted olive-cake, poultry manure and industrial residues of agro-food activity for soil amendment. *Bioresource Technol.* 99, 1177-1188.
- Stolz A., 2001. Basic and applied aspects in the microbial degradation of azo dyes. *Appl. Microbiol. Biotechnol.* 56, 69-80.
- Suarez-Garcia F., Martinier- Alonso, A., Tascon J.D., 2002. Pyrolysis of apple pulp: chemical activation with phosphoric acid. *Anal. Appl. Pyrol.* 63, 283- 301.
- Tan I.A.W., Ahmad A.L., Hameed B.H., 2008. Adsorption of basic dye on high-surface-area activated carbon prepared from coconut husk: equilibrium, kinetic and thermodynamic studies. *J. Hazard. Mater.* 154, 337-346.
- Vernersson T., Bonelli P.R., Cerrela E.G., Cukierman A.L., 2002. *Arundo donax* cane as a precursor for activated carbons preparation by phosphoric acid activation. *Bioresource Technol.* 83, 95-104.
- Vijaykumar M.H., Veeranagouda Y., Neelakanteshwar K., Karegoudar, T.B. 2006. Decolorization of 1:2 metal complex dye Acid Blue 193 by a newly isolated fungus, *Cladosporium cladosporioides*. *World J. Microb. Biotechnol.* 22, 157-162.
- Weber W. J., Morris, J. C. 1963. Kinetics of adsorption on carbon from solutions. *J. Sanit. Eng. Div. Am. Soc. Civ. Eng.* 89, 31-60.
- Yang T., Chong L.A., 2006. Textural and chemical proprieties of zinc chloride activated carbons prepared from pistachio- nut shells. *Mater. Chem. Phys.* 100, 438-444.

#### 4.2.2: Modeling of adsorption isotherms and kinetics of a tannery dye onto an activated carbon prepared from an agricultural by-product

---



**Abstract**

The potential of an activated carbon prepared from an agricultural by-product for the removal of a tannery dye from aqueous solution was investigated. The effects of contact time, solution pH and temperature were evaluated. The results indicated that the equilibrium data were perfectly represented using a Langmuir isotherm. The maximum monolayer adsorption capacity was found to be  $146.31 \text{ mgg}^{-1}$  at  $25 \text{ }^\circ\text{C}$ . The kinetic studies indicated that the adsorption process followed a pseudo-second-order model. The application of an intra-particle diffusion model revealed that the adsorption mechanism of the concerned dye is a rather complex process and that diffusion is involved in the overall rate of the adsorption process, but it is not the only rate-controlling step. The calculated thermodynamics parameters revealed the spontaneous and endothermic nature of the adsorption process. The activation energy,  $E_a = 9.50 \text{ kJ mol}^{-1}$ , could indicate a physical adsorption process. Despite the presence of other components in the real effluent, the adsorbent was able to remove the target dye. The present study indicates that activated carbon prepared from olive-waste cakes is a promising candidate as a low cost adsorbent for the removal of a tannery dye from industrial wastewater.

**Keywords:** olive-waste cakes, tannery dye, isotherm, thermodynamics, real effluent.

### **1. Introduction**

The removal of dyes from industrial effluents is an area of research receiving increasing attention because government legislation regarding the release of contaminated effluents is becoming increasingly stringent (Nigam et al., 2000). Industrial tanneries discharge enormous amounts of colored wastewater, which leads to severe environmental problems. Most of the dyes used for leather dyeing are toxic, mutagenic and carcinogenic, and they are usually of synthetic origin and have complex aromatic molecular structures (Fu and Viraraghavan, 2001). Additionally, these dyes are unusually resistant to degradation. Therefore, many aspects should be considered when selecting proper treatment processes including both economic and environmental aspects. Recently, environmental friendly methods for treating effluents have been receiving considerable attention. Application for some of the waste products could help in this regard. Meanwhile, the reuse of wastes can be an advantage. Adsorption using activated carbon (AC) has proven to be very effective in treating effluents (Namasivayam and Kavitha, 2002, Binupriya et al., 2008). Besides, AC adsorption has been cited by the United States Environmental Protection Agency (USEPA) as being one of the best available environmental control technologies (Hamdaoui and Naffrechoux, 2007). However, the widespread use of AC adsorption is restricted because of the high cost of conventional and commercial carbons. Therefore, in recent years, many researchers have tried to produce ACs using renewable and cheaper precursors which are mainly industrial and agricultural by-products (lignocellulosics). The reuse of these waste materials not only produces a useful and low cost adsorbent for the purification of contaminated environments, but also contributes to minimizing solid wastes.

In the present study, an activated carbon prepared from olive-waste cakes, an agro-food waste predominantly produced in the Mediterranean countries, was prepared by chemical activation with phosphoric acid and was used for the removal of a tannery dye that is extensively used in a tannery located in Sfax, Tunisia. The equilibrium and kinetics data of the adsorption process were analyzed to study the adsorption characteristics and the mechanism of adsorption. Finally, to investigate the efficiency of the prepared AC towards the Black Dycem TTO tannery dye, the adsorption of a real tannery effluent solution from an industrial bath was also tested.

## **2. Materials and methods**

### **2.1. Adsorbent**

The AC was prepared from the chemical activation of exhausted olive-waste cakes, which were obtained from an oil factory, “Agrozitex”, located in Sfax-Tunisia. Phosphoric acid (analytical grade) was used as a dehydrating agent. The activated carbon was prepared using a method described in a previous work (Baccar et al., 2009). The activated carbon has particle sizes ranging between 100 and 160  $\mu\text{m}$ . The surface area ( $S_{\text{BET}}$ ), the total pore volume and the average pore diameter of the prepared adsorbent, determined after application of the BET (Brunauer–Emmett and Teller) model, are  $793 \text{ m}^2 \text{ g}^{-1}$ ,  $0.49 \text{ cm}^3 \text{ g}^{-1}$  and 4.2 nm, respectively (Vernersson et al., 2002). The pH at point of zero charge ( $\text{pH}_{\text{pzc}}$ ) is 5.03, which indicates that the majority of the functional groups on the adsorbent are acidic.

### **2.2. Adsorbate and chemicals**

Black Dycem TTO is a patented commercial dye that is extensively used in an industrial tannery “Société Tunisienne de Chamoisage” located in Sfax, Tunisia. This dye is supplied to this factory by “Colorantes Industriales, S.A” (Barcelona, Spain). According to its technical specifications, the black, water soluble dye, is not rapidly biodegraded, and the effluent containing this dye must be recycled. This dye is classified as an acidic dye, the principal chemical classes of which are azo, anthraquinone, triphenylmethane, azine, xanthene, nitro and nitroso (Gupta and Suhas, 2009). Analysis of the metal content in the dye, using acetylene-air flame absorption spectrophotometer (HITACHI Model Z-6100), indicated that it contained Cr ( $0.56 \text{ mg g}^{-1}$ ); therefore, it is considered to be a metal complex dye. The maximum absorption wavelength of the dye (462 nm) was obtained by scanning an aqueous solution of the dye over the visible range.

The real effluent was also provided from the same industrial tannery. This effluent originates from the different process units of tanning; therefore, it is a complex mixture of the Black Dycem TTO dye, metals and additives whose exact composition is unknown. Nevertheless, the characteristics of this as-received industrial effluent, which exhibited an intense dark blue color, are shown in Table 1. All other chemicals used in this study were of analytical grade.

**Table 1:** Physico-chemical characteristics of the real tannery effluent

Parameter	Numerical value
pH	3.13
Conductivity (ms cm <sup>-1</sup> )	14.71
COT (mg L <sup>-1</sup> )	7524
COD (mg L <sup>-1</sup> )	10940
DBO <sub>5</sub> (mg L <sup>-1</sup> )	3800
N total ( mg L <sup>-1</sup> )	607
P (mg L <sup>-1</sup> )	1.47

### 2.3. Adsorption studies

#### 2.3.1. Sorption isotherms and kinetic studies

The equilibrium and kinetics of the dye adsorption were studied at approximately 25 °C. To determine the equilibrium isotherm, adsorption tests were performed by adding various amounts of adsorbent (0.10, 0.30, 0.50, 0.70 and 1.00 g) to a series of 500 mL Erlenmeyer flasks that were filled with a 300 mL solution containing 150 mg L<sup>-1</sup> of the Black Dycem TTO dye. The solution was maintained at its natural pH of 6.66. The flasks were shaken at 200 rpm with a magnetic stirrer for 120 hours to ensure that adsorption equilibrium was reached. Then, each dye solution was separated from the sorbent by centrifuging at 13000 rpm for 5 min. The residual concentration of Black Dycem TTO was measured at 462 nm using a UV-Visible scanning spectrophotometer (UDV-2950).

The amount of dye adsorbed at equilibrium  $q_e$  (mg g<sup>-1</sup>) can be calculated from the following equation (Eq. (1)):

$$q_e = \frac{(C_0 - C_e)V}{m_{AC}} \quad (1)$$

where  $C_0$  and  $C_e$  (mg L<sup>-1</sup>) are the initial and equilibrium liquid phase dye concentrations, respectively,  $V$  is the volume of the solution (L) and  $m_{AC}$  is the mass of the activated carbon used in the experiment (g).

The procedure for kinetic test was basically identical to the procedure for the equilibrium test. Nevertheless, for each carbon/dye solution, liquid samples were collected for analysis at preset time intervals. The amount of dye adsorbed at time  $t$ ,  $q_t$  ( $\text{mg g}^{-1}$ ), was calculated using Eq. (1) by substituting  $C_e$  with  $C_t$ . The magnitude of  $C_t$  represents the concentration of the liquid-phase dye at any time  $t$ .

### **2.3.2. Effect of pH on the dye adsorption**

The effect of pH on the dye uptake by the adsorbent was investigated using synthetic solutions containing  $150 \text{ mg L}^{-1}$  of the Black Dycem TTO at  $25 \text{ }^\circ\text{C}$ . Adsorption tests were performed by adding  $1.00 \text{ g}$  of the activated carbon to a series of  $500 \text{ mL}$  Erlenmeyer flasks that were filled with  $300 \text{ mL}$  of the above solution at different pH values. The initial pHs of the solutions were adjusted to between 2 and 9 by adding either HCl (1M) or NaOH (1 M). The pHs of the solutions were measured using a pH-meter (Metrohm, model 632) that was equipped with a combined glass electrode (Metrohm). Each suspension was magnetically stirred for 72 h at 250 rpm. Then, each dye solution was separated from the sorbent by centrifuging at 13000 rpm for 5 min. The residual concentration of the Black Dycem TTO was determined as previously described, and the amount of adsorbed dye was calculated using Eq. (1).

### **2.3.3. Effect of temperature**

The effect of the temperature on the dye sorption process was investigated using time-based analyses, where the adsorption systems were analyzed until the concentration of the residual dye in the solution became constant (equilibrium state). The kinetic adsorption runs were performed at three different temperatures, i.e. 15, 25 and  $40 \text{ }^\circ\text{C}$ , using the same stock solution that contained  $150 \text{ mg L}^{-1}$  of the Black Dycem TTO - at its natural pH of 6.66 - mixed with  $1.00 \text{ g}$  of the adsorbent. The mixture was agitated using a magnetic stirrer at 250 rpm. For each temperature,  $C_t$ ,  $q_t$ ,  $C_e$  and  $q_e$  were determined as described above.

### **2.3.4. Adsorption of a real tannery dye effluent**

To evaluate the efficiency of the prepared activated carbon towards the removal of the Black Dycem TTO dye, a real tannery effluent solution from the industrial bath containing the target dye was used. The adsorption of Black Dycem TTO from the real



effluent was performed at 25 °C. The adsorption test was carried out by adding 1.00 g of the adsorbent to a 500 mL Erlenmeyer flask that was filled with 300 mL of the real effluent. The separation of the solution from the sorbent and the measurement of the residual concentration of the dye were conducted using the same methods described above for the commercial dye.

### 3. Theoretical background

#### 3.1. Adsorption isotherms

##### 3.1.1. Langmuir model

The Langmuir isotherm is described by Eq. (2):

$$q_e = \frac{q_{\max} K_L C_e}{1 + K_L C_e} \quad (2)$$

where  $q_{\max}$  and  $K_L$  are Langmuir constants related to the adsorption capacity (maximum amount adsorbed per gram of adsorbent) ( $\text{mg g}^{-1}$ ) and energy of sorption ( $\text{L m g}^{-1}$ ), respectively. The essential characteristics of the Langmuir isotherm can be expressed in terms of a dimensionless constant separation factor  $R_L$ , which is defined as follows:

$$R_L = \frac{1}{1 + K_L C_0} \quad (3)$$

where  $C_0$  is the initial concentration of the solute. The value of  $R_L$  indicates the type of isotherm: unfavorable ( $R_L > 1$ ), linear ( $R_L = 1$ ), favorable ( $0 < R_L < 1$ ) or irreversible ( $R_L = 0$ ) (Hameed et al., 2007).

Eq. (2) can be linearized to five different forms, as shown in Table 2, which main difference are related to the data distribution and consequently to the accuracy in the parameter determination.

##### 3.1.2. Freundlich model

The empirical Freundlich model is expressed by Eq. (4):

$$q_e = K_F C_e^{1/n} \quad (4)$$

where  $K_F$  and  $n$  are the Freundlich constants related to the adsorption capacity and adsorption intensity, respectively. These parameters can be calculated from the intercept

and the slope of the linear plot of  $\log q_e$  versus  $\log C_e$ . The magnitude of the exponent,  $n$ , indicates the favorability of adsorption.

Conventionally,  $q_{max}$  is determined from the Langmuir model. However, this parameter can also be estimated from the Freundlich model. Therefore, it is necessary to operate with a constant initial concentration  $C_0$  and variable weights of adsorbents; therefore,  $\log q_m$  is the extrapolated value of  $\log q_e$  for  $C=C_0$  (Hamdaoui and Naffrechoux, 2007). According to Halsey (1952):

$$K_F = \frac{q_m}{C_0^{1/n}} \quad (5)$$

where  $C_0$  is the initial concentration of the solute in the solution ( $\text{mg L}^{-1}$ ) and  $q_m$  is the Freundlich maximum adsorption capacity ( $\text{mg g}^{-1}$ ).

**Table 2:** Langmuir isotherm and its linear forms

Isotherm	Linear form	Plot
Langmuir-1	$\frac{1}{q_e} = \frac{1}{K_L q_m} \frac{1}{C_e} + \frac{1}{q_m}$	$\frac{1}{q_e}$ vs. $\frac{1}{C_e}$
Langmuir-2	$\frac{C_e}{q_e} = \frac{1}{q_m} C_e + \frac{1}{q_m K_L}$	$\frac{C_e}{q_e}$ vs. $C_e$
Langmuir-3	$q_e = \frac{q_m K_L C_e}{1 + K_L C_e}$ $q_e = -\frac{1}{K_L} \frac{q_e}{C_e} + q_m$	$q_e$ vs. $\frac{q_e}{C_e}$
Langmuir-4	$\frac{q_e}{C_e} = -K_L q_e + K_L q_m$	$\frac{q_e}{C_e}$ vs. $q_e$
Langmuir-5	$\frac{1}{C_e} = K_L q_m \frac{1}{q_e} - K_L$	$\frac{1}{C_e}$ vs. $\frac{1}{q_e}$

### 3.1.3. Temkin model

The Temkin isotherm can be expressed by Eq. (6):

$$q_e = \frac{RT}{b} \ln(AC_e) \quad (6)$$

where constant  $B = RT/b = (RT/\Delta E)q_{max}$ ,  $R$  is the universal gas constant ( $8.314 \text{ J mol}^{-1}\text{K}^{-1}$ ),  $T$  is the temperature (K),  $\Delta E = (-\Delta H)$  is the variation of adsorption energy ( $\text{J mol}^{-1}$ ),  $A$  is the Temkin equilibrium constant ( $\text{L m g}^{-1}$ ) corresponding to the

maximum binding energy and  $q_{\max}$  is the adsorption (maximum) capacity (Hamdaoui and Naffrechoux, 2007, Kundu and Gupta, 2006). If the adsorption obeys the Temkin equation, A and B can be obtained from the slope and intercept of the plot  $q_e$  against  $\ln C_e$ .

### 3.1.4. Dubinin–Radushkevich (D–R) isotherm

To distinguish between physical and chemical adsorption, the adsorption data can be further interpreted using Dubinin–Radushkevich (D–R) isotherm (Tan et al., 2008). The D–R equation is given as follows:

$$q_{\varepsilon} = q_m \exp(-\beta\varepsilon^2) \quad (7)$$

with

$$\varepsilon = RT \ln\left(1 + \frac{1}{C_e}\right) \quad (8)$$

where  $q_m$  is the maximum amount adsorbed and can be called the adsorption capacity,  $\beta$  is a constant related to the adsorption energy ( $\text{mol}^2 \text{kJ}^{-2}$ ),  $\varepsilon$  is the potential energy of the surface, R is the gas constant ( $\text{kJ mol}^{-1} \text{K}^{-1}$ ) and T is the absolute temperature. The constant B gives the free energy E ( $\text{kJ mol}^{-1}$ ) of the transfer of 1 mol of solute from infinity to the surface of an adsorbent, and can be computed using the following relationship (Onyango et al., 2004):

$$E = \frac{1}{\sqrt{2B}} \quad (9)$$

The D–R equation can be linearized as follows:

$$\ln q_{\varepsilon} = \ln q_m - \beta\varepsilon^2 \quad (10)$$

A plot of  $\ln q_e$  versus  $\varepsilon^2$  gave straight lines. The values of  $q_m$  ( $\text{mg g}^{-1}$ ), B ( $\text{mol}^2 \text{kJ}^{-2}$ ) and thus the mean free energy of adsorption E ( $\text{kJ mol}^{-1}$ ) were obtained from the intercept and slope of the straight line.

## 3.2. Adsorption kinetics

### 3.2.1. Pseudo-first and pseudo-second order equations

The adsorption kinetics was investigated using two common models, namely, the Lagergren pseudo-first order and pseudo-second order models. The linear forms of these two models are expressed by equations (11) and (12), respectively:

$$\ln(q_e - q_t) = \ln q_e - K_1 t \quad (11)$$

$$\frac{t}{q_t} = \frac{1}{K_2 q_e^2} + \frac{1}{q_e} t \quad (12)$$

where  $q_e$  and  $q_t$  have the same previously mentioned meaning and are expressed in  $\text{mg g}^{-1}$ ,  $K_1$  and  $K_2$  are the pseudo-first order and the pseudo-second order model rate constants, expressed in  $\text{min}^{-1}$  and  $\text{g mg}^{-1} \text{min}^{-1}$ , respectively.

### 3.2.1. Intra-particle diffusion model

The intra-particle diffusion model based on the theory proposed by Weber and Morris (1963) was used to identify the diffusion mechanism. According to this theory, the adsorbate uptake  $q_t$  varies almost proportionally with the square root of the contact time,  $t^{1/2}$  rather than  $t$ :

$$q_t = K_{id} t^{1/2} + C \quad (13)$$

where  $C$  is the intercept and  $k_{id}$  ( $\text{mg g}^{-1} \text{h}^{-1/2}$ ) is the intra-particle diffusion rate constant. If intra-particle diffusion occurs, then  $q_t$  versus  $t^{1/2}$  will be linear, and if the plot passes through the origin, then the rate limiting step is only due to intra-particle diffusion. Otherwise, some other mechanisms along with intra-particle diffusion are involved. In most cases, this plot gives general features of three stages: initial curved portion, followed by an intermediate linear portion and a plateau. The initial sharper, is due to the instantaneous adsorption or external surface adsorption (external mass transfer). The intermediate linear part is due to intra-particle diffusion and the plateau arises from the equilibrium stage where intra-particle diffusion starts to slow down because of the extremely low solute concentrations in the solution.

### 3.3. Thermodynamics studies

The rate and equilibrium data, which were obtained at the three temperatures considered, were used to evaluate the activation energy ( $E_a$ ) and the thermodynamic parameters ( $\Delta G^\circ$ ,  $\Delta H^\circ$  and  $\Delta S^\circ$ ) of the dye adsorption process.

The activation energy  $E_a$  was determined using the Arrhenius equation:

$$\ln k_2 = \ln A - \frac{E_a}{RT} \quad (14)$$

where  $k_2$  is the pseudo-second order rate constant,  $A$  is the Arrhenius factor and the other terms have their usual meaning.

The equilibrium constant,  $K_D$ , of the adsorption process, expressed in  $L g^{-1}$ , can be used to estimate the thermodynamic parameters due to its dependence on temperature. The changes in standard free energy ( $\Delta G^\circ$ ), enthalpy ( $\Delta H^\circ$ ) and entropy ( $\Delta S^\circ$ ) of the adsorption process were determined by using Eqs. (15)–(17):

$$K_D = \frac{q_e}{c_e} \quad (15)$$

$$\Delta G^\circ = -RT \ln K_D \quad (16)$$

$$\ln K_D = \frac{\Delta S^\circ}{R} - \frac{\Delta H^\circ}{RT} \quad (17)$$

## 4. Results and discussion

### 4.1. Effect of contact time on dye adsorption

Figure 1 shows the residual dye concentration versus contact time. The curves relative to all the adsorbent doses tested (0.10, 0.30, 0.50, 0.70 and 1.00 g) are presented. The results indicate that the contact time needed to reach the adsorption equilibrium of Black Dycem TTO on activated carbon is approximately 48 h for all of the sorbent loadings considered. Therefore, the chosen contact time of 120 h, used in our experiments, is more than sufficient to reach equilibrium.

As shown in Figure 1 the rate of adsorption of the dye was initially rapid, and then gradually slowed until it reached an equilibrium; once equilibrium was reached, there was no significant increase in the dye removal. This observation can be explained by the fact that the adsorption rate is fast at the beginning, because the dye is adsorbed by the exterior surface of the activated carbon. When the exterior adsorption surface reaches saturation, the dye enters into the pores of the adsorbent and is adsorbed by the interior surface of the particles. This phenomenon requires a relatively long contact time. For example, Chen et al. (2001) used 5 days as the contact time for the adsorption isotherm of dyestuffs on pitch. To ensure that full equilibrium was attained, Hameed et al. (2007) used 48 h as a contact time for the adsorption of acid green 25 dye.

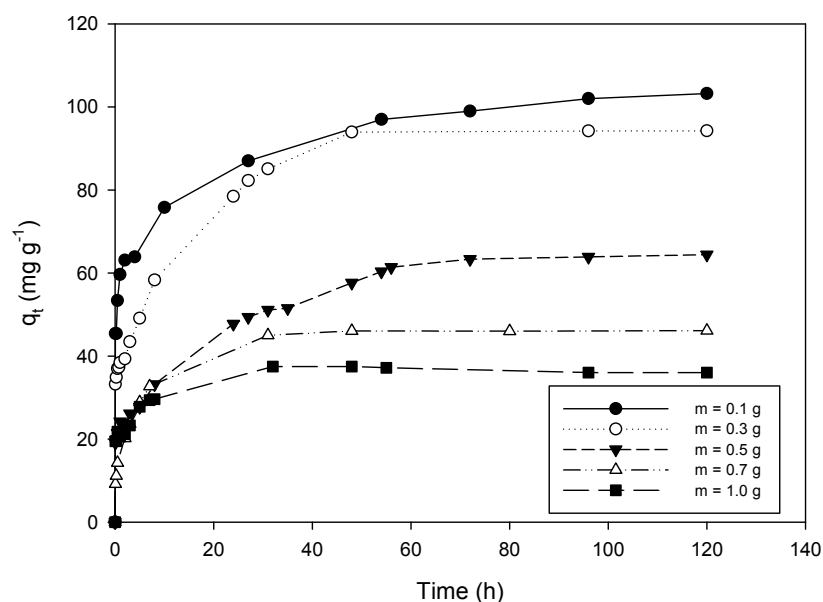


**Figure 1:** Effect of contact time on Black Dycem TTO adsorption for different amounts of adsorbent ( $C_0 = 150 \text{ mg L}^{-1}$ ;  $T = 25 \text{ }^\circ\text{C}$ ).

#### 4.2. Effect of pH

The effect of the solution pH on the adsorption of the tannery dye on activated carbon prepared from olive-waste cakes was examined under the following conditions: a temperature of  $25 \text{ }^\circ\text{C}$ , a constant initial concentration of  $150 \text{ mg L}^{-1}$ ,  $0.30 \text{ g}$  of adsorbent and  $125 \text{ rpm}$  agitation speed. The solution pH range was adjusted between 2 and 9. The experimental results showed no significant variation in the amount of solute adsorbed in the examined pH range (Figure not shown). According to reported studies on the adsorption of dyes with different chemical structures, the effect of pH on the solute uptake by activated carbons can be highly, moderately or slightly significant (Tsai et al., 2004). The adsorption is affected by the changes in the pH of the solution because this parameter affects the degree of ionization of the dye and the surface properties of the sorbents. As a general rule, pH values lower than  $\text{pH}_{\text{pzc}}$  result in lowering the number of negatively charged sites of the activated carbon, thereby increasing the number of positively charged sites which enhances the adsorption of anionic dyes. At pH values greater than  $\text{pH}_{\text{pzc}}$ , the hydroxyl ion concentration increases and the number of negatively charged sites on the surface of the carbon increases so that the extent of adsorption of acidic dyes is decreased because of ionic repulsion between the negatively charged surface and the anionic dye molecules (Hameed et al., 2007). For the dye used

in this work, the results related to the pH effect are apparently surprising. However, a plausible explanation of this behavior may be the presence of both negatively and positively charged functional groups in the dye molecules. Independent of the origin of this insignificant effect of the pH, this finding is quite meaningful in the adsorption process application since it makes any pH adjustment of the effluent before treatment not indispensable.

### 4.3. Modeling of adsorption isotherm

The distribution of the adsorbate between the liquid and the solid phases when the adsorption process reaches an equilibrium state is indicated by the adsorption isotherm. The shape of the isotherm is the first experimental tool used to diagnose the nature of the adsorption phenomenon. The isotherms have been classified by Giles et al. (1974) into four main groups: L, S, H and C. The experimental adsorption isotherm for the adsorption of the Black Dycem TTO dye onto the activated carbon prepared from olive-waste cakes is presented in Figure 2.

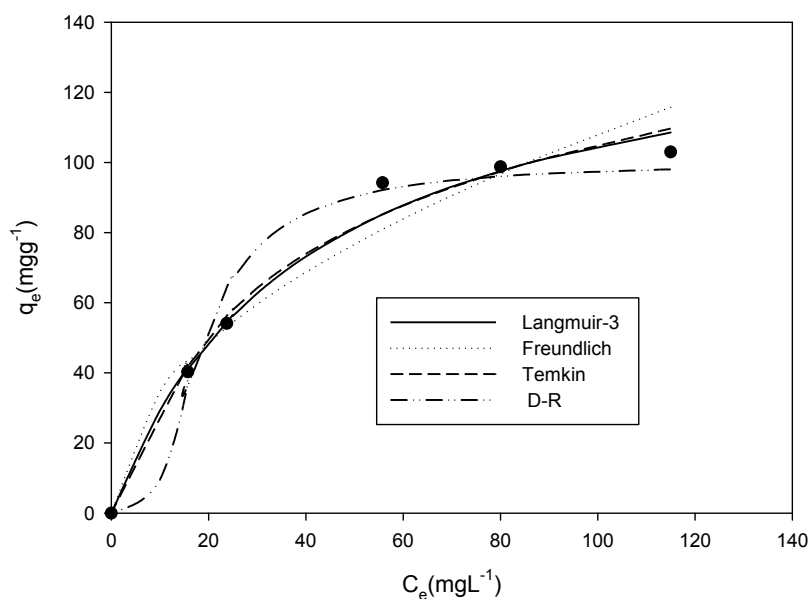


**Figure 2:** Equilibrium adsorption isotherms of Black Dycem TTO dye onto activated carbon at 25 °C.

According to the cited classification, the isotherm for the Black Dycem TTO displayed an L curve pattern. The isotherm had a concavity toward the abscissa axis, which indicated that as more sites in the substrate are filled, it becomes more difficult for a fresh solute molecule to find a vacant site (Cabrita et al., 2010).

Four isotherm models related to the adsorption equilibrium have been tested in the present study. The equilibrium data were modeled using the Langmuir (five linearized expressions), Freundlich, Temkin and Dubinin–Radushkevich (D–R) models.

To compare the validity of each isotherm model, the normalized standard deviation  $\Delta q$  (%) was calculated using Eq. (18):

$$\Delta q (\%) = 100 \sqrt{\frac{\sum \left( \frac{q_{\text{exp}} - q_{\text{cal}}}{q_{\text{exp}}} \right)^2}{N-1}} \quad (18)$$

where  $q_{\text{exp}}$  and  $q_{\text{cal}}$  are the experimental and calculated amounts, respectively, of the dye adsorbed at equilibrium onto the activated carbon and  $N$  is the number of measurements performed. The normalized standard deviation,  $\Delta q$ , represents the fit between the experimental and predicted values of the adsorption capacity, whereas the linear correlation coefficients ( $R^2$ ) represent the fit between the experimental data and linearized forms of the isotherm equations (Hamdaoui and Naffrechoux, 2007).

Table 3 summarizes the parameters from the four models tested, the  $R^2$  and  $\Delta q$  (%) values. From table 3, it was observed that the values of Langmuir parameters from the five linear expressions were different. This difference arises because each of these transformations changes the original error distribution (for better or worse). From the  $R^2$  values, it appears that the best fit was obtained using Langmuir-1 or Langmuir-5 equations compared with the other Langmuir linear equations and the others models: Freundlich, Temkin and (D–R) equations because they present the highest correlations coefficients ( $R^2 = 0.99$ ). It has been reported that the use of the correlation coefficient of a linear regression analysis for comparing the best fits of different isotherms is inappropriate (Ho, 2004). According to Kinniburgh (1986), the best transformation is not necessarily the one that gives the highest correlation coefficient, but rather the one where the resulting error distribution most closely matches the “true” error distribution. Despite the extremely high coefficients of correlations ( $R^2 = 0.99$ ), the two linear forms of the Langmuir equation, Langmuir-1 and 5 presented higher values of standard deviation percentage than Langmuir-3, therefore they did not perfectly describe the equilibrium data. Additionally, it was observed that the  $\Delta q$  (%) values for the five different linearized Langmuir isotherm equations were lower than those for the Freundlich, Temkin and D-R equations. These results indicate that the adsorption of the



Black Dycem TTO on the prepared AC follows the Langmuir isotherm and that the corresponding parameters the adsorption capacity ( $q_{\max}$ ) and  $R_L$  were determined from the linear form Langmuir-3 model and found to be  $146.31 \text{ mg g}^{-1}$  and 0.21, respectively. The value of  $R_L$  indicates favorable adsorption.

**Table 3:** Langmuir, Freundlich, Temkin and D–R isotherm model parameters correlation coefficients and  $\Delta q$  (%) values for adsorption of Black Dycem TTO at 25 °C.

<b>Isotherm</b>	<b>Parameters</b>			
<b>Langmuir</b>	$K_L$	$q_{\max}(\text{mg g}^{-1})$	$R^2$	$\Delta q$ (%)
Langmuir-1	0.022	153.84	0.991	6.336
Langmuir-2	0.028	138.88	0.982	6.601
Langmuir-3	0.025	146.31	0.907	5.684
Langmuir-4	0.023	153.44	0.907	5.912
Langmuir-5	0.022	157.63	0.991	6.301
<b>Freundlich</b>	n	$q_{\max}(\text{mg g}^{-1})$	$R^2$	$\Delta q$ (%)
	2.025	131.98	0.940	10.22
<b>Temkin</b>	A	B	$R^2$	$\Delta q$ (%)
	0.222	33.85	0.958	6.66
<b>D–R isotherm</b>	$\beta$	$q_{\max}(\text{mg g}^{-1})$	$R^2$	$\Delta q$ (%)
	42.09	99.94	0.945	10.58

For the sake of comparison, the values of some adsorbent capacities towards dyes available in the literature are shown in Table 4. The  $q_{\max}$  value in this study ( $146.31 \text{ mg g}^{-1}$ ) is higher than those in most previous studies. This finding suggests that the Black Dycem TTO tannery dye could be readily adsorbed by activated carbon prepared from the olive-waste cakes.

**Table 4:** Comparison of adsorption capacities of the AC prepared from olive-waste cakes and others adsorbents for different dyes

<b>Adsorbent</b>	<b>Adsorbate</b>	<b><math>q_{\max}</math> (mg g<sup>-1</sup>)</b>	<b>References</b>
AC from olive-waste cakes	Black Dycem TTO	146.3	This study
Activated palm ash	Acid green 25	123.4	(Hameed et al., 2007)
Pine sawdust	Metal complex yellow	82.0	(Ozacar and Sengyl, 2004)
AC from pinewood	Anionic acid blue	11.8	(Tseng et al., 2003)
AC from rice husk	Acid blue	50.0	(Mohamed, 2004)
Orange peel	Anionic acid violet 17	19.9	(Sivaraj et al., 2001)

The free energy  $E^-$  calculated from the D–R isotherm model – was found to be  $0.108 \text{ kJ mol}^{-1}$ , which is lower than the typical range of bonding energies for ion exchange mechanisms ( $8\text{-}16 \text{ kJ mol}^{-1}$ ) indicating that physisorption could play a significant role in the adsorption process of the Black Dycem TTO dye onto the prepared activated carbon (Jain et al., 2009).

#### 4.4. Adsorption kinetics

##### 4.4.1. Pseudo-first and pseudo-second order equations

The adsorption kinetics were modeled using two common models, specifically, the Lagergren pseudo-first order and pseudo-second order models.

The calculated  $q_e$ ,  $K_1$ ,  $K_2$  and the corresponding linear regression coefficient  $R^2$  values are presented in Table 5. The applicability of the kinetic model is compared by judging the correlation coefficients,  $R^2$ , and the agreement between the calculated and the experimental  $q_e$  values. In light of these considerations, we can conclude that the pseudo-second-order mechanism is predominant. Similar kinetic results have also been reported for the adsorption of acid blue 193 onto BTMA-bentonite (Ozcan et al., 2005).

**Table 5:** Parameters of the pseudo-first and pseudo-second order kinetics models at different adsorbent amounts.

Adsorbent amounts (g)	$q_{e,exp}$ ( $\text{mg g}^{-1}$ )	Pseudo-first order kinetic model			Pseudo-second order kinetic model		
		$K_1$ ( $\text{h}^{-1}$ )	$q_{e,cal}$ ( $\text{mg g}^{-1}$ )	$R^2$	$K_2$ ( $\text{g mg}^{-1} \text{h}^{-1}$ )	$q_{e,cal}$ ( $\text{mg g}^{-1}$ )	$R^2$
m=0.10	103.22	0.011	45.14	0.719	0.042	96.15	0.980
m=0.30	94.23	0.059	60.17	0.997	0.004	96.15	0.997
m=0.50	64.41	0.104	22.72	0.957	0.031	65.79	0.992
m=0.70	46.11	0.136	21.13	0.737	0.004	43.47	0.999
m=1.00	36.01	0.217	17.02	0.959	0.037	36.63	0.999

#### 4.4.2. Intra-particle diffusion

The plot of the adsorbed quantity of Black Dycem TTO against the square root of time is shown in Figure 3. As illustration, the curves relative to 0.30, 0.50 and 1.00 g are only presented. It can be observed that the plots are not linear over the entire time range and the graphs reflect a dual nature, with the initial linear portion followed by a plateau. The fact that the first curved portion of the plots seems to be absent implies that the external surface adsorption (stage 1) is very fast elapsed and the stage of intra-particle diffusion (stage 2) is rapidly attained and continued to 48 h. Finally, the equilibrium adsorption (stage 3) begins after 48 h. The dye molecules are slowly transported via intra-particle diffusion into the particles and are finally retained in the pores. The linear portion of the curve does not pass through the origin and the latter stage of dye adsorption does not follow the Webber–Morris equation. It may be concluded that the adsorption mechanism of this adsorbate is a rather complex process and that the intra-particle diffusion was not the only rate-controlling step. The obtained results agree with those found by Monser and Adhoum (2009) for the adsorption of tartrazine onto activated carbon.

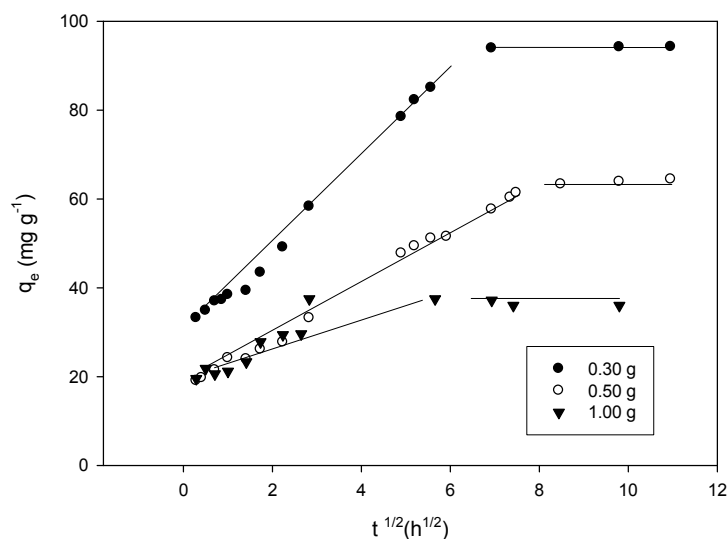


**Figure 3:** Plots of tannery dye uptake against square root of contact time.

#### 4.5. Effect of temperature

Adsorption experiments were performed for different contact times at three different temperatures: 15, 25 and 40 °C. For each temperature considered, the values of  $C_e$  and

$q_e$  corresponding to the equilibrium state were also determined. The results related to the time dependence of  $q_t$  are shown in Figure 4.

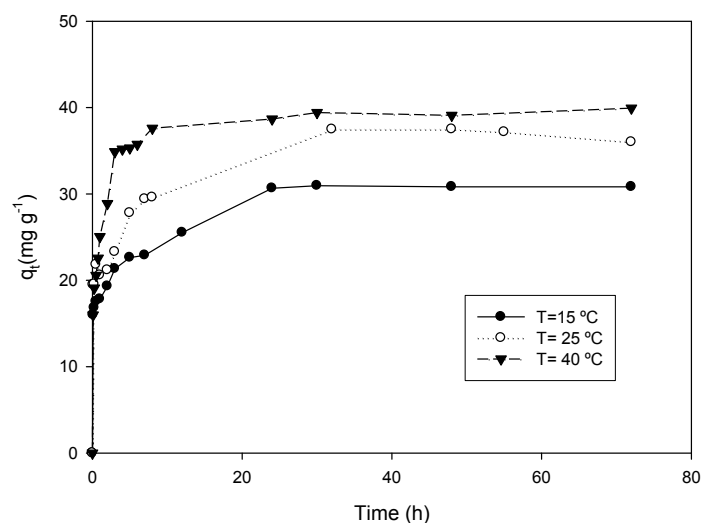


**Figure 4:** Variation of dye uptake with contact time at different temperatures (15, 25 and 40 °C).

It was found that the uptake of the dye by the sorbent adsorption capacity increases with increasing temperature from 15 to 40 °C, indicating that the adsorption is an endothermic process (Al-Degs et al., 2008). According to Hameed et al. (2007), the increase in the adsorption may be a result of increase in the mobility of the dye with increasing temperature. An increasing number of molecules may also acquire sufficient energy to undergo an interaction with active sites at the surface. Furthermore, increasing temperature may produce a swelling effect within the internal structure of the activated palm ash, thereby enabling large dye to penetrate further. Bouberka et al. (2005) reported that the amount of yellow 4GL (acid dye) adsorbed on modified clays increases with increasing temperature from 30 to 50 °C. Alkan et al. (2005) also reported that the adsorption capacity of sepiolite for acid blue 62 dye at 55 °C is higher than at 25 °C.

A Van't Hoff plot of  $\ln K_D$  as a function of  $1/T$  (figure not shown) yields a straight line. The  $\Delta H^\circ$  and  $\Delta S^\circ$  parameters were calculated from the slope and intercept of the plot, respectively. The values of the thermodynamic parameters are listed in Table 6.

The positive value of  $\Delta S^\circ$  indicates that there is an increase in the randomness at the solid/solution interface during the adsorption of the dye on the activated carbon (Azizz et al., 2009). This positive value may be explained as follows: during the adsorption of the dye, the adsorbate species displace the adsorbed solvent molecules to gain more

translational entropy than was lost by the adsorbate, thus allowing randomness in the system. The  $\Delta H^\circ$  parameter was found to be  $49.02 \text{ kJ mol}^{-1}$ . The positive value of  $\Delta H^\circ$  further confirms the endothermic nature of the adsorption process (Ruhan et al., 2009). The decrease in the  $\Delta G^\circ$  values shows the feasibility of adsorption as temperature is increased. Similar results were reported by Li et al. (2009) for the adsorption of 2-nitroaniline onto activated carbon prepared from cotton stalk fibers. Considering the time- profiles of dye uptake presented in Figure 4, the effect of temperature on the adsorption kinetics was also investigated using the Lagergren pseudo-first order and pseudo-second order models. The parameters related to each model were presented in Table 7.

As previously observed, the results fit the second-order-model for the three considered temperatures. The correlation coefficients of the second-order model for  $15^\circ\text{C}$  and  $25^\circ\text{C}$  and  $40^\circ\text{C}$  were greater than 0.98 and greater than those of the pseudo-first order model. The data given in Table 6 also show that the pseudo-second order rate constant,  $K_2$ , increases with temperature, which indicates that the adsorption kinetics are enhanced as the temperature increases. This enhancement also reflects the endothermic nature of the adsorption process. The activation energy,  $E_a$ , for the adsorption of the Black Dycem TTO was determined from the slope of the Arrhenius plot of  $\ln K_2$  versus temperature ( $1/T$ ) (figure not shown), and was found to be  $9.50 \text{ kJ mol}^{-1}$ . The magnitude of the activation energy provides insight about the type of adsorption, which is mainly physical or chemical. The physisorption processes usually have energies in the range of  $5 - 40 \text{ kJ mol}^{-1}$ , while higher activation energies ( $40 - 800 \text{ kJ mol}^{-1}$ ) suggest chemisorption processes (2007). Consequently, the relatively low activation energy ( $9.50 \text{ kJ mol}^{-1}$ ) obtained for the adsorption of Black Dycem TTO onto the activated carbon may involve a physical sorption, which confirmed the results found previously from the D–R isotherm model.

**Table 6:** Thermodynamic parameters for the adsorption of Black Dycem TTO onto activated carbon prepared from Tunisian olive-waste cakes at different temperatures.

$\Delta S^\circ$ (jmol <sup>-1</sup> K <sup>-1</sup> )	$\Delta H^\circ$ (kJ mol <sup>-1</sup> )	$\Delta G^\circ$ (kJ mol <sup>-1</sup> )		
		278 K	298 K	310 K
178.119	53.459	47.503	47.075	46.754

**Table 7:** Parameters of the pseudo-first and pseudo-second order kinetic models at various temperatures.

	Pseudo-first order kinetic model				Pseudo-second order kinetic model		
	$q_{e,exp}$ (mg g <sup>-1</sup> )	$K_1$ (h <sup>-1</sup> )	$q_{e,cal}$ (mg g <sup>-1</sup> )	$R^2$	$K_2$ (g mg <sup>-1</sup> h <sup>-1</sup> )	$q_{e,cal}$ (mg g <sup>-1</sup> )	$R^2$
T = 15 °C	30.82	0.319	18.21	0.841	0.017	24.03	0.990
T = 25 °C	36.01	0.217	17.02	0.959	0.037	36.63	0.999
T = 40 °C	39.92	0.244	10.85	0.385	0.170	25.00	0.984

#### 4.6. Adsorption of dye from real tannery effluent

The results related to the time dependence of  $q_t$  of the commercial dye and the real effluent are shown in Figure 5. The time dependence curve evolves in the same way as the curve of the commercial dye with slightly lower adsorption removal, due to the lower dye concentration in the exhausted bath and the presence of other components in the real effluent that can compete with the target dye.

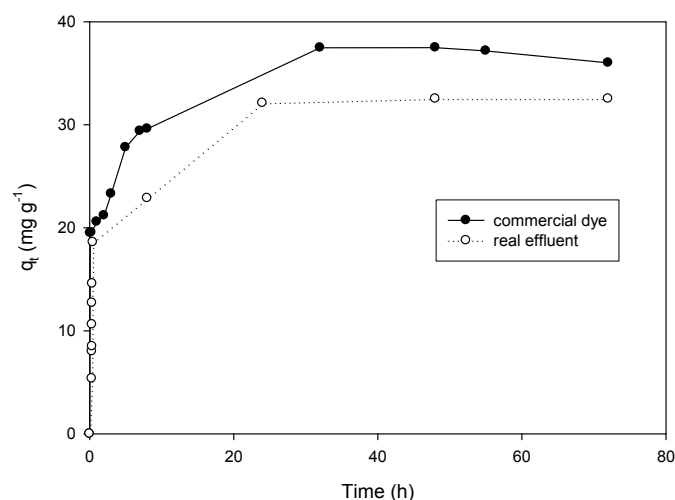


**Figure 5:** Plots of the uptake of the commercial dye and real effluent along the time at 25 °C.

## 5. Conclusions

The adsorption of a tannery dye using activated carbon prepared from olive-waste cakes was investigated. The thermodynamics and kinetics aspects of the adsorption were then evaluated. In the equilibrium study, it was found that the Langmuir model provided the best fit, and that this model is correlated with a monolayer adsorption for the considered dye. The adsorption capacity of the activated carbon was determined to be  $146.31 \text{ mg g}^{-1}$ , which is in good agreement with those of other sorbents prepared from agricultural wastes. Time-based investigations revealed that the adsorption process followed the pseudo-second order model.

Based on the obtained results it appears that the activated carbon prepared from Tunisian olive-waste cakes constitutes a good adsorbent for removing a commercial tannery dye and a real effluent containing the target dye.

## Acknowledgements

The authors wish to thank Mr. H. Ben Arab from the industrial tannery for providing the commercial tannery dye and the real effluent. The authors would like also to thank the Spanish Ministry of Foreign Affairs and Cooperation, AECID, for the predoctoral scholarship of R. Baccar.



## REFERENCES

- Al-Degs Y.S., El-Barghouthi M.I., El-Sheikh A.H., Walker G.M., 2008. Effect of solution pH, ionic strength, and temperature on adsorption behavior of reactive dyes on activated carbon. *Dyes Pigments* 77, 16–23.
- Alkan M., Çelikçapa S., Demirbas O., Dogan M., 2005. Sorption study of an acid dye from an aqueous solution using modified clays. *Dyes Pigments* 65, 251–259.
- Aziz A., Ouali M.S., El Hadj E., De Menorval L.C.H., Lindheimer M., 2009. Chemically modified olive stone: a low-cost sorbent for heavy metals and basic dyes removal from aqueous solutions. *J. Hazard. Mater.* 163, 441–447.
- Baccar R., Bouzid J., Feki M., Montiel A., 2009. Preparation of activated carbon from Tunisian olive-waste cakes and its application for adsorption of heavy metal ions. *J. Hazard. Mater.* 162, 1522–1529.
- Binupriya A.R., Sathishkumar M., Swaminathan K., Ku C.S., Yun S.E., 2008. Comparative studies on removal of congo red by native and modified mycelia pellets of *Trametes versicolor* in various reactor modes. *Bioresour. Technol.* 99, 1080–1088.
- Bouberka Z., Kacha S., Kameche M., Elmaleh S., Derriche Z., 2005. Sorption study of an acid dye from an aqueous solution using modified clays. *J. Hazard. Mater.* 119, 117–124.
- Cabrita I., Ruiz B., Mestre A.S., Fonseca I.M., Carvalho A.P., Ania C.O., 2010. Removal of an analgesic using activated carbons prepared from urban and industrial residues. *Chem. Eng. J.* 163, 249–255.
- Chen B.N., Hui C.W., McKay G., 2001. Film-pore diffusion modeling and contact time optimization for the adsorption of dyestuffs on pitch, *Chem. Eng. J.* 84, 77–94.
- Fu Y., Viraraghavan T., 2001. Fungal decolorization of dye wastewaters: a review. *Bioresour. Technol.* 79, 251–262.
- Giles C.H., Smith D., Huiston A., 1974. A general treatment and classification of the solute adsorption isotherm. I. Theoretical. *J. Colloid Interf. Sci.* 47, 755–765.
- Gupta V.K., Suhas, 2009. Applications of low-cost adsorbents for dye removal-A review. *J. Environ. Manage.* 90, 2313–2342.
- Hamdaoui O., Naffrechoux E., 2007. Modeling of adsorption isotherms of phenol and chlorophenols onto granular activated carbon Part II. Two-parameter models and

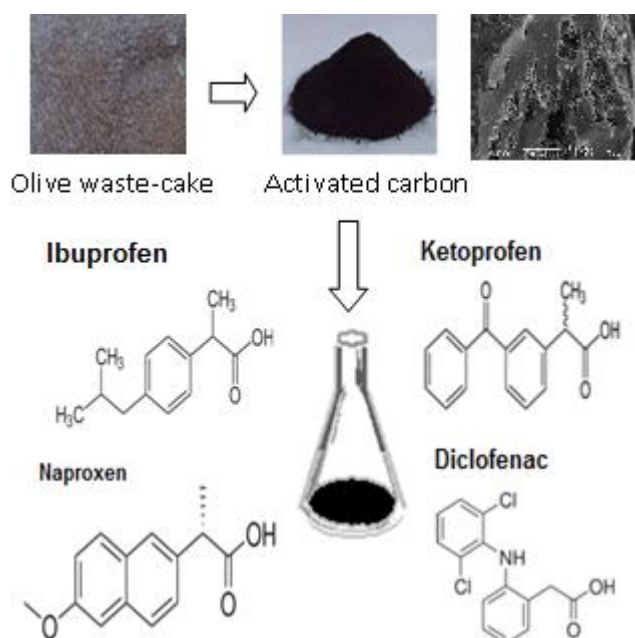
- equations allowing determination of thermodynamic parameters. *J. Hazard. Mater.* 147, 381–394.
- Hameed B.H., Ahmad A.A., Aziz N., 2007. Isotherms, kinetics and thermodynamics of acid dye adsorption on activated palm ash. *Chem. Eng. J.* 133, 195–203.
- Hasley G.D., 1952. The role of surface heterogeneity. *Adv. Catal.* 4, 259–269.
- Ho Y.S., 2004. Selection of optimum sorption isotherm. *Carbon* 42, 2113–2130.
- Jain M., Garg V.K., Kadirvelu K., 2009. Chromium (VI) removal from aqueous system using *Helianthus annuus* (sunflower) stem waste. *J. Hazard. Mater.* 162, 365–372.
- Kinniburgh D.G., 1986. General purpose adsorption isotherm. *Environ. Sci. Technol.* 20, 895–904.
- Kundu S., Gupta A.K., 2006. Arsenic adsorption onto iron oxide-coated cement (IOCC): regression analysis of equilibrium data with several isotherm models and their optimization. *Chem. Eng. J.* 122, 93–106.
- L. Monser, N. Adhoum, Tartrazine modified activated carbon for the removal of Pb(II), Cd(II) and Cr(III), *J. Hazard. Mater.* 16 (2009) 263–269.
- Li K., Zheng Z., Xingfa H., Guohua Z., Jingwei F., Jibiao Z., 2009. Equilibrium, kinetic and thermodynamic studies on the adsorption of 2-nitroaniline onto activated carbon prepared from cotton stalk fiber. *J. Hazard. Mater.* 166, 213–220.
- Mohamed M.M., 2004. Acid dye removal: comparison of surfactant-modified mesoporous FSM-16 with activated carbon derived rice husk, *J. Colloid. Interf. Sci.* 272, 28–34.
- Namasivayam C., Kavitha D., 2002. Removal of Congo Red from water by adsorption onto activated carbon prepared from coir pith, an agricultural solid waste. *Dyes Pigments* 54, 47–58.
- Nigam P., Armour G., Banat I.M., Singh D., Marchant R., 2000. Physical removal of textile dyes from effluents and solid-state fermentation of dye-adsorbed agricultural residues. *Bioresour. Technol.* 72, 219–226.
- Onyango M.S., Kojima Y., Aoyi O., 2004. Adsorption equilibrium modeling and solution chemistry dependence of fluoride removal from water by trivalent-cation-exchanged zeolite F-9. *J. Colloid. Interface Sci.* 279, 341–350.
- Ozacar M., Sengyl I.A., 2004. Two-stage batch sorber design using second-order kinetic model for the sorption of metal complex dyes onto pine sawdust. *Biochem. Eng. J.* 21, 39–45.

- Ozcan A.S., Erdem B., Ozcan A., 2005. Adsorption of Acid Blue 193 from aqueous solutions onto BTMA-bentonite. *Colloids Surf. A: Physicochem Eng. Aspect* 266, 73–81.
- Ruhan A.A., Sari A., Tuzen M., 2009. Equilibrium, thermodynamic and kinetic studies on biosorption of Pb(II) and Cd(II) from aqueous solution by macrofungus (*Lactarius scrobiculatus*) biomass. *Chem. Eng. J.* 15, 255–261.
- Sivaraj R., Namasivayam C., Kadirvelu K., 2001. Orange peel as an adsorbent in the removal of Acid violet 17 (acid dye) from aqueous solutions. *Waste Manage.* 2, 105–110.
- Tan I.A.W., Ahmad A.L., Hameed B.H., 2008. Adsorption of basic dye on high-surface-area activated carbon prepared from coconut husk: equilibrium, kinetic and thermodynamic studies. *J. Hazard. Mater.* 154, 337–346.
- Tsai W.T., C.Y. Chang, C.H. Ing, C.F. Chang, 2004. Adsorption of acid dyes from aqueous solution on activated bleaching earth. *J. Colloid Interf. Sci.* 275, 72–78.
- Tseng R.L., Wu F.C., Juang R.S., 2003. Liquid-phase adsorption of dyes and phenols using pinewood-based activated carbons. *Carbon* 41, 487–495.
- Vernersson T., Bonelli P.R., Cerrela E.G., Cukierman A.L., 2002. *Arundo donax* cane as a precursor for activated carbons preparation by phosphoric acid activation. *Bioresource Technol.* 83, 95–104.
- Weber W.J., Morris J.C., 1963. Kinetics of adsorption on carbon from solutions. *J. Sanit. Eng. Div. Am. Soc. Civ. Eng.* 89, 31-60.



### 4.2.3: Removal of pharmaceutical compounds by activated carbon prepared from agricultural by-product

---



**Abstract**

Adsorption of ibuprofen, ketoprofen, naproxen and diclofenac onto a low-cost activated carbon, prepared at the laboratory scale from olive-waste cakes, has been investigated. Single and mixture drug solutions were considered. The equilibrium adsorption data obtained at 25 °C were analyzed by Langmuir and Freundlich models. The former provides the best fit of the experimental data. The adsorption capacities of the carbon for the four drugs were quite different and were linked essentially to their p<sub>ka</sub> and their octanol/water coefficient. The adsorption kinetics of these adsorbates have been investigated and the results indicated that the adsorption process followed the pseudo-second-order kinetic model for the four tested drugs. The effect of pH and temperature on the drugs uptake by the adsorbent was also investigated. Increasing pH gradually reduced the uptake of the four drugs, and this effect was more perceptible when the pH became alkaline. The increase of temperature in the range 4–40 °C does not have a perceptible effect on the adsorption process for all the studied drugs.

**Keywords:** Low cost adsorbent, olive-waste cakes, naproxen, ibuprofen, diclofenac, ketoprofen.

## 1. Introduction

Pharmaceuticals are compounds with biological activity developed to promote human health and well being. Nevertheless, because a considerable amount of the dose taken is not adsorbed by the body, a variety of these chemicals – including painkillers, tranquilizers, anti-depressants, antibiotics, birth control pills and chemotherapy agents – are finding their way into the environment via human and animal excreta from disposal into the sewage system and from landfill leachate that may impact groundwater supplies (Cabrita et al., 2010). Most substances of pharmaceutical origins are not biodegradable and often not completely eliminated due to their ability to escape to conventional wastewater treatments (Villaescusa et al., 2011; Domínguez et al., 2011). Therefore, residual quantities remain in treated water, or have been found in drinking water (Cabrita et al., 2010). According to a survey in German wastewater treatment plants, clofibric acid and carbamazepine were poorly removed (Ternes, 1998). Moreover, Urase and Kikuta (2005) emphasized the low removal of ketoprofen and naproxen by the conventional activated sludge process.

The removal of pharmaceuticals by adsorption on commonly efficient adsorbents is one of the most promising techniques because of its convenience when applied in current water treatment processes (Domínguez et al., 2011). To date, several reports related to the adsorption of pharmaceuticals onto natural materials or components of natural materials e.g. soils (Figueroa and MacKay, 2005), clays (Figueroa et al., 2004; Pils and Laird, 1993), hydrous oxides (Gu and Karthikeyan, 2005) and silica (Bui and Choi, 2010) have been published. To our knowledge, only few studies have been reported that address the removal of pharmaceuticals from aqueous media by activated carbons, and in most of the cases, commercially available carbons were employed (Yoon et al., 2003; Tsai et al., 2006; Onal et al., 2007). In this work, an activated carbon prepared from a Tunisian agricultural by-product was used to study the adsorption potential of four pharmaceuticals. As probe molecules, nonsteroidal anti-inflammatory acid drugs (NSAIDs), namely ibuprofen, ketoprofen, naproxen and diclofenac, have been selected because they are widely used and ubiquitously detected in aqueous environments (Bui and Choi, 2010; Onal et al., 2007). These pharmaceuticals are also considered to be compounds with high environmental risk (Hernando et al., 2006). Indeed, although their concentrations are generally at trace levels ( $\text{ng L}^{-1}$  to low  $\mu\text{g L}^{-1}$ ) in the environment,

this amount can be sufficient to induce toxic effects (Hernando et al., 2006). On the other hand, the current investigations, reported in bibliography, reveal the high toxicity (“very toxic class”) of anti-inflammatories, such as diclofenac, ibuprofen, naproxen or ketoprofen to bacteria (Daughton and Ternes, 1999; Farré et al., 2001). Other authors have also reported the toxic effects of diclofenac and ibuprofen on invertebrates and algae (Cleuvers, 2003).

Taking into account all the above, the main objective of this research is to evaluate the adsorption potential of prepared carbon for the considered probe molecules. For this purpose, the adsorbent was first prepared at the laboratory scale from olive-waste cakes via chemical activation using phosphoric acid as a dehydrating agent. Then, the adsorption of the pharmaceutical products was studied, while considering the kinetic and thermodynamic aspects of the retention process. Single and mixture drug solutions were considered in this work.

## **2. Materials and methods**

### **2.1. Preparation of the activated carbon**

In the present study, exhausted olive-waste cake was collected from an oil factory “Agrozitex” located in Sfax, Tunisia. It was used as raw material to produce activated carbon via chemical activation using phosphoric acid (analytical grade) as a dehydrating agent. The preparation of the activated carbon was conducted as follows: 40 g of the crushed ( $\text{Ø} < 1.5 \text{ mm}$ ) and dried precursor was mixed with a  $\text{H}_3\text{PO}_4$  solution with a concentration 60%  $\text{H}_3\text{PO}_4$  in weight. The impregnation ratio, defined by the weight ratio of impregnant ( $\text{H}_3\text{PO}_4$ ) to precursor, was 1.75. The impregnation was conducted in a stirred Pyrex reactor equipped with a reflux condenser. Stirring was used to ensure the acid had access to the interior of the olive-waste cake particles. The temperature and the duration of the reaction were 104 °C and 2 h, respectively. Agitation and heating were ensured using a heating magnetic stirrer with connected temperature regulator probe made of Teflon. The pyrolysis of the impregnated material was conducted in a cylindrical stainless steel reactor, inserted into a tubular regulated furnace under continuous nitrogen flow ( $0.5 \text{ L min}^{-1}$ ). The pyrolysis temperature and pyrolysis time were maintained at 450 °C and 2 h, respectively. After cooling down to room temperature under the same flow of nitrogen, the obtained activated carbon was thoroughly washed with hot distilled water until it reached neutral pH. The sample was



then dried at 105 °C overnight, ground (to a granulometry ranging between 100 and 160  $\mu\text{m}$ ) and finally kept in a hermetic bottle for subsequent use.

More details of the preparation of the activated carbon and the optimization of various synthesis conditions as well as their effect on the properties of the prepared adsorbent have been discussed in a previous study (Baccar et al., 2009); thus, they are beyond the scope of this paper. Nevertheless, some of its characteristics are shown herein for data interpretation purposes.

## **2.2. Characterization of the activated carbon**

Textural characteristics of the prepared activated carbon including surface area ( $S_{\text{BET}}$ ), total pore volume ( $V_{\text{tot}}$ ) and pore size distribution were determined from  $\text{N}_2$  adsorption at 77 K using an Autosorb1-Quantachrome instrument. To gain further knowledge regarding important aspects of the surface chemistry of the adsorbent, the pH of the point of zero charge ( $\text{pH}_{\text{pzc}}$ ) has been determined according to the method described by Furlan et al. (2010). It is noted that  $\text{pH}_{\text{pzc}}$  is considered as the pH at which the electric charge density of a given surface equals zero. This parameter was obtained through mixtures of 0.1 g of activated carbon with 50 mL of 0.01 M NaCl standard solution in nine Erlenmeyer flasks to which appropriate quantities of HCl or NaOH were added to obtain the following pH values: 2.5; 4.0; 5.0; 6.0; 7.0; 8.0; 9.0; 10.0 and 11.0. The mixtures were shaken for 48 h at room temperature. Then, the equilibrium pH of each mixture was measured. A high-precision pH meter (Metrohm, model 632) equipped with a combined glass electrode (Metrohm) was used. Preliminary calibration was systematically carried out using suitable buffer solutions.  $\text{pH}_{\text{pzc}}$  is the pH at which the initial value is the same as the final value. Depending on the precursor origin and the preparation mode (chemical or physical), activated carbons can have an acidic, basic or neutral nature depending on the  $\text{pH}_{\text{pzc}}$ .

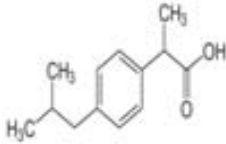
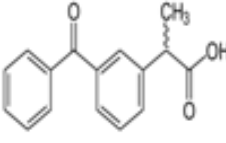
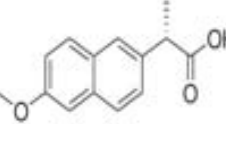
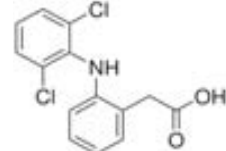
## **2.3. Adsorption studies**

### **2.3.1. Chemicals**

All chemicals used in this work were of analytical grade. The four pharmaceuticals: ibuprofen, ketoprofen naproxen and diclofenac were purchased from Sigma–Aldrich (Barcelona, Spain). The chemical structure and physicochemical properties of each

adsorbate are depicted in Table 1. Solutions of each drug were prepared in deionized water (Millipore Direct Q<sub>4</sub> Water Purification System).

**Table 1:** Molecular structure and some physicochemical properties of pharmaceuticals

Pharmaceutical trade name	Structure	Chemical formula	Molecular Mass (g mol <sup>-1</sup> )	log K <sub>ow</sub> *	pK <sub>a</sub> *
Ibuprofen		C <sub>13</sub> H <sub>18</sub> O <sub>2</sub>	206.29	3.97	4.91
Ketoprofen		C <sub>16</sub> H <sub>14</sub> O <sub>3</sub>	254.28	3.12	4.45
Naproxen		C <sub>14</sub> H <sub>14</sub> O <sub>3</sub>	230.25	3.18	4.15
Diclofenac		C <sub>14</sub> H <sub>11</sub> Cl <sub>2</sub> NO <sub>2</sub>	296.14	4.51	4.15

\* Vieno et al., 2007; K<sub>ow</sub>: octanol/water partition coefficient

### 2.3.2. Sorption isotherms and kinetic studies

Equilibrium and kinetics of the pharmaceuticals adsorption were studied essentially at 25 °C. To determine the equilibrium isotherm, adsorption tests were carried out by adding various amounts of adsorbent (0.10, 0.15, 0.25, 0.35, 0.4 and 0.45 g) to a series of 500 mL Erlenmeyer flasks filled with a 300 mL solution of either: naproxen, ketoprofen, diclofenac or ibuprofen. The initial concentrations were 19.78, 19.28, 14.80 and 10.04 mg L<sup>-1</sup> for naproxen, ketoprofen, diclofenac and ibuprofen, respectively. The solutions were maintained at their natural pH of 4.1. The flasks were shaken at 200 rpm with a magnetic stirrer for 26 h to reach adsorption equilibrium. Then each solution was separated from the sorbent by centrifugation at 13,000 rpm for 5 min and filtered with 13 mm Millex filters.

The initial and the equilibrium concentrations of the four drugs were analyzed using a Dionex 3000 Ultimate HP LC equipped with a UV detector at 230 nm. Chromatographic separation was achieved on a GraceSmart RP 18 column (250 mm × 4 mm, particle size 5 μ). The column temperature was 30 °C. The mobile phase consisted of 6.9 mmol L<sup>-1</sup> acetic acid in water adjusted to pH 4 (by NaOH) with 35% v/v acetonitrile. It was delivered isocratically at 1 mL min<sup>-1</sup> as described by Stafiej et al. (Stafiej et al., 2007). A sample volume of 20 μL was injected from a Dionex autosampler. Retention times were 19.13, 17.00, 12.07 and 11.20 min for ibuprofen, diclofenac, naproxen and ketoprofen, respectively.

From the initial and the equilibrium concentrations, the amount of the drug adsorbed at equilibrium  $q_e$  (mg g<sup>-1</sup>) can be calculated from the following equation:

$$q_e = \frac{(C_0 - C_e)V}{m_{AC}} \quad (1)$$

where  $C_0$  and  $C_e$  (mg L<sup>-1</sup>) are the initial and equilibrium liquid phase pharmaceutical concentrations, respectively,  $V$  the volume of the solution (L) and  $m_{AC}$  is the mass of the activated carbon used in the experiment (g).

Analysis of the equilibrium data allows the maximum adsorption capacity ( $q_{max}$ ) of the adsorbent to be calculated. To check the influence of some characteristics of the adsorbates on the  $q_{max}$  values, linear regression analysis was performed using the software SPSS 17.

The kinetic test procedure was basically identical to the equilibrium test. Nevertheless, for each carbon/pharmaceutical solution mixture liquid samples were taken at preset time intervals for analysis. The amount of drug adsorbed at time  $t$ ,  $q_t$  ( $\text{mg g}^{-1}$ ), was calculated using Eq. (1) by substituting  $C_e$  with  $C_t$ . The magnitude  $C_t$  represents the pharmaceutical liquid phase concentration at any time  $t$ .

### **2.3.3. Effect of pH on the pharmaceutical adsorption**

The effect of pH on each pharmaceutical uptake by the adsorbent was investigated at 25 °C at various pH levels: 2.01, 4.12 (natural pH solution) and 8.61. Adsorption tests were conducted by adding 1.0 g of activated carbon to a series of 500 mL Erlenmeyer flasks filled with 300 mL of one of the pharmaceutical solution.

The pH of the solutions was adjusted with either HCl (1 M) or NaOH (1 M). Each suspension was magnetically stirred for 26 h at 200 rpm. At the end of each experiment, the separation of the drug solution from the sorbent and the measurement of the residual concentration ( $C_e$ ) of each pharmaceutical were conducted using the same method mentioned above.

### **2.3.4. Effect of temperature on adsorption**

The effect of temperature on the pharmaceutical uptake by the sorbent was investigated by time-based analyses. For each temperature, a stock solution of a known concentration for each pharmaceutical at its natural pH 4.12 was used. The kinetic adsorption runs were performed at three different temperatures, i.e. 4, 25 and 37 °C. The adsorption systems were analyzed until the residual drug concentration in the solution became constant (equilibrium state). The mixture was agitated by a magnetic stirrer at 200 rpm. For every temperature, the quantities:  $C_t$ ,  $q_t$ ,  $C_e$  and  $q_e$  were determined as described above.

### **2.3.5. Competitive adsorption from mixture drug solution**

The adsorption kinetics of a mixture of three drugs (naproxen, ketoprofen and ibuprofen) was studied. In this case, 50 mL of solution containing a mixture of three pharmaceuticals (with concentrations of 20, 20 and 10  $\text{mg L}^{-1}$  of naproxen, ketoprofen and ibuprofen, respectively) was added to 0.3 g of activated carbon and the sorption process was investigated by time-based analysis until the equilibrium state was reached.

For the sake of comparison with the individuals systems previously studied, the experiment was conducted at 25 °C and at pH 4.12.

### 3. Results and discussions

#### 3.1. Characteristics of the activated carbon

Nitrogen adsorption data provide quantitative information about the specific surface area (BET surface), the total pore volume ( $V_{\text{tot}}$ ), pore size distribution and the average pore volume of the carbonaceous adsorbents. These essential textural characteristics govern the adsorption capacity of the activated carbon and its ability to fix either small or large molecules (Yang and Chong, 2006).

The nitrogen adsorption isotherm of the prepared activated carbon is characterized by a wide knee at low relative pressures and a gradually upward increase at relative pressures above 0.2 (Figure 1). The isotherm features an intermediate between types I and II of the IUPAC classification (Yang, 1985), indicating that the adsorbent has a combination of microporous and mesoporous structures.

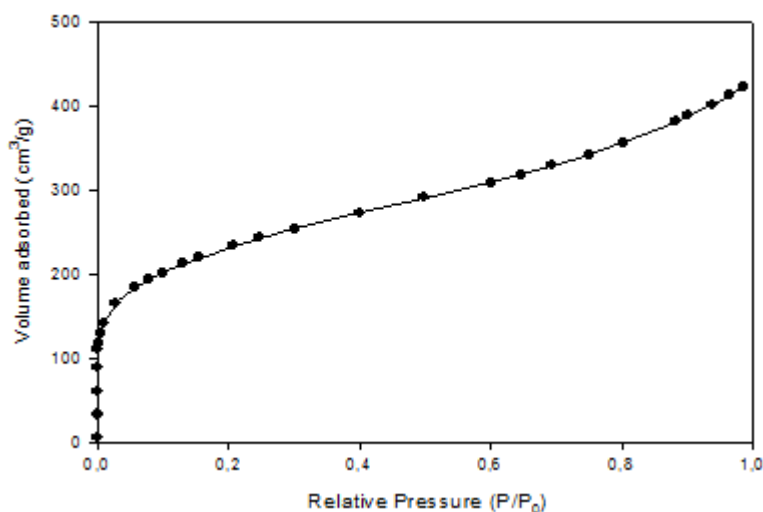


**Figure 1:** Adsorption isotherm of nitrogen at 77 K of the prepared activated carbon

The textural characteristics of activated carbon obtained from N<sub>2</sub> adsorption analysis are summarized in Table 2, indicating that the adsorbent has a large specific area (793 m<sup>2</sup> g<sup>-1</sup>). Comparing the magnitude of the mesopore volume with the total pore volume – which contributes to about 82 % of the total pore volume – indicates the high mesoporosity of the adsorbent. The average pore diameter of the prepared activated

carbon, obtained from Barrett–Joyner–Hanlenda (BJH) method, was found to be 4.2 nm which indicated that the activated carbon derived from olive waste cakes was mainly mesoporous in character with a minor presence of micropores. This finding is particularly interesting because applications of the adsorbent phenomenon may require specific pore sizes. Thus, for an adsorbent used in the liquid–solid system, the ability of solutes to access small pores of the adsorbent could be handicapped due to capillarity effects. Thus, the adsorbent should possess a well-developed mesoporous texture because mesopores may act as channels leading to micropores. However, for the use of adsorbents in the gas–solid system, significant amounts of micropores are usually required (Ould-Idriss et al., 2011). In the present work, the presence of mesopores is favorable for the adsorption of large molecules like the studied drugs.

The pH of point of zero charge ( $\text{pH}_{\text{pzc}}$ ) of an activated carbon depends on the chemical and electronic properties of the functional groups and it is a good indicator of these properties (Song et al., 2010). The  $\text{pH}_{\text{pzc}}$  of the AC was found to be 5.03, which indicates its acidic character.

**Table 2:** Textural characteristics of activated carbon

$S_{\text{BET}}^{\text{a}}$ ( $\text{m}^2 \text{g}^{-1}$ )	$S_{\text{mic}}^{\text{b}}$ ( $\text{m}^2 \text{g}^{-1}$ )	Total pore volume <sup>c</sup> ( $\text{cm}^3 \text{g}^{-1}$ )	Micropore volume <sup>d</sup> ( $\text{cm}^3 \text{g}^{-1}$ )	Micropore volume /total pore volume (%)	Mesopore volume <sup>e</sup> ( $\text{cm}^3 \text{g}^{-1}$ )	Mesopore volume /total pore volume (%)	Average pore diameter <sup>f</sup> (nm)
793	136.29	0.59	0.07	14.20	0.49	83.05	4.2

<sup>a</sup> Specific surface area (multipoint BET method)

<sup>b</sup> Micropore surface area (*t*-plot method)

<sup>c</sup> Calculated from the amount of  $\text{N}_2$  adsorbed at  $P/P_0 = 0.95$

<sup>d</sup> Obtained from *t*-plot method

<sup>e</sup> Calculated from the amount of  $\text{N}_2$  adsorbed between relative pressure  $P/P_0$ : 0.1 - 0.95

<sup>f</sup> Obtained from Barrett–Joyner–Hanlenda (BJH) method.

### 3.2. Adsorption isotherms

The adsorption isotherm indicates how the adsorbate is distributed between the liquid and the solid phases when the adsorption process reaches an equilibrium state. The

shape of the isotherm is the first experimental tool used to diagnose the nature of the adsorption phenomenon. The isotherms have been classified by Giles et al. (1974) into four main groups: L, S, H and C. According to this classification, the isotherms of all considered pharmaceutical products displayed an L curve pattern. The isotherms have a concavity toward the abscissa axis in all cases, indicating that as more sites in the substrate are filled, it becomes more difficult for a fresh solute molecule to find a vacant site (Cabrita et al., 2010). The isotherms related to the adsorption of the four drugs on the prepared activated carbon are presented in Figure 2.

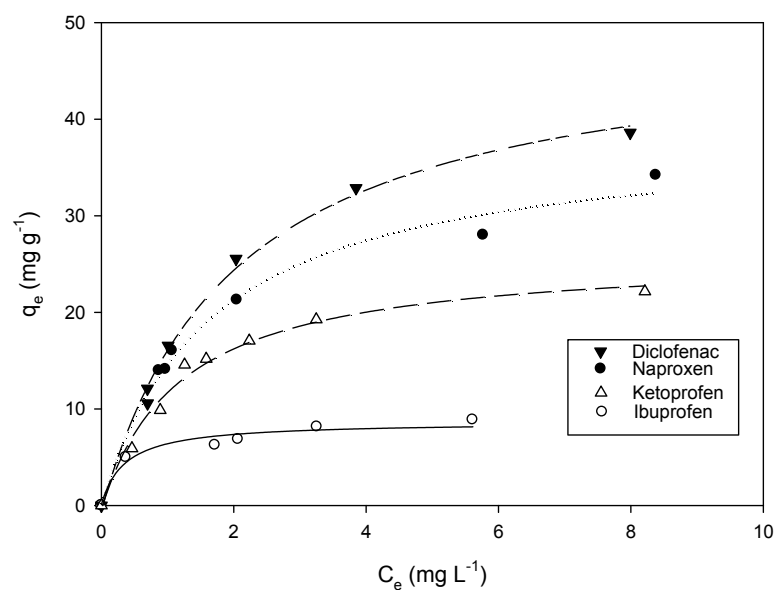


**Figure 2:** Equilibrium adsorption isotherms of ketoprofen (---△---), naproxen (—●—), ibuprofen (.....○.....) and diclofenac (—◊—) onto activated carbon at 25 °C

Two isotherm models related to adsorption equilibrium have been tested in the present study, i.e., Langmuir and Freundlich isotherm models.

The Langmuir model assumes monolayer adsorption onto a surface containing a finite number of adsorption sites of uniform energies of adsorption with no transmigration of adsorbate in the plane of surface. The Langmuir isotherm is described by the following equation:

$$q_e = \frac{q_{\max} K_L C_e}{1 + K_L C_e} \quad (2)$$



where  $q_{\max}$  and  $K_L$  are Langmuir constants related to the adsorption capacity (maximum amount adsorbed per gram of adsorbent ( $\text{mg g}^{-1}$ )) and energy of sorption ( $\text{L m g}^{-1}$ ), respectively. Values of  $q_{\max}$  and  $K_L$  can be calculated from the slope and intercept of the linear plot of  $C_e/q_e$  against  $C_e$ .

The essential characteristics of the Langmuir isotherm can be expressed in terms of dimensionless constant separation factor  $R_L$ , which is defined as follows:

$$R_L = \frac{1}{1 + K_L C_0} \quad (3)$$

where  $C_0$  is the initial solute concentration.  $R_L$  values less than unity confirm the favorable uptake of the sorbent (Hameed et al., 2007).

The empirical Freundlich model, which is known to be satisfactory for low concentrations and based on sorption on a heterogeneous surface, is expressed by the following equation:

$$q_e = K_F C_e^{1/n} \quad (4)$$

where  $K_F$  and  $n$  are Freundlich constants related to the adsorption capacity and adsorption intensity, respectively. These parameters can be calculated from the intercept and the slope of the linear plot  $\log q_e$  versus  $\log C_e$ . The magnitude of the exponent  $n$  indicates the favorability of adsorption.

Conventionally,  $q_{\max}$  is determined from the Langmuir model. However, this parameter can also be estimated from the Freundlich model. Thus, it is necessary to operate with constant initial concentration  $C_0$  and variable weights of adsorbents; therefore,  $\log q_m$  is the extrapolated value of  $\log q_e$  for  $C = C_0$  (Hamdaoui and Naffrechoux, 2007). According to Halsey (1952):

$$K_F = \frac{q_m}{C_0^{1/n}} \quad (5)$$

where  $C_0$  is the initial concentration of the solute in the solution ( $\text{mg L}^{-1}$ ) and  $q_m$  is the Freundlich maximum adsorption capacity ( $\text{mg g}^{-1}$ ).

The comparison of the applicability of each model was made essentially on the basis of the linear coefficient correlation  $R^2$  values. To further validate the results of this comparison, a normalized standard deviation  $\Delta q$  (%) was also calculated, for the two obtained models, using the following equation:

$$\Delta q (\%) = 100 \sqrt{\frac{\sum \left( \frac{q_{\text{exp}} - q_{\text{cal}}}{q_{\text{exp}}} \right)^2}{N-1}} \quad (6)$$

where  $q_{\text{exp}}$  and  $q_{\text{cal}}$  are, respectively, the experimental and calculated amounts adsorbed at equilibrium for each pharmaceutical and  $N$  is the number of measurements made. As seen, the normalized standard deviation  $\Delta q$  indicates the fit between the experimental and predicted values of adsorbed amounts while the linear correlation coefficients ( $R^2$ ) show the fit between the experimental data and linearized forms of the isotherm equations (Hamdaoui and Naffrechoux, 2007). The higher is the value of  $R^2$  and the lower is the value of  $\Delta q$ , the better will be the goodness of fit.

The adsorption data at 25 °C onto activated carbon for the four drugs considered were used to fit linearized expressions of Langmuir and Freundlich. Good linearity was obtained in all cases. As an illustration, Figures 3a and 3b shows the Langmuir and Freundlich isotherm plots for the adsorption of ketoprofen.

Table 3 summarizes the parameters related to the Langmuir and Freundlich isotherms. From the  $R^2$  values, the fit to the Langmuir equation was better than that to the Freundlich. Moreover, the values of  $\Delta q$  (%) for the Langmuir equation were lower than those for the Freundlich equation. Consequently, the values of maximum adsorption capacity obtained using the Langmuir equation match better with the experimental data than those calculated by the Freundlich equation.

The dimensionless constant separation factors  $R_L$  for naproxen, ketoprofen, diclofenac and ibuprofen were, respectively, 0.08, 0.04, 0.15 and 0.15. The  $R_L$  values were less than 1, indicating favorable uptake of the four pharmaceuticals. The adsorption capacities ( $q_{\text{max}}$ ) determined from the Langmuir model were 56.17, 39.52, 24.69 and 10.83 mg g<sup>-1</sup> for diclofenac, naproxen, ketoprofen and ibuprofen, respectively. The results indicated that there is a difference in the adsorption affinity of the activated

carbon toward the four drugs tested. The maximum adsorption capacity of ibuprofen was approximately 5 times lower than that for diclofenac.

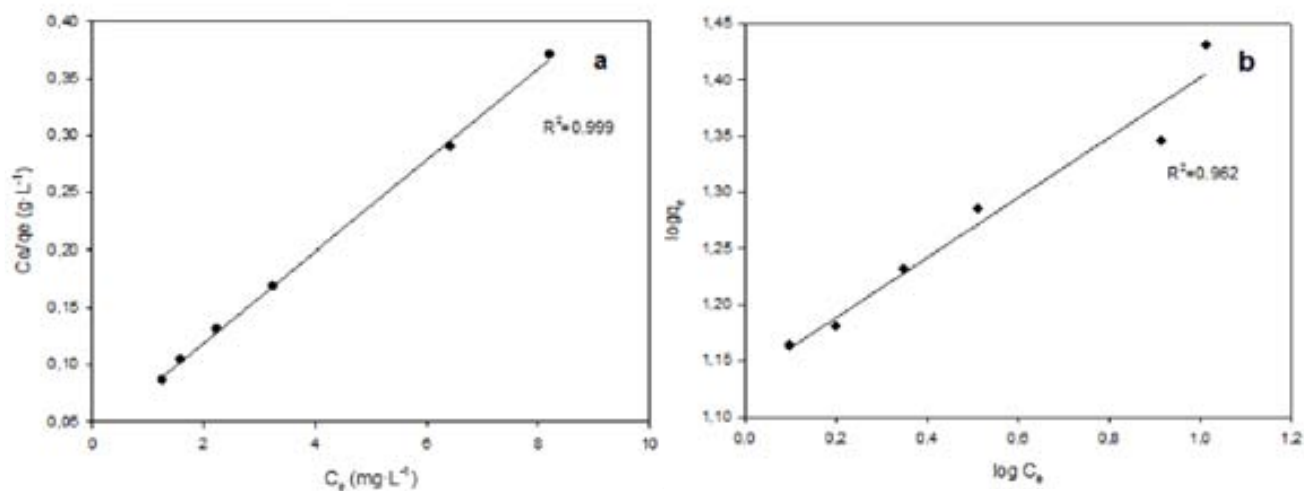


**Figure 3:** Langmuir (a) and Freundlich (b) isotherm plots for the adsorption of ketoprofen

**Table 3:** Langmuir and Freundlich isotherm constants for the four pharmaceuticals at 25 °C.

Isotherm	Naproxen	Ketoprofen	Diclofenac	Ibuprofen
<b>Langmuir</b>				
$K_L$	0.58	1.05	0.38	0.55
$q_{max}$	39.5	24.7	56.2	12.6
$R^2$	0.987	0.996	0.967	0.971
$\Delta q$ (%)	4.5	2.2	6.9	3.4
<b>Freundlich</b>				
$n$	2.62	4.33	1.57	2.94
$q_{max}$	46.9	27.7	83.1	14.4
$R^2$	0.983	0.962	0.962	0.956
$\Delta q$ (%)	4.9	32.1	9.4	4.6

### 3.3. Adsorption kinetics

Adsorption kinetics experiments were used to investigate the effect of contact time on drugs adsorption. As illustration, Figure 4 presented only the curves relatives to residual

ketoprofen concentration versus contact time for different amounts of adsorbent (0.10, 0.15, 0.25, 0.35, 0.4 and 0.45 g). Similar plots, having similar general feature, were also determined for diclofenac, ibuprofen and naproxen. Time-based results indicated that the residual concentration of adsorbate decreases with time and, at some point in time, it reaches a constant value beyond which no more adsorbate is further removed from the solution. At this point the amount of drug desorbing from the activated carbon is in a state of dynamic equilibrium with the amount of drug being adsorbed on the carbon.

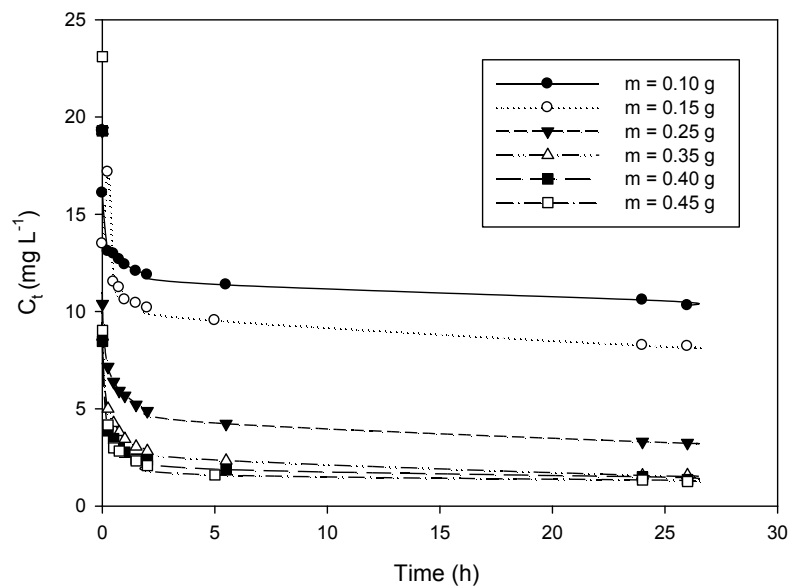


**Figure 4:** Effect of contact time on ketoprofen adsorption for different amounts of adsorbent at 25 °C

The adsorption kinetics model was also investigated using three models, namely, the Lagergren pseudo-first order and pseudo-second order models as well as the Elovich equation.

### 3.3.1. Theoretical background

#### 3.3.1.1. Pseudo-first and second order kinetic models

The Lagergren pseudo-first order and pseudo-second order models, in the linear form, are expressed by Eqs. (7) and (8), respectively:

$$\ln(q_s - q_t) = \ln q_s - K_1 t \quad (7)$$

$$\frac{t}{q_t} = \frac{1}{K_2 q_e^2} + \frac{1}{q_e} t \quad (8)$$

where the terms  $q_e$  and  $q_t$  have the same meaning previously mentioned and are expressed in  $\text{mg g}^{-1}$  and  $K_1$  and  $K_2$  are the pseudo first-order and second-order model rate constants, expressed in  $\text{min}^{-1}$  and  $\text{g m g}^{-1} \text{min}^{-1}$ , respectively. Straight lines of  $\ln(q_e - q_t)$  versus  $t$  and  $t/q_t$  versus  $t$  suggest the applicability of one of these kinetic models and that the kinetic parameters can be determined from the slope and intercept of the plot.

### 3.3.1.2. Elovich equation

The Elovich equation is one of the most useful models for describing chemisorption (Tan et al., 2009) and is given as follows:

$$q_t = \frac{1}{b} \ln(ab) + \frac{1}{b} \ln t \quad (9)$$

where  $a$  ( $\text{mg g}^{-1}\text{h}^{-1}$ ) is the initial sorption rate and  $b$  ( $\text{mg g}^{-1}$ ) is related to the extent of surface coverage and activation energy for chemisorption. The parameters  $(1/b)$  and  $(1/b) \ln(ab)$  can be obtained from the slope and intercept of the linear plot of  $q_t$  versus  $\ln t$ . The value of  $1/b$  is indicative of the number of sites available for adsorption, while the  $(1/b) \ln(ab)$  value is the adsorption quantity when  $\ln t$  is equal to zero (Tan et al., 2009).

### 3.3.2. Modeling of adsorption kinetics

The calculated  $q_e$ ,  $K_1$ ,  $K_2$ ,  $a$  and  $b$  and the corresponding linear regression coefficient  $R^2$  values are presented in Table 4. The applicability of the kinetic model is compared by judging the correlation coefficients  $R^2$ .

The correlation coefficients for the pseudo-second order kinetic plots were almost equal to unity for all pharmaceuticals, where those relating to the first-order and Elovich model were relatively lower. This result indicates that the sorption systems do not kinetically follow a pseudo-first order or Elovich model and that the pseudo-second order sorption mechanism is dominant. This result is in agreement with those reported in several papers dealing with adsorption of organic solutes on activated carbons (Hamdaoui and Naffrechoux, 2007; Mestre et al., 2007; Onal et al., 2007).

**Table 4:** Pseudo-first order model, pseudo second order model and Elovich equation constants and correlation coefficients for adsorption of the four studied pharmaceuticals on the olive-waste activated carbon at 25 °C

Adsorbate	First-order Kinetic model				Second-order Kinetic model			Elovich equation		
	$q_{e,exp}$ ( $mg\ g^{-1}$ )	$K_1$ ( $L\ min^{-1}$ )	$q_{e,cal}$ ( $mg\ g^{-1}$ )	$R^2$	$K_2$ ( $gmg^{-1}\ min^{-1}$ )	$q_{e,cal}$ ( $mg\cdot g^{-1}$ )	$R^2$	$a$ ( $mg\ g^{-1}\ min^{-1}$ )	$b$ ( $gmg^{-1}$ )	$R^2$
Naproxen	19.076	0.236	2.656	0.947	0.582	19.120	1	$1.13\ 10^9$	1.241	0.945
Ketoprofen	18.126	0.227	3.671	0.978	0.354	18.214	0.999	1.08	1.117	0.593
Ibuprofen	9.083	0.188	1.011	0.896	1.491	9.099	1	-1.72	2.842	0.966
Diclofenac	13.776	2.0773	9.622	0.815	0.698	13.812	1	$4.05\ 10^7$	1.636	0.754

### **3.4. Effect of temperature**

Generally, the temperature affects the adsorption process. To mitigate the effect of this parameter, adsorption experiments were conducted for different contact time at three temperatures: 4, 25 and 37 °C. The results did not reveal a perceptible effect of the studied parameter on the adsorption process in the considered temperature range for the four studied drugs (figure not shown). The results agree with those of Mestre et al. (2007) who noticed that temperatures (25 - 40 °C) had no significant influence on ibuprofen adsorption process onto powder activated carbon. Villaescusa et al., (2011) also observed the negligible influence of temperature on paracetamol sorption onto grape stalk between 5 and 30 °C and indicated that this sorption is almost athermic. One possible explanation of this athermicity is that the molecule drugs are well solvated in their aqueous solution (Naseem and Tahir, 2001). In order for the drugs molecules to be adsorbed, they have to lose part of their hydration sheath. This dehydration phenomenon requires energy (endothermic phenomenon). This endothermicity practically equals the exothermicity of the molecules getting attached to the surface. Consequently, the overall adsorption process is nearly athermic.

### **3.5. Effect of pH on the pharmaceuticals adsorption**

The role of pH on the adsorption of the four pharmaceuticals by the olive waste-cakes activated carbon was studied. The results, expressed in term of removal percentage of each drug with different pH values, are shown in Figure 5. It was observed that high pH reduced the uptake of the four drugs, and this effect was more perceptible when the pH became alkaline. This trend is comparable to the finding by Cho et al. (2011), who reported that the sorption of the ibuprofen onto carbon nanotubes decreased as the pH increased from 4 to 10. Behera et al. (2010) also reported that the sorption of Triclosan, a widely used disinfectant present in numerous commercial products, with activated carbon, kaolinite, and montmorillonite gradually decreased as the pH increased from 3 to 10.

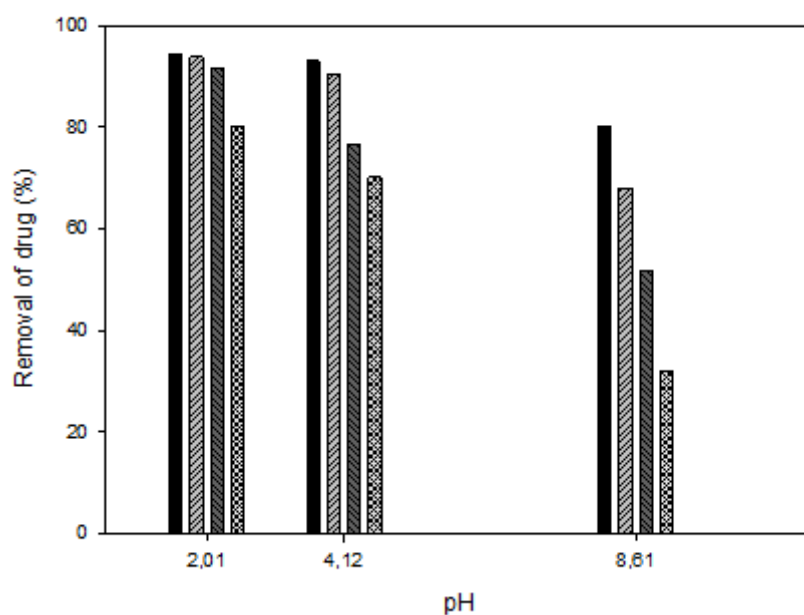


**Figure 5:** Effect of pH on the removal of diclofenac (■), naproxen (▨), ketoprofen (▩) and ibuprofen (▧) with activated carbon

From Figure 5, it is also noteworthy that pH acted differently in the adsorption of the four drugs.

According to the literature, some authors reported that interactions between the activated carbon and aromatics may imply dispersion forces between  $\pi$ -electrons in aromatics and  $\pi$ -electrons in activated carbon (Hamdaoui and Naffrechoux, 2007, Moreno-Castilla, 2004). Other authors indicated that many mechanisms, namely: electrostatic interactions, hydrogen bonding, and hydrophobic-hydrophobic mechanism should be taken into account to explain some experimental adsorption data.

With regards to the effect of pH observed in the study (Figure 5), it seems that interactions between the  $\pi$ -electrons of the adsorbate aromatic ring and those of the carbon grapheme layers cannot explain alone the decrease of percentage removal versus pH. Since the pH affects the nature of the adsorbate and the surface properties of the adsorbent, other mechanisms may interfere. For a given activated carbon and in accordance with its amphoteric character, it is known that the surface of carbon is neutral at  $\text{pH} = \text{pH}_{\text{pzc}}$ , negatively charged for pH higher than  $\text{pH}_{\text{pzc}}$  and positively charged at pH below the  $\text{pH}_{\text{pzc}}$  (Noh, and Schwarz, 1989). Concerning the adsorbates, their charges will be based on their  $\text{pK}_a$  values (Table 1). The four acid drugs are essentially neutral molecules at pH below their  $\text{pK}_a$  value. However, they acquired



negative charge when the pH is above the pka value because of the dissociation of the drug molecules into carboxylate anions. Thus, the adsorption of pharmaceuticals onto activated carbon can be partially controlled by interactions others than  $\pi$ - electrons ones. For  $pH < pH_{pzc}$  ( $pH = 2.01$ ), the activated carbon is positively charged, while the acid drugs are neutral ( $pH < pka$ ); thus, adsorption most likely involves hydrogen bonding and/or van der Waals interaction (Domínguez et al., 2011). At pH 4.12, a pH value in the vicinity of the pka value of the four pharmaceuticals, approximately two forms exist: molecule and ionic. From the fundamental acid-base relation:

$$pH = pka + \log \frac{[A^-]}{[HA]} \quad (10)$$

where  $A^-$  refers to the ionized species and HA refers to the neutral species. The ionization percentage can be calculated using the following equation:

$$\% \text{ ionization} = \frac{100}{1 + 10^{(pka-pH)}} \quad (11)$$

At pH 4.12, approximately 48.28% of naproxen and diclofenac, 31.94 % of ketoprofen and 13.95 % of ibuprofen species had negative charge and the removal percentage slightly decreased. Similarly, for  $pH > pH_{pzc}$  ( $pH = 8.61$ ), the surface of the adsorbent is negatively charged and a higher proportion of the acid drugs too ( $pH > pka$ ), leads to an electrostatic repulsion between the adsorptive anions and the surface of the adsorbent. Consequently the removal of pharmaceuticals decreased (Figure 5).

For more convenience, the difference between the individual behaviors of each pharmaceutical as the pH varies will be discussed in the following section.

### 3.6. Relation between adsorption capacity and adsorbate characteristics

As mentioned above, the solution pH affects globally the uptake of all considered pharmaceuticals with activated carbon. However, even at the same pH, the drugs behave differently toward adsorption phenomenon. Similarly, the adsorption capacities ( $q_{max}$ ), from the Langmuir model also varied from one drug to another. This behavior variability has only one root: the differences among the characteristics of the four adsorbates.

According to Moreno-Castilla (2004), the characteristics of the adsorbate that mainly influence the adsorption process are the molecular size, solubility in water, pka and the

nature of the substituent in the benzene ring if they are aromatic. The molecular size controls the accessibility to the pores of the carbon while the pKa governs the dissociation of the adsorptive if it is an electrolyte. Solubility determines the hydrophobic interactions and is conditioned by the value of the octanol/water partition coefficient,  $K_{ow}$ . Some authors reported that  $K_{ow}$  is directly proportional to the adsorption capacity (Hamdaoui and Naffrechoux, 2007). Westerhoff et al. (2005) found that compounds with low  $\log K_{ow}$  seem to be the most difficult to remove with powder-activated carbon. According to our results, no direct correlation appears between the adsorption capacity ( $q_{max}$ ) and the available quantified characteristics pKa and  $\log K_{ow}$  (Tables 1 and 3). Thus, linear regression analysis was performed to determine the influence of these two characteristics: hydrophobicity ( $\log K_{ow}$ ) and pKa on  $q_{max}$  values, using the software SPSS 17. The obtained results showed that the highest statistical trend exists between the two characteristics pKa and  $\log K_{ow}$  ( $R^2 = 0.999$ ) with a higher negative effect of pKa and a lower positive effect of  $\log K_{ow}$ , as described by the following equation:

$$q_{max} = 211.87 - 50.62 pKa + 12.02 \log K_{ow} \quad (12)$$

A high statistical trend is also obtained from the removal percentage

$$(\% \text{ removal} = 276.97 - 56.83 pka + 8.64 \log K_{ow}, \text{ at pH } 8.61; R^2 = 0.999) \dots (13).$$

Thus, diclofenac, for example, is adsorbed better than naproxen, which presents the same pKa, due to their difference in hydrophobicities:  $\log K_{ow} = 3.18$  for naproxen and 4.51 for diclofenac. At pH 4.12, ibuprofen presents the lowest percentage of ionization (13.95 %) compared to the other drugs. When only the pKa values were compared, it was expected that ibuprofen would be the most adsorbed because it has the lowest electrostatic repulsive interaction between its deprotonated form and the negative charge of the adsorbent. However, this outcome does not occur. Therefore, it is possible to ascribe its lowest uptake to the chemical structure of its molecules which may favor aggregation between them through hydrophobic interactions and make the ibuprofen difficult to access and to adsorb on activated carbon.

Adsorption tests of a solution containing a mixture of three drugs: ketoprofen, naproxen and ibuprofen on activated carbon were conducted, and the percentages of removal were measured (Table 5).

**Table 5:** Percentages removal of naproxen, ketoprofen and ibuprofen from mixture drug solution at 25 °C

Drug	Percentage removal (%)
Naproxen	90.45
Ketoprofen	88.40
Ibuprofen	70.07

Although, these values were lower than those for the removal of individual drugs, the extent of adsorption follows the same trend identified above. Lastly, large quantities of drugs were adsorbed in the mixture, which is worth noting. These results indicate the ability of the prepared adsorbent to adsorb multiple drugs.

In addition to the two characteristics cited above, the functional groups and other structural properties (i.e., planner structure) of organic molecules may also play a role in their adsorption onto activated carbon Cho et al., (2011). Ketoprofen, which contained both ketone and carboxylate groups (Table 1), may have a higher complexing affinity to activated carbon than the other drugs. The chloro group is an electron-withdrawing group; therefore, the electron density in the aromatic ring decreases as the number of chloro groups increases (Hamdaoui and Naffrechoux, 2007). Diclofenac presents two chloro groups; thus, it may present the highest affinity to the  $\pi$ -electrons in activated carbon.

A systematic study involving a larger list of drugs will be necessary to more thoroughly investigate the correlation between adsorbate characteristics and the extent of adsorption on activated carbon.

#### 4. Conclusions

The adsorption of four pharmaceuticals, naproxen, diclofenac, ibuprofen, and ketoprofen on activated carbon prepared from olive-waste cakes was investigated. After structural characterization of the sorbent, the thermodynamics and kinetics aspects of the adsorption were investigated. In an equilibrium study, it was found that the Langmuir model provided the best fit and this model is in agreement with a monolayer

adsorption for the four considered pharmaceuticals. Time-based investigations showed that adsorption process followed the second-order model. Large quantities of drugs are adsorbed in a mixture indicating the ability of the prepared adsorbent to adsorb multiple drugs.

Based on a linear regression analysis of the obtained data, the uptake of the four drugs was first linked in this paper to the  $pK_a$  and  $\log K_{ow}$  characteristics of the adsorbates. To further evaluate the correlation between adsorbate characteristics and the extent of adsorption on activated carbon, more drugs must be studied.

### **Acknowledgements**

The authors would like to thank Maria Giner Molina for her contribution in the experimental work. The authors would also like to thank the Spanish Ministry of Foreign Affairs and Cooperation, AECID, for the predoctoral scholarship of R. Baccar.

### **REFERENCES**

- Baccar R., Bouzid J., Feki M., Montiel A., 2009. Preparation of activated carbon from Tunisian olive-waste cakes and its application for adsorption of heavy metal ions. *J. Hazard. Mater.* 162, 1522-1529.
- Bhera S. K., Oh S.Y., Park H.S., 2010. Sorption of triclosan onto activated carbon, kaolinite and montmorillonite: effects of pH, ionic strength, and humic acid. *J. Hazard. Mater.* 179, 684-691.
- Bui T.X., Choi H. 2010. Influence of ionic strength, anions, cations, and natural organic matter on the adsorption of pharmaceuticals to silica. *Chemosphere* 80, 681-686.
- Cabrita I., Ruiz B., Mestre A.S., Fonseca I.M., Carvalho A.P., Ania C.O., 2010. Removal of an analgesic using activated carbons prepared from urban and industrial residues. *Chem. Eng. J.* 163, 249-255.
- Cho H.H., Huang H., Schwab K., 2011. Effects of solution chemistry on the adsorption of ibuprofen and triclosan onto carbon nanotubes. *Langmuir* 27, 12960-12967.
- Cleuvers M., 2003. Aquatic Ecotoxicity of pharmaceutical including the assessment of combination effects. *Toxicol. Lett.* 142, 185-194.
- Daughton C.G., Ternes T.A., 1999. Pharmaceuticals and personal care products in the environment: agents of subtle change? *Environ. Health Perspect.* 107, 907.

- Domínguez J.R., González T., Palo P.E., Cuerda-Correa M., 2011. Removal of common pharmaceuticals present in surface waters by Amberlite XAD-7 acrylic-ester-resin: Influence of pH and presence of other drugs. *Desalination* 269, 231-238.
- Farré M., Ferrer I., Ginebreda A., Figueras M., Olivella L.; Tirapu L., Vilanova M., Barcelo D., 2001. Determination of drugs in surface water and wastewater samples by liquid chromatography-mass spectrometry: methods and preliminary results including toxicity studies with *Vibrio fischeri*. *J. Chromatogr. A* 938, 187-197.
- Figuerola R.A., Leonard A., MacKay A.A., 2004. Modeling tetracycline antibiotic sorption to clays. *Environ. Sci. Technol.* 38, 476-483.
- Figuerola R.A., MacKay A.A., 2005. Sorption of oxytetracycline to iron oxides and iron oxide-rich soils. *Environ. Sci. Technol.* 39, 6664-6671.
- Furlan F.R., M. Da Silva L. G., Morgado A. F., De Souza A.A.U., De Souza S. M. A.G.U., 2010. Removal of reactive dyes from aqueous solutions using combined coagulation/flocculation and adsorption on activated carbon. *Res. Conserv. Recycling* 54, 283-290.
- Giles C.H., Smith D., Huiston A., 1974. A general treatment and classification of the solute adsorption isotherm. I. Theoretical. *J. Colloid Interface Sci.* 47 755-765.
- Gu C., Karthikeyan K.G., 2005. Interaction of tetracycline with aluminum and iron hydrous oxides. *Environ. Sci. Technol.* 39, 2660-2667.
- Hamdaoui O., Naffrechoux E., 2007. Modeling of adsorption isotherms of phenol and chlorophenols onto granular activated carbon: Part I. Two-parameter models and equations allowing determination of thermodynamic parameters. *J. Hazard. Mater.* 14, 381-394.
- Hameed B.H., Din A.T.M., Ahmad A.L., 2007. Adsorption of methylene blue onto bamboo-based activated carbon: kinetics and equilibrium studies. *J. Hazard. Mater.* 141, 819-825.
- Hasley G.D., 1952. The role of surface heterogeneity. *Adv. Catal.* 4, 259-269.
- Hernando M.D., Mezcuca M., Fernández-Alba A.R., Barceló D., 2006. Environmental risk assessment of pharmaceutical residues in wastewater effluents, surface waters and sediments. *Talanta* 62, 334-342.
- Mestre A.S., Pires J., Nogueira J.M.F., Carvalho A.P., 2007. Activated carbons for the adsorption of ibuprofen. *Carbon* 45, 1979-1988.

- Moreno-Castilla C., 2004. Adsorption of organic molecules from aqueous solutions on carbon materials. *Carbon* 42, 83-94.
- Naseem R., Tahir S. S., 2001. Removal of Pb (II) from aqueous/acidic solutions by using bentonite as an adsorbent. *Water Res.* 35, 3982–3986.
- Noh J.S., Schwarz J.A., 1989. Estimation of the Point Zero Charge of simple oxides by mass titration. *J. Colloid Interface Sci.* 130, 157.
- Onal Y., Akmil-Başar C., Sarici-Ozdemir C., 2007. Elucidation of the naproxen sodium adsorption onto activated carbon prepared from waste apricot: kinetic, equilibrium and thermodynamic characterization. *J. Hazard. Mater.* 148, 727-734.
- Ould-Idriss A., Stitou M., Cuerda-Correa E.M., Fernandez-Gonzalez C., Macias-Garcia A., Alexandre-Franco M.F., Gomez-Serrano V., 2011. Preparation of activated carbons from olive-tree wood revisited. II. Physical activation with air. *Fuel Process. Technol.* 92, 266-270.
- Pils J.R.V., Laird D.A., 2007. Sorption of tetracycline and chlortetracycline on K- and Ca-saturated soil clays, humic substances, and clay–humic complexes. *Environ. Sci. Technol.* 41, 1928-1933.
- Sing K.S.W., Everett D.H., Haul R.A.W., Moscow L., Pierotti R.A., Rouquérol J., Siemieniewska T., 1985. Reporting physisorption data for gas/solid system, *Pure Appl. Chem.* 57, 603-619.
- Song X., Liu H., Cheng L., Qu Y., 2010. Surface modification of coconut-based activated carbon by liquid-phase oxidation and its effects on lead ion adsorption. *Desalination* 255, 78-83.
- Stafiej A., Pyrzyńska K., Regan F., 2007. Determination of anti-inflammatory drugs and estrogens in water by HPLC with UV detection. *J. Sep. Sci.* 30, 985-991.
- Tan I.A.W., Ahmad A.L., Hameed B.H., 2009. Adsorption isotherms, kinetics, thermodynamics and desorption studied of 2,4,6-trichlorophenol on oil palm empty fruit bunch- based activated carbon. *J. Hazard. Mater.* 164, 473-482.
- Ternes, T.A. 1998. Occurrence of drugs in German sewage treatment plants and rivers. *Water Res.* 32, 3245-3260.
- Tsai W.T., Lai C.W., Su T.Y., 2006. Adsorption of bisphenol-A from aqueous solution
- Urase T., Kikuta T., 2005. Separate estimation of adsorption and degradation of pharmaceutical substances and estrogens in the activated sludge process. *Water Res.* 39, 1289-1300.

- Vieno N.M., Härkki H., Tuhkanen T., Kronberg L., 2007. Occurrence of pharmaceuticals in river water and their elimination in a pilot-scale drinking water treatment plant. *Environ. Sci. Technol.* 41, 5077-5084.
- Villaescusa I., Fiol N., Poch J., Bianchi A., Bazzicalupi C., 2011. Mechanism of paracetamol removal by vegetable wastes: The contribution of  $\pi$ - $\pi$  interactions, hydrogen bonding and hydrophobic effect. *Desalination* 270, 135-142.
- Westerhoff P., Yoon Y., Snyder S., Wert E., 2005. Fate of endocrine-disruptor, pharmaceutical, and personal care product chemicals during simulated drinking water treatment processes. *Environ. Sci. Technol.* 39, 6649-6663.
- Yang T., Chong L.A., 2006. Textural and chemical properties of zinc chloride activated carbons prepared from pistachio-nut shells. *Mater. Chem. Physics*, 100, 438-444.
- Yoon Y., Westerhoff P., Snyder S.A., Esparza M., 2003. HPLC-fluorescence detection and adsorption of bisphenol A, 17 $\beta$ -estradiol, and 17  $\alpha$ -ethynyl estradiol on powdered activated carbon. *Water Res.* 37, 3530-3537.





## Topic 3: Biological treatment

---

In this topic, the biological process using white- rot fungi is adapted to decolorize a tannery dye. For the selection of the best strain, screenings in solid and liquid medium are realized. The efficiency of the best fungus is tested in single and repeated batches in an air-pulsed bioreactor. The following publication 4.3.1 encompass this issue:

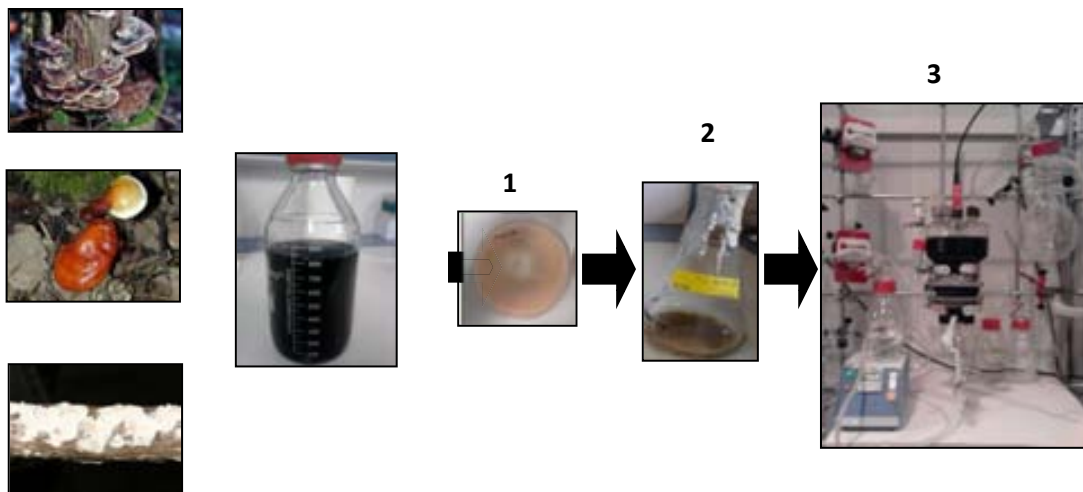
### **4.3.1. Decolorization of a tannery dye: from fungal screening to bioreactor application**

*Biochemical Engineering Journal, 56 (2011) 184–189*



### 4.3.1. Decolorization of a tannery dye: from fungal screening to bioreactor application

---



**Abstract**

In the present work, the potential of three white-rot fungi (WRF) (*Trametes versicolor*, *Ganoderma lucidum* and *Irpex lacteus*) to decolorize the commercial tannery dye – Black Dycem – was investigated. The decolorization ability of the three strains was studied in primary and secondary screenings. The results indicated that *T. versicolor* displayed the greatest decolorization ability, both in terms of extent and rapidity. To assess the potential of *T. versicolor*, decolorization tests were performed in single and repeated batches in an air-pulsed bioreactor with biomass reuse. Although low enzyme activity was detected during the repeated batches, the decolorization capability of the fungus did not decrease, and *T. versicolor* was able to remove 86–89% of the dye. Further experiments were conducted in order to elucidate the enzymatic activities involved in the dye biodegradation process. The results proved that the biodegradation mechanism plays a noticeable role in the decolorization process of the dye, in addition to adsorption phenomenon occurring on the fungal surface. Moreover, it was shown that laccase is involved in the decolorization process, although a mediator is required. Killed fungus presented an appreciable color removal even in repeated batches, suggesting that dead cells are an effective biosorbent.

**Keywords:** white-rot fungi, tannery dye, sequence batch reactor, enzymatic system.

## 1. Introduction

The process of tanning is one of the oldest industrial procedures in the world. Currently, these industrial activities are based on chemical processes involving several organic and inorganic compounds, including acids, chromium salts, dyes, auxiliaries and other chemical additives (Paschoal et al., 2009). The dyeing of leather is one of the most important steps in post-tanning operations in leather production, and it requires a substantial amount of water. As a result, the process produces enormous amounts of colored wastewater that can cause severe environmental problems. Indeed, dyes are usually synthetic origin with complex aromatic molecular structures (Fu and Viraraghavan, 2009). Most dyes are toxic, mutagenic and carcinogenic. Moreover, they are unusually resistant to degradation. Scientists have been trying to develop a single economical method for the treatment of dyes, but it still remains an unsolved challenge (Pant et al., 2008). A number of chemical and physico-chemical strategies have been proposed to treat dye-containing wastes and wastewaters. These methods (Gupta and Suhas, 2004) include chemical oxidative degradation and electrochemical decomposition, coagulation, flocculation and adsorption. However, these processes present high costs and/or limited applicability as the main disadvantages (Robinson et al., 2001). Special attention is given to biological process since they are generally cost effective and environmentally friendly (Sathiya moorthi et al., 2007).

A wide variety of microorganisms, including some bacteria, fungi and algae are capable of decolorizing a wide range of dyes (Fu and Viraraghavan, 2009). Among the microorganisms tested, white-rot fungi (WRF) were found to be able to degrade various recalcitrant pollutants, including different types of dyes, through their highly oxidative and non-specific ligninolytic enzymes (Ozfer et al., 2003, Blázquez et al., 2004, Prachi and Anushree, 2009, Anastasi et al., 2010). Two major strategies have been developed for use of white-rot fungi for degradation of pollutants (Borras et al., 2008). One is the treatment with enzymes, such as laccases, manganese peroxidases and lignin peroxidases, either in purified form or using broths from fungi cultures (Pant and Adholeya, 2009). The other strategy is direct degradation of pollutants using active cultures of fungi. A fungus capable of decolorizing one dye may have different capacities for other dyes (Wesenberg et al., 2003, Fu and Viraraghavan, 2009).

The main objective of this work was to assess the potential of three common WRF (*Trametes versicolor*, *Ganoderma lucidum* and *Irpex lacteus*) to decolourize a

commercial tannery dye, Black Dycem TTO. To our knowledge, no reports have been devoted to the degradation of this dye by WRF. Moreover, the Black Dycem TTO containing wastewater poses a serious industrial problem since there is at present, no process technically and economically acceptable for dye's removal.

The decolorization efficiency of the three strains was investigated in primary screening on a solid medium (Petri dishes). A secondary screening was conducted in aqueous medium in Erlenmeyer flasks. To assess the potential of the best strain selected from the previous experiments, decolorization tests were performed in single and repeated batches in an air-pulsed bioreactor. Fungal pellets formed during the first batch were retained for repeated-batch mode. The repeated batch process maintains the activity of the pellets for a long period of time and may achieve better results, in comparison to batch cultivation (Birhanli and Yesilada, 2006). Finally, enzyme assays were performed to elucidate the enzymatic system involved in the degradation process.

## **2. Materials and methods**

### **2.1. Microorganisms**

The strain *T. versicolor* 42530 was acquired from the American Type Culture Collection (ATCC). *G. lucidum* (Leysser) Karsten FP-58537-Sp was provided by the US Department of Agriculture Forest Products Laboratory, Madison, Wis. *I. lacteus* (AX1) was isolated from agricultural soils at the Long Term Ecological Research site at Michigan State University. *G. lucidum* and *I. lacteus* were a gift from Dr. C. A. Reddy (Michigan State University). All fungi were maintained on 2% malt extract agar slants at 25 °C until use. Subcultures were routinely made.

### **2.2. Chemicals**

Black Dycem TTO is a commercial patented dye that is, extensively used in a tannery industry located in Sfax, Tunisia. It is supplied to this factory by "Colorantes Industriales, S.A" (Barcelona, Spain). According to its technical specifications, the black, water soluble dye, is not rapidly biodegraded, and the effluent containing this dye must be recycled. It is classified as an acid dye, the principal chemical classes of which are azo, anthraquinone, triphenylmethane, azine, xanthene, nitro and nitroso (Gupta and Suhas, 2004).

The maximum absorption wavelength of the dye (462 nm) was obtained by scanning an aqueous solution of dye over the visible range. All other chemicals used were of analytical grade.

### **2.3. Culture methods**

A mycelial suspension of each fungus was obtained by inoculation of four 1 cm diameter plugs, from the fungus growing zone on 2% malt agar, in a 500 mL Erlenmeyer flask containing 150 mL of 2% (w/v) malt extract medium. This was incubated at 25 °C under orbital agitation (135 rpm, r = 25 mm). After 4–5 days, a dense mycelial mass was formed. It was separated from the culture medium, resuspended in an equal volume of a sterile saline solution (0.85% (w/v) NaCl) and then disrupted with an X10/20 homogenizer (Ystral GmbH). The resulting mycelial suspension was stored at 4 °C until use. The suspension was used to obtain fungal pellets by inoculating 1 mL of the suspension in 250 mL malt extract medium (2%) (adjusted to pH 4.5) in a 1 L Erlenmeyer flask. The flask was incubated in an orbital shaker (135 rpm, r = 25mm) at 25 °C for 5–6 days. The pellets thus obtained can be stored in sterilized saline solution (0.85% NaCl) at 4 °C, where they will remain active for up to 2 months without losing their morphology (Blázquez et al., 2004).

### **2.4. Decolorization tests**

#### **2.4.1. Decolorization on Petri dishes**

The three WRF: *T. versicolor*, *I. lacteus* and *G. lucidum*, were subjected to a primary screening based on the ability of each fungus to remove the dye. The experiments were performed on solid medium plates containing 20 g malt extract (ME), 15 g agar and 50 mg of the target dye Black Dycem TTO per liter. The medium was autoclaved and poured into Petri dishes. Plates were then inoculated with 1 cm diameter plugs, cut from the growing zone of the fungi, and incubated at 25 °C for 10 days. Uninoculated plates served as controls for abiotic decolorization. The experiments were performed in duplicate for each culture.

### 2.4.2. Decolorization tests in Erlenmeyer flasks

The decolorization tests were performed out in 0.5 L Erlenmeyer flasks filled with 100 mL of medium. Two different liquid media were employed to select the most appropriate one for the dye decolorization: defined medium (DM) and malt extract medium (ME). The DM contained 8 g glucose, 1.9 g NH<sub>4</sub>Cl, 1.168 g 2,2-dimethylsuccinate (DMS) buffer, 10 mL macronutrients solution (20 g KH<sub>2</sub>PO<sub>4</sub>, 5 g MgSO<sub>4</sub>·7H<sub>2</sub>O, 1 g CaCl<sub>2</sub> per liter) and 1 mL micronutrients solution (1.5 g nitrilo triacetic acid, 3.0 g MgSO<sub>4</sub>·7H<sub>2</sub>O, 0.5 g MnSO<sub>4</sub>·H<sub>2</sub>O, 1.0 g NaCl, 0.1 g FeSO<sub>4</sub>·7H<sub>2</sub>O, 0.1 g CoSO<sub>4</sub>, 0.1 g ZnSO<sub>4</sub>·7H<sub>2</sub>O, 0.1 g CaCl<sub>2</sub>·2H<sub>2</sub>O, 0.01 g CuSO<sub>4</sub>·5H<sub>2</sub>O, 0.01 g AlK(SO<sub>4</sub>)<sub>2</sub>·12H<sub>2</sub>O, 0.01 g H<sub>3</sub>BO<sub>3</sub>, 0.01 g NaMoO<sub>4</sub> per liter) and 10 mg thiamine per liter. The ME contained 20 g L<sup>-1</sup> malt extract (Sharlau, Barcelona, Spain).

Dyestuff (150 mg L<sup>-1</sup>) was added to each medium and the pH was adjusted to 4.5. The flasks were inoculated with 1 mL of mycelium of the three mentioned white-rot fungi and were maintained at 25 °C under orbital agitation (135 rpm, r=25mm) for 8 days.

All the treatments were done in triplicate.

### 2.4.3. Single batch decolorization in an air-pulsed bioreactor

A glass air-pulsed bioreactor, with a working volume of 1500 mL, was used for the decolorization process. The air-pulse frequency was 0.16 s<sup>-1</sup>, allowing fluidization and liquid phase homogenization of the biomass. The bioreactor was equipped with a pH controller in order to maintain the pH at 4.5 and the temperature was maintained at 25 °C (Figure 1) (Blázquez et al., 2004). The growth medium (GM) proposed by Borrás et al. (2008) for fungal pellet production was used. It contained 7 g glucose, 2.1 g NH<sub>4</sub>Cl, 10 mg thiamine, 100 mL macronutrients solution and 10 mL micronutrients solution per liter. The dye was added to the GM at a concentration of 150 mg L<sup>-1</sup>. The pH was adjusted to 4.5 and the temperature was maintained at 25 °C. The bioreactor was inoculated with 5mL of the mycelial suspension of *T. versicolor* per liter of medium.



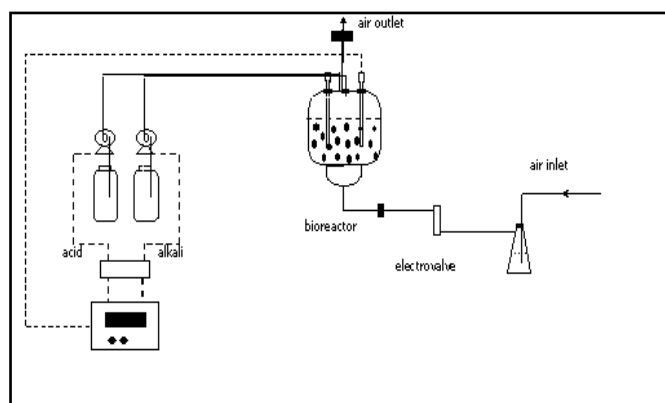


**Figure 1:** Scheme of the lab-scale bioreactor (1.5 L)

#### **2.4.4. Repeated batch decolorization tests in an air-pulsed bioreactor**

Repeated-batch operations were performed to assess the long-term activity of the fungus *T. versicolor* in tannery dye removal. The experiment started with a normal batch containing the same GM described previously. After a 4-day start-up period, the medium was exchanged for a fresh medium (FM) limited by nitrogen, and the same pellets formed during the first batch, were used 3 times in the subsequent batches. The FM contained 150 mg of the dye, 10 mL macronutrients solution and 1 mL micronutrients solution per liter. The ammonium chloride concentration in the FM was limited to  $8.13 \text{ mg L}^{-1}$  in order to avoid fungal growth. The glucose was fed continuously at a specified uptake rate ( $0.09 \text{ g (g}^{-1} \text{ DW d}^{-1})$ ) from a concentrated solution ( $150 \text{ g L}^{-1}$ ).

#### **2.4.5. Enzyme assays and cytochrome P450 inhibition experiment**

To elucidate the enzymatic system involved in the dye decolourization process, several experiments were performed.

A commercial laccase decolorization experiment was conducted in a 100 mL Erlenmeyer flask using a purified laccase of *T. versicolor* from Sigma Aldrich. A volume of 50 mL of the dye solution, with a concentration of  $300 \text{ mg L}^{-1}$ , was added to 50 mL of laccase solution at a final measured enzyme activity of  $68.31 \text{ AU} \cdot \text{L}^{-1}$ . The Erlenmeyer flask was placed in an orbital shaker at  $25 \text{ }^\circ\text{C}$ . The dye concentration and the enzyme activity were measured over 96 h. Un-inoculated media served as controls for abiotic decolorization.

The effect of the most commonly used mediators, 2,2-azino-bis-(3-ethylbenzthiazoline-6-sulfonic acid) diammonium salt (ABTS) and hydrate 1-hydroxy-benzotriazol (HOBT), on the laccase activity was tested. Each mediator was added to the above solution (containing dye and commercial laccase) to a final concentration of 1 mM. The Erlenmeyer flasks were incubated in an orbital shaker (135 rpm) at 25 °C for 24 h.

Repeated batch experiments in Erlenmeyer flasks were also performed to study the effect of a cytochrome P 450 inhibitor. The inhibitor, 1-aminobenzotriazole (ABT) was added to a final concentration of 1 mM to 100 mL of defined medium containing 10 g of wet pellet of *T. versicolor* (equivalent to 3.1g L<sup>-1</sup> dry weight). Over 4 days after each 24 h-period, the medium was exchanged for a fresh medium (FM) limited by nitrogen which contained the inhibitor (ABT) and the same pellets. The pellets were kept for 3 times in subsequent batches. The same repeated batch experiments were performed with two types of controls: one without the inhibitor (control (1)) and another using killed fungus (control (2)).

Killed controls consisted of adding 4 mL of toxic sodium azide solution (5g L<sup>-1</sup> NaN<sub>3</sub>) to 100 mL of the medium- containing pellets. The pellets had been pre-grown for 7 days under conditions identical to those of the experimental cultures.

All the repeated batch experiments for the cytochrome P 450 inhibitor were done in triplicate.

## **2.5. Analytical methods**

Visible spectrophotometry at 462 nm was used to determine the dye concentration. A standardization curve was plotted by measuring the absorbances of different dye solutions at the maximum absorption wavelength. Absorbances were measured with a Varian UV/vis Cary spectrophotometer.

Glucose concentrations were measured with a YSI 2700 enzymatic analyzer (Yellow Springs Instruments and Co).

Laccase activity was measured using a modified version (Kaal and De Jong, 1983) of the first step of the method used for the determination of manganese peroxidase (MnP) (Wariishi et al., 1992), where 2,6-dimethoxyphenol (DMP) is oxidized by laccase, even in the absence of a cofactor. One activity unit (AU) was defined as the number of micromoles of DMP oxidized per minute. The DMP extinction coefficient was

24800 M<sup>-1</sup> cm<sup>-1</sup>. The pH determinations were conducted with a Basic 20 pH meter (Crison, Barcelona, Spain). The dry weight of pellets was determined after vacuum filtration through reweighed glass microfiber filters (Whatman GF/A, 47 mm diameter) and drying at 105 °C to a constant weight. The results are the mean of reactions performed at least in duplicates.

A Microtox system from Microbics Corporation was used. The assay is based on the percentage of decrease in the amount of light emitted by the bioluminescent marine bacterium *Vibrio fischeri* upon contact with the sample. Toxicity is inversely proportional to the intensity of light emitted after contact with the toxic substances. The effective concentration, EC<sub>50</sub>, is defined as the concentration that produces a 50% light reduction. The EC<sub>50</sub> was measured after 5 and 15 min of contact time. A color correction was done according to the Microtox instructions. To obtain 50% inhibition, the fractions were diluted wherever necessary with purified water containing 2% NaCl. This diluent was also used as a non-toxic control. Effluent toxicity is expressed in units of EC<sub>50</sub>.

All experiments in Erlenmeyer flasks were performed in triplicate and mean values are presented. Calculation of average values and analyses of standard deviations (represented as error bars) were performed using Excel 2007. Analysis of variance (ANOVA) was used to evaluate the effect of the cytochrome P-450 inhibitor (ABT) on the decolorization. Data were analyzed using SPSS (17) for Windows.

### **3. Results and discussion**

#### **3.1. Primary screening on Petri dishes**

Initial evaluation of the capability of the three fungi to decolorize the tannery dye, Black Dycem TTO, was performed on solid medium plates. The result showed by visual inspection that all of the three fungi tested are capable of removing the dye. However, *T. versicolor* displayed the greatest decolorization ability both in terms of extent and rapidity of decolorization. By day 4, decolorization began with the formation of a clear zone around the colonies. After a 10-day period, the dye was almost completely decolorized by *T. versicolor*, while faintly decolorized by *I. lacteus* and *G. lucidum*. It should be noted that some authors have also shown the capabilities of *T. versicolor* to degrade anthraquinone dyes including acid green (Knapp et al., 1995), azo dyes including Amaranth (Swamy and Ramsay, 1999), synthetic dyes including reactive

violet (Lucas et al., 2008) and metal complex dyes including Lanaset Grey G (Blázquez et al., 2008). To simultaneously confirm and determine the efficiency of the dye decolorization by the three fungi quantitatively, a secondary screening was conducted in Erlenmeyer flasks.

### 3.2. Secondary screening in liquid systems

The performances of fungi in the decolorization of the tannery dye were evaluated in two liquid media: ME and DM. The initial pH was 4.5. The results showed that the three tested fungi were able to grow under the reaction conditions and to decolorize the dye. In ME after 2 days, the decolorization level was greater than 90% in all cases (Figure 2A). In DM, *T. versicolor* was observed to have the most rapid dye decolorization of the fungi tested. About 94% of the dye was decolorized during 48 h. However, the yields of dye decolorization observed over the same period for *I. lacteus* and *G. lucidum* were 76% and 90%, respectively (Figure 2B).

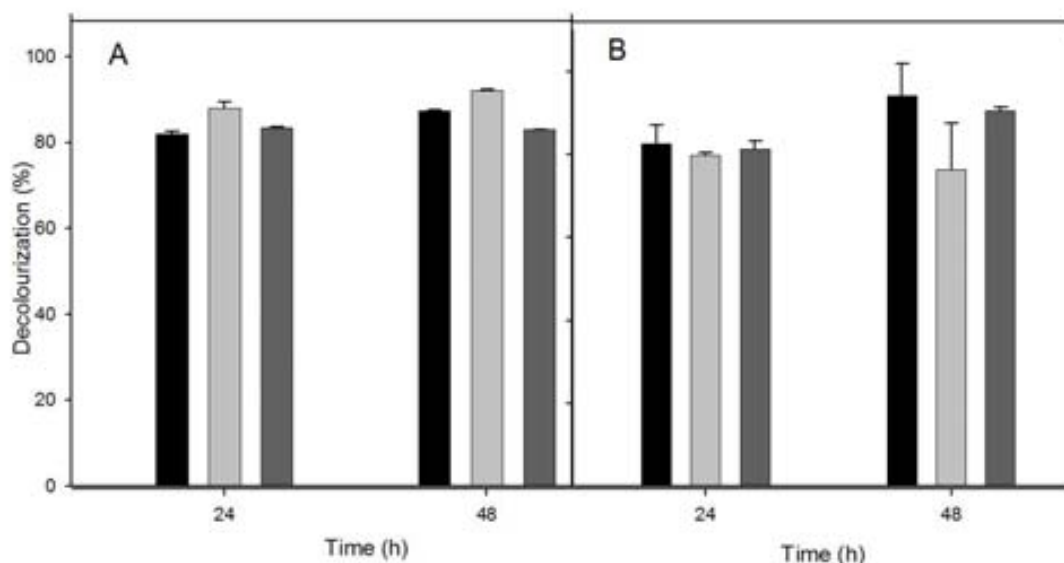


**Figure 2:** Decolourization of the dye Black Dycem TTO by white-rot fungi: *T.versicolor* (■), *I. lacteus* (□) and *G. lucidum* (▒) in ME (A) and DM (B)

Although succinic acid was used as a buffer in DM, the broth pH decreases up to pellet growth inhibition level, while in ME the pH variation was less dramatic for the three fungi (pH ranging from 2.44 to 3.42 and from 3.92 to 4.12 for DM and ME,

respectively). Jang et al. (2002) reported a pH of 4.5 as the optimal value for the growth and laccase production activity of *T. versicolor*.

Results obtained in the Erlenmeyer flasks experiments also showed that *T. versicolor* was able to reach very high decolorizing level (95%) even with a very low biomass level (0.92 g dry weight·L<sup>-1</sup>). This means the fungus has a high specific degradation level with DM. In addition to this advantage, the cost of DM is significantly lower than ME (Borras et al., 2008).

Taking into account the above results, DM and *T. versicolor* were used in the subsequent experimental work, and experiments were conducted in a laboratory scale bioreactor with a pH controller in order to avoid pH inhibitory effects on fungal growth.

### 3.3. Single batch decolorization in an air-pulsed bioreactor by *T. versicolor*

The pH value of the aqueous medium was automatically adjusted at 4.5 with 1 M NaOH solution, during the course time of the experiment.

Figure 3 shows the results obtained in the fluidized bioreactor inoculated with mycelium of *T. versicolor*. After 24 h, the decolorization level was only 60%, but reached 97% at 96 h (the end of the experiment) when the biomass of the formed pellets was 2.26 g·dry weight L<sup>-1</sup>. As seen in Figure 3, glucose measurements displayed prominently that it was exhausted after 96 h. Moreover, low levels of extracellular laccase were observed during the treatment and the maximum activity (28 AU L<sup>-1</sup>) was measured at the end of the experiment.

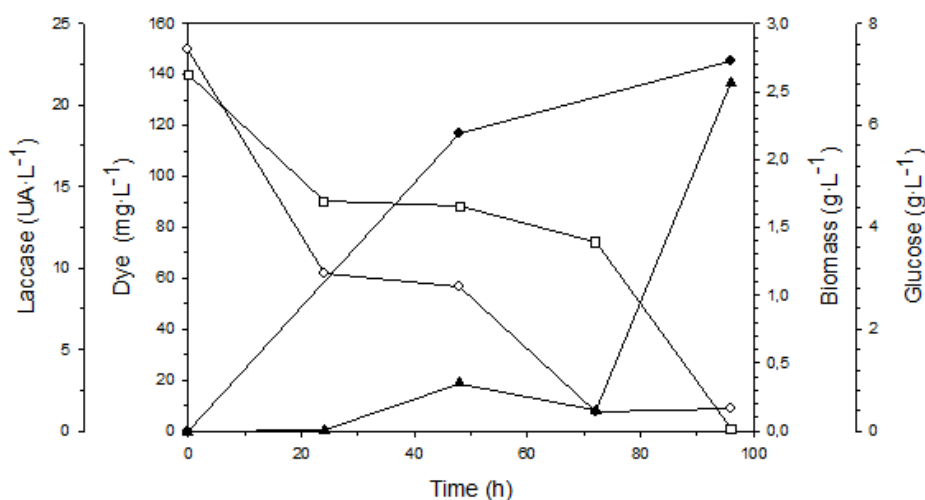


**Figure 3:** Time course of dye (◇), biomass (◆) and glucose (◻) concentrations and laccase activity (▲) in the bioreactor inoculated with mycelium of *T. versicolor*.

In addition, a toxicity test was performed by measuring the  $EC_{50}$ , where the solution is considered toxic when its value is lower than 3%. The initial synthetic dye solution has an  $EC_{50}$  of  $22\% \pm 1\%$ , which is recalculated to  $124\% \pm 62\%$  when the color correction is applied, while the fungal decolorized solution has an  $EC_{50}$  of  $33\% \pm 5\%$ , where no color correction is required. So neither the initial solution nor the treated solution are toxic.

To investigate the decolorization potential of the fungus more fully, batch multistage tests were undertaken.

### **3.4. Repeated batch experiments**

The longevity of *T. versicolor* decolorization activity was investigated in a repeated batch reactor. The experiment was initiated under the same conditions described for the single batch previously. After a 4-day period (first batch), the aqueous solution was drawn and a growth-limited medium was refilled. This medium limited the growth because of low nitrogen content. The pellet biomass obtained during the first batch was kept for the three subsequent batches. The duration of each latter batch was approximately 36 hours. The dye concentration and the laccase level were analyzed over the course of the experiment (Figure 4). During the first batch, the laccase activity reached its maximum value ( $70 \text{ AU L}^{-1}$ ). However, low enzyme activities were detected during subsequent batches. Although low enzyme activity was detected, the decolorization capability of the fungus did not decrease significantly and *T. versicolor* was able to remove 86–89% of the Black Dycem TTO dye over the three batches. This implies that the biodegradation mechanism seems to play an important role in the decolorization process of the dye, in addition to an adsorption phenomenon occurring on the surface of the pellets. Otherwise, the biomass would be saturated by dye adsorption and consequently no new dye removal could occur. The ability of the fungus to survive and to decolorize during three sequential batches at relatively high dye concentration (150 ppm) is an adaptive feature that makes it a promising candidate for wastewater treatment.

Returning to the laccase activity observed during the repeated batches, our results agree with those of Blázquez et al. (2004) who showed that only low enzyme activity is probably necessary to catalyze the decolorization of a dye solution. These authors,

Blázquez et al. (2004) have also observed that no direct relationship between laccase activity and the decolorization rate exists.

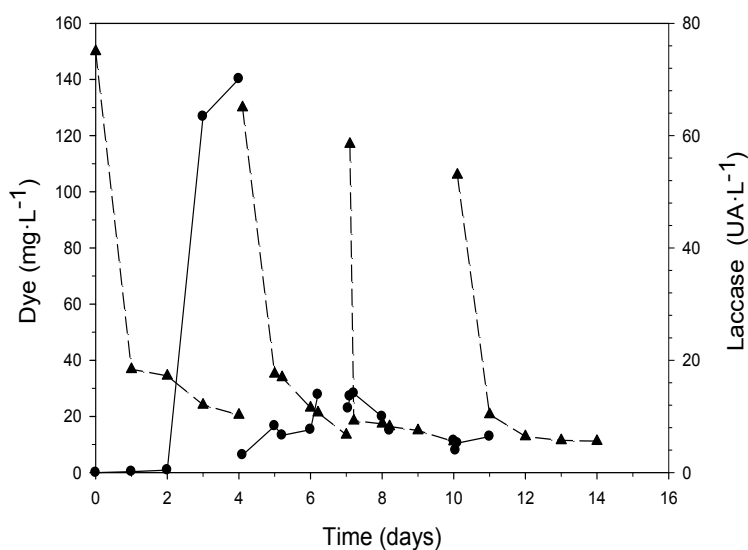


**Figure 4:** Dye concentration ( $\blacktriangle$ ) and laccase activity ( $\bullet$ ) during the repeated-batch experiment

Data of a typical time-dependent visible spectrum of the dye solution during the first 4 days of the repeated batch process showed that the dye's main absorbance peak at  $\lambda = 462$  nm disappeared within approximately 24 h, followed by an insignificant change for the next 72 h. These results, confirmed that the fungus was efficacious in decolorization of the studied tannery dye and demonstrated the speed of the removal process. The absorbance spectrum of the dye at the end of experiment is different from the initial one. Moreover, the pellets, that were dark in the first few hours of the treatment (owing to adsorption phenomenon), became quite discolored at the end of the experiment. These findings indicated that the overall color removal by *T. versicolor* is due to two mechanisms: adsorption and biodegradation. Consequently, further investigations on the enzymatic activities involved in the dye biodegradation process are necessary.

### 3.5. Enzyme assays and cytochrome P450 inhibition experiment

The relative contribution of enzymes to the decolorization of dyes may be different for each fungus. *T. versicolor* releases laccase as its major extracellular enzyme (Fu and Viraraghavan, 2009), which is able to catalyze the oxidation of a variety of organic substances coupled to the reduction of molecular oxygen. Furthermore, the presence of

redox mediators enhances the range and the rates of compounds to be oxidized (including recalcitrant dyes) by the so-called laccase–mediator systems (LMS) (Cristóvão et al., 2009). Intracellular systems, that are generally present in most fungi, such as cytochrome P 450 monooxygenase, may also be involved in dye decolorization. Several experiments were conducted to determine whether laccase or cytochrome P450 were involved in the decolorization of the tannery dye studied.

Preliminary results related to the treatment of the dye treated with a commercial laccase from *T. versicolor* had shown that pure laccase did not decolorize the dye. These results indicated that the presence of a mediator is required or another enzymatic system may be involved in the decolorization process. It should be noted that some reports have also shown that laccase alone does not decolorize some types of textile dyes (Kandelbauer et al., 2004, Rodríguez, et al., 1999). However, no decolorization was observed in the abiotic control. This means that there were not interferences of physical phenomenon in the decolorization of the dye.

Various fungal metabolites such as 2,2-azino-bis-(3-ethylbenzthiazoline-6-sulfonic acid) diammonium salt (ABTS) and hydrate 1-hydroxy-benzotriazol (HOBT), are known to act as mediators for laccase and to enhance pollutant degradation (Asgher et al., 2008). The effect of these two mediators was examined here. The results showed remarkable differences in their abilities to enhance dye decolorization. In the presence of ABTS, no decolorization was observed. Conversely, when using HOBT, the percentage of decolorization reached 65%, indicating that both laccase and HOBT are involved in the degradation of the tannery dye. This great difference in the activity of mediators, on dye decolorization, agrees with the findings of Li et al. (1999). These authors argue that if one laccase mediator is more effective than another with a particulate substrate, this does not necessarily mean that the same order of effectiveness would remain with other laccases because the reaction depends on both laccase and mediator, and the combination thereof (Nyanhongo et al., 2002).

The results related to the repeated Erlenmeyer batches with the inhibitor of cytochrome P450 and the two corresponding controls are shown in Figure 5. Over the course of the experiment, the cytochrome P 450 inhibitor (ABT) did not affect the effectiveness of the decolorization process because the fungus presents the same percentages of decolorization as the control (1) (without inhibitor) during the three batches ( $P > 0.05$  ( $P$



= 0.801)). This result suggests that the enzyme cytochrome P 450 is not involved in degradation of this tannery dye.

Figure 5 shows a significant difference ( $P < 0.05$  ( $P = 0.000$ )) in decolorization percentages observed with living fungus in absence of inhibitor (control (1)) and with killed fungus (control (2)). The killed fungus presented lower color removal (59%) than the living cells (82%) during the first 24 h and during the three sequential batches. Since the only mechanism for dead cells is biosorption (Fu and Viraraghavan, 2009), the higher color removal observed for living cells can be explained only by the intervention of two mechanisms: biosorption and enzymatic degradation.

Killed fungus presented appreciable color removal during the first 24 h and continued to decolorize during the subsequent batches, but with gradually decreasing capacities. This great capacity for decolorization may be due to the increased surface area of killed fungi, resulting from cell rupture upon death. Similar results were reported by Fu and Viraraghavan (2009) when they compared living and dead cells, suggesting that dead cells served as an effective biosorbent.

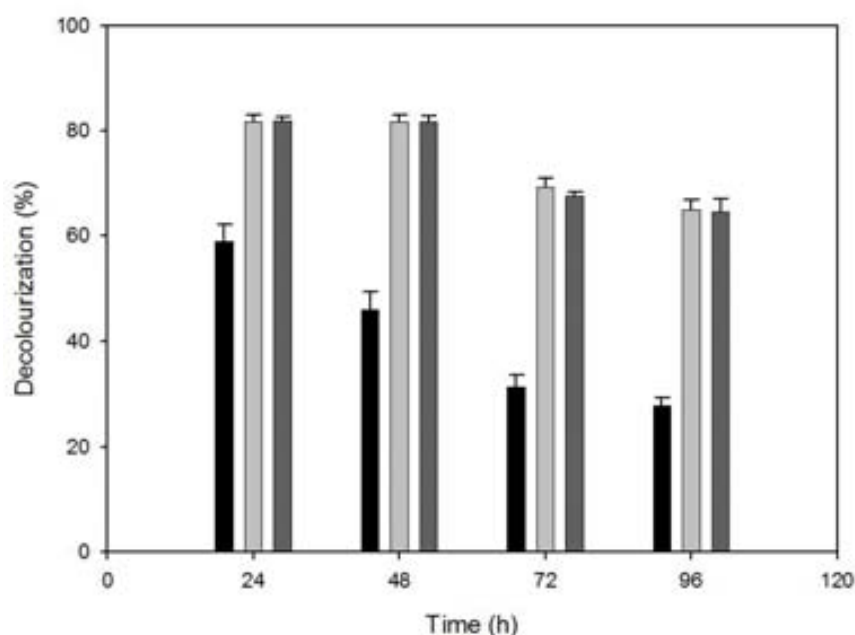


**Figure 5:** Decolourization of the dye Black Dycem TTO by white-rot fungus *T.versicolor* in repeated batch experiment in the presence of cytochrome P450 inhibitor ABT (■), in the absence of the inhibitor (control (1)) (■) and with killed fungus ((control (2)) (■)).

## **Conclusion**

In this study, the ability of three white-rot fungi to remove a tannery dye was evaluated. The wide range of experiments performed provided evidence of the following:

- the fungus *T. versicolor* displayed the greatest decolorization ability both in terms of extent and rapidity of decolorization on Petri dishes and in Erlenmeyer flasks;
- the decolorization rate of the fungus did not decrease during the sequential batches in the bioreactor, and *T. versicolor* continues to remove the Black Dycem TTO dye over three sequential batches, although a low enzyme activity was detected;
- the overall color removal by *T. versicolor* is due to two mechanisms: adsorption and biodegradation;
- the extracellular enzyme laccase is involved in the decolorization process but a mediator is required. However, the intracellular enzyme cytochrome P 450 is not involved in the studied tannery dye degradation;
- the appreciable color removal observed by dead cells suggested their use as an effective biosorbent.

According to these results, the fungus seems to be highly promising for development of effective bioremediation processes for tannery dye decolorization. This study strengthens the prospects of the strain to be developed for industrial scale processes for the treatment of tannery dyes.

## **5. REFERENCES**

- Anastasi A., Spina F., Prigione V., Tigini V., Giansanti P., Varese G.C., 2010. Scale-up of a bioprocess for textile wastewater treatment using *Bjerkandera adusta*. *Bioresour. Technol.* 101, 3067-3075.
- Asgher M., Bhatti H.N., Ashraf M., Legge R.L., 2008. Recent developments in biodegradation of industrial pollutants by white rot fungi and their enzyme system. *Biodegradation.* 19, 771-783.
- Birhanli E., Yesilada O., 2006. Increased production of laccase by pellets of *Funalia trogii* ATCC 200800 and *Trametes versicolor* ATCC 200801 in repeated-batch mode. *Enzyme. Microb. Technol.* 39, 1286-1293.

- Blánquez P., Casas N., Font X., Gabarrell X., Sarrà M., Caminal G., Vicent T., 2004. Mechanism of textile metal dye biotransformation by *Trametes versicolor*. *Water Res.* 38, 2166-2172.
- Blánquez P., Sarrà M., Vicent T., 2008. Development of a continuous process to adapt the textile wastewater treatment by fungi to industrial conditions. *Process Biochem.* 43, 1-7.
- Borras E., Blánquez P., Sarrà M., Caminal G., Vicent T., 2008. *Trametes versicolor* pellets production: low-cost medium and scale-up. *Biochem. Eng. J.* 42, 61–66.
- Cristóvão O. R., Tavares A. P.M., Ferreira L. A., Loureiro J.M., Boaventura R.A.R., Macedo E. A., 2009. Modeling the discoloration of a mixture of reactive textile dyes by commercial laccase. *Bioresour. Technol.* 100, 1094-1099.
- Fu Y., T. Viraraghavan, Fungal decolorization of dye wastewaters: a review. *Bioresour. Technol.* 79 (2001) 251-262.
- Gupta V.K., Suhas, 2009. Applications of low-cost adsorbents for dye removal- A review. *J. Environ. Manage.* 90, 2313-2342.
- Jang M.Y., Ryu W.R., Cho M.H., 2002. Laccase production from repeated batch cultures using free mycelia of *Trametes sp.* *Enzyme Microb. Technol.* 30, 741-746.
- Kaal E.E.J., De Jong E., Field J.A., 1993. Stimulation of ligninolytic peroxidase activity by nitrogen nutrients in the white rot fungus *Bjerkandera sp.* Strain BOS55. *Appl. Environ. Microb.* 59, 4031–4036.
- Kandelbauer A., Maute O., Kessler R.W., Erlacher A., Gubitz G.M., 2004. Study of dye decolorization in an immobilized laccase enzyme-reactor using online spectroscopy. *Biotechnol. Bioeng.* 87, 552–563.
- Knapp J.S., Newby P.S., Reece L.P., 1995. Decolorization of dyes by wood rotting basidiomycete fungi. *Enzyme Microb. Technol.* 17, 664–668.
- Li K., Xu F., Eriksson K.E.L., 1999. Comparison of fungal laccases and redox mediators in oxidation of a nonphenolic lignin model compound. *Appl. Environ. Microb.* 65, 2654-2660.
- Lucas M., Mertens V., Corbisier A.M., Vanhulle S., 2008. Synthetic dyes decolourisation by white-rot fungi: development of original microtitre plate method and screening. *Enzyme Microb. Technol.* 42, 97-106.

- Nyanhongo G.S., Gomes J., Ubitz G.M.G., Zvauya R., Readd J., Steiner W., 2002. Decolorization of textile dyes by laccases from a newly isolated strain of *Trametes modesta*. *Water Res.* 36, 1449-1456.
- Ozfer Y., Dilek A., Cing S., 2003. Decolorization of textile dyes by fungal pellets. *Process. Biochem.* 38, 933-938.
- Pant D., Adholeya A., 2009. Concentration of fungal ligninolytic enzymes produced during solid-state fermentation by ultrafiltration. *World J. Microb. Biotechnol.* 25, 1793-1800.
- Pant D., Singh A., Satyawali Y Gupta., R. K., 2008. Effect of carbon and nitrogen source amendment on synthetic dyes decolourizing efficiency of white-rot fungus, *Phanerochaete chrysosporium*. *J. Environ. Biol.* 29, 79-84.
- Paschoal F.M.M., Anderson M.A., Zanoni M.V.B., 2009. Simultaneous removal of chromium and leather dye from simulated tannery effluent by photoelectrochemistry. *J. Hazard. Mater.* 166, 531-537.
- Prachi K., Anushree M., 2009. Fungal dye decolourization: recent advances and future potential. *Environ. Int.* 35, 127-141.
- Robinson T., McMullan G., Marchant R., Nigam P., 2001. Remediation of dyes in textile effluent: a critical review on current treatment technologies with a proposed alternative. *Bioresour. Technol.* 77, 247-255.
- Rodríguez E., M.A. Pickard, R. Vazquez- Duhalt, 1999. Industrial dye decolorization by laccases from ligninolytic fungi. *Curr. Microbiol.* 38, 27-32.
- Sathiya moorthi P., Periyar selvam S., Sasikalaveni A., Murugesan K., Kalaichelvan P.T., 2007. Decolorization of textile dyes and their effluents using white rot fungi. *Afr. J. Biotechnol.* 6, 424-429.
- Swamy J., Ramsay J.A., 1999. Effects of glucose and NH<sub>4</sub> concentrations on sequential dye decoloration by *Trametes versicolor*. *Enzyme Microb. Technol.* 25, 278-284.
- Wariishi H., Valli K., Gold M.H., 1992. Manganese (II) oxidation by manganese peroxidase from the basidiomycete *Phanerochaete chrysosporium*. *J. Biol. Chem.* 267, 23688-23695.
- Wesenberg D., Kyriakides I., Agathos S.N., 2003. White-rot fungi and their enzymes for the treatment of industrial dye effluents. *Biotechnol. Adv.* 47, 161-187.

## **Chapter 5:**

### General conclusions and suggestions for further research

---

This chapter summarizes the general conclusions drawn from this dissertation and presents some suggestions for future research.

## **5.1. GENERAL CONCLUSIONS**

Based on the results obtained within the framework of this study, it appears that the two-applied processes -adsorption on activated carbon prepared from the by-product olive-waste cakes and the biological treatment using white-rot fungi- demonstrated their effectiveness for the removal of the target contaminants in the studied conditions. Through the research study, the main conclusions that can be drawn from the current investigation are given below:

- Concerning the adsorption process, the results showed that olive-waste cakes may constitute a suitable precursor for the manufacture of a powerful activated carbon through chemical activation with phosphoric acid. The most efficient activated carbon is that obtained under the following optimal conditions: an acid concentration equal to 60%  $\text{H}_3\text{PO}_4$ , an impregnation ratio of 1.75, and a pyrolysis temperature of 450 °C. The adsorption characteristics of the prepared adsorbent under these conditions compare well, and sometimes more favorably than the previously reports for activated carbon in literature.
- The study of the environmental impact assessment of activated carbon preparation via life cycle assessment tool, demonstrated that the impregnation step presented the highest environmental impact and that the total cumulative energy demand was shared equally between the steps involving impregnation, drying the washed AC and pyrolysis. Certain modifications could entail a reduction on the environmental impact if they are incorporated into the production system of AC, such as gas recovery derived from the pyrolysis step for reuse as an energy source and recovery of phosphoric acid after AC washing.
- Column adsorption tests showed the high capacity of the activated carbon to reduce  $\text{KMnO}_4$  into insoluble manganese (IV) oxide ( $\text{MnO}_2$ ) which impregnated the sorbent surface. Adsorption experiments of copper on column, through treated and untreated activated carbon bed with  $\text{KMnO}_4$ , reveal that the capacity

for copper sorption was enhanced by a factor of up to 3 after modification of the produced activated carbon by permanganate treatment under specified conditions.

- The prepared adsorbent was also shown to be effective in removing organic pollutants especially textile and tannery dyes from individual and real effluents and emerging contaminants such as pharmaceuticals from single and mixture solutions. Moreover, the adsorption capacity of the adsorbent towards the dyes compares well those of other sorbents prepared from agricultural wastes and even better than the commercial granular AC “CAL” from Chemviron Carbon towards the metal complex dye Lanaset grey G dye. Concerning the pharmaceuticals, the adsorption test demonstrates that the uptake of the four drugs studied was quite different and that large quantity of drugs was adsorbed in the mixture.
- Several isotherm and kinetic models were employed to understand the sorption behavior and in the most cases Langmuir and pseudo-second models present the best fit except for the adsorption textile dye in which the kinetics studies follow the pseudo-first kinetic model. The effect of pH and temperature on the adsorption process shows that these parameters react differently towards the dyes and the pharmaceuticals. Indeed, pH variation doesn't affect the adsorption of the textile and tannery dyes. However, its variation should be considered in the removal of the studied drugs. On the contrary, the temperature influences the adsorption of dyes though no effect is noticed on the drugs uptake.
- For the biological treatment, the ability of three white-rot fungi: *Trametes versicolor*, *Ganoderma lucidum* and *Irpex lacteus*, to remove a tannery dye was evaluated. After a primary (on Petri dishes) and a secondary (in Erlenmeyer's scale) screenings, the results demonstrate that the fungus *Trametes versicolor* displayed the greatest decolorization ability, both in terms of extent and rapidity.
- Decolorization tests performed using the best strain *Trametes versicolor*, retained from the previous experiments, in single and repeated batches in an air-

pulsed bioreactor with biomass reuse, show high efficiency of this fungus to remove the tannery dye. The overall color removal by *T. versicolor* is due to two mechanisms: the adsorption and biodegradation involved by the extracellular enzyme laccase.

In general and according to these conclusions both processes: the production of an activated carbon from olive-waste cake seems to be an interesting alternative to valorize this agro-waste where is produced in large amounts especially in the Southern and Easter Mediterranean countries and the fungus *Trametes versicolor* seems to be highly promising for development of effective bioremediation processes for recalcitrant removal.

However, the results presented in Annex 1, concerning the combination of the two processes using first the biological treatment followed by adsorption on the prepared activated carbon for the removal of an effluent containing the textile metal complex dye: Grey Lanaset G, show lower capacities of adsorption of Cr and Co which led to think about the modification of the AC in order to ameliorate its adsorption capacity towards these metals species like the case of copper.

## **5.2. SUGGESTIONS FOR FUTURE RESEARCH**

The following recommendations are proposed for future work that could be undertaken and could give more knowledge about the dissertation:

- Focusing on the full scale implementations, the preparation of activated carbon may be scaled up from laboratory to pilot plant while considering the suggestions proposed in the life cycle assessment study.
- It will be interesting to do an economic analysis determining the cost of preparation of activated carbon from the by-product olive waste cakes in order to have a complete idea about this adsorbent.
- Desorption and regeneration of the activated carbon so that it could be reused saving cost and avoiding environmental problem with its disposal.



- Further studies are needed to improve the results related to the combination of the two studied processes. Using adsorption followed by desorption and biological treatment of the desorbed solution could be a good solution for the removal of emerging contaminants, such as drugs, found in low concentrations in real effluents. It would be also interesting to operate in continuous operation.



## **Annexes:**

---

Annexed information presented some unpublished results and provides some useful supporting information. In the annexed information A 1, the results related to a tentative of combination of the two studied processes: the biological treatment and the adsorption on activated carbon to remove a metal complex dye are presented. Annexes A.2 and A.3 present the technical specifications of the dyes Lanaset grey G and Black dycem TTO, respectively.

### **A.1. Metal complex dye degradation by the fungus *Trametes versicolor* followed by metal adsorption with a low cost activated carbon derived from Tunisian olive-waste cakes**

*Presented in the international congress first IMAW (International Association of Mediterranean Agro-industrial Waste) International Symposium "Agro-industrial by-products: waste or resource" in ECOMONDO Rimini-Italy.*

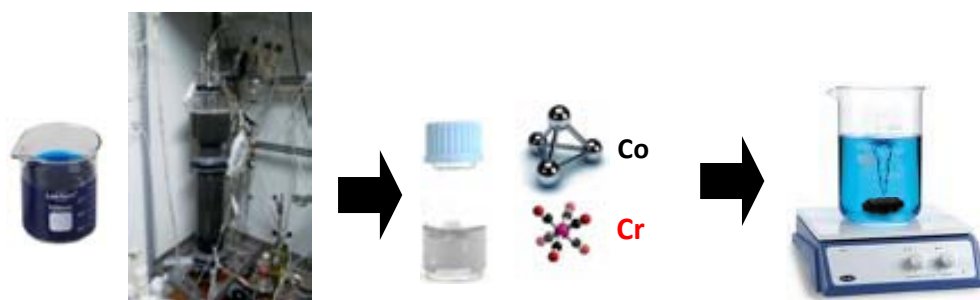
### **A.2. Technical specifications of the textile dye Lanaset grey G**

### **A.3. Technical specifications of the tannery dye Black dycem TTO**

### **A.1. Metal complex dye degradation by the fungus *Trametes versicolor* followed by metal adsorption with a low cost activated carbon derived from Tunisian olive-waste cakes**

---

The last issue of the present doctoral consists of the development of a combined biological and physico-chemical process to purify a textile effluent. The textile dye, Lanaset grey G, is chosen as a representative of a metal complex dye to carry out this experimentation.



## **Abstract**

The production of activated carbon (AC) from Tunisian olive-waste cakes, a cheap and abundant by-product of the manufacture of olive oil mills, via chemical activation, was studied in this work. The activated carbon was fully characterized considering its adsorption properties as well as its chemical structure and morphology. As application, the adsorption equilibrium of a commercial metal complex dye, Grey Lanaset G, on this activated carbon was determined. The results indicate that the maximum adsorption capacity was  $109 \text{ mg g}^{-1}$ , which is between the adsorption capacities of two commercial granular AC from Chemviron Carbon: Filtrasorb 400 ( $454.54 \text{ mg g}^{-1}$ ) and CAL ( $56.82 \text{ mg g}^{-1}$ ). On the other hand, the metal complex dye was successfully biodegraded in a fluidized pulsed bioreactor with pellets of *Trametes versicolor*. The dye is first adsorbed into the biomass, then degradation occurs resulting to the releasing of the metals into the medium. The results, found from the application of biological treatment followed by the adsorption on the AC show low adsorption capacities of Cr and Co. These, led us to modify the AC in order to ameliorate its capacity of adsorption.

## **1. Introduction**

Textiles industry effluents can damage the environment, if they are discharged directly into the surface waters or into wastewater treatment plant, as they contain dyes with complex and variable chemical structure. Activated carbon (AC) is the most commonly used and most effective adsorbent (Chen et al., 2003). Nevertheless, its application fields are restricted due to its high cost. Natural materials and certain waste products from industries and agricultural operations, which must be available in large quantities, may have potential as inexpensive precursors for activated carbon production. Several suitable agricultural by-products (lignocellulosics) including peach stones (Molina-sabio et al., 1995), date stones (Girgis and El-hendawy, 2002; Haimour and Emeish, 2006), pistachio-nut shells (Yang and Lua, 2006) and grain sorghum (Diao and Walawender, 2002) have been investigated in the last years as activated carbon precursors and are still receiving renewed attention. In comparison, olive-waste cakes received much less consideration as lignocellulosic material for activated carbon production (Cimino et al., 2005; Baçaoui et al., 2001).

---

Olive-waste cakes (olive pomace) is the remaining residue of oil extraction process predominantly produced in the Mediterranean countries. In Tunisia, olive-waste cakes represent a yearly average of  $2 \cdot 10^5$  tons depending on the crop (Sellami et al., 2008). The use of this material as precursor for the preparation of activated carbon produces not only a useful adsorbent for the purification of contaminated environments, but also contributes to minimizing the solid wastes. On the other hand, the research group of “biodegradation of industrial contaminants and waste valorization” (UAB, Barcelona) has developed a biological process for the treatment of dyes using a fluidized pulsed bioreactor filled with pellets of the ligninolytic fungus *Trametes versicolor*.

The results show that the microorganism is capable of degrading several dyes such as Grey Lanaset G which is a mixture of metal complex dyes containing Cr and Co. With the biological treatment the effluent is almost totally decolorized but a high proportion of the metals are released from the dye. So in order to be able to reuse the effluent, the metals must be removed from the medium. The present work has explored the complementarities of two processes the biological treatment in a bioreactor by pellets of *Trametes versicolor* and the physical process of adsorption on activated carbon prepared from Tunisian olive-waste cakes, in order to purify the textile metal complex dye: Grey Lanaset G. The biodegradation of the dye, in batch mode, was evaluated from the results of spectrophotometric color analysis and metal atomic absorption analysis.

Performances of the prepared activated carbon are expressed in terms of some properties, among which: specific surface area, cation-exchange capacity (CEC), bulk density, iodine and methylene blue numbers. Scanning electron microscopy (SEM) was employed to visualize adsorbent morphology. In order to evaluate the adsorption potential of the adsorbent for metal complex dyes, adsorption tests were made by using the commercial mixture Grey Lanaset G as adsorbate. The Langmuir and Freundlich isotherms were used to fit the equilibrium data.

## **2. Materials and methods**

### **2.1. Preparation of activated carbon**

Exhausted olive-waste cakes, obtained from an oil factory “Agrozitex” located in Sfax, Tunisia, was used as raw material for the production of activated carbons via chemical activation. For this purpose, phosphoric acid was retained as a dehydrating agent. Each preparation test was conducted as follows: 40 g of the crushed (diameter <1.5mm) and

dried precursor was mixed with H<sub>3</sub>PO<sub>4</sub> solution having a concentration 60% H<sub>3</sub>PO<sub>4</sub> in weight. The impregnation ratio, defined by the weight ratio of impregnant (H<sub>3</sub>PO<sub>4</sub>) to precursor was 1.75. The impregnation was carried out in a stirred pyrex reactor equipped with a reflux condenser. Stirring was used to ensure the access of the acid to the interior of the olive-waste cake particles. The temperature and the duration of the reaction were 104 °C and 2 h, respectively. Agitation and heating were ensured by a heating magnetic stirrer with connected temperature regulator probe made of teflon. The pyrolysis of the impregnated material was conducted in a cylindrical stainless steel reactor, inserted into a tubular regulated furnace under continuous nitrogen flow (0.5 L min<sup>-1</sup>). Pyrolysis temperature and time were 450 °C and 2 h respectively. After cooling down to room temperature, under the same flow of nitrogen, the obtained activated carbon was thoroughly washed with hot distilled water until neutral pH. The sample was then dried at 105 °C overnight, ground and finally kept in hermetic bottle for subsequent uses.

The values of Brunauer-Emmett-Teller (BET) surface area, average pore diameter and pore volume were obtained from adsorption of N<sub>2</sub> at 77 K using physiochemical BET analyzer model ASAP 2020 (Micrometrics). The chemical composition of the adsorbent was determined using X-ray spectrometer Philips, model X Pert. The structure of the activated carbon was analyzed by scanning electron microscopy (SEM) using a Philips XL30 microscope.

## **2.2. Biological treatment**

### **2.2.1. Microorganism:**

*Trametes versicolor* was obtained from the American type culture collection (ATCC# 42530). The fungus was maintained on 2% malat agar slants at 25 °C until use. Pellets of *Trametes versicolor* were obtained as described previously (Blázquez et al., 2006).

### **2.2.2. Equipment and techniques:**

A glass bioreactor with a useful volume of 500 mL and pellets of *T. versicolor* with a 3 mm diameter approximately were used to carry out the decolourisation experiments. Biomass fluidization and biomass liquid phase homogenization conditions were maintained by an electrovalve.

The bioreactor was equipped with pH control in order to maintain pH at 4.5 and the temperature was maintained at 25 °C. The batch medium contained per liter: 8 g glucose, 1.9 g NH<sub>4</sub>Cl, 11 mL of a supplemented medium (Kirk et al., 1978) and 0.15 g Grey Lanaset G dye. The color was measured by a PV 8620 Philips spectrophotometer at the visible maximum adsorbance 590 nm. Laccase activity was measured using a modified version of the method for the determination of manganese peroxidase (Wariishi et al., 1992).

### 2.3. Chemicals

Grey Lanaset G, a mixture of metal complex dyes, was supplied by Ciba (ref. 080173.5). All other chemicals used were of analytical grade. Solutions were prepared by dissolving the corresponding reagent in bidistilled water.

## 3. Results

### 3.1. Characterization of the prepared activated carbon

The characteristics of the AC obtained in this work are presented in Table 1. As it can be seen, the characteristics of this adsorbent compare well and sometimes even favorably with those of the other sorbents. The X-ray diffraction analysis of activated carbon did not show any peak indicating amorphous nature of the carbon prepared from olive-waste cakes (Figure 1) It was found that the BET surface area, total pore volume and average pore diameter of the activated carbon were 793.39 m<sup>2</sup>g<sup>-1</sup>, 0.492 cm<sup>3</sup> g<sup>-1</sup> and 4.199 nm, respectively.

The sorbent surface exhibits a clear porous structure and a predominately microporous character (Figure 2).

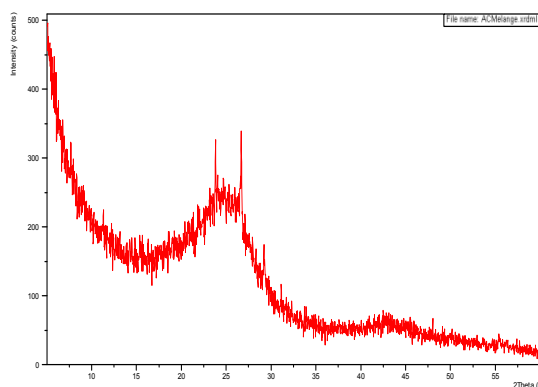


**Figure 1:** RX spectrum of the activated carbon



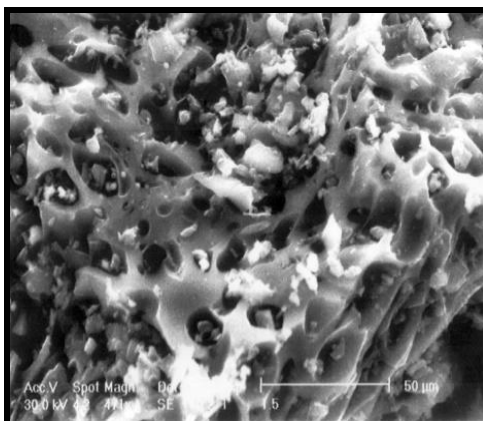


**Figure 2:** *SEM micrograph of the activated carbon*

The adsorption isotherm of the Grey Lanaset G was carried out at 25°C. The results were interpreted in terms of Langmuir and Freundlich equations. The following table presents the parameters corresponding to the Langmuir and Freundlich. From the regression coefficients it can be concluded that Langmuir equation provides the best fit. The value of  $R_L$  in the present investigation values were found to be 0.0452 and confirmed that the activated carbon is favorable for the adsorption of the dye Grey Lanaset G.

**Table 1:** Compared characteristics of the optimal activated carbon

Raw material	Activation process	Adsorbents characteristics			References
		I <sub>2</sub> (mg g <sup>-1</sup> )	BM (mg g <sup>-1</sup> )	S <sub>BET</sub> (m <sup>2</sup> g <sup>-1</sup> )	
Olive-waste cakes	Chemical (H <sub>3</sub> PO <sub>4</sub> )	583	312.5	793.39	(Baccar et al., 2009)
Coconut shell	Chemical (H <sub>3</sub> PO <sub>4</sub> )	*-	-	-	(ASTEE, 2006)
Grain sorghum	Chemical (H <sub>3</sub> PO <sub>4</sub> )	-	-	182-508	(Diao and Walawender, 2002)
Peach stones	Chemical (H <sub>3</sub> PO <sub>4</sub> )	-	-	632	(Molina-Sabio et al., 1995)
Olive-seed waste	Chemical (KOH)	-	190-262	367-506	(Stavropoulos and Zabanioutou, 2005)
Olive-waste waste	Physical (steam)	-	-	514-1271	(Baçaoui et al. 2001)
Olive stones	Physical (steam and N <sub>2</sub> gas mixture)	574	-	-	(Galiastatou et al., 2002)

**Table 2:** Langmuir and Freundlich isotherm constants for Grey Lanaset G at 25 °C.

Langmuir isotherm		Freundlich isotherm	
R <sup>2</sup>	0.9986	R <sup>2</sup>	0.837
q <sub>max</sub>	108.69	n	5.767
R <sub>L</sub>	0.0452	K <sub>F</sub>	48.337

**Table 3:** Comparison of the maximum capacity adsorption of the AC prepared from olive-waste cakes and the commercial AC F400 and CAL

Type of AC	AC prepared from olive-waste cakes	Commercial ACs	
		F400	CAL
q <sub>max</sub> (mg g <sup>-1</sup> )	108.69	454.54	56.82

As it can be seen from the table 3, the maximum adsorption capacity of the carbon obtained in this work is less than the one for commercial activated carbon F400 but it is almost the double of the other commercial sorbent CAL.

### 3.2. Biological treatment

Figure 3 shows the results obtained in a bioreactor with a useful volume of 500 mL. The most substantial colour reduction occurred within the first 24 hours. However, low enzyme activity was noticed in the first day. It is demonstrated in a previous study of the group that the colour is eliminated due to an adsorption process in the biomass in a first step followed by a step that transfers it into the cells and finally the metals are released into the medium. The initial and final metal concentrations of Cr and Co in the solution are presented in the table 4.

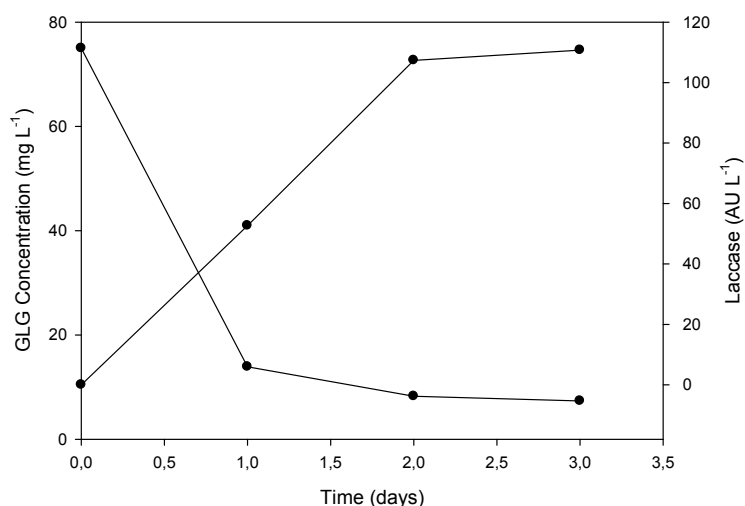


**Figure 3:** Laccase activity and colour evolution during the biological process

**Table 4:** Concentration of Cr and Co in the medium in the beginning and the end of the biological process

	Begining of the process	End of the process
Chromuim (mg L <sup>-1</sup> )	0.11	1.19
Cobalt (mg L <sup>-1</sup> )	0.14	0.38

### 3.3. Biological treatment followed by adsorption

In order to remove Cr and Co, the effluent was treated by adsorption on activated carbon prepared from Tunisian olive-waste cakes. The adsorption capacity of Cr by one g of activated carbon in function of time is presented in table 5. We noticed low adsorption capacities of Cr and the same results were found for the Co. These results led us to think about the reasons of these low capacities because this adsorbent presented a good adsorption capacity of copper in a previous work (Baccar et al., 2009). One reason could be that the AC is unable to adsorb low quantities of metals; a second possible reason could be related to the presence of other components in the medium such as anti foam which could compete the adsorption of Cr and Co.

**Table 5:** variation of the capacity of adsorption of Cr on activated carbon at 25 °C

<b>Time (min)</b>	10	20	40	60	90	120	180
<b>q Cr (mg g<sup>-1</sup>)</b>	0.11	0.11	0.11	0.13	0.12	0.13	0.13

#### **4. Conclusions**

The metal complex dye is successfully biodegraded in a fluidized pulsed bioreactor filled with pellets of *Trametes versicolor*. The dye is first adsorbed onto the biomass, followed by its transfer into cells. Then degradation occurs within cells and the resulting metals are finally released into the medium.

The prepared activated carbon from Tunisian olive-waste cakes presented a good adsorption capacity of the metal complex dye: Grey Lanaset G comparing to commercial ACs. The results, found from the application of biological treatment followed by the adsorption on the AC, in order to purify the Grey Lanaset G, show low capacities of adsorption of Cr and Co. These, led us to modify the AC in order to ameliorate its adsorption capacity.

#### **REFERENCES**

- ASTEE, 2006. Association Scientifique et Technique pour l'Eau et l'Environnement. Réglementation et traitement des eaux destinés à la consommation humaine. 1<sup>ère</sup> Edition. Paris.
- Baçauoui A., Yaacoubi A., Dahbi A., Bennouna C., Phan Tan Luu R., Maldonado-Hodar F. J., Rivera- Utrilla J., Moreno-Castilla, C. 2001. Optimization of conditions for the preparation of activated carbons from olive-waste cakes. *Carbon* 39, 425-432.
- Baccar R., Bouzid J., Feki M., Montiel A., 2009. Preparation of activated carbon from Tunisian olive waste cakes and its application for adsorption of heavy metal ions. *J. Hazard. Mater.* 162, 1522- 1529.
- Blánquez P., Sarrà M., Vicent M.T., 2006. Study of the cellular retention time and the partial biomass renovation in a fungal decolourisation continuous process. *Water Res.* 40, 1650-1656.

- Chen J. P., Yoon J.T., Yiacoumi S., 2003. Effects of chemical and physical properties of influent on copper sorption onto activated carbon fixed-bed columns. *Carbon* 41, 1635-1644.
- Cimino G., Cappello R.M, Caristi C., Toscazo G., 2005. Characterisation of carbons from olive cake by sorption of wastewater pollutants. *Chemosphere* 61, 947-955.
- Diao W.P., Fan Walawender L.T., 2002. Activated carbon prepared from phosphoric acid activation of grain sorghum. *Bioresour. Technol.* 81, 45-52.
- Galiatsatou P., Metax As M., Arapoglou D., Kasselouri-rigopoulou V., 2002. Treatment of olive mill waste water with activated carbons from agricultural by-products. *Waste Manage.* 22, 803-812.
- Girgis B.S., El-hendawy A.N.A., 2002. Porosity development in activated carbons obtained from date pits under chemical activation with phosphoric acid. *Micropor. Mesopor. Mat.* 52, 105-117.
- Haimour N.M., Emeish S., 2006. Utilization of date stones for production of activated carbon using phosphoric acid. *Waste Manage.* 26, 51-60.
- Kirk T.K., Schulz E., Connors W.j., Lorenz L.F., Zeikus J.G., 1978. Influence of cultural parameters on lignin metabolism by *Phanerochaete chrysosporium*. *Arch. Microbiol* 117, 277–284.
- Molina-Sabio M., Rodríguez-reinoso F., Catarla F., Sellés M.j., 1995. Porosity in granular carbons activated with phosphoric acid. *Carbon* 33, 1105-1113.
- Sellami F., Jarboui R., Achica S., Medhioub K., Ammar E., 2008. Co-composting of oil exhausted olive cake, poultry manure and industrial residues of agro-food activity for soil amendment. *Bioresour. Technol.* 99, 1177-1188.
- Stavropoulos G.G., Zabaniotou A., 2005. Production and characterization of activated carbon from olive seed waste residue. *Micropor. Mesopor. Mater.* 82, 79-85.
- Wariishi H., Valli K., Gold M.H., 1992. Manganese (II) oxidation by manganese peroxidase from the basidiomycete *Phanerochaete chrysosporium*. *J. Biol. Chem.* 267, 23688–23695.
- Yang T., Chong Lua, A., 2006. Textural and chemical proprieties of zinc chloride activated carbons prepared from pistachio- nut shells. *Mater. Chem. Physics* 100, 438-444.

## **A.2. Technical specifications of the textile dye Lanaset grey G**

---



**Ciba Specialty Chemicals**  
**COLORS Y CONSUMER CARE**  
 HOJA DATOS DE SEGURIDAD (91/155/CE)

1/4  
 Código del producto 080173.5  
 Fecha 06.01.1998  
 Sustituye HDS fecha 28.01.1997

<b>NOMBRE COMERCIAL</b>				
GRIS LANASET G				
<b>1. IDENTIFICACION DE LA SUSTANCIA/ PREPARADO Y LA EMPRESA</b>				
Descripción química	Mixture of metal complex dyes			
Fabricante	Ciba Specialty Chemicals, CH-4002 Basel			
Departamento responsable	Ecotox TD 2.5 Fax 0041 61 636 7996			
Proveedor	Ciba Specialty Chemicals s.a. Balmes, 117 08008 Barcelona			
Teléfono de emergencia	(93) 404 03 00	Fax (93) 404 03 03		
<b>2. COMPOSICION/ INFORMACION SOBRE LOS COMPONENTES</b>				
Información sobre los componentes	%	No. CAS	Símbolo	Frases R
No aplicable				
<b>3. IDENTIFICACION DE LOS PELIGROS</b>				
Sin clasificación de riesgo según EC				
<b>4. PRIMEROS AUXILIOS</b>				
Inhalación				
Contacto con la piel	Quitarse las ropas contaminadas. Lavarse las zonas del cuerpo afectadas con jabón y abundante agua.			
Contacto con los ojos	Lávese inmediata y abundantemente con agua durante 10 minutos como mínimo.			
Ingestión	Enjuáguese la boca con agua. Beber abundante agua.			
Información para el médico	Tratamiento sintomático			
<b>5. MEDIDAS DE LUCHA CONTRA INCENDIOS</b>				
Medios de extinción adecuados	Agua, espuma, polvo seco, anhídrido carbónico.			
Medios de extinción que no deben utilizarse	Sin restricciones.			
Riesgo de fuego/ explosión	Ninguno.			
Gases de combustión	Oxidos de carbono, nitrógeno y azufre			
Protección personal	Aparato de respiración autónoma.			
<b>6. MEDIDAS A TOMAR EN CASO DE VERTIDO ACCIDENTAL</b>				
Precauciones individuales				
Precauciones para la protección del medio ambiente	No verter en medio acuático			
Métodos de limpieza	Colocarlos en envases señalizados para su eliminación como residuo químico.			
Información adicional				

-- No aplicable



<b>7. MANIPULACION Y ALMACENAMIENTO</b>		
Higiene laboral	Evitese su ingestión, inhalación y contacto con los ojos y la piel. Manipularlo de acuerdo con los principios de higiene industrial y estipulaciones legales pertinentes.	
Prevención del fuego		
Medios de almacenamiento	Almacenar en lugar fresco y seco con adecuada ventilación	
Segregación	No son necesarias precauciones especiales	
Condiciones de almacenamiento	No son necesarias precauciones especiales	
<b>8. CONTROLES DE EXPOSICION Y PROTECCION PERSONAL</b>		
Componentes con límites de exposición	Ninguna	
Protección personal		
<b>9. PROPIEDADES FISICAS Y QUIMICAS</b>		
Aspecto	Estado Color Olor	Polvo Negro Ninguno
<b>DATOS DE SEGURIDAD IMPORTANTES</b>		
Punto de fusión	--	°C
Punto de ebullición	--	°C
Punto de destello	--	°C
Descomposición térmica	> 200	°C
Temperatura de inflamación	> 450	°C
Autoinflamabilidad		BAM
Propiedades oxidantes	Ninguna	
Límites de explosión	Inferior	Superior
Presión de vapor	--	mbar
Densidad		a
Solubilidad en agua	100	g/l
	100	g/l
pH	7.5-8.5	
Coefficiente de reparto		log Pow
Viscosidad	--	mPa.s
		a
		30
		°C
		90
		°C
		1
		g/l
		°C
<b>10. ESTABILIDAD Y REACTIVIDAD</b>		
Condiciones a evitar	Ninguna	
Materiales a evitar	Ninguno.	
Productos de descomposición peligrosos	Ninguno.	
Información adicional		

GRIS LANASET G

3/4  
 Código del producto 080173.5  
 Fecha 06.01.1998

11. INFORMACION TOXICOLOGICA							
Toxicidad aguda	(LD50)	> 5000	mg/kg				Ratas (oral)
Irritación primaria	(Piel)	Non irritante	EC 83	OECD 404			Conejos
	(Ojos)	Non irritante	EC 83				Conejos
Efectos negativos en el hombre		No se conocen efectos negativos					
Información adicional							
12. INFORMACIONES ECOLOGICAS							
Bioeliminación		70-80%, Análisis DOC,					OCDE 302B
Resumen		Eliminación po adsorción sobre lodo					
DATOS ECOTOXICOLOGICOS							
Toxicidad para el efluente bacterias	BST CI50	> 300	mg/l				
Toxicidad para los peces	CL0 CL50	6 18	mg/l		48 h trucha arcoiris		OECD 203
Resumen		Nocivo para los organismos acuáticos (Modelo CE)					
Comportamiento en las plantas de tratamiento		No produce inhibición. No se conocen efectos nitrificadores inhibidores					
INFORMACION ECOLOGICA ADICIONAL							
DBO5	25	mgO2/g	DQO	1000	mgO2/g	COT	34.4 %
Contenido de nitrógeno		5.7	%				
Contenido de fósforo		0.1	%		as phosphate		
Contenido en halógeno orgánico		-	%				
Contenido de metales		0.79 2.5	%		Cobalt as organo-metal complex Chromium as CrIII organo-metal complex		
Producto ensayado		Basado en datos conocidos de los componentes					
13. CONSIDERACIONES SOBRE LA ELIMINACION							
Producto		Incinerar, verter. Observar las disposiciones legales.					
Clasificación de los residuos (91/689/CE)							
Embalaje contaminado		Tratar como residuos químicos los envases vacíos contaminados.					

**PRAT BELTRAN, S. L.**  
 Narciso Monturiol, 35. Apartado 5  
 Tel. (93) 379 43 44 - Fax (93) 370 34 52  
 08820 El Prat de Llobregat (Spain)

GRIS LANASET G

4/4  
 Código del producto 080173.5  
 Fecha 06.01.1998

<b>14. INFORMACION RELATIVA AL TRANSPORTE</b>		<b>MANTENER LEJOS DE ALIMENTOS</b>		
Número UN ADR/RID	FREE	Clase ADR/RID	FREE	
Nombre para el transporte ADR/RID				
Número UN IMO	FREE	Clase IMDG	FREE	Grupo de embalaje
Nombre para el transporte IMO				
Número UN ICAO	FREE	Clase ICAO	Grupo de embalaje	
Nombre para el transporte ICAO				
<b>15. INFORMACION REGLAMENTARIA</b>				
<b>CLASIFICACION Y ETIQUETADO</b>			83/467 CE	
Símbolo y clasificación	--	--		
Frases R				
Frases S				
Contiene				
<b>16. OTRAS INFORMACIONES</b>				
<b>17. INFORMACIONES APLICABLE EN SU USO COMO</b>				
Colorante textil				
<p>Los productos de la División de Colorantes y Productos Químicos de Ciba Specialty Chemicals son de calidad técnica y si no se ha especificado lo contrario, están recomendados únicamente para su utilización en aplicaciones industriales de preparación, tintura o acabado de textiles, papel o cuero. Si se desean utilizar para otras aplicaciones, inclusive en productos de consumo sujetos a estándares o legislaciones específicas, deben ser consultado al proveedor. Los datos indicados en las H.D.S. son aplicables únicamente a los productos de Ciba Specialty Chemicals comercializados bajo sus propias designaciones. A petición de las autoridades competentes, Ciba Specialty Chemicals facilitará la información técnica en que se basan dichos datos.</p>				

member of ETAD



**A.3. Technical specifications of the tannery dye Black dycem TTO**

---



COLORANTES INDUSTRIALES, S.A.  
 Óptica, 11 P. Ind. Santa Rita  
 08755 - Castellbisbal - BCN  
 SPAIN

Tel. +34 93 771 1830  
 Fax +34 93 771 1670  
 www.colorantesindustriales.com



## Feuille de Specifications Techniques

DATE : 22/10/2001

PRODUIT : NOIR DYCEM TTO

PARAMETRES DE QUALITÉ	TOLÉRANCE	SPECIFICATION
Concentration. Extinction	+/- 2.5 %	100 %
Concentration. Rémission	+/- 2.5 %	100 %
Différence totale de Couleur C.M.C. (2:1)	-	Máx. 1.00
Solubilité (grs./ltro.)	-	Min. -
Test de la poudre	-	Min. 3

Colorantes Industriales, S.A.



COLORANTES INDUSTRIALES, S.A.  
 Óptica, 11 P.Ind. Santa Rita  
 08755 - Castellbisbal - BCN  
 SPAIN

Tel. +34 93 771 1830  
 Fax +34 93 771 1970  
 www.colorantesindustriales.com



Página 1 de 4

### Fiche de Données de Sécurité

En accord avec la directive 1907/2006/CE (REACH)

Date d'EMISION : 20/02/2009 Date de REVISION : 01/06/2007

#### 1. IDENTIFICATION DU PRODUIT ET DE LA SOCIETE

Substance ou Préparato : NOIR DYCEM TTO



C.INDEX FORMULE / DESCRIPTION : COLORANT ACIDE  
 C.A.S. E.I.N.E.C. REACH

Utilisation de la substance ou préparé : Préparation, Teinture ou Finissages pour les Industries Textiles, du Bois, du Papier ou du Cuir.

Fournisseur : COLORANTES INDUSTRIALES, S.A.  
 C/ OPTICA, 11 - P.IND. SANTA RITA  
 08755 - CASTELLBISBAL (Barcelona- SPAIN)  
 Tel. +34 93 771 1830 - Fax. +34 93 771 1970  
 colorantes@colorantesindustriales.com

Téléphone d'urgence : + 34 93 771 1830 en Horario de Oficina

#### 2. IDENTIFICATION DES DANGERS

DL50 > 3550 mg / kg. (oral-rot)

#### 3. COMPOSITION ET INFORMATION SUR LES COMPOSANTS

Nom	Concentration	Iconne	Phrase R	REACH	C.A.S.
-----	---------------	--------	----------	-------	--------

#### 4. MESURES DE PREMIERS SECOURS

INHALATION : Mettre rapidement à l'abri la personne touchée.

INGESTION : Si la personne est consciente, donner du lait et faire vomir.

PEAU / YEUX : Laver immédiatement et abondamment les parties atteintes avec de l'eau et du savon, pour les yeux utiliser que de l'eau pendant au moins 15 minutes.

MESURES GENERALES : Appeler un médecin.



COY CIANANES INDUSTRIAS S.A.  
 Ofi. 1001 P. 122 Santa Rita  
 08755 - Casle Basca - ESPAÑA

Tel. +34 93 771 1833  
 Fax +34 93 771 1970  
 www.coyci.com/ingles/ingles.htm



Página 2 de 4

#### 6. ALGUNTAS DE LUTYÉ CONTRE L'INCENDIE

UTILISER DES EXTINGUEURS : A poudre, à mousse ou à l'eau peur vérifiée.

PRODUITS DE DECOMPOSITION DANGEREUX : En principe, aucun.

MESURES SPECIALES : Peur vérifier de l'eau pour refroidir les surfaces exposées au feu et pour protéger la personne. Eloigner du feu les produits inflammables. Ne pas utiliser de l'eau à pression pour ne pas disperser de produit.

DANGERS SPECIAUX : Le produit est combustible.

#### 8. MESURES APRES FOITE OU DEVERSEMENT ACCIDENTEL

PRECAUTIONS PER L'ENVIRONNEMENT : Eviter que le produit arrive aux cours d'eau.

RECUPERER LE PRODUIT : Avec l'aide de pelles et de saucis, le mettre dans des conteneurs appropriés pour son recyclage et éviter la formation de poudre.

PRECAUTION INDIVIDUELLE : Travailler avec des gants et avec des lunettes de protection. Ne pas fumer et éviter l'inhalation du produit.

#### 7. STOCKAGE ET MANIPULATION

MANIPULATION : Eviter la formation de poudre et le contact direct avec le produit. Porter l'équipement de protection pour produit chimique.

STOCKAGE : Conserver les emballages fermés. Ne pas manipuler, déplacer ou ouvrir à proximité d'une flamme ou d'une température de façon possible entre + 25°C.

#### 8. CONTROLE DE L'EXPOSITION / PROTECTION INDIVIDUELLE

Produit	E.I.N.E.C.S.	STEL		TWA	
		PPM	MG/M3	PPM	MG/M3

PROTECTION INDIVIDUELLE : Pour les manipulations où la contact avec le produit est probable, il est recommandé de porter des gants adaptés aux produits chimiques, des vêtements à manches longues ainsi que des lunettes de protection. En cas de risque de surexposition, il est nécessaire de porter un appareil respiratoire adapté.

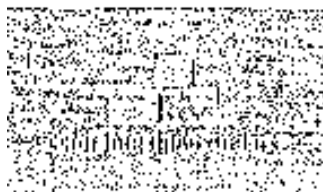
#### 9. PROPRIETES PHYSIQUES ET CHIMIQUES

ETAT PHYSIQUE :	POUDRE	PROPRIETES D'EXPLOSION :	NP
POINT D'EGRESSION :		POINT DE FUSION :	> 250°C
POINT D'INFLAMMATION :		DENSITE (g/ml) :	
PH (10 g/l. de l'eau) :	7	VISCOSITE (cP) :	
SOLUBILITE (20°C quant. dans l'eau) :	39		

#### 10. STABILITE ET REACTIVITE

STABILITE :	Stable à température d'ambiance.
INCOMPATIBILITE :	Agents oxydants forts.
RISQUE DE POLYMERISATION :	NP
CONDITIONS A EVITER :	NP





COLOMANTE INDUSTRIALES S.A.  
 Office: 11 Pined, Santa Rita  
 69750 - Castañubal - BZH  
 SPAIN

Tel: +34 93 771 1630  
 Fax: +34 93 771 1670  
 www.coloman.es/industriales.com



Página 3 de 4

**11. INFORMATIONS TOXICOLOGIQUES**

INGESTION (DL50) > 3500	Essais sur rat
CONTACT AVEC LA PEAU : -	(CEE/83)
CONTACT AVEC LES YEUX : -	(CEE/83)

**12. INFORMATIONS ECOLOGIQUES**

**DEGRADABILITE :** Ce produit est classé comme **NON BIODEGRADABLE RAPIDEMENT**. Cette substance est supposée être éliminée dans une station d'épuration d'eau.

**ECOTOXICITE ET BIOACCUMULATION :** Probablement, sans effets néfastes pour les organismes aquatiques :

Toxicité : CL 50 < 300 mg/litre/94 heures.	
AOX (%) : -	BOD5 (mgO2/g) : COD (mgO2/g) :

Le produit ne contient pas de métaux pesants dangereux pour l'eau.  
 Ce produit ne contient pas de chlore libre par faveur l'oxydation.  
 Le produit ne contient pas de Phosphore actif.

**13. CONSIDERATIONS RELATIVES A L'ELIMINATION**

**ELIMINATION :** Considérer la recyclabilité du produit.

Ce produit NE PEUT, ni être mis à la décharge, ni être évacué dans les égouts, les caniveaux, les eaux d'égout, les puits ou les rivières. Les fûts vides doivent être nettoyés pour recueillir le produit résiduel ou destruction par des sociétés agréées. Dans tous les cas, le respect des réglementations européennes, nationales et locales doit être obtenu.

**14. TRANSPORT**

**PRECAUTIONS SPECIALES :** Stable à température ambiante pendant le transport. Transporter en emballage bien fermé et identifié.

**INFORMATION COMPLIMENTAIRE :**

Transport	ONU	CLASSE	DANGER	GROUP
ADR/RIC :				
IMDG :				
IATA/ICAO :				

**MARINE POLLUANT :** NON

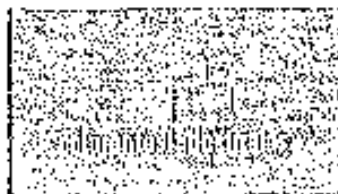
**15. INFORMATION REGLEMENTAIRE**

**ETIQUETAGE :**



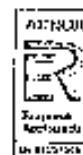
**CONNE :**

NP      Aucun Danger selon le règlement 2001/56/CE



COLONIAS INDUSTRIAL CO. S.A.  
 C/Alca, 11 P. Inc. Santo Pile  
 04705 - Castellón de la Plana - HCN  
 ESPAÑA

Tel. +34 93 771 1930  
 Fax +34 93 771 1970  
[www.coloniasindustriales.com](http://www.coloniasindustriales.com)



Página 4 de 4

#### 16. AUTRES INFORMATIONS

Cette fiche complète la Fiche technique d'utilisation, mais ne la remplace pas. Les renseignements qu'elle contient sont basés sur l'état de nos connaissances relatives au produit concerné, à ce jour. Ils sont donnés de bonne foi. L'attention des utilisateurs est en outre attirée sur les risques éventuellement encourus lorsqu'un produit est utilisé à d'autres usages que ceux pour lequel il est conçu.

Aucune garantie ne peut être donnée sur l'exactitude des informations contenues dans cette fiche. Celle-ci, est offerte de bonne foi à notre clientèle, dans le seul but de l'informer et de l'aider dans ses recherches et n'entraîne aucune garantie formelle ou implicite quant à son utilisation. En conséquence, Colonias Industriales, S.A. ou les sociétés affiliées du groupe, ne pourront être tenues pour responsables des dommages de quelque nature qu'ils soient, résultant de la publication de ce document.

De même, aucune des informations qu'il contient ne doit être interprétée comme une approbation ou une recommandation d'emploi de produits qui pourraient des droits protégés de propriété industrielle.